Modulation of the JAK2/STAT3 pathway in vivo : understanding reactive astrocyte functional features and contribution to neurodegenerative diseases

Lucile Ben Haim

▶ **To cite this version:**

Lucile Ben Haim. Modulation of the JAK2/STAT3 pathway in vivo : understanding reactive astrocyte functional features and contribution to neurodegenerative diseases. Neurons and Cognition [q-bio.NC]. Université Pierre et Marie Curie - Paris VI, 2014. English. NNT : 2014PA066534 . tel-01165032

HAL Id: tel-01165032

https://theses.hal.science/tel-01165032

Submitted on 18 Jun 2015

HAL is a multi-disciplinary open access archive for the deposit and dissemination of scientific research documents, whether they are published or not. The documents may come from teaching and research institutions in France or abroad, or from public or private research centers.

L'archive ouverte pluridisciplinaire **HAL**, est destinée au dépôt et à la diffusion de documents scientifiques de niveau recherche, publiés ou non, émanant des établissements d'enseignement et de recherche français ou étrangers, des laboratoires publics ou privés.

Université Pierre et Marie Curie

Ecole Doctorale Cerveau, Cognition, Comportement

Laboratoire des maladies neurodégénératives, CEA-CNRS URA2210

Thèse de doctorat de Neurosciences

Lucile BEN HAIM

Modulation of the JAK2/STAT3 pathway *in vivo*: understanding reactive astrocyte functional features and contribution to neurodegenerative diseases.

Dirigée par Dr. Carole Escartin

Soutenue publiquement le 11 décembre 2014

Composition du jury

Président	Pr. Jean Mariani	CNRS UMR 7102 UPMC
Rapporteurs	Dr. Jean-Charles Liévens	CNRS UMR 7286 CRN2M
	Dr. Frank Pfrieger	CNRS UPR 3212 INCI
Examinateurs	Dr. Christian Lobsiger	INSERM U-1127 UPMC
	Dr. Stéphane Oliet	INSERM Neurocentre Magendie
Directrice de thèse	Dr. Carole Escartin	CEA-CNRS URA2210

« Before you know, you must imagine »
Nobel laureate Richard Axel

Abstract

Astrocytes become reactive in response to pathological conditions in the CNS including neurodegenerative diseases (ND) such as Alzheimer's (AD) and Huntington's (HD) diseases. Reactive astrocytes (RA) are identified by morphological changes but their functional features and influence on neuronal survival are poorly understood. They have mainly been studied in acute injuries, but less is known for chronic diseases like ND. In this context, we aimed at 1) identifying the signaling cascades involved in astrocyte reactivity in ND conditions, 2) evaluating RA contribution to chronic neuronal dysfunction in ND models and 3) deciphering RA functional features.

The JAK2/STAT3 pathway is a known trigger of astrocyte reactivity in many CNS acute injury models. Here, we show that this pathway is a universal inducer of astrocyte reactivity in several ND mouse models of both AD and HD. We developed new viral vectors that target the JAK2/STAT3 cascade *in vivo*, in astrocytes of the adult rodent brain, to selectively modulate astrocyte reactivity. Using these original tools, we were able to investigate the contribution of RA to disease progression and neuronal dysfunction in two different models of HD: the lentiviral-based model of HD and the N171-82Q HD mice. Our results show that RA do not primarily influence disease phenotype in these models. Finally, we manipulated the JAK2/STAT3 pathway to activate astrocytes in WT mice in order to characterize the functional features of RA *in vivo*. We show that astrocyte activation through the JAK2/STAT3 pathway triggers transcriptional changes of numerous genes involved in important cellular functions such as metabolism, protein degradation pathways and immune response. Furthermore, we show that astrocyte reactivity alters synaptic plasticity in the mouse hippocampus.

Our results identify the JAK2/STAT3 pathway as a central cascade for astrocyte reactivity. The viral vectors developed in this project represent powerful tools to 1) manipulate this pathway and decipher RA contribution to chronic neuronal dysfunction in various ND models and 2) characterize RA functional features *in vivo.* Better understanding RA functions may eventually lead to the identification of new therapeutic targets for ND.

Key words: Reactive astrocytes, JAK2/STAT3 pathway, Neuroinflammation, Huntington's disease, Alzheimer's disease, Viral vectors, Transcription regulation.

Résumé

Les astrocytes deviennent réactifs en réponse à toute situation pathologique dans le SNC, en particulier dans les maladies neurodégératives (MND) comme la maladie d'Alzheimer (MA) et de Huntington (MH). Les astrocytes réactifs (AR) sont identifiés par des changements morphologiques bien caractérisés mais les conséquences fonctionnelles de leur réactivité sont peu connues, notamment dans les MND. La contribution des AR dans les situations pathologiques a principalement été étudiée dans des modèles de lésions aigües mais leur rôle dans les MND est peu connu. Dans cette étude, nous avons évalué 1) les voies de signalisation impliquées dans la réactivité astrocytaire, 2) la contribution des AR à la dysfonction neuronale dans des modèles de MND et 3) les caractéristiques fonctionnelles des AR.

La voie JAK2/STAT3 est une voie de signalisation impliquée dans la réactivité astrocytaire, dans des conditions pathologiques aigües. Dans cette étude, nous avons montré que cette voie universelle induit également la réactivité astrocytaire des modèles murins de MA et MH. Nous avons développé de nouveaux vecteurs viraux permettant de cibler la voie JAK2/STAT3, *in vivo*, sélectivement dans les astrocytes, dans le cerveau de rongeur adulte. A l'aide de ces outils, nous avons étudié la contribution des AR à la dysfonction neuronale observée dans deux modèles murins de la MH. Nos résultats suggèrent que les AR ne jouent pas un rôle central dans la dysfonction neuronale et la progression de la maladie dans ces deux modèles.

Enfin, nous avons induit la réactivité dans les astrocytes de souris sauvages, en ciblant la voie JAK2/STAT3. L'activation de la voie JAK2/STAT3 dans les astrocytes du striatum module très fortement l'expression de gènes impliqués dans des fonctions cellulaires importantes comme le métabolisme oxydatif, les voies de dégradation des protéines ou la réponse immunitaire. De plus, nous avons observé que l'induction de la réactivité astrocytaire dans l'hippocampe de souris sauvage conduit à une diminution de la plasticité synaptique.

En conclusion, nous avons montré que la voie JAK2/STAT3 est une voie centrale et conservée dans les AR. Les vecteurs viraux développés au cours de ce projet représentent des outils innovants pour évaluer 1) la contribution des AR à la dysfonction neuronale dans de nombreux modèles de MND et 2) caractériser les propriétés fonctionnelles des AR *in vivo*. L'étude des AR pourra permettre d'identifier de nouvelles cibles moléculaires pour manipuler ces cellules pléiotropes à des fins thérapeutiques.

Mots-clés : Astrocytes réactifs, Voie de signalisation JAK2/STAT3, Neuroinflammation, Maladie de Huntington, Maladie d'Alzheimer, Vecteurs viraux, Régulation transcriptionnelle

Remerciements

Je tiens à remercier les membres de mon jury pour avoir accepté d'examiner mon travail et de participer à ma soutenance de thèse. En particulier mes rapporteurs Jean-Charles Liévens et Frank Pfrieger pour l'évaluation de mon manuscrit.

Je voudrais remercier toutes les personnes qui m'ont aidé, de toutes les manières que ce soit, au cours de ma thèse.

Je remercie Philippe Hantraye pour avoir accepté que je réalise mon stage de Master 2 et ma thèse à MIRCen.

Je voudrais remercier ma directrice de thèse, Carole, qui aura éprouvé, en plus de ces deux grossesses, une sorte de troisième accouchement en encadrant officiellement sa première thèse. Merci pour tes encouragements constants, à l'épreuve de mon pessimiste et de mon instatisfaction. Merci pour ton encadrement, pour la confiance que tu m'as accordé, dès le Master 2 sur ce projet. Merci de m'avoir permis de présenter mon travail et de le défendre à de nombreux congrès. Merci de ton aide, de ton soutien et de tes conseils pour la thèse et aussi pour la suite.

Je tiens à remercier Gilles pour avoir été mon maître de stage de Master 2 par intérim, pour ton expérience, tes conseils, tes encouragements et pour l'organisation des team-meetings qui m'ont fait beaucoup progressé sur la communication de mes résultats (pour la partie valorisation, ça vient petit à petit).

Merci à Emmanuel pour m'avoir accueillie dans le laboratoire et encadré au cours de mon stage de Master 1. Merci pour ta gentillesse, pour le temps que tu as toujours su m'accorder pour parler de mon projet de thèse, de science en général ou de la carrière de chercheur.

Merci aux différentes personnes qui ont partagé mon bureau pour avoir éprouvé ma taciturnité au cours de ces trois ans et demi. Laetitia, merci pour ton optimisme, ton calme et ton humour (pas toujours bien placé), pour nos discussions existentielles sur la thèse et sur la suite. Merci à Noémie pour ta bonne humeur et ton humour, malgré que tu aies partagé notre bureau au cours des mois les plus stressants de ces 3 ans. Bon courage pour la suite. Merci à María pour ton soutien, tes encouragements et ta sagesse, de laquelle je vais m'efforcer de m'inspirer en recherche et dans la vie en général. Merci à Fabien pour ton aide, qui a été très précieuse pour mon projet de thèse mais surtout merci pour ton humour qui nous manque à tous.

Merci à Juliette et Emilie pour leur soutien, leur humour et tous les moments qu'on a partagé. Juliette, nos échanges 9gag resteront associés à ma thèse pour toujours. Emilie, tu es un exemple de courage et de persévérance (et aussi de résistance à la bière).

Merci à Karine pour m'avoir formée et pour ton aide pour les expériences de comportement. Je garde un souvenir tout particulier de l'atelier peinture pour le test de la marche.

Merci à Marie-Claude pour m'avoir formée à la qPCR, pour ton aide et tes nombreux conseils.

Merci à Noëlle, Charlène, Nicole et Alexis pour le design et la production des quelqu…nombreux virus dont je me suis servie au cours de ma thèse. Nöelle et Charlène, merci pour votre humour, votre enthousiasme et votre bonne humeur qui font partie des choses qui rendent l'ambiance à MIRCen particulièrement agréable.

Merci à Gwen, Martine et Diane pour votre investissement et votre efficacité pour mes manips d'injection, qui j'espère resteront dans le top 10 des manips de stéréotaxie les plus compliquées de MIRCen. Un merci particulier à Gwen pour ta polyvalence, ton efficacité et pour avoir été toujours prête à aider les thésardes en détresse.

Merci à Fanny, Caro et Pauline de m'avoir formée aux joies de l'histo, pour votre aide et votre expérience. J'ai quand même gagné deux prix de posters avec mes belles immunos, c'est grâce à vous !

Je voudrais remercier nos collaborateurs pour leur aide et leur expertise, qui ont beaucoup apporté à ce projet.
Merci à Paolo pour m'avoir initiée à l'electrophysiologie dans le striatum, j'ai beaucoup apprécié aller à Marseille et découvrir un autre laboratoire.

Merci à Aude et Julien pour les manips d'electrophysiologie sur les souris JAK2. Aude, je te remercie chaleureusement d'avoir accepté d'être jury à mon comité de mi-thèse puis pour ton aide, tes conseils et encouragmeents sur mon projet mais aussi sur le post-doc.

Merci à Ian Bayer et Nathalie Deschamps pour les expériences de FACS. C'était une manip ambitieuse et nous avons réussi à générer des données très importantes grâce à votre collaboration. Merci à Nathalie pour ta patience, ton aide pour le tri et ton intérêt pour notre projet.

Merci à Robert Olaso, Céline Derbois et Virginie Lavilla pour leur expertise et leur aide pour la réalisation de l'étude transcriptomique sur les astrocytes triés. J'ai beaucoup apprécié de faire ce développement technique avec vous et repousser les limites des kits de biologie moléculaire.

Je voudrais remercier Thierry Kortulewski, Lamya Irbah, Jean-Yves Thuret et Régis Courbeyrette pour leur aide technique au microscope confocal.

Je remercie Christian Lobsiger et Romain Parillaud pour les échantillons de souris intoxiquées au MPTP.

Merci à Marie-Laure et Marie-Christine pour votre aide et votre efficacité pour m'avoir guidé dans les méandres administratifs du CEA.

Je voudrais remercier toutes les personnes qui travaillent à MIRCen et avec lesquelles j'ai eu le plaisir d'interagir pendant ces 3 ans et demi. Je garderai un excellent souvenir de ma thèse à MIRCen, grâce à votre présence à tous.

Enfin, je voudrais remercier ma famille, en particulier mes parents et ma sœur, qui m'on supporté avec mon fichu caractère et ma coquille, surtout pendant ces 3 ans. Merci pour votre soutien et pour votre patience, merci de m'avoir soutenu dans mes choix pour me destiner au métier passionnant et inédit de chercheur.

Figures

INTRODUCTION

I. GENERAL INTRODUCTION

Astrocytes are now recognized as essential participants of in many brain functions. They are pleiotropic cells responsible for the maintenance of the cellular environment for neurons to function properly. Astrocytes regulate ionic and water homeostasis, they participate in the formation and maintenance of the blood-brain barrier (BBB), they provide neurons with trophic, metabolic support as well as antioxidant defense. Astrocytes display a strategic anatomical location as they contact blood vessels as well as ensheath synapses. They reuptake glutamate from the synaptic cleft through specific glutamate transporters and thus prevent excitotoxicity. Astrocytes also modulate synaptic transmission and release synaptically active molecules called gliotransmitters.

Because of their close interactions with neurons as well as other glial cells, astrocytes are key sensors of brain homeostasis. Indeed, they detect and react to pathological conditions in the CNS in a phenomenon called astrocyte reactivity (**Sofroniew, 2009**). It occurs in a variety of pathological conditions, both acute (trauma, ischemia, infection…) and chronic (neurodegenerative diseases (ND)). Reactive astrocytes are mainly identified by morphological changes ranging from hypertrophy and upregulation of intermediate filaments to the formation of a glial scar (**Sofroniew, 2009**).

Astrocyte reactivity is a complex phenomenon, involving multiple extracellular triggers (cytokines, nucleotides, aggregated proteins…) that may activate different intracellular pathways (JAK/STAT, NF-κB, MAPK) (**Kang and Hebert, 2011**). However, the functional changes that are elicited by these signaling cascades in reactive astrocytes are poorly understood. One of the reasons is the lack of appropriate tools to evaluate the consequences of reactive astrocyte functions and neighboring neurons study the causal link between these pathways and astrocyte reactivity, particularly in chronic pathological conditions such as in ND.

Astrocyte reactivity and its impact on neurons has mainly been studied in acute injuries, involving glial scar formation (**Sofroniew, 2009**). By contrast, neuronal dysfunction in ND does not involve external stimulus such as a mechanical lesion and thus, are most likely to involve different pathological mechanisms. ND such as Alzheimer's (AD), Huntington's (HD), Parkinson's (PD) diseases or amyotrophic lateral sclerosis (ALS) are characterized by the selective loss of vulnerable neurons in specific regions of the CNS. ND are characterized by common cellular alterations, including apoptosis, mitochondrial dysfunction, oxidative stress, protein aggregation or inflammation (**Burda and Sofroniew, 2014**). Interestingly, many of these functions involve neuron-astrocyte interactions in the healthy brain.

It is widely debated whether reactive astrocytes can influence neuron survival and disease phenotype, especially in ND. Evidence suggests that reactive astrocytes play a pivotal role and can exert both beneficial and detrimental effects on neurons according to the pathological situation.

This work is centered on reactive astrocytes and ND. Specifically, we aimed to investigate: 1) the signalling pathways involved in astrocyte reactivity in the context of ND, 2) the contribution of astrocyte reactivity to neuronal dysfunction in HD, a prototypic ND, and 3) to model and study the functional changes occurring in reactive astrocytes.

II. INTRODUCTION

A. Astrocytes are pleitropic cells essential for brain functions

1) General characteristics of astrocytes

a) What is an astrocyte?

In 1846, Virchow first described that nerve cells were embedded in a connective tissue that he called 'nervenkitt' or nerve glue. In 1909, Ramón y Cajal used gold impregnation to reveal the morphology of star-shaped cells called astrocytes (**Garcia-Marin et al., 2007**). He identified two main types of astrocytes that are distinguished according to their morphology and anatomical localization. Fibrous astrocytes are found in the white matter, they display an elongated morphology with thin and long processes. By contrast, protoplasmic astrocytes are found in the grey matter, they have more numerous and irregular processes than fibrous astrocytes (**Garcia-Marin et al., 2007**).

The number of astrocytes and its relation to the brain complexity is controversial. In the literature, authors often refer to astrocytes as the most abundant cell type in the brain or that the number of astrocytes per neuron (glia/neuron ratio) is drastically increased in high-order primates. In fact, a recent study showed that the glial/neuron ratio varies consistently across brain structures in a variety of mammalian species (rodents, insectivores, non-human and human primates) (**Herculano-Houzel, 2014**). In addition, another study determined that astrocytes only represent approximately 20% of the total glial cells in the human neocortex (**Pelvig et al., 2008**). Thus, it appears that astrocyte complexity rather than number increases with brain size, especially in humans (**Oberheim et al., 2009**).

b) Functional and anatomical organization

Astrocytes display a star-shaped morphology and can be identified by the expression of several markers including glial fibrillary acid protein (GFAP), an intermediate filament protein and the Ca^{2+}-binding protein B (S100β). More recently, aldehyde dehydrogenase 1 family, member L1 (Aldh1L1) has been identified as a new marker for astrocytes and allows the labeling of most astrocytes in the rodent brain (**Cahoy et al., 2008; Yang et al., 2011**).

Interestingly, dye-filling experiments and more recently, reporter mice with fluorescent astrocytes, have allowed the visualization of the real morphology of these cells. In fact, astrocytes have a complex morphology, with highly ramified processes (**Wilhelmsson et al., 2004**) (**Figure 1A**). Indeed, the GFAP labeling only represents approximately 15% of the total volume occupied by an astrocyte (**Bushong et al., 2002**). In addition, astrocytes are organized in separate, non-overlapping spatial domains (**Bushong et al., 2002**) (**Figure 1C**).

Both protoplasmic and fibrous astrocytes display a unique anatomical localization. Fibrous astrocytes contact nodes of Ranvier and blood vessels in the white matter. Protoplasmic astrocytes ensheath synapses and contact blood vessels in the grey matter (**Figure 1B, E and F**) (**Barres, 2008**). Each astrocyte encompasses 300-600 neuronal dendrites (**Halassa et al., 2007**) and 140 000 hippocampal synapses (**Bushong et al., 2002**) in the mouse brain. Astrocyte processes also contact blood

capillaries through their perivascular endfeets (**Figure 1E, F**). This anatomical particularity allows astrocytes to control water and ion homeostasis (**Alvarez et al., 2013**). Furthermore, astrocytes are organized as a network, coupled by gap-junctions channels (**Giaume et al., 2010**) (**Figure 1D**). Gap-junction channels are formed by the apposition of two connexons, each resulting of the assembly of six connexins. The main astroglial connexins are the connexins 43 and 30. These channels are permeable to small molecules (<1.2kDa) including ions (Ca^{2+}, K^{+}…), second messengers (cyclic adenosine monophosphate (AMP), inositol-3-phosphate (IP_3) or ATP…), energy substrates (glucose, glycogen…) or amino acids (glutamate) (**Giaume et al., 2010; Escartin and Rouach, 2013**).

This peculiar organization allows astrocytes to maintain a tight homeostasis for neuron to function properly. Very interestingly, Lugaro has already suggested, more than a century ago, most of these roles for astrocytes uniquely based on the observation of their morphology. He hypothesized that astrocytes were able to uptake metabolites and release toxic molecules in the blood flow through their endfeets (**Somjen, 1988**). Remarkably, he also proposed that astrocytes were able to take-up molecules that were released at the synapse during neuronal communication (**Somjen, 1988**).

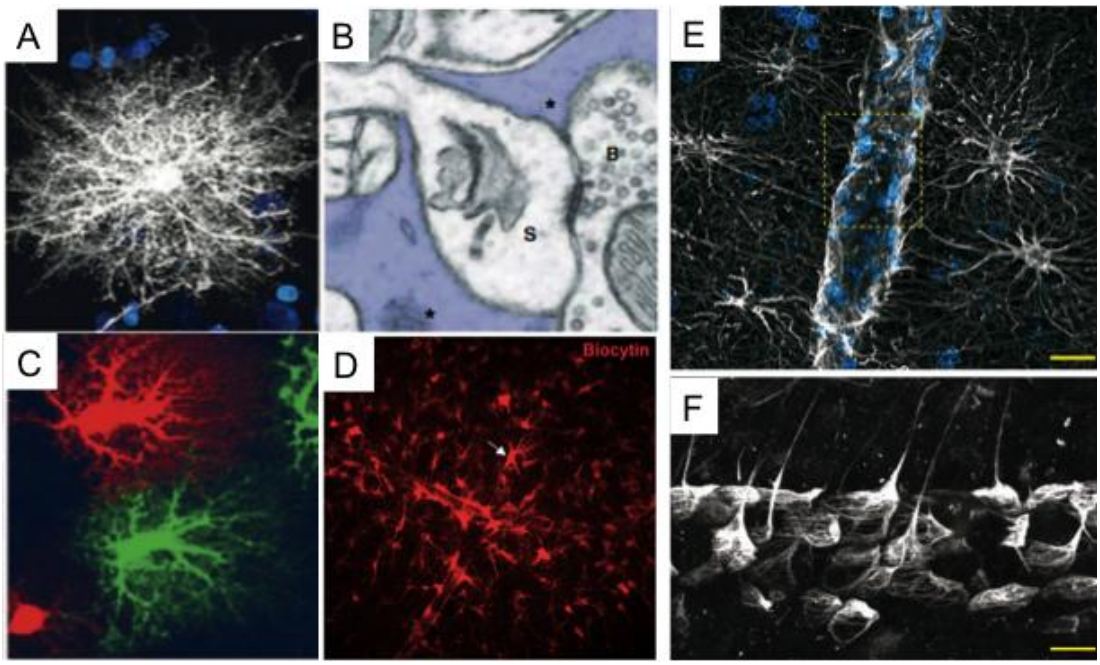

Figure 1. Anatomical characteristics of protoplasmic astrocytes.
A, Protoplasmic astrocytes are star-shaped cells and display a bushy morphology. **B**, Astrocytes (blue) ensheath synapses and form with the pre- (**B**) and post-synaptic (S) elements, the tripartite synapse. **C**, Astrocytes are organized in non-overlapping spatial domains. Dye-filling experiment shows the morphology of adjacent astrocytes in the mouse brain. **D**, Astrocytes are organized as a network and are coupled through gap-junctions. In the mouse hippocampus, one astrocyte (arrow) has been filled with a fluorescencent label (biocytin), which has diffused in the astroglial network of coupled astrocytes. **E-F**, Astrocytes contact blood vessels through perivascular endfeets that cover the surface of the vessel basal lamina to form the BBB (**F**). Adapted from (**Belanger and Magistretti, 2009; Allaman et al., 2011; Escartin and Rouach, 2013**).

c) Astrocyte-like cells and radial glial cells share common features with mature astrocytes

Invertebrates such as Caenorhabditis elegans (C.elegans) and Drosophila melanogaster have astrocyte-like glial cells suggesting that specialized glia appeared very early in evolution (**Freeman and Rowitch, 2013**). C.elegans cephalic sheath glia is necessary for nerve ring formation, are closely associated with synapses and support neuronal functions (**Oikonomou and Shaham, 2011**). Drosophila displays two populations of glial cells analogous to mammalian astrocytes: the cortical glial cells and drosophila astrocytes. Cortical glial cells enwrap neuronal soma while drosophila astrocytes are component of the CNS blood-brain barrier. As their mammalian astrocyte counterparts, glial cells in Drosophila are involved in neurite outgrowth, secrete neuronal trophic factors and express neurotransmitter transporters (**Freeman and Rowitch, 2013**).

Neurons and astrocytes are derived from radial glia. Cortical neurogenesis begins at E9-10 in mouse, when radial glia cells divide to generate intermediate progenitor cells (**Figure 2**). At the end of this developmental period, gliogenesis occurs when radial glia cells lose their ventricle attachment and migrate though the developing cortex (**Kriegstein and Alvarez-Buylla, 2009**). In mammals, radial glial cells generate astrocytes and intermediate progenitor cells (**Figure 2**). The latter proliferate locally in the postnatal brain to expand astrocyte populations (**Ge et al., 2012; Tien et al., 2012**). Radial glial cells express several markers such as GFAP, GLAST, GLT-1, sex determining region Y box 2 (Sox2), hairy and enhancer of split 5 (Hes5), Prominin 1 or brain lipid binding protein (BLBP) (**Dimou and Gotz, 2014**). Interestingly, some of these markers are expressed also by mature astrocytes in the adult brain and/or are upregulated by astrocytes in pathological conditions.

Furthermore, radial glial cells are maintained during adulthood, in restricted brain areas (**Kriegstein and Alvarez-Buylla, 2009**). The subependymal zone (SEZ) located below the ependymal layer of the lateral ventricles is the most active zone of neurogenesis in the adult brain in mice. Radial glial cells in the SEZ give rise to intermediate neural progenitors and to neuroblasts that proliferate and migrate in the rostral migratory stream towards the olfactory bulb (**Dimou and Gotz, 2014**). Neuroblasts give rise to different types of neurons in the olfactory bulb. In the subgranular zone (SGZ) of the dentate gyrus, radial glial cells locally proliferate and give rise to new granule cells throughout adult life in mammals including humans (**Spalding et al., 2013**).

Thus, radial glial cells that give rise to the majority of brain cells and astrocyte-like cells found in invertebrates share common features with mature astrocytes of the mammalian brain. Astrocytes appear as highly conserved through evolution underlying their essential roles for brain functions.

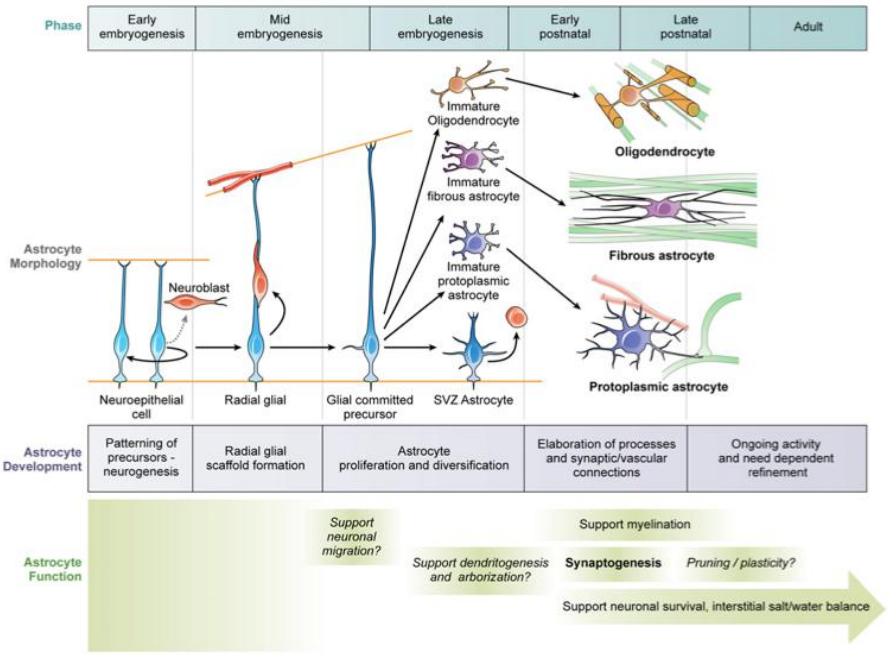

Figure 2. Neurodevelopmental changes in astrocyte morphology and functions.
Neuroepithelial cells are formed during early embryogenesis and give rise to radial glial cells. These cells perform asymmetric division to generate neural precursor cells that will give rise to neurons. Once neurogenesis is achieved, radial glial cells acquire a glial-restricted potential and differentiate in glial precursors cells of oligodendrocytes and astrocytes. Glial precursors cells are maintained in neurogenic areas of the adult brain in the subependymal zone of the lateral ventricles and in the dentate gyrus of the hippocampus. Adapted from (**Molofsky et al., 2012**)

Astrocytes are involved in a wide variety of functions in the healthy CNS ranging from development to information processing. The following part of the manuscript will highlight the main functions of astrocytes. Appreciating the crucial role of astrocytes is needed to understand how changes in any of these functions may impact CNS and neurons, especially in the context of diseases.

2) Astrocyte are involved in a variety of brain functions

a) Astrocytes regulate synapse formation, maturation and elimination

Astrocytes are in contact with thousands of synapses and are able to regulate synapse number during synaptogenesis (**Ullian et al., 2001**). A wide body of evidence shows that astrocytes are involved in neural circuit development by regulating the formation, maturation, functionality and elimination of synapses (**Pfrieger, 2009; Clarke and Barres, 2013**). Most of these molecules have been primarily identified in retinal ganglion cell (RGCs) culture model, whereby viable RGCs are able to grow and survive without glial environment (**Pfrieger and Barres, 1997**). However, when RGCs are grown in the presence of astrocytes or of astrocyte-conditioned medium, it strongly increases the formation of excitatory synapses (**Pfrieger and Barres, 1997**), in an activity dependent manner (**Ullian et al.,**

2001). Several astrocyte-secreted molecules have been shown to control synapse formation including BDNF, cholesterol, glypicans, hevin, thrombospondins (TSPs) and transforming growth factor beta 1 (TGFβ1) (**Clarke and Barres, 2013**). For example, Mauch and colleagues demonstrated that in RGCs, the formation of numerous and efficient synapses depends on the import of glia-derived cholesterol via apolipoprotein E-containing lipoproteins (**Mauch et al., 2001**). Further investigations showed that cholesterol is necessary for dendrite differentiation, which limits the formation of synapses in RGCs (**Goritz et al., 2005**). Particularly, cholesterol promotes the differentiation of presynaptic terminals during synaptogenesis, but it is also required for the functional stability of synapses over time (**Goritz et al., 2005**). Interestingly, these changes appear to be mediated by a transcriptional regulation in RGC. Indeed, glia-conditioned medium or cholesterol treatment induces change in the expression of genes involved in the development of dendrites as well as the regulation of cholesterol and fatty acid metabolism (**Goritz et al., 2007**).
Besides cholesterol, many other factors have been involved in the regulation of synapse formation. For example, Hevin and SPARC are secreted by astrocytes and have been shown to control excitatory synapse formation both *in vivo* and *in vitro* through antagonistic effects (**Kucukdereli et al., 2011**). In addition, other factors such as TSPs bind to a voltage-gated Ca^{2+} channel on neurons, which lead to the recruitment at the membrane of scaffolding and adhesion molecules at synaptic sites (**Sigrist and Plested, 2009**). However, TSP and Hevin/SPARC- induced synapses are functionally silent and other factors are involved in the conversion of silent to active synapse. For example, glypicans 4 and 6 allow synapse maturation by promoting functional clustering of AMPA receptor subunits at the post-synaptic membrane in RGCs (**Allen et al., 2012**). In addition, contact interactions are also involved in the astrocyte modulation of synapse formation. For example, in the hippocampus, neuronal Ephrin A4 receptor interacts with Ephrin A3, expressed by astrocytic processes surrounding synapses. Carmona et al. showed that Ephrin A3 is required for maintaining Ephrin A4 receptor activation and spine morphology *in vivo* (**Carmona et al., 2009**).

During development, synapses are made and eliminated to establish neuronal connectivity. In the mature CNS, the refinement of neuronal networks is a dynamic activity-dependent process involving synapse elimination (**Clarke and Barres, 2013**). Evidence from drosophila shows an important role of glial cells in the engulfment of mushrooms body neurons during metamorphosis (**Awasaki and Lee, 2011**). In addition, several studies have provided evidence for a direct role of astrocytes-secreted molecules in synapse elimination in rodents. Astrocytes induce the expression of C1q, the initiating protein of the complement cascade in RGCs (**Stevens et al., 2007**). In the developing reticulogeniculate system, upregulation of C1q at synapses is necessary for their elimination and the refinement of synaptic connections (**Stevens et al., 2007**).
In addition, a recent study showed that astrocytes are able to engulf synapses to mediate synaptic connections refinement in the reticulogeniculate system (**Chung et al., 2013**). This mechanism is dependent upon the MEGF10 and MERTK phagocytic pathways in astrocytes as well as neuronal

activity. Furthermore, in the mature CNS, astrocytes engulf both excitatory and inhibitory synapses (**Chung et al., 2013**).

Thus, astrocytes have a predominant role in synaptogenesis as well as in the refinement of synaptic connexions to establish viable neuronal networks in the adult brain.

b) Astrocytes reuptake and recycle neurotransmitters

A major role of astrocytes is to reuptake neurotransmitters. Indeed, astrocytes reuptake released glutamate from the synaptic cleft by through specific transporters, apposed to glutamatergic terminals (**Kullmann and Asztely, 1998; Danbolt, 2001**) (Figure 3). Astrocytes express high affinity glutamate transporters GLT-1 (EAAT2) and GLAST (EAAT1). GLT-1 is highly expressed in the hippocampus, the cortex and the striatum. It is responsible for the majority of glutamate uptake in the forebrain (**Rothstein et al., 1994; Tanaka et al., 1997**). By contrast, GLAST is highly expressed in the cerebellar Bergmann glia (**Rothstein et al., 1994; Regan et al., 2007**).

Together, neuronal and astrocyte transporters limit glutamate action on its pre- and post-synaptic receptors and decrease α-amino-3-hydroxy-5-methyl-4-isoxazolepropionic acid receptor (AMPAR) and N-methyl-D-aspartate receptor (NMDAR) currents (**Mennerick and Zorumski, 1994; Diamond and Jahr, 1997; Bergles and Jahr, 1998; Tsukada et al., 2005**). They also prevent glutamate from activating extrasynaptic receptors or crosstalk between excitatory synapses (**Huang and Bergles, 2004**).

Under physiological conditions, glutamatergic transmission is involved in integrated functions such as learning and memory (**Riedel et al., 2003**). However, excessive glutamate release or inadequate reuptake is toxic for neurons (**Dong et al., 2009**). This phenomenon, called excitotoxicity, is involved in neuronal cell death in many pathological conditions including ischemia (**Mitani and Tanaka, 2003**) or ND such as HD, PD and ALS (**Maragakis and Rothstein, 2006**). Indeed, GLT-1 KO mice display elevated extracellular glutamate levels, spontaneous seizures and early death (**Tanaka et al., 1997**). These mice show increased neuronal death upon short-term ischemia (5 min).

When glutamate is uptaken from the synaptic cleft, it is then metabolized in astrocytes by glutamine synthase (GS). This enzyme transaminates glutamate into glutamine, which is then transported back to neurons to replenish the glutamate pool in synaptic vesicles (**Allaman et al., 2011**) (**Figure 3**).

Thus, astrocytes, spatially and temporally buffer glutamate, through the expression of high affinity transporters, to maintain its homeostasis and prevent excitotoxicity. Astrocytes are also responsible for the recycling of glutamate into glutamine, necessary for neuronal activity.

Astrocytes also reuptake y-aminobutyric acid (GABA) as they express GABA transporters (GAT) (**Gadea and Lopez-Colome, 2001**). GAT1 is located on astrocyte processes near synapses whereas GAT3 is expressed at distal sites. GAT1 is involved in the termination of GABA signaling at the synaptic cleft and GAT3 regulates the action of GABA on pre-synaptic GABAB receptors

(**Beenhakker and Huguenard, 2010**). These transporters also allow astrocytes to release GABA (**Gallo et al., 1991**). Interestingly, alteration of GABA release is associated with various pathological conditions such as epilepsy (**Pirttimaki et al., 2013**) and ND including AD (**Jo et al., 2014; Wu et al., 2014**) and HD (**Wojtowicz et al., 2013**).

c) Astrocytes provide metabolic support to neurons

Whilst representing only 2% of the body mass, the brain oxygen and glucose consumption represent 20% of those of the whole organism. Such metabolic needs are required to restore ionic gradients altered by synaptic activity. Thus, glucose consumption is tightly coupled to synaptic activity (**Magistretti, 2006**). This phenomenon, called the neuro-metabolic coupling, is the basis of imaging techniques such as positron emission tomography (PET) allowing to detect radioactive glucose uptake in specific brain areas during behavioral tasks (**Magistretti, 2006**).

The cellular basis of the neuro-metabolic coupling has been proposed to involve astrocytes as a key player, located at the interface of blood vessels and synapses. According to their model, Pellerin and Magistretti proposed that, glutamate released at excitatory synapses, is uptaken by astrocytes through glutamate transporters along with Na^+. Accumulation of Na^+ in astrocytes activates the Na^+/K^+ ATPase pump that creates a deficit in ATP. Increased ADP and Pi concentrations activate glycolysis and increase glucose uptake through the astrocytic glucose transporter, GLUT1. Lactate, the terminal product of astrocytic glycolysis, is then transported back to neurons through the astrocyte membrane via monocarboxylate transporters (MCT) 1 and 4. Lactate is translocated into neurons through MCT2 and then metabolized into pyruvate to enter the tricyclic acid (TCA) cycle (**Pellerin and Magistretti, 1994; Magistretti et al., 1999**) (**Figure 3**).

Astrocytes are coupled through gap-junction channels (see § II. A.1.b). This peculiar organization plays an important role in the metabolic coupling in the brain. Indeed, it has been shown that glutamatergic activity increases glucose uptake from blood vessels as well as its trafficking in the astroglial network through gap junctions towards the most active synapses (**Rouach et al., 2008**).

Another source of energy for the brain is glycogen. Interestingly, glycogen granules are predominantly found in astrocytes. Upon intense neuronal activity or hypoglycemia, astrocytic glycogen is able to sustain neuronal function being transformed into lactate and transported to neurons to be used as energy substrate (**Brown and Ransom, 2007**). Glycogenolysis is stimulated by neuromodulators such as noradrenaline or vasoactive intestinal peptide (**Magistretti et al., 1999**). This regulation participates to the metabolic plasticity of glycogen involved for example in the regulation of sleep (**Petit et al., 2002**) or as more recently demonstrated, in learning (**Suzuki et al., 2011**). In their elegant study, Suzuki et al. have demonstrated the role of the astrocyte-neuron metabolic coupling in long-term memory formation. Authors showed that inhibition of glycogen metabolism in astrocytes prevents long-term memory formation in the rat hippocampus. Furthermore, disruption of astrocytic MCTs leads to

an alteration of long but not short-term memory in the inhibitory avoidance task. This amnesia was associated with impaired synaptic plasticity. Both amnesia and synaptic plasticity were rescued by L-lactate but not glucose suggesting a central role of the astrocyte-neuron transport of lactate in long-term memory formation (**Suzuki et al., 2011**).

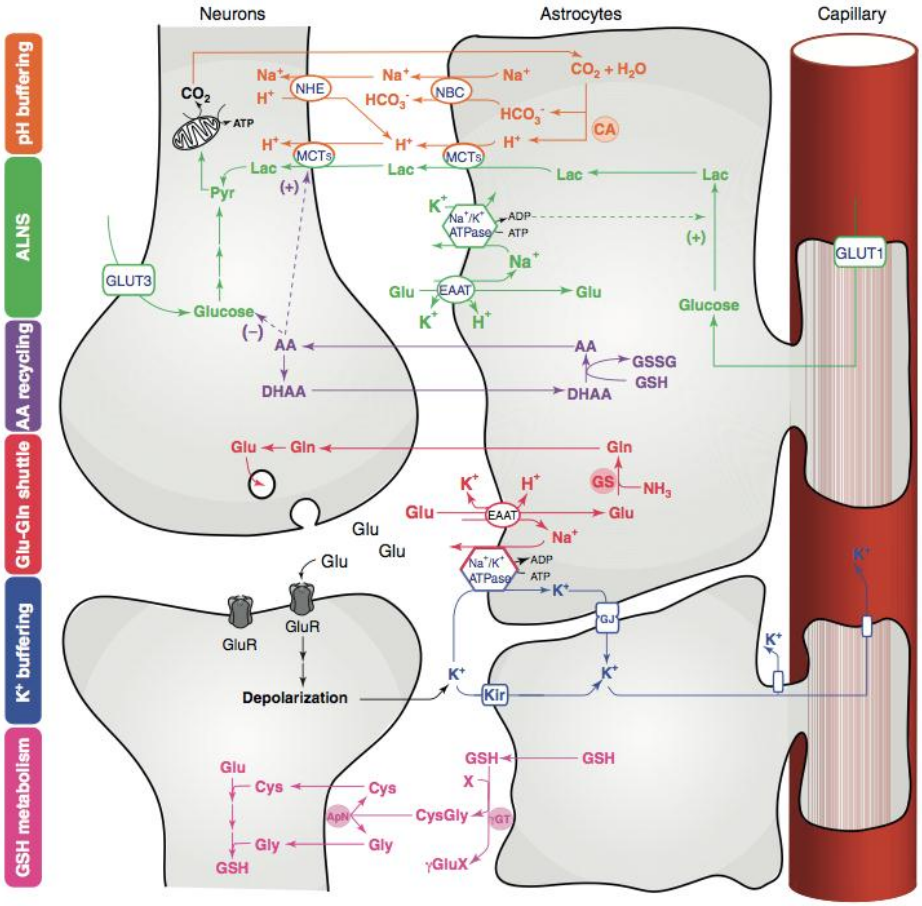

Figure 3. Astrocytes provide trophic support, metabolic substrates and antioxidant defense to neurons.
Astrocytes participate in the regulation of ionic homeostasis and pH buffering by the activity of the anhydrase carbonide that breaks up CO_2 in $HCO3^-$ and H^+ (orange pathway). Ions are released in the extracellular medium through the Na^+/HCO_3^- co-transporter (NBC). Synaptic activity results in the release of glutamate in the synaptic cleft, which is uptaken in astrocytes through glutamate transporters (EAAT) along with the import of Na^+ and H+ and the export of K^+ (red and green pathways). The electrogenic transport of Na^+ by the Na^+/K^+ ATPase increases ADP and Pi levels that stimulate glucose uptake from blood vessels (green pathway). Upon reuptake, GS converts glutamate into glutamine. It is then transported back to neurons to be transformed in glutamate and stored into synaptic vesicles. Glutamate reuptake thus couples synaptic activity with increase glucose uptake from blood vessels through the glucose transporter GLUT-1. After glycolysis, the lactate generated in astrocyte cytoplasm is transported to neurons though monocarboxylate transporters (MCT) 1 and 4 (green pathway). Lactate is transported into neurons by MCT2 and used as energy substrate to produce ATP through the TCA cycle. Astrocytes uptake excess of K^+ released during synaptic transmission through K^+ inward rectifier (Kir) channels. K^+ diffuses by gap junctions throughout the astroglial network or is released into the blood flow (blue pathway). Astrocytes provide neurons with molecules with antioxidant properties such as ascorbic acid (AA) (purple pathway) and gluthatione (GSH) (pink pathway). From (**Allaman et al., 2011**).

d) Astrocytes provide trophic support and antioxidant defense to neurons

Astrocytes secrete various factors exhibiting trophic effects on neurons. Among those factors, astrocytes release growth factors (BDNF, nerve growth factor, basic fibroblast growth factor (bFGF) etc), cytokines, neurosteroids as well as adhesion molecules involved in neurite outgrowth (**Muller et al., 1995; Hamby and Sofroniew, 2010; Sofroniew and Vinters, 2010**). Furthermore, astrocytes release other neuroactive molecules able to modulate synaptic transmission such as glutamate, D-serine, GABA or ATP (see § II.A.2.h) (**Araque et al., 2014**).

In addition to the release of trophic molecules, astrocytes play an important role in the antioxidant defense of the brain. Cellular respiration produces reactive oxygen species (ROS). The production of ROS is tightly regulated by antioxidant defense in the brain. Indeed, uncontrolled ROS production is deleterious for neurons and involved many pathological conditions. In this context, astrocytes play a central role in the antioxidant defense of the brain. They express high levels of detoxifying enzymes including glutathione peroxidase and catalase. More importantly, they release antioxidant molecules such as glutathione (GSH), superoxide dismutases 1, 2 and 3 and ascorbate (**Allaman et al., 2011**). Such molecules can then be used by neurons as ROS scavengers. Particularly, the nuclear factor erythroid 2- related factor 2 (Nrf2) pathway plays an important role in the antioxidant capacity of astrocytes. Nrf2 is a transcription factor that controls the expression of gene encoding ROS detoxifying enzymes (**Itoh et al., 1997; Venugopal and Jaiswal, 1998**). Upon oxidative stress, activation of Nrf2 results in increased GSH synthesis, which has neuroprotective effects in several models of neurodegenerative diseases including ALS (**Vargas et al., 2008**), PD (**Chen et al., 2009; Gan et al., 2012**) and HD (**Calkins et al., 2010**) (see II. B. 3 b, c and C. 4)

e) Astrocytes are components of the BBB and regulate the cerebral blood flow

The blood-brain barrier (BBB) is a physical barrier between the blood and the brain parenchyma. The BBB is composed of the endothelial cells of the blood capillary, a basal lamina, the pericytes and the perivascular endfeets of astrocytes (**Figure 4**). Endothelial cells are linked through tight junctions to control the entry of substrates into the brain parenchyma (**Abbott et al., 2006**).

Astrocytes provide the link between blood vessels and neurons. Furthermore, they release angiogenic factors (vascular endothelial growth factor, TGFβ) involved in the formation and the maintenance of the BBB phenotype (**Alvarez et al., 2013**).

The BBB phenotype is altered in many pathological conditions including ischemia, trauma, tumor epilepsy and in ND such as multiple sclerosis, AD or PD (**Abbott et al., 2006**). Disruption of astrocyte endfeet-endothelial cells interactions and the inflammatory environnement contribute to BBB alterations. In trauma, bradykinin stimulates the release of interleukin-6 (IL-6) by astrocytes, increasing BBB permeability (**Abbott et al., 2006**). In PD, the release of reactive oxygen species (ROS) by activated microglia alters endothelial cells, pericytes and increases BBB permeability (**Cabezas et al., 2014**).

Perivascular astrocytes contacting the BBB participate in the maintenance of ionic and water homeostasis. During neuronal activity, large amounts of potassium are released in the extracellular space to allow the repolarization of the post-synaptic element (**Alvarez et al., 2013**). Astrocytes express high levels of potassium channels, especially the potassium inward rectifier channel 4.1 (Kir4.1), near synapses and at vascular endfeets. Astrocytes export potassium ions from the extracellular space to the blood flow, thus providing spatial buffering for potassium (**Alvarez et al., 2013**).

Astrocytes also participate in the regulation of water homeostasis. Glucose consumption linked to neuronal activity generates water that needs to be extruded to prevent cellular swelling (**Abbott et al., 2006**). Astrocytes transport water to the cerebral blood flow (CBF) through the water channel aquaporin 4 (AQP4), enriched at vascular endfeets. Interestingly, in brain tumours, both AQP4 and Kir4.1 channels are redistributed at astrocyte endfeets, which participate in the BBB disruption. Upregulation of AQP4 is observed in many pathological conditions (ischemia, trauma, AD) and is associated with cell swelling (**Abbott et al., 2006**).

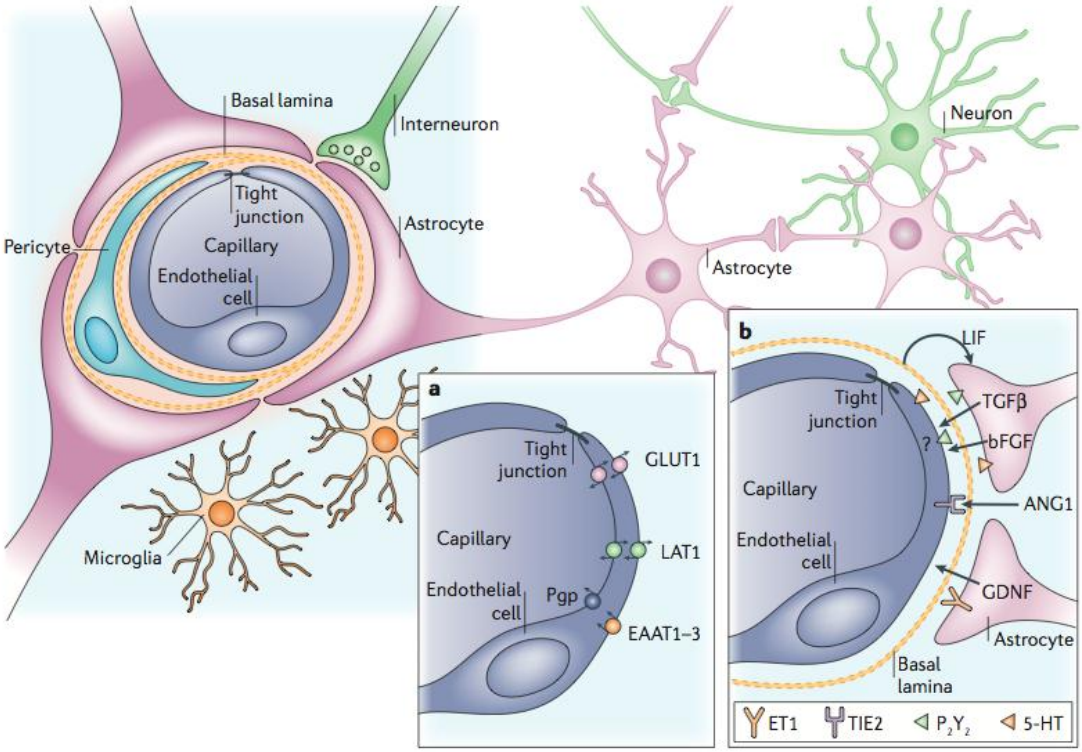

Figure 4. Astrocytes are involved in the maintenance of the BBB.
Endfeet of perivascular astrocytes form the BBB along with the pericytes, the basal lamina and the endothelial cells. Astrocytes are the link between blood vessels and neurons. Thus, astrocytes can control the flux and nature of molecules that penetrate in the neuronal compartment. Astrocytes uptake metabolic substrates from the blood flow through the expression of specific transporters such as GLUT-1. Astrocytes release factors such as TGFβ or bFGF that modulate the BBB phenotype. From (**Abbott et al., 2006**)

In the brain, during neuronal activity, an increase in oxygen and glucose consumption is followed by an increase in local CBF (**Magistretti, 2006**). This phenomenon, called the neuro-vascular coupling. Increase in oxygen consumption with neuronal activity is much less important than the local CBF. Therefore, there is a mismatch between oxygen and CBF local changes during neuronal activity. This alteration is the basis of blood-oxygenation level dependent (BOLD) fMRI, which detects changes in levels of deoxygenated hemoglobin and cerebral blood in the brain during a given bevioral task (**Magistretti, 2006**).

Several recent studies have demonstrated the implication of astrocytes, as key player in neuro-vascular coupling *in vivo*. For example, two-photon imaging of Ca^{2+} signaling with Ca^{2+} photolysis in astrocytes causes vasodilation of neighboring arterioles. In their interesting study, Schummers et al. have shown that visual stimulation elicits Ca^{2+} signals in astrocytes in the ferret primary visual cortex that are associated with hemodynamic changes (**Schummers et al., 2008**).

This dynamic coupling between excitatory neuronal activity and regulation of CBF is in part performed through the release by astrocytes of active molecules such as arachidonic acid, prostaglandins or epoxyeicosatrienoic acids (EETs). These molecules cause vasodilation or vasoconstriction depending on the local O2 concentration (**Attwell et al., 2010**).

In conclusion, astrocytes are anatomical and functional components of the BBB. They are also key players in the neuro-vascular coupling, essential for physiological brain function.

f) Astrocytes regulate ionic homeostasis

Astrocytes regulate the homeostasis of several ions including K^+, Na^+ and Cl^-, through highly controlled transport mechanisms. In addition to Kir4.1 channels, they uptake potassium through the Na^+/K^+ ATPase or $Na^+/K^+/2Cl^-$ co-transporters (**Allaman et al., 2011**) (**Figure 3**).

Sodium homeostasis in astrocytes has gain more and more interest in the past years. Sodium concentration in astrocytes in mainly controlled via the Na^+/K^+ ATPase that exchanges three intracellular sodium ions for two extracellular potassium ions and consumes ATP. Sodium influx also occurs through the $Na^+/K^+/2Cl^-$ co-transporters and is linked to pH homeostasis through the $Na^+/HCO3^-$ co-transporter and the Na^+/H^+ exchanger. In addition, glutamate transport through GLT-1 and GLAST is coupled to the import of sodium (**Rose and Karus, 2013**) (**Figure 3**).

Although increase in intracellular sodium appears less attractive than calcium, because it is not linked to the activation of intracellular cascades, it is interesting to observe that increased synaptic activity causes sodium transients in astrocytes (**Rose and Karus, 2013**). Application of glutamate elicits increase in sodium concentration that is mainly dependent upon glutamate transport in cortical astrocytes in culture (**Chatton et al., 2000**) and in slices (**Uwechue et al., 2012**).

A physiological role for transient sodium elevation in astrocytes is the activation of the Na^+/K^+ ATPase that leads to increase glucose uptake and induces glycogenolysis to sustain neuron energy needs (see § II.A.2.c) (**Rose and Karus, 2013**).

Alteration of sodium homeostasis in astrocytes is observed in several pathological conditions such as ischemia or epilepsy (**Rose and Karus, 2013**). For example, it has been recently reported that astrocyte NF-κB pathway mediates astrocyte swelling and activation of the $Na^+/K^+/2Cl^-$ co-transporters in brain edema after traumatic brain injury (**Jayakumar et al., 2014**) .

Astrocytes participate in the regulation of extracellular pH in the brain. They metabolize CO_2 into $HCO3^-$ and H^+ and export both ions in the extracellular space through the $Na^+/HCO3^-$ co-transporter (**Allaman et al., 2011**). Astrocytes also maintain pH homeostasis through the Na^+/H^+ exchanger. Interestingly, in pathological such as ischemia, pH homeostasis is altered. During ischemia, oxygen and glucose deprivation prevent aerobic metabolism (**Schurr et al., 1997**). Astrocytes produce lactate from their glycogen stores to sustain neuron energy needs. Lactate accumulates and causes glial acification (**Mutch and Hansen, 1984**). In a recent study, Beppu et al. have used elegant optogenetic tools to demonstrate that glial acidification during ischemia is detrimental for neurons and contribute to excitotoxicity (**Beppu et al., 2014**).
Thus, astrocytes participate in the maintenance of ionic homeostasis in the brain. This function is essential for neuronal activity and, in the case of Na^+, serves as a link with the astrocyte metabolic support to neurons.

g) The tripartite synapse and the regulation of synaptic transmission

Astrocyte processes ensheath synapses and form, along with the pre- and post-synaptic elements, the tripartite synapse (**Araque et al., 1999**). Although astrocytes are considered as electrically silent cells compared to neurons, they express a variety of neurotransmitter receptors (**Porter and McCarthy, 1997**). Astrocytes are able to detect neuronal activity even elicited by minimal synaptic activity (**Di Castro et al., 2011; Panatier et al., 2011**). Furthermore, astrocytes respond to neuronal activity by Ca^{2+} and Na^+ signals (**Dallerac et al., 2013; Araque et al., 2014**). Ca^{2+} signals in astrocytes have complex patterns and kinetics depending on the synaptic system or brain region. Increased Ca^{2+} concentration in astrocytes leads to the release via exocytic and non-exocytic mechanisms of so-called gliotransmitters such as glutamate, ATP, D-serine, GABA or TNF-α (**Hamilton and Attwell, 2010; Araque et al., 2014**). Gliotransmitters can act on different neuronal receptors both at the pre- and post-synaptic levels to modulate neuronal activity and synaptic plasticity. Several mechanisms of action of gliotransmitters have been described including: modulation of basal synaptic transmission, increase neuronal excitability, neuronal network synchronization, synaptic potentiation, modulation of synaptic plasticity or heterosynaptic depression (**Araque et al., 2014**). Most of these effects have been demonstrated in the hippocampus for glutamate, ATP (converted to adenosine) and D-serine (the co-agonist of NMDARs) in brain slices. Especially, D-serine is the preferential co-agonist of synaptic NMDARs, involved in LTP (**Papouin et al., 2012**). It was elegantly demonstrasted that the Ca^{2+}-dependent release of D-serine by astrocytes controls NMDAR-dependent LTP in the mouse hippocampus (**Henneberger et al., 2010**).

Besides the release of gliotransmitters, astrocytes can modulate synaptic transmission through morphological changes that impact the tripartite synapse function. Indeed, astrocyte processes coverage changes with neuronal activity and in pathological conditions. For example, a recent study has reported that induction of LTP in the hippocampus leads to increased synaptic coverage by astrocyte processes through Ca^{2+}-dependent mechanisms (**Bernardinelli et al., 2014**). In addition, whisker stimulation increases astrocyte synaptic coverage of excitatory dendritic spines in the barrel cortex as observed *in vivo* or *ex vivo* (**Genoud et al., 2006**). In contrast, reduced synaptic coverage is observed during lactation in the supraoptic nucleus of the thalamus in the rat (**Oliet et al., 2001**). These mechanisms regulate the distribution of astrocyte glutamate transporters at the synapse leading to an increase in glutamate concentration in the synaptic cleft that modulates the synaptic transmission.

In these studies, modulation of the synaptic coverage by astrocyte processes was induced by neuronal activity. Interestingly, specific alteration of astrocyte feature can also influence the morphology of the tripartite synapse. In a recent study, Pannasch et al. elegantly demonstrated that Cx30 regulates synaptic transmission by controlling the extension of astrocytic processes into the synaptic cleft. In Cx30 KO mice, glutamatergic transmission is decreased in parallel with increased glutamate transport in astrocytes. The mechanism underlying this observation is very surprising. In Cx30 KO mice, astrocyte processes form protrusions into the synaptic cleft that increase glutamate uptake through GLT-1. This function of Cx30 is independent of its channel function and is mediated through protein-protein interactions by its intracellular C-terminal domain (**Pannasch et al., 2014**).

Several recent studies strongly suggest that astrocyte actively modulate complex behaviors. For example, using two-photon microscopy and Ca^{2+} imaging in behaving mice, Nimmerjahn et al. reported Ca^{2+} excitation in Bergmann glia cells during locomotor activity as well as differential Ca^{2+} signals in awake, still animal (**Nimmerjahn et al., 2009**). Additionnally, Halassa et al. demonstrated that modulation of neuronal activity during sleep was dependent on the purinergic gliotransmission, with a transgenic approach to prevent exocytotic release of molecules from astrocytes (**Halassa et al., 2009**). Another interesting example is the astrocyte regulation of neuronal activity in the respiration center in the brainstem. This mechanism is a physiological reflex that adapts respiration to maintain blood pH and CO_2 concentrations to non-toxic levels. Gourine et al. showed that in this particular brain region, astrocytes detect pH changes and react by elevating their intracellular Ca^{2+} concentration. In turn, they release ATP, which modulates neuronal activity and control breathing (**Gourine et al., 2010**).

An elegant study from D. Bergles's lab showed that norepinephrine, released during arousal states, is able to diffuse throughout the brain and modulates astrocyte Ca^{2+} signals elicited during behavioral tasks (locomotion, visual stimulation) (**Paukert et al., 2014**).

Astrocyte network is also involved in the astrocyte modulation of integrated functions. Indeed, deletion of Cx30 and Cx43 in astrocytes of transgenic mice leads to cognitive impairment, abnormal motor behavioral as well as altered synaptic transmission and plasticity (**Pannasch and Rouach, 2013**).

Astrocytes receive an incredible number of signals through complex interactions with various cell types including neurons, endothelial cells and other glial cells. In addition, they form a network and can integrate spatially distant signals. Evidence from outstanding studies demonstrates the active participation of astrocytes to modulate synaptic transmission, plasticity and even neuronal networks underlying complex behaviors.

3) Astrocytes heterogeneity

As neurons, astrocytes from different brain regions are characterized by distinct morphological and functional features. Astrocyte heterogeneity has been observed in rodents and in humans, based morphological criteria (**Emsley and Macklis, 2006; Sosunov et al., 2014**).

Emsley and Macklis have defined a classification of CNS astrocytes based on the expression of astrocytic proteins GFAP and S100β in GFAP-GFP reporter mice. Nine classes of astrocytes were classified: cerebellar Bergmann glia, ependymal glia, white matter fibrous astrocytes, grey matter protoplasmic astrocytes, tanycytes, velate glia, radial glia, marginal glia and perivascular glia (**Emsley and Macklis, 2006**). Furthermore, human and high-order primate-specific astrocytes have been identified in the cortex: the varicose and intralaminar astrocytes (**Oberheim et al., 2009**). Human astrocytes appear undoubtedly more complex than their rodent counterparts. For instance, human cortical protoplasmic astrocytes are 2.6 fold larger and display 10 fold more $GFAP^+$ processes than rodent astrocytes (**Oberheim et al., 2009**).

Besides the well-established morphological differences between astrocytes in different brain regions, they also differ by their molecular profile (**Doyle et al., 2008**), expression of ion channels, transporters or receptors (**Matyash and Kettenmann, 2010; Oberheim et al., 2012**). For example, one of the major roles of astrocytes is to reuptake glutamate from the synaptic cleft through high-affinity transporters. Using promoter-driven expression of fluorescent proteins, Regan et al. showed that, in the adult brain, while GLT-1 is the major glutamate transporter expressed in the forebrain, GLAST is primarly expressed in the cerebellar Bergmann glial cells and in white matter fibrous astrocytes. This differential expression is established during development and may have an important functional influence on astrocytes capacity to uptake glutamate (**Regan et al., 2007**)

Evidence supports a functional role for astrocyte heterogeneity between brain regions and within the same area. For instance, spontaneous Ca^{2+} oscillations observed in the cortex of anesthetized rats display layer-specific pattern between layer 1 and layer 2/3 (**Takata and Hirase, 2008**). Similarly, Ca^{2+}-signals elicited by locomotor activity in Bergmann glia cells display significantly different dynamics than cortical protoplasmic astrocytes (**Nimmerjahn et al., 2009**).

The network organization of astrocytes also shows region-specific patterns. In particular, astrocyte coupling in the somatosensory cortex is greater within a barrel than in the region delimiting two barrels (the septa). This organization suggests that the astrocytic network is adapted to the peculiar anatomy of sensory neurons in the barrels (**Houades et al., 2008**).

Recent studies point towards a developmental origin of astrocyte morphological and functional heterogeneity. Indeed, astrocytes are allocated to restricted spatial domains during development, which may underlie functional specificity in the adult CNS (**Tsai et al., 2012**). For example, in an elegant study, Molofsky et al. showed that a subset of spinal astrocytes express position-specific proteins. This regional patterning of astrocytes is involved in the establishment of specific neuronal networks during postnatal development (**Molofsky et al., 2014**).
These results suggest that all astrocytes in the CNS are not the same and that this heterogeneity can influence their functions as well as their interactions with neurons in specific brain regions.
This large body of evidence illustrates that astrocytes are involved in virtually all brain functions. Thus, any alteration of the above-mentioned astrocytic functions is susceptible to have a dramatic effect on neurons as well as general brain homeostasis.

B. Astrocytes become reactive in response to pathological conditions

In addition to their pleiotropic roles in the physiological CNS, astrocytes are able to react to pathological conditions in a phenomenon referred to as astrocyte reactivity. Reactive astrocytes are mainly identified by universal morphological changes whereas their functional alterations are still poorly understood. Reactive astrocytes are observed in acute pathological conditions such as mechanical lesions of the brain and spinal cord, brain trauma, ischemia, infection or epilepsy. Astrocyte reactivity is also a feature of chronic conditions such as aging or ND (**Pekny and Nilsson, 2005; Escartin and Bonvento, 2008; Sofroniew and Vinters, 2010**).

Reactive astrocytes are classically identified by hypertrophy of their primary processes and upregulation of intermediate filament proteins such as GFAP, vimentin and nestin. These morphological changes can be associated with alteration of the non-overlapping organization of astrocyte domains in specific disease models. Indeed, Oberheim et al. found that reactive cortical astrocytes displayed an increased number of overlapping processes between distinct astrocyte territories, in various mouse models of epilepsy (**Oberheim et al., 2008**). Interestingly, this phenomenon was not observed in acute traumatic injuries such as entorhinal cortex lesion and electrically induced injury of the cerebral cortex (**Wilhelmsson et al., 2006**) or in a mouse model of AD (**Oberheim et al., 2008**). Thus, while overexpression of intermediate filament proteins appears as a conserved feature in reactive astrocytes, they can display various morphological alterations, according to the type of injury or disease.

Terminology

In this manuscript, I will not use the term “reactive astrogliosis” because it implies the notion of astrocyte proliferation. In fact, in most injury or disease models, astrocytes do not proliferate (see next paragraph) and thus, reactive astrogliosis is a confounding term. I will use “astrocyte reactivity” or “reactive astrocytes” to refer to astrocytes that respond to a pathological condition in the CNS. Regarding the literature, I will consider that astrocytes are reactive as compared to dysfunctional, based on their hypertrophic morphology and upregulation of intermediate filaments (GFAP, vimentin). Alternatively, I will use “activated astrocytes” to designate astrocytes that have been experimentally activated (by cytokines or genetic manipulation). This terminology is different from “activated astrocytes” mentioned in the literature referring to astrocytes activated by neurotransmitters and that display Ca^{2+} signals. “Glial scar” will refer to specific scar-forming astrocytes that organize around the lesion core in the case of acute CNS injury or at the site of the needle track after intracerebral injections. I will use the term “neuroinflammation” to define the reactivity of astrocytes, microglia and peripheral immune cells in pathological conditions.

Upon acute injuries such as traumatic injury, stroke, infection or autoimmune inflammation, the lesioned tissue is invaded with fibrotic and immune cells, such as macrophages, as a result of a local BBB disruption. Astrocytes form a glial scar that demarcates the lesioned tissue from the healthy parenchyma. Glial scar formation has been observed for more than a century and widely described and studied since then (**Yiu and He, 2006**). Indeed, glial scar is considered as the major impediment to axon regrowth especially in the field of spinal cord injury (SCI) and thus many therapeutic strategies have aimed to interfere or inhibit glial scar formation (**Sofroniew, 2009; Brosius Lutz and Barres, 2014**). However, this simplistic view is evolving as new approaches have provided insights into the molecular mechanisms and regulations of glial scar formation. Especially, the work of Sofroniew and colleagues has made an important contribution to demonstrate that scar-forming astrocytes can exert both beneficial and detrimental effects on neurons in the context of many acute injury models (see § II.D.3).

The classical definition of astrocyte reactivity includes the notion of proliferation. However, recent evidence suggests that only a subset of specific scar-forming astrocytes actually undergo proliferation (**Bardehle et al., 2013; Wanner et al., 2013**). The notion that the number of astrocytes was increased after injury is based on the misleading interpretation of an increased number of $GFAP^+$ cells after CNS injury (**Dimou and Gotz, 2014**). Most astrocytes in the CNS expressed GFAP at undetectable levels under physiological conditions. Upon injury or disease, astrocytes become reactive and upregulate GFAP, therefore increasing the number of $GFAP^+$ cells. The elegant work of M. Götz's laboratory used live imaging monitoring of fluorescently labeled astrocytes to study their reaction following cortical stab wound injury (**Bardehle et al., 2013**). Surprisingly, they found that most of cortical astrocytes do no react to the cortical lesion (80%). By contrast, 10% of cells polarize their processes towards the injury site and only 16% undergo active proliferation. These proliferating astrocytes correspond to a subset of astrocytes with their soma in direct contact with endothelial cells of blood vessels (**Bardehle et al., 2013**). These results suggest that these proliferating astrocytes may receive signals from the blood flow that specifically elicit their proliferation perhaps to repair the breached BBB. In accordance, studies have shown that there are proliferative astrocytes in the lesioned area after SCI and that ablation of those cells disrupts the formation of the glial scar. Recently, Wanner et al. described a subset of elongated proliferative astrocytes at the borders of the glial scar after SCI. These elongated astrocytes efficiently secluded infiltrating immune cells both *in vitro* and *in vivo* (**Wanner et al., 2013**). By contrast to acute injury involving glial scar formation, astrocyte proliferation is very limited in ND models. Indeed, the number of astrocytes represented less than 5% of the total proliferating cells in a mouse model of AD (**Sirko et al., 2013**) and than 20% in a model of ALS (**Lepore et al., 2008**).

Reactive astrocytes are, in some aspects, reminiscent of radial glial cells. For example, they re-expressed proteins that are downregulated in mature astrocytes. Furthermore, as mentioned above, specific subsets of reactive astrocytes undergo proliferation under pathological conditions (**Dimou and**

Gotz, 2014). The neural stem cell (NSC) potential of reactive astrocytes refers to the property of some reactive astrocytes to be differentiated in neurons and other glial cells when they are grown *in vitro* (**Dimou and Gotz, 2014**). This property of reactive astrocytes is particularly appealing for thepeutic strategies involving cell replacement, particularly in ND. However, many evidence suggests that most astrocytes in the CNS remain committed to their lineage both in physiological and pathological conditions (**Barnabe-Heider et al., 2010**). Nevertheless, upon injury, specific subsets of reactive glial cells isolated from the lesioned tissue, display NSC properties *in vitro*. Genetic fate mapping identified a subset of cortical astrocytes that are able to generate multipotent cells *in vitro* (**Buffo et al., 2008; Sirko et al., 2013**). Importantly, reactive cortical astrocytes acquire NSC potential only after acute injuries such as mechanical trauma or ischemia but not in the case of chronic pathological condition such as AD (**Sirko et al., 2013**). In the spinal cord, ependymal cells lining the central canal behave as NSC upon SCI as they can give rise to both astrocytes and oligodendrocytes (**Barnabe-Heider et al., 2010**). These cells generate the majority of newborn scar-forming astrocytes. Furthermore, a recent study showed that the progeny of these NSCs is critical for scar formation and strongly promotes neuronal survival by releasing neurotrophic factors (**Sabelstrom et al., 2013**).

Astrocyte reactivity appears as a complex process that involves profound changes in astrocyte properties and most likely, functions. Efforts to understand the functional changes associated with reactive astrocytes are needed to determine how reactive astrocytes impact surrounding neurons (**Sofroniew, 2009; Burda and Sofroniew, 2014**). In this context, it is crucial to characterize the inducers and signaling cascades that mediate astrocyte reactivity.

1) Molecular triggers of astrocyte reactivity

In pathological conditions, various molecules are released by different sources including microglia, endothelial cells, leukocytes or degenerating neurons (**Figure 5**). They act on various astrocyte receptors to trigger and modulate astrocyte reactivity. These factors include nucleotides (ATP, DNA), glutamate, nitric oxide, chaperones, extracellular matrix proteins (fibrin, thrombin), serum proteins (albumin), pro- and anti-inflammatory cytokines (IL-1β, TNFα, IL-6, TGFβ, CNTF, INF-γ, IL-10), morphogens (BMP), endothelins, FGFs (**Burda and Sofroniew, 2014**) (**Figure 5**).

For instance, IL-1β, TNFα, IL-6, TGFβ activate signaling pathways that regulate the expression of pro- or anti-inflammatory genes such as inducible nitric oxide synthase (iNOS) or cyclooxygenase-2. Furthermore, they can induce the expression immediate early genes such as *c-fos* and heat shock protein genes both in culture (**Eddleston and Mucke, 1993**) and *in vivo* (**Dragunow and Hughes, 1993**).

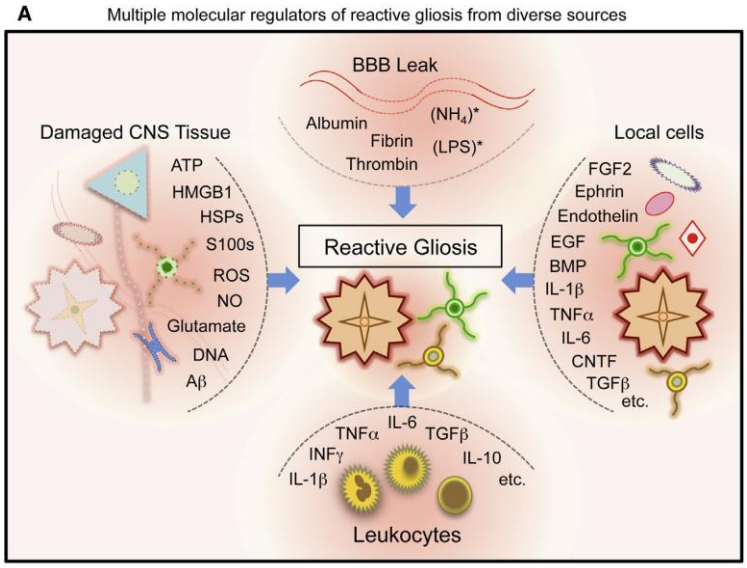

Figure 5. Various molecules released in pathological conditions trigger astrocyte reactivity. Astrocyte reactivity can be elicited by the release of molecules from microglial cells, infiltrating immune cells (leukocytes), other glial cells (oligodendrocytes, NG2 cells), endothelial cells or directly by the damaged tissue. Microglial cells and leukocytes mainly release cytokines and chemokines. Damaged neurons and other cells release potentially toxic molecules such as glutamate, aggregated proteins, purines or ROS. In pathological conditions where there is an alteration of the BBB, serum proteins also enter the CNS, which serves as an additional trigger for astrocyte reactivity. From (**Burda and Sofroniew, 2014**)

However, while the variety of molecules released upon inflammatory reaction following injury is well documented, the intracellular signaling cascades that they trigger and the consequences of their activation on astrocyte functions are less characterized (**Kang and Hebert, 2011**). The identification of these intracellular signaling pathways mostly relies on the histological or biochemical detection of activated (phosphorylated) key factors in reactive astrocytes in pathological conditions.

2) Multiple intracellular signaling pathways are associated with astrocyte reactivity in the CNS

a) The NF-κB pathway

i) Description of the pathway

The nuclear factor of kappa light polypeptide gene enhancer in B-cells (NF-κB) signaling pathway is a ubiquitous cascade, activated by the binding of cytokines such as IL-1, TNFα, LPS or growth factors to their specific cell-surface receptor. These ligands activate the canonical NF-κB pathway. This results in the activation of the IKK complex that phosphorylates IκB, the master inhibitor of NF-κB signaling. Once phosphorylated, IκB is degraded by the proteasome and the p65 and p50 subunits of the NF-κB complex, relocates to the nucleus. The NF-κB complex then binds specific promoter sequences to regulate target gene expression (**Perkins, 2007; Dong et al., 2009**) (**Figure 6**). For example, the NF-

κB pathway regulates the transcription of pro-inflammatory molecules such as cytokines or the iNOS (**Hoffmann and Baltimore, 2006**).

Other pathways can lead to the translocation of NF-κB complex in the nucleus including the non-canonical pathway, activated by lipopolysaccharide (LPS) or atypical pathways either IKK dependent (genotoxic stress) or IKK independent (hypoxia, oxidative stress) (**Figure 6**).

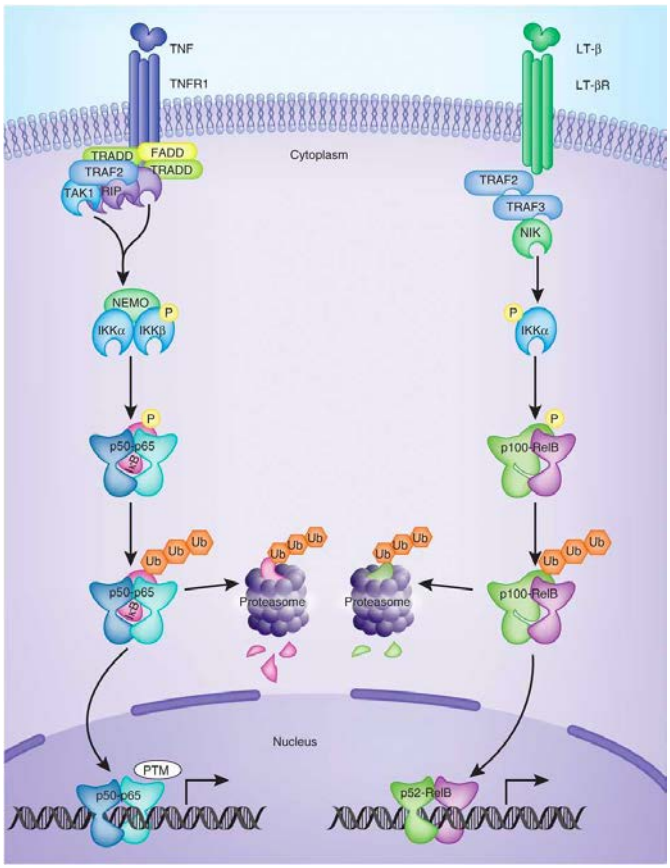

Figure 6. Canonical and non-canonical pathways of NF-κB activation.
Under resting conditions, NF-κB dimers are bound to inhibitory IκB proteins, which sequester inactive NF-κB complexes in the cytoplasm. Stimulus-induced degradation of IκB proteins is initiated through phosphorylation by the IκB kinase (IKK) complex, which consists of two catalytically active kinases, IKKα and IKKβ, and the regulatory subunit IKKγ (NEMO). Phosphorylated IκB proteins are targeted for ubiquitination and proteasomal degradation, which thus releases the bound NF-κB dimers so they can translocate to the nucleus. NF-κB signaling is often divided into two types of pathways. The canonical pathway (left) is induced by most physiological NF-κB stimuli and is represented here by TNFR1 signaling. Stimulation of TNFR1 leads to the binding of TRADD, which provides an assembly platform for the recruitment of FADD and TRAF2. TRAF2 associates with RIP1 for IKK activation. In the canonical pathway (right), IκBαis phosphorylated in an IKKβ- and NEMO-dependent manner, which results in the nuclear translocation of mostly p65-containing heterodimers. Transcriptional activity of nuclear NF-κB is further regulated by PTM. In contrast, the noncanonical pathway, induced by certain TNF family cytokines, such as CD40L, BAFF and lymphotoxin-β (LT-β), involves IKKα-mediated phosphorylation of p100 associated with RelB, which leads to partial processing of p100 and the generation of transcriptionally active p52-RelB complexes. IKKα activation and phosphorylation of p100 depends on NIK, which is subject to complex regulation by TRAF3, TRAF2 and additional ubiquitin ligases. LT-βR, receptor for lymphotoxin-β. From (**Oeckinghaus et al., 2011**).

ii) The NF-κB pathway and astrocyte reactivity

The NF-κB pathway is involved in many cellular processes including immune response, inflammation, cell division and apoptosis. It is well described that inflammatory molecules (LPS, IL-1, TNFα) known to activate the NF-κB pathway result in the activation of microglia and astrocytes (**Kaltschmidt et al., 2005**). Evidence from *in vitro* studies showed that the NF-κB pathway regulates the expression of key astrocyte proteins. For instance, cultured astrocytes stimulated with neuroprotective molecules such as epidermal growth factor or TGF-β result in an NF-κB -mediated increase in GLT-1 expression while pro-inflammatory factors like TNFα reduces GLT-1 levels through the NF-κB pathway (**Su et al., 2003**).

Activation of the NF-κB pathway is considered to be involved with astrocyte reactivity in pathological conditions (**Brambilla et al., 2009; Dvoriantchikova et al., 2009; Bracchi-Ricard et al., 2013**). In fact, data from the literature showed that this ubiquitous cascade could be activated in many cell types such as neurons, microglia, astrocytes or macrophages. For example, after stroke, activation of NF-κB was observed in neurons (**Schneider et al., 1999**). Following SCI, activation of NF-κB was observed in macrophages/ microglia, endothelial cells and neurons (**Bethea et al., 1998**). Activation of the NF-κB pathway has also been observed in neurons, astrocytes and microglia in patients and in rodent models of ND including AD, PD, ALS, HD and multiple sclerosis (MS) (**Mattson and Camandola, 2001; Khoshnan and Patterson, 2011; Medeiros and LaFerla, 2013**). Thus, these data do not evidence a predominant activation of the NF-κB pathway in reactive astrocytes. Only few studies have used cell-type specific approaches to determine the contribution of NF-κB activation to glial cell activation. In a recent study, Crosio et al. showed that inhibition of the NF-κB pathway in astrocytes of SOD1G93A mice, model of ALS, only transiently attenuates their reactivity at the onset of the disease (**Crosio et al., 2011**).

While the NF-κB pathway is classically considered to be involved in glial cell activation, at least in the case of astrocytes, clear evidence of its activation in chronic disease models is still lacking.

b) The MAPK pathways

ii) Description of the MAPK pathways

Binding of growth factors, cytokines or extracellular matrix proteins to their specific cell-surface receptors activates different mitogen-activated protein kinase (MAPK) pathways (**Jeffrey et al., 2007**). Growth factors such as FGF, platelet derived growth factor and epidermal growth factor transduce the signal through activation of small GTP-ase proteins (Ras) that in turn activate the core cascade of a MAPKKK (Raf), MAPKK (MEK1/2) and MAPK (Erk) (**Figure 7**). Extracellular matrix proteins such as integrins activate the c-jun N-terminal kinase (JNK) cascade though activation of Rac1 and MEK1/4 that in turn activate JNK1/2/3. Last, IL-1β signals through TFAF6-TAB1/2 to activate MEK6 and p38 MAPK (**Jeffrey et al., 2007**).

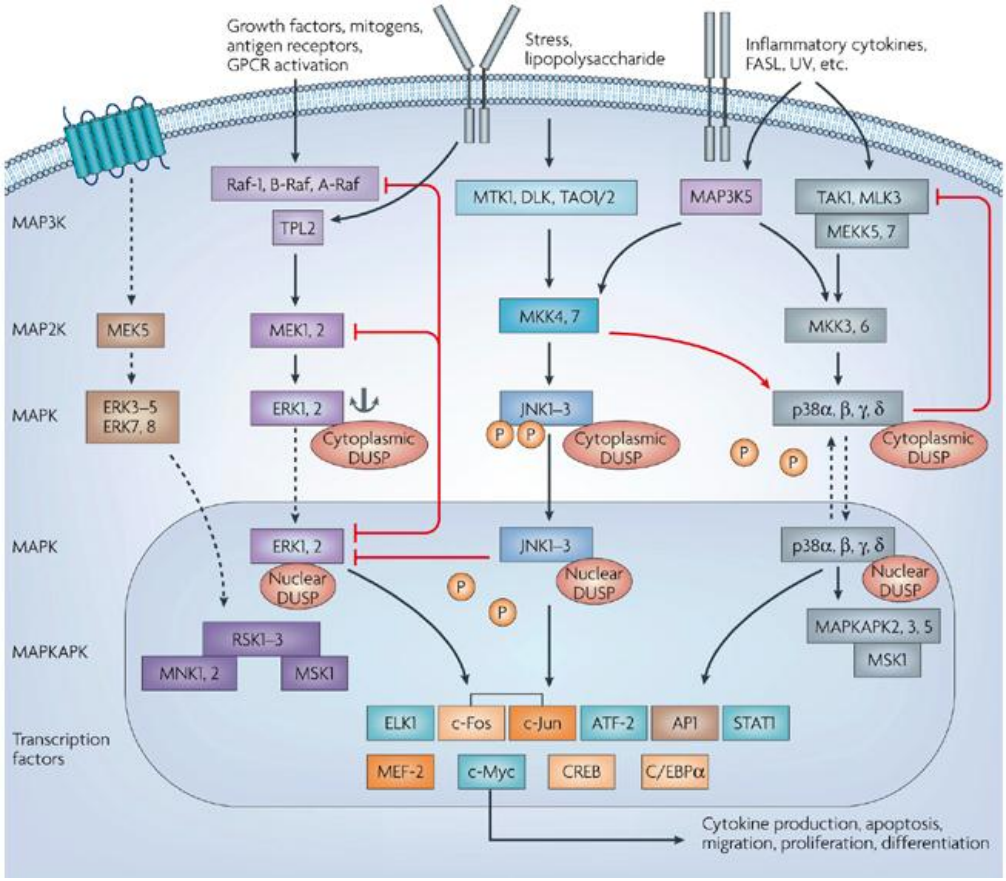

Figure 7. The MAPK pathways.
The three main arms of the mitogen-activated protein kinase (MAPK) pathway, ERK (extracellular signal-regulated kinase), JNK (c-Jun N-terminal kinase) and p38, that mediate immune cell functional responses to stimuli through multiple receptors such as chemoattractant receptors, Toll-like receptors and cytokine receptors are shown. The MAPK pathways cascades leads to activated MAPKs entering the nucleus to trigger immediate early gene and transcription factor activation for cellular responses such as cytokine production, apoptosis and migration. The main classes of mammalian MAPKs consist of ERK1 and ERK2, and the more recently identified larger kinases ERK3 (α and β), ERK4 (ERK1b), ERK5, ERK7 and ERK8; p38 MAPKs (p38α, β, γ, δ); and JNKs, also known as stress-activated protein kinases (SAPK1, 2, 3). A general feature of MAPK pathways is the three-tiered kinase canonical cascade consisting of a MAPK, a MAPK kinase (MAP2K, MAPKK, MKK or MEK) and a MAPK kinase kinase (MAP3K or MAPKK). For receptor tyrosine kinases (RTKs) and G-protein coupled receptors (GPCRs), MAPK cascade activation is initiated by small GTP-binding proteins, STE20-like kinases or by adaptor proteins that transmit the signal to MAP3Ks. MAP3Ks then transfer the signal to MAP2Ks to induce MAPK activation. From (**Jeffrey et al., 2007**).

ii) The MAPK pathways and astrocyte reactivity

In cultured astrocytes, phospho-ERK is induced after scratch injury (**Mandell et al., 2001**). In mice, after TBI, phospho-ERK is increased in cortical astrocytes up to 30 days post-lesion (**Carbonell and Mandell, 2003**). Phospho-JNK is detected in reactive astrocytes in the hippocampus in the kindling model of temporal lobe epilepsy in the rat (**Cole-Edwards et al., 2006**). Furthermore, in human brains with infarct, trauma or epilepsy, phospho-ERK is detected in reactive astrocytes (**Mandell and VandenBerg, 1999**). By contrast, p38 MAPK activation was not observed in Alzheimer's disease (AD)

models (**Koistinaho et al., 2002**). Thus, there is evidence that this ubiquitous pathway might be activated in reactive astrocytes. Although a causal link between MAPK pathway activation and induction of astrocyte reactivity has not been investigated.

c) The JAK/STAT pathway

i) Description of the JAK/STAT pathway

The JAK/STAT pathway is a ubiquitous cascade that predominantly mediates cytokine signaling in cells. It regulates the expression of genes involved in a variety of functions including cell growth, proliferation, differentiation and inflammation. Cytokines of the IL-6 family composed of IL-6, IL-11, leukemia inhibitory factor (LIF), oncostatin M (OsM), cardiotrophin-1 (CT-1), ciliary neurotrophic factor (CNTF) and cardiotrophin-like cytokine (CLC) signal through specific cell-surface receptors sharing the gp130 subunit. Upon binding, cytokines trigger the assembly of multimeric receptors, formed by specific subunits (**Ernst and Jenkins, 2004**) (**Figure 8**).

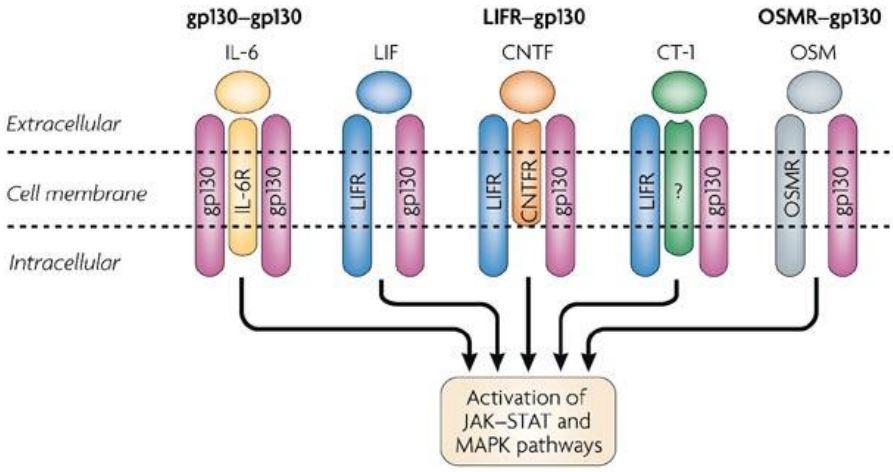

Figure 8. Combinations of receptor subunits and intracellular pathways involved in cytokine signaling.
GP130 homodimers associate with specific interleukin (IL) receptors such as the IL-6 receptor (IL-6R) to mediate the actions of IL-6. Leukaemia inhibitory factor (LIF) binds to heterodimers of LIF receptor (LIFR) and gp130. LIFR–gp130 heterodimers can also associate with other receptor subunits to bind ciliary neurotrophic factor (CNTF) and cardiotrophin 1 (CT-1). The oncostatin M receptor (OSMR) forms heterodimers with gp130 to bind oncostatin M (OSM). The signal-transducing subunit gp130 is found in all complexes, and is responsible for the intracellular activation of the Janus-activated kinase–signal transducer and activator of transcription (JAK–STAT) and the mitogen-activated protein kinase (MAPK) pathways. From (**Bauer et al., 2007**).

JAKs

Janus kinases (JAKs) are serine-threonine protein kinases, associated with the intracellular domain of cytokine receptors. JAKs are involved in the signal transduction process triggered by cytokine binding to their specific receptors (**Shuai and Liu, 2003**). Cytokine binding elicits conformational changes allowing the transphosphorylation of JAKs on tyrosine residues (**Brooks et al., 2014**). Activated JAKs phosphorylate the cytokine receptor, which unmask its binding site for the Src-homology domain 2

(SH2) of signal transducer and activator of transcription (STATs) proteins. When STATs are recruited at the cytokine receptor, JAKs phosphorylate STATs (**Leonard, 2001**) (**Figure 9A**).

In mammals, the JAK family includes JAK1, JAK2, JAK3 and TYK2. JAKs contain eight domains: a tyrosine-kinase domain JAK homology 1 (JH1), a pseudo-kinase domain (JH2), a SH2-like domain (JH3) and a domain containing protein 4.1, ezrin, radixin and moesin (FERM) (**Figure 9B**) (**Shuai and Liu, 2003**). The FERM domain is necessary for binding to the cytokine receptor, the SH2-like domain binds phosphotyrosine residues in proteins and the pseudo-kinase domain negatively regulates the kinase domaine activity (**Shuai and Liu, 2003**).

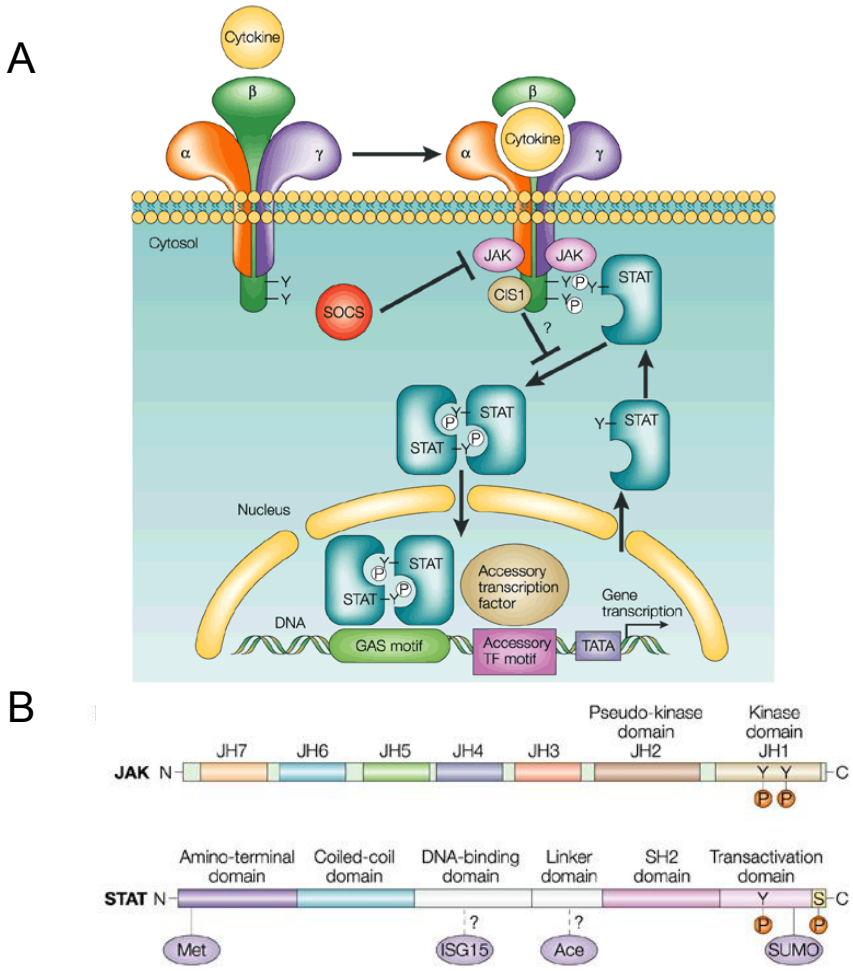

Figure 9. The JAK/STAT pathway.
A, Schematic representation of the JAK/ STAT pathway. Activation of JAKs after cytokine stimulation results in the phosphorylation of STATs, which dimerize and translocate to the nucleus to activate gene transcription by binding to specific promoting sequences on target genes. **B**, Domain structures of JAKs and STATs.JAK- The JH1–JH7 domains are based on sequence similarity of four known JAKs. JH1 is the kinase domain, which contains two tyrosines that can be phosphorylated after ligand stimulation. JH2 is the pseudo-kinase domain. The JH6 and JH7 domains mediate the binding of JAKs to receptors. STAT- The activity of STATs can be regulated by protein modification, including tyrosine and serine phosphorylation, methylation (Met), sumoylation (SUMO), ISGylation (ISG15) and acetylation (Ace). The modification sites of ISGylation and acetylation have not been identified. Adapted from (**Leonard, 2001; Shuai and Liu, 2003**).

STATs

Upon cytokine binding, STATs are recruited to the activated receptor through reciprocal interactions of their SH2 domains with those of gp130. This interaction allows JAKs to phosphorylate STATs. Phosphorylated STATs dimerize and translocate to the nucleus where they regulate the transcription of target genes (**Levy and Darnell, 2002**) (**Figure 9A**).

There are seven STATs: STAT1, STAT2, STAT3, STAT4, STAT5A, STAT5B, STAT6. STATs can form homodimers or/ and heterodimers. They contain a C-terminal transactivation domain, a SH2 domain, a DNA-binding domain, a coiled-coil domain and the amino-terminal domain (**Figure 9B**). Phosphorylation on Tyr705, located between the SH2 and the transactivation domain, is necessary for STATs dimerization and nuclear translocation. Phosphorylation of Serine 727, located at the C-terminus of STATs increases STATs transcriptional induction.

Once activated, STATs dimers translocate to the nucleus. This transport is dependent on the activity of specific transporters. Recently, it has been shown that the nuclear import of STAT3 is mediated through its interaction with importin- α3 (**Riedel et al., 2003**) and depends on Ran-GTPase and importin β 1 activities (**Cimica et al., 2011**). Once in the nucleus, STATs regulate the transcription of genes carrying consensus STAT-binding elements (TTCnnnGAA) on their promoter.

As previously mentioned, dysregulation of the JAK/STAT pathway can lead to uncontrolled cell proliferation and cancer (see §II.B.2.c.ii). Therefore, STATs signaling is tightly regulated through three mechanisms: the internalization of cytokine receptors, the activity of intracellular protein phosphatases and of specific inhibitory proteins such as protein inhibitor of STATs and suppressor of cytokine signaling (SOCS) (**Kiu and Nicholson, 2012**). Cytokine receptors can be internalized by endocytic vesicles and then degraded by the ubiquitin-proteasome or lysosomal pathways. For example, both proteasome and lysosome are required for the degradation of erythropoietin receptor/ligand complex in order to rapidly decrease cell sensitivity to erythropoietin. The degradation signal and receptor ubiquitinylation is dependent upon JAK2 activation (**Walrafen et al., 2005**). But the most potent negative regulator of the JAK/STAT signaling is the SOCS family of proteins.

SOCS

SOCS proteins are inducible inhibitors of cytokine signaling. Remarkably enough, three independent groups concurrently discovered SOCS proteins named as SOCS1, jak-binding protein 1 (JAB1) and STAT-induced STAT inhibitor 1 (SSI1, respectively (**Endo et al., 1997; Naka et al., 1997; Starr et al., 1997**). The SOCS family of proteins also includes the cytokine-inducible SH2 domain-containing protein 1 (CIS1), which blocks IL-2, IL-3 and Epo5 signaling through inhibition of STAT5 (**Yoshimura et al., 1995; Ram and Waxman, 1999**). Expression of SOCS proteins is rapidly induced by cytokines and thus acts as a negative feedback loop to regulate the JAK/STAT pathway activation (**Yoshimura et al., 2007**).

There are eight SOCS proteins in mammals: SOCS1-7 and CIS. They all contain a C-terminal SOCS box, the SH2 domain and a variable N-terminal region.

SOCS proteins regulate the JAK/STAT signaling in different ways. First, SOCS proteins contain a SOCS box, which is an adapter for substrate polyubiquitinilation and targeting to the proteasome (**Kile et al., 2002**) (**Figure 10A**). Indeed, the SOCS box interacts with elongin B anc C, which then bind to the Cullin 5 and to an E3 ubiquitin ligase (**Zhang et al., 2001; Babon et al., 2009**). Therefore, all proteins interacting with the central SH2 domain of SOCS proteins (phospho-JAKs, phospho-STATs and others phosphotyrosine-containing proteins) can be a substrate for this degradation. This mechanism is involved in the termination of cytokine signaling by SOCS (**Kile et al., 2002**).
In addition, SOCS1 and SOCS3 have a short N-terminal domain allowing them to inhibit the catalytic activity of JAKs, the kinase inhibitor region (KIR) (**Babon and Nicola, 2012**) (**Figure 10 A and B**). The crystal structure of the gp130/JAK2/SOCS3 complex was recently resolved (**Kershaw et al., 2013b**). It revealed that SOCS3 binds the gp130 receptor on its SH2 domain. However, by contrast to what was previously thought, the structure showed that SOCS3 does not directly interact with phosphotyrosines on JAK2 but rather blocks the docking site for JAK2 substrates, thus preventing its activity (**Figure 10B**). For this reason, SOCS3 is only able to inhibit JAK1, JAK2 and TYK2 but not JAK3 because of the absence of a specific sequence on the substrate-docking site (**Babon and Nicola, 2012**).

The importance of cytokine signaling by SOCS proteins has been highlighted by loss of function studies in KO mice. *Socs1* and *socs3* KO are lethal. *Socs1*$^{-/-}$ mice die during neonatal period from inflammatory disease involving excessive activation of T cells and a hyper- responsiveness to IFNγ (**Starr et al., 1998; Alexander et al., 1999**). *Socs3*$^{-/-}$ mice die embryonically from placental defects due to uncontrolled LIF signaling (**Takahashi et al., 2003; Robb et al., 2005**). These results show the key importance of SOCS proteins in the regulation of cytokine signaling.
SOCS proteins negatively regulate cytokine signaling by attenuating the JAK/STAT pathway in various cell types. For example, SOCS3 preferentially regulates G-CSF and gp130-mediated signaling through inhibition of the JAK2/STAT3 cascade. SOCS3 is involved in the regulation of cellular functions in many organs including immune system, brain, spinal cord, retina or liver (**Yoshimura et al., 2007; Boyle and Robb, 2008**).

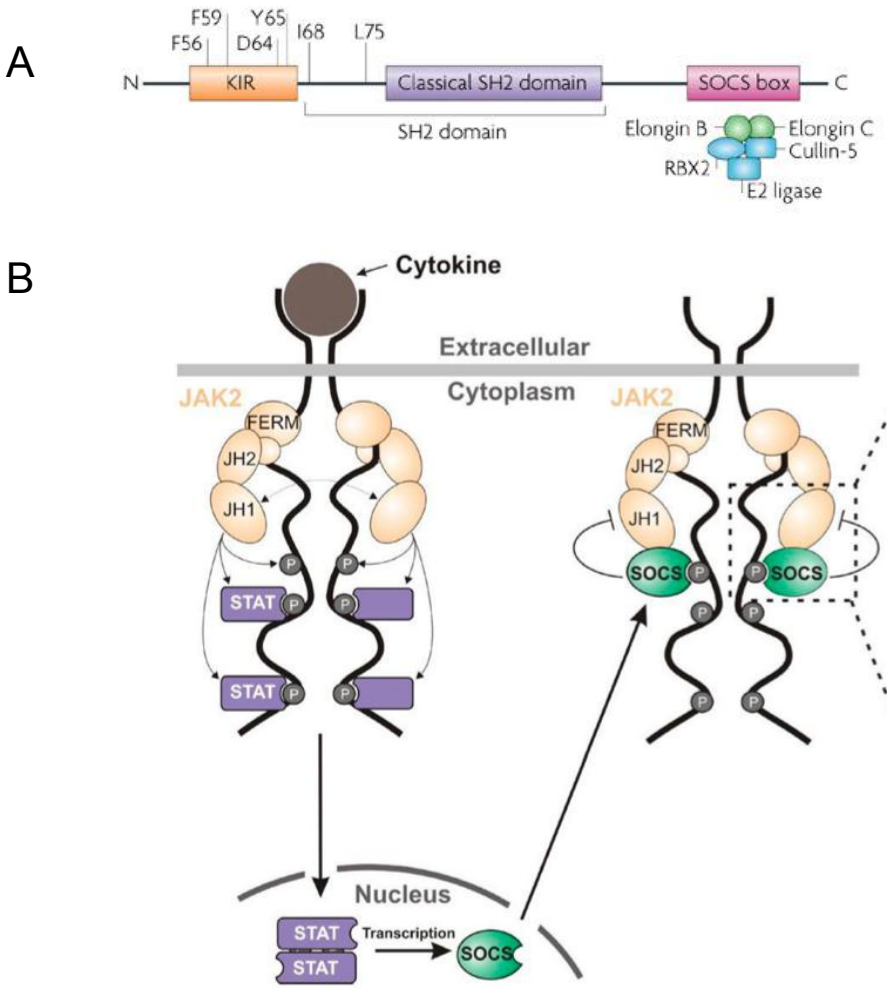

Figure 10. The structure of SOCS proteins and mechanism of JAK2 inhibition.
A, Structure of suppressor of cytokine signalling 1 and 3 (SOCS1, 3). The SOCS box is conserved in all cytokine-inducible SRC homology 2 (SH2)-domain-containing protein (CIS)–SOCS-family proteins. The function of the SOCS box is the recruitment of the ubiquitin-transferase system. The SOCS box interacts with a complex containing elongin B, elongin C, cullin-5, RING- box-2 (RBX2) and E2 ligase. CIS–SOCS-family proteins, as well as other SOCS-box- containing molecules, function as E3 ubiquitin ligases and mediate the degradation of proteins that they associate with through their amino-terminal regions. Therefore, SOCS proteins target the entire cytokine-receptor complex, including Janus kinase (JAK) proteins and SOCS protein themselves, for proteasomal degradation. **B**, Mechanism of JAK2 inhibition by SOCS3. In addition to the generic ubiquitylation mechanism of protein degradation, SOCS1 and 3 can inhibit the catalytic domain (JH1) of JAK2. SOCS3 inhibits the catalytic activity of JAKs by binding to the activation loop of the catalytic domain through both its KIR and SH2 domains. Adapted from (**Yoshimura et al., 2007; Kershaw et al., 2013a**).

The JAK/STAT pathway controls the transcription of target genes

It is somewhat remarkable that a unique signaling cascade can exert as many different functions in such a variety of cell types. Recent studies have provided insight into the transcriptional regulation by STATs, especially by STAT3. By comparing STAT3 target genes in different cell lines, Hutchins et al.

showed that the induction of genes involved in the regulation of the JAK/STAT pathway and cell growth, were systematically induced by STAT3, independently of the cell type. Particularly, STAT3 induces its own transcription (**Hutchins et al., 2013**). By contrast, they found non-canonical STAT3 DNA binding sites that were only present in specific cell types. Although, these sequences could not account for the wide variety of cell-specific STAT3 target genes, they could serve as platform for the interactions with co-factors or epigenetic regulators of gene expression in specific cell types (**Hutchins et al., 2013**). However, this study was performed on cell lines from immune and neural-derived cells. In a recent study, Hamby et al. investigated the changes in gene expression elicited in cultured astrocytes by cytokine or LPS stimulation. Primary astrocyte cultures were treated with various cytokines (TGF-β1, IFN-γ) or LPS, alone and in combination. They found that the combinatorial stimulation with the cytokine cocktail altered the expression of more than 6800 genes (**Hamby et al., 2012**). In astrocytes, cytokines increase the expression of genes involved in immune signaling, cell death, growth, and proliferation. In addition, in this study, they observed the modulation of several genes encoding G-protein coupled receptors (GPCR) linked to Ca^{2+} signaling in astrocytes. Using electrophysiology, they were able to show that cytokine stimulation of cultured astrocyte led functional changes in Ca^{2+} signaling consistent with changes in GPCR gene expression (**Hamby et al., 2012**). Taken together, these results suggest that the JAK/STAT pathway regulates the expression of many genes, some of which in a cell-type specific manner. In particular, in cultured astrocytes, activation of the JAK/STAT pathway might regulates the ability of astrocytes to signal and interact with neighboring cells.

Crosstalk between JAK/STAT and other signaling pathways

There are multiple levels of crosstalk between the JAK/STAT and other signaling pathways, which increases the range of its regulation in cells. In particular, STAT3 and NF-κB have been shown to interact in various ways: physical interaction, cooperation to regulate the transcription of target genes or the reciprocal negative regulation through their respective inhibitors (**Grivennikov and Karin, 2010**).

Synergistic interactions between STAT3 and NF-κB are involved the development and progression of colon, gastric and liver cancers by promoting inflammatory processes (**Grivennikov and Karin, 2010**). First, STAT3 and NF-κB act synergistically to regulate the expression a common subset of target genes including *serpine1*, *Bcl-3* and *Bcl-2* (**Oeckinghaus et al., 2011**). Second, physical interaction between STAT3 and NF-κB can regulate the activity of gene promoters or enhancers. For example, Yu et al. showed that in IL-1β and LPS+ IFNγ -stimulated mesangial cells, STAT3 forms a physical complex with NF-κB p50 and p65 (**Yu et al., 2002**). In addition, overexpression of STAT3 inhibits the activity of the inducible nitric oxide synthase (iNOS) promoter, which is NF-κB-dependent and does not carry STAT-responsive elements (**Yu et al., 2002**). Thus, when highly expressed, STAT3 negatively regulates NF-κB activation and subsequent regulation of NF-κB-dependent gene expression. In hepatic cell lines, Yoshida et al. found that p65 can interact with unphosphorylated STAT3 (U-STAT3) to inhibit STAT3-responsive elements (**Yoshida et al., 2004**). By contrast, in

epithelial cell lines, IL-6 triggers the accumulation of U-STAT3, which forms a complex with NF-κB to activate the transcription of NF-κB-dependent genes such as *ccl5* (RANTES), *IL-6* or *IL-8* (**Yang et al., 2007**).

Last, SOCS1 and SOCS3, the endogenous inhibitors of STATs, negatively regulate Toll-like receptor signaling, classically associated with activation NF-κB (**Yoshimura et al., 2003**).

However, most of these data have been obtained in cultured cell lines, using cytokine, toxin or expression of constitutively activated mutant proteins to activate JAK/STAT and NF-κB pathways. Whether any of these STAT3/NF-κB interactions occur in physiological conditions *in vivo* remains to be demonstrated.

ii) Physiological roles of the JAK/STAT pathway

The JAK/STAT pathway outside of the CNS

Cellular proliferation and cancer

Constitutive activation of the JAK/STAT pathway is associated with various diseases including inflammatory conditions and tumors. Indeed, STATs regulate the expression of genes involved in cell growth and proliferation. For example, STAT3 controls the expression of genes involved in cell cyle (*cyclin D1* and *p53*) and in cell survival (*Bcl-xl*, *Bcl-2*, *fas*) (**Levy and Darnell, 2002**).

A range of tumors and tumor-derived cell lines display mutations of JAK2 and STAT3 proteins that result in the constitutive activation of the JAK2/STAT3 pathway (**Kiu and Nicholson, 2012**). For example, constitutively activated STAT3 is observed in head and neck cancers or myelomas (**O'Shea et al., 2013a**). Thus, *stat3* can be considered as an oncogene. Further evidence came from the work of Bromberg and colleagues that designed a constitutively activated STAT3 (STAT3C) mutant by the substitution of two cysteine residues in the STAT3 SH2-domains (**Bromberg et al., 1999**). Thus, two STAT3C molecules can dimerize spontaneously through the formation of a disulfide bridge between the two cysteines, leading to a stimulus-independent activation of the STAT3 pathway. Fibroblasts expressing STAT3C elicited tumors when transplanted into nude mice. STAT3C expression was associated with the upregulation of genes involved in cell cycle and cell survival (**Bromberg et al., 1999**).

Likewise, several point mutations in JAK2 have been associated with hematologic diseases and cancers (**O'Shea et al., 2013a; Vainchenker and Constantinescu, 2013**). The JAK2V617F mutation in JAK2 pseudokinase domain has been found in most patients with polycythemia vera as well as 50-60% of patients with essential thrombocythemia and primary myelofibrosis. The JAK2K539L mutation in the linker region between the pseudo-kinase has been found in patients with idiopathic erythrocytosis (**O'Shea et al., 2013a**). Finally, the JAK2T875N mutation resulting in a constitutively active kinase domain, has been identified in patients suffering from acute megakaryoblastic leukemia (**Zou et al., 2011**)

Immunity

The JAK/STAT pathway is involved in the formation and maintenance of lymphoid cells including T cells, natural killer and B cells. Especially, TYK2 and JAK3 appear to play a crucial role in the development of lymphocytes as mutations in *tyk2* and *jak3* genes are associated with primary immunodeficiencies in humans (**O'Shea et al., 2013b**). Further mutations of STAT1 and STAT3 proteins are associated with immune deficiencies and high susceptibility to microbial infections. STATs play a central role in immune cell functions and altered STAT signaling is involved in many immune diseases (**Figure 11**).

STAT	Cellular functions	Major diseases
1	• Cell growth and apoptosis • T_H1 cell-specific cytokine production • Antimicrobial defence	• Atherosclerosis • Infection • Immune disorders
2	• Mediation of IFNα/IFNβ signalling	• Cancer • Infection • Immune disorders
3	• Cell proliferation and survival • Inflammation • Immune response • Embryonic development • Cell motility	• Cancer
4	• T_H1 cell differentiation • Inflammatory responses • Cell proliferation	• Experimental autoimmune encephalomyelitis (multiple sclerosis) • Systemic lupus erythematosus
5A	• Cell proliferation and survival • IL-2Rα expression in T lymphocytes • Mammary gland development • Lactogenic signalling	• Cancer • Chronic myelogenous leukaemia
5B	• Cell proliferation and survival • IL-2Rα expression in T lymphocytes • Sexual dimorphism of body growth rate • NK cell cytolytic activity	• Cancer • Chronic myelogenous leukaemia
6	• Inflammatory and allergic immune response • B cell and T cell proliferation • T_H2 cell differentiation	• Asthma • Allergy

Figure 11. Roles of the JAK/STAT pathway in the immune system.
Summary of the cellular functions and diseases associated with loss-of-function of STAT proteins. These results highlight the crucial role of STAT proteins in immune system development and maintenance. From (**Miklossy et al., 2013**)

The JAK/STAT pathway in the CNS

The JAK/STAT pathway is expressed in all cells. In the CNS, its functions have mainly been investigated in neurons and in radial glial cells during development.

Development

As mentioned previously (see § I.A.2.a) during development, radial glial cells generate intermediate progenitors that give rise to neurons (neurogenic phase). At the onset of astrogliogenesis, radial glial cells differentiate into intermediate precursor cells and astrocytes. This neuron-astrocyte switch is regulated in NSCs and the JAK/STAT pathway appears to be a central player in this developmental

step. During the neurogenic period, the JAK/STAT pathway is inhibited to prevent early astrocyte differentiation. This inhibition involves both epigenetic control of gene expression as well as interaction of STAT3 with inhibitory proteins. Indeed, promoter sequences of mature astrocyte-specific genes such as GFAP or S100β are methylated, preventing gene transcription. In addition, STAT3 and its co-activator complex, the CREB-binding protein (CBP)/ p300 complex is sequestrated in the cytoplasm by pro-neuronal transcription factors (**Kanski et al., 2014**).

When the neurogenic phase terminates, several molecules trigger the neuron-astrocyte regulatory switch. Cytokines or morphogens such as BMPs induce gliogenesis at specific time points in cultured progenitor cells. In addition, the gliogenic switch can be promoted by other signaling cascades, which ultimately activate the JAK/STAT pathway. For example, activation of NOTCH induces the binding of its effectors Hes1 and Hes5 to STAT3 to promote its phosphorylation by JAK2 (**Kamakura et al., 2004**). Furthermore, it was shown that activation of the JAK/STAT pathway during the gliogenic period in cultured cortical progenitors leads to a positive autoregulatory loop of STAT1 and STAT3 to strengthen the induction of astrogliogenesis (**He et al., 2005**). In accordance with these results, conditional deletion of *stat3* in neural stem cells promotes neurogenesis and inhibits astrogliogenesis (**Cao et al., 2010**). Taken together, these results demonstrate the involvement of the JAK2/STAT3 pathway in regulating a critical step during CNS development.

Regulation of hormone signaling

Various hormones including leptin, gonadotropin-releasing hormone (GnRH) or prolactin act on specific neuronal populations in the hypothalamus to regulate energy homeostasis, food intake, reproduction and lactation. These hormones signal through their cognate receptors and activate the JAK/STAT pathway. For example, leptin regulates food intake and energy expenditure by acting on hypothalamic arcuate neurons. Particularly, leptin binds its receptor and leads to the release of the anorexigenic peptide from pro-opiomelanocortin (POMC) from neurons (**Villanueva and Myers, 2008**). This effect depends on the activation of the JAK2/STAT3 pathway. Indeed, *stat3* and *stat5* KO in POMC neurons reduced POMC expression and increased food intake causing mild obesity in mice (**Villanueva and Myers, 2008**). Furthermore, leptin signaling induces SOCS3 expression that acts as a negative feedback mechanism. SOCS3 expression is increased in various models of obesity. Loss-of-function studies have shown that SOCS3 is critical to maintain leptin sensitivity in POMC neurons and thus regulates food intake (**Villanueva and Myers, 2008; Ernst et al., 2009**).

In addition, JAK2, STAT3 and STAT3 are expressed in hypothalamic GnRH neurons. For example, *jak2* KO mice display reduced GnRH levels and thus results in altered gonad development and infertility in female mice (**Nicolas et al., 2013**).

Synaptic plasticity

The JAK/STAT pathway is also involved in the regulation of synaptic plasticity underlying learning and memory. First, hormones as well as cytokines that signal through the JAK/STAT pathway lead to

reduced LTP in slices. For example, in rat hippocampal slices treated with IL-6, LTP is reduced in CA1 pyramidal cells. In addition, AG490 JAK inhibitor causes spatial memory impairment (**Chiba et al., 2009**). However, cytokines as well as AG490 modulate the JAK/STAT pathway in multiple cell types. Therefore, the cellular basis of this observation is not clear. In this context, Nicolas et al. showed, in a recent paper that the JAK2/STAT3 pathway in neurons mediates NMDAR dependent LTD but not LTP in hippocampal slices and organotypic cultures. They used intracellular injection of pharmacological inhibitors of JAK and STAT and knockdown of *jak2* and *stat3* genes in pyramidal cells on organotypic slices. They found that activation of STAT3 was necessary to trigger NMDAR-LTD but it was not dependent on STAT3 nuclear localization and its effects on gene expression. Alternatively, they suggest that unknown effects of STAT3 in the cytoplasm of pyramidal cells are responsible for the induction of LTD (**Nicolas et al., 2012**).

Axon-growth promoting effects

The JAK/STAT pathway is also a central player in axonal regeneration. This function has particularly been investigated in optic nerve injury (**Park et al., 2009; Sun et al., 2011**). Indeed, several studies reported that *socs3* deletion in RGCs enhances axon regeneration after crush injury *in vivo* (**Smith et al., 2009; Sun et al., 2011**). In their elegant study, Smith et al. showed that this effect is dependent on gp130-related signaling. They performed cell-specific deletion of both *socs3* and *gp130* genes in RGCs with $socs3^{fl/fl}$ and $gp130^{fl/fl}$ mice and induced gene deletion by intravitreal injection of an adeno-associated viral vector encoding the Cre recombinase. Intravitreal injection of CNTF further improves axon regeneration in *socs3*-deleted RGCs. Furthermore, axon-growth promoting effects in RCG after lens injury is also dependent on CNTF and LIF that signal through the gp130/JAK/STAT pathway (**Leibinger et al., 2009**). Very interestingly, by contrast to mammals, in the zebrafish, RCG display an endogenous capability for axon regeneration after optic nerve injury (**Roos et al., 1999; McDowell et al., 2004**). A recent study from D. Goldman's laboratory investigated whether this intrinsic capability was associated with an alteration of the inhibitory effects of SOCS3 in the zebrafish eye. Indeed, after optic nerve injury, expression of several cytokines that signal through the gp130/JAK/STAT pathway was induced including CNTF, LIF or IL-11 and increased axon regeneration. In this model, SOCS3 expression was induced but did not inhibit the JAK/STAT-mediated axonal regeneration after optic nerve injury (**Elsaeidi et al., 2014**).

Overall, these data demonstrate a central role of the JAK/STAT pathway both in the CNS and in peripheral organs. Interestingly, most of the JAK/STAT pathway functions in the CNS have mainly been studied in neurons. Its physiological role in astrocytes in the adult brain is poorly known. By contrast, in pathological conditions, activation of the JAK/STAT pathway is frequently observed in reactive astrocytes.

Activation of the JAK/STAT pathway is associated with astrocyte reactivity

The JAK/STAT pathway is critical for glial scar formation (**Sofroniew, 2009**). Several studies from different groups have well demonstrated STAT3 involvement in glial scar formation after acute injuries. Okada et al. investigated the effects of targeting the JAK2/STAT3 pathway in reactive astrocytes. To this end, they deleted *stat3* or *socs3* with the Cre-loxP system in nestin-expressing cells. Nestin is expressed during development by progenitor cells and in the adult brain by NSCs in neurogenic areas (**Kriegstein and Alvarez-Buylla, 2009**). Under acute pathological or direct stimulation by cytokines, nestin expression can be induced in reactive astrocytes (**Clarke et al., 1994; Lin et al., 1995; Escartin et al., 2006**). Therefore, nestin promoter was used to interfere with the JAK2/STAT3 pathway in reactive astrocytes after SCI. Conditional deletion of *stat3* (*nes-stat3*$^{-/-}$) resulted in altered migration of reactive astrocytes and wound healing. By contrast, conditional deletion of *socs3* (*nes-socs3*$^{-/-}$) enhanced glial scar formation (**Okada et al., 2006**). Similarly, *stat3* deletion in reactive astrocytes (*gfap-stat3*$^{-/-}$) attenuated GFAP upregulation and disrupted glial scar formation after SCI (**Herrmann et al., 2008**). By interfering with the JAK/STAT pathway, these studies demonstrate that the JAK/STAT pathway in reactive astrocytes is necessary for glial scar formation.

In addition, activation of STAT3 was observed in reactive astrocytes, in many injury models including TBI (**Oliva et al., 2012**), neonatal brain injury (**Nobuta et al., 2012**), axotomy (**Tyzack et al., 2014**), infection (**Na et al., 2007**), glaucoma (**Zhang et al., 2013**), epilepsy (**Xu et al., 2011**), ischemia (**Amantea et al., 2011**) and in after exposure to neurotoxins (**Sriram et al., 2004; O'Callaghan et al., 2014**). STAT3 activation was also reported in chronic pathological conditions such as ND. By contrast to acute injury models, activation of STAT3 was detected in reactive astrocytes as well as neurons and activated microglia. In AD patients and mouse models, Wan et al. mainly observed STAT3 activation in neurons and very few reactive astrocytes (**Wan et al., 2010**). In patients and mouse models of ALS, activated STAT3 was detected in motorneurons, reactive astrocytes and activated microglia (**Shibata et al., 2009; Shibata et al., 2010**). In models of neuropathic, activation of STAT3 was observed in reactive astrocytes (**Tsuda et al., 2011**) and activated microglia (Dominguez et al., 2010).

These studies mainly rely on the detection of the phosphorylated form of STAT3 or the nuclear localization of STAT3, both reflecting its activation. However, this approach does not evidence the instrumental role of the JAK2/STAT3 pathway in mediating astrocyte reactivity in these models. Only few have investigated the direct requirement of this pathway to mediate astrocyte reactivity. For example, Sriram et al. showed that STAT3 was strongly upregulated in reactive astrocytes in the MPTP model of PD in mice. Pharmacological blockade of JAK2 with AG490, resulted in the attenuation of astrocyte reactivity after MPTP injection (**Sriram et al., 2004**). Nobuta et al. used a conditional deletion of *stat3* in reactive astrocytes (*gfap-stat3*$^{-/-}$) in a model of neonatal white matter injury (WMI). LPS subcutaneously injected in the early postnatal period reproduces astrocyte reactivity observed in WMI in newborns. By contrast to WT mice, *gfap-stat3*$^{-/-}$ mice failed to display astrocyte hypertrophy and GFAP upregulation after LPS injection (**Nobuta et al., 2012**). After peripheral nerve

injury, a model of neuropathic pain, reactive astrocytes in the spinal cord have been shown to proliferate. Pharmacological inhibition of JAKs and STATs decreases astrocyte reactivity along with proliferation in the spinal cord (**Tsuda et al., 2011**).

Taken together, these data strongly suggest that the JAK/STAT pathway has an important role in astrocyte reactivity *in vivo*. However, due to the large number of models that have been studied, involving various pathological mechanisms, CNS regions and even cell types, it is difficult to dissect out the specific contribution of the JAK/STAT pathway activation in reactive astrocytes to injury/disease processes. In fact, only very few studies have investigated the requirement of this pathway, especially in ND models.

d) Other signaling pathways associated with astrocyte reactivity

i) The calcineurin-regulated signaling pathways

The Ca^{2+}/calmodulin-dependent serine/threonine phosphatase calcineurin (CN) is involved in the regulation of gene expression through the modulation transcription factors such as nuclear factor of activated T-cells (NFATs) and NF-κB (**Furman and Norris, 2014**). CN is a ubiquitous protein, although expressed at high levels in the brain. It regulates the growth, differentiation and cellular processes in T-cells, osteoclasts or myocytes (**Hogan et al., 2003**).

In addition, CN is activated upon inflammatory conditions. In primary cultures of astrocytes, CN is activated by known-inducers of astrocyte reactivity such as pro-inflammatory cytokines (IL1β, TNFα, IFNγ) or Aβ peptide (**Furman and Norris, 2014**). Several studies have linked NFAT/CN pathway to astrocyte reactivity, in particular in the context of AD. Indeed, CN immunoreactivity is increased in aged mice and around amyloid plaques both in AD patients and mouse models (**Furman and Norris, 2014**). Overexpression of a constitutively activated form of CN in astrocytes resulted in enhanced GFAP expression after brain injury of LPS injection (**Fernandez et al., 2007**). However, there are some discrepancies in the literature towards the effects of CN activation in reactive astrocytes in AD models. Pharmacological inhibition of CN restored cognitive deficits in the Tg2576 mouse model of AD (**Dineley et al., 2007**). Viral-mediated overexpression of the blocking peptide VIVIT to prevent NFAT/CN activation, resulted in the attenuation of astrocyte reactivity around amyloid depositions in APP/PS1 AD mice (**Furman et al., 2012**). By contrast, constitutive activation of CN in the same mouse model resulted in decreased amyloid load, attenuated astrocyte and microglia reactivity and restored cognitive deficits (**Fernandez et al., 2012**).

Interestingly, when activated, this pathway has been shown to regulate glutamate uptake in cultured astrocytes. Indeed, inhibition of NFAT/CN pathway by VIVIT prevented the decrease in GLT-1 expression observed after stimulation with IL-1β and Aβ. Furthermore, by decreasing extracellular glutamate, VIVIT protected neurons from excitotoxicity (**Sama et al., 2008**).

In conclusion, the NFAT/CN pathway is an additional pathway associated with astrocyte reactivity. However, manipulation of this pathway in reactive astrocytes provided controversial results, especially in the context of AD.

ii) The FGF signaling pathway

There is a large body of evidence reporting that fibroblast growth factor (FGF) signaling is associated with astrocyte reactivity both in primary astrocyte culture (**Brambilla et al., 2003; Chadi and Gomide, 2004**) and *in vivo* (**Eclancher et al., 1990; Eclancher et al., 1996; Avola et al., 2004; Fischer et al., 2004**). After TBI in the rat cortex, FGFR-1 and its ligand FGF-2 are localized in reactive astrocyte nuclei, reflecting activation of the pathway. An interesting and recent study suggests that FGF signaling is required to maintain astrocytes in a resting state upon physiological conditions (**Kang et al., 2014**). They used transgenic mice with tamoxifen-inducible deletion of *fgfr-1*, *fgfr-2* and *fgfr-3* (*fgfr-1*$^{fl/fl}$ *x fgfr-2*$^{fl/fl}$ *x fgfr-3*$^{-/-}$) or transgenic mice overexpressing a mutated form of *fgfr-3* leading to a constitutively active FGF signaling in nestin-expressing astrocytes. Authors studied astrocyte reactivity after acute brain injury when FGF signaling was either disrupted or stimulated. In *fgfr-1*$^{fl/fl}$ *x fgfr-2*$^{fl/fl}$ *x fgfr-3*$^{-/-}$ mice, astrocyte reactivity was enhanced at the site of stab wound injury. By contrast, *fgfr-3* mutant mice did not show astrocyte reactivity after cortical injury (**Kang et al., 2014**). Together, these data suggest that FGF signaling can act as a negative regulator of astrocyte reactivity.

Overall, multiple signaling pathways are associated with astrocyte reactivity both in acute and chronic pathological conditions. Yet, relatively few studies have directly investigated the direct requirement for these signaling pathways in mediating astrocyte reactivity, especially, in chronic pathological such as ND.

C. Reactive astrocytes in neurodegenerative disorders

1) Huntington's disease

a) General characteristics of Huntington's disease

i) Epidemiology

Huntington's disease (HD) is a fatal genetic neurodegenerative disease caused by an autosomal dominant mutation in the huntingtin gene (*htt*) (The Huntington's disease Collaborative Research **Group, 1993**). This mutation consists in a pathological expansion of CAG repeats encoding a polyglutamine (polyQ) track in the mutant Htt (mHtt) protein. A length of 36 to 39 CAG repeats in *htt* is associated with uncomplete penetrance of HD phenotype. Above 40 CAG repeats, the penetrance is complete and mHtt carriers will develop HD. There is an inverse correlation between the number of CAG repeats and the onset of symptoms in patients with HD. Thus, juvenile forms of HD are observed in 5-10% of HD cases, in persons carrying a large number of CAG repeats (>60 CAG) (**Ross and Tabrizi, 2011**). The mean disease onset for HD is approximately 45 years of age (**Ross et al., 2014**). The prevalence of the disease is about 6 per 100 000 in Europe, North American, and Australian populations. By contrast, the prevalence for HD is lower in Asia with 0.40 per 100 000 (**Pringsheim et al., 2012**).

ii) Symptoms

HD can be divided in pre-manifest and manifest periods (**Figure 12**). The pre-manifest period refers to the presymptomatic phase of HD, whereby mhtt carriers display no symptoms of the disease. The manifest period begins with a prodromal phase, which is defined by subtle behavioral and motor abnormalities. HD diagnosis relies on the presence of extrapyramidal movement disorders along with emotional alterations. Early, moderate and advanced stages of HD pathology are characterized by the progressive worsening of HD symptoms with time, ultimately leading to patient death (**Shoulson and Fahn, 1979**).

HD is characterized by motor, cognitive and psychiatric symptoms. The first extrapyramidal movement disorder that appears in early and late-onset HD is chorea. Then, HD progression is characterized by the appearance of further motor symptoms involving impairment of voluntary movements, bradykinesia and rigidity (**Walker, 2007**). However, patients with HD also suffer from alterations of cognitive functions including decreased attention, abnormal planning and perseverative behaviors (**Ross et al., 2014**). Lastly, patients with HD display psychiatric symptoms such as major depressive syndrome, suicidal behavior and irritability (**Ross et al., 2014**). Interestingly, a recent study showed that apathy is one of the most well correlated symptoms with disease progression. This psychiatric alteration can even be detected at the presymptomatic stage (**Ross et al., 2014**).

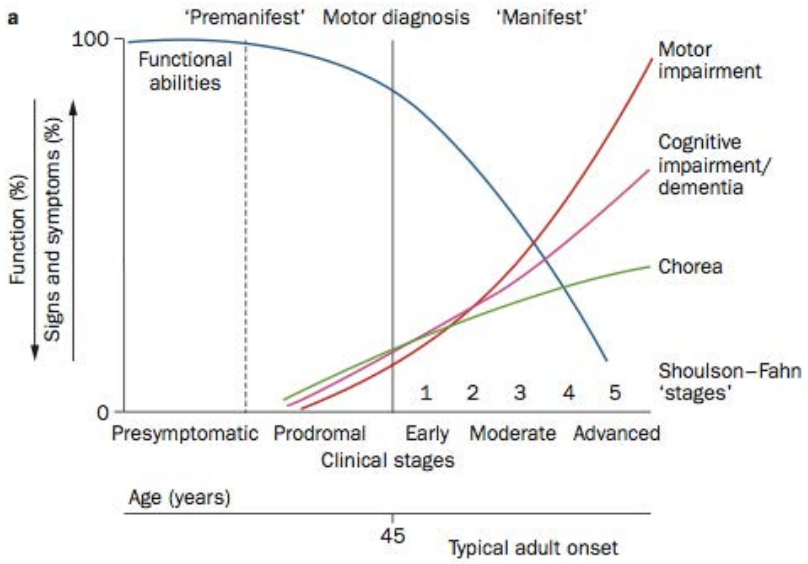

Figure 12. Clinical evolution of HD symptoms.
The progression of HD is characterized by a pre-manifest period that consists in the pre-symptomatic stage, where mHtt carriers are undistinguishable or healthy subjects. During prodromal HD, patients start displaying subtle motor and behavioral changes. The mean disease onset for HD is 45 years of age. HD patients progressively develop motor symptoms (chorea, incoordination, bradykinesia and rigidity) and cognitive impairment including dementia. Adapted from (**Ross et al., 2014**)

iii) Neuropathology

Histologically, HD is characterized by the dramatic loss of neurons in the caudate and putamen structures of the striatum. Disease stage closely correlates with histological alterations observed in the striatum of patients with HD (**Vonsattel et al., 1985**). Over the course of the disease, cortical grey matter atrophy also occurs at the level of the motor cortex. Other brain regions such as the globus pallidus, the thalamus or the hippocampus also undergo atrophy in HD (**Vonsattel et al., 1985**). In the striatum, the most vulnerable neuronal population is the medium-sized GABAergic spiny neurons (MSNs). By contrast, the encephalin$^+$ and substance P$^+$ striatal interneurons are relatively spared (**Ross and Tabrizi, 2011**). Another hallmark of HD is the presence of mHtt aggregates.

Motor disturbances can be explained by alterations of the basal ganglia circuitry due to the dysfunction and subsequent death of MSNs (**Sepers and Raymond, 2014**). The basal ganglia direct and indirect pathways act together to promote or inhibit movement. In HD, due to the dysfunction and loss of dopamine 2 receptor (D2R)-expressing MSNs, this circuitry is unbalanced leading to cortical hyperexcitability (**Sepers and Raymond, 2014**). Furthermore, dopamine acts on D2R to decrease glutamate release in the striatum (**Surmeier et al., 2007**). It has been hypothesized that the convergence between an increase in glutamate release from cortical inputs and the loss of D2R in the striatum contributes to the selective demise of MSN in HD (**Surmeier et al., 2007**). Therefore, even if MSN are predominantly vulnerable, the dysfunction of the whole basal ganglia circuitry is involved in

motor dysfunctions in HD. Indeed, conditional expression of the pathogenic N-terminal fragment of mHtt in striatal neurons is not sufficient to induce motor defects and neuropathology in mice (**Gu et al., 2005**). In fact, expression of mHtt in other neuronal types such as cortical interneurons participate in HD pathogenesis by disrupting cell-cell interactions (**Gu et al., 2005; Gu et al., 2007**).

HD pathogenesis is characterized by alterations of many cellular functions due to both a loss of normal functions of Htt and a gain of toxic functions conferred by the polyQ track. Here, I will only describe some of the main physiological roles of normal Htt as well as the most prominent cellular dysfunctions observed in HD. The molecular basis underlying HD pathogenesis is described in detail in outstanding reviews (**Landles and Bates, 2004; Cattaneo et al., 2005; Zuccato et al., 2010; Arrasate and Finkbeiner, 2012; Sepers and Raymond, 2014**).

b) The normal function of Htt

Htt is expressed throughout the body, in multiple cell types. It is a large protein (350 kDa), involved in many cellular functions, through numerous protein-protein interactions. Although its primary amino acid structure is known, it only gives limited insights into its functions (**Cattaneo et al., 2005**). Htt contains conserved amino-acid sequences involved in protein-protein interactions, consensus cleavage sites by several proteases and a polyQ track located at the N-terminus. The N-terminal part of Htt is involved in its interactions with transcription factors and can be cleaved in multiple N-terminal fragments (**Cattaneo et al., 2005**). Furthermore, Htt sequence carries several sites for post-translational modifications such as phosphorylation, acetylation and sumoylation. Htt also has a nuclear localization and nuclear export signal sequences, which can be involved in the transport of proteins or transcription factors between the nucleus and the cytoplasm (**Ross and Tabrizi, 2011**).

Htt is required for normal development, as total KO of Htt is lethal at the gastrulation stage of embryonic developmental (**Cattaneo et al., 2005**). *In vitro*, reduction of Htt expression or KO of *Htt* ($Hdh^{-/-}$) in stem cells results in reduced production of neurons, suggesting an important role of Htt in neurogenesis and maintenance of neurons (**White et al., 1997**). Accordingly, deletion of *Htt* in the postnatal brain results in progressive neurodegeneration in mice (**Dragatsis et al., 2000**). Htt also has neuroprotective functions. For example, overexpression of Htt in a transgenic mouse model of HD (YAC18) protected neurons from ischemic damage after MCAO (**Zhang et al., 2003**). In addition, Htt has anti-apoptotic functions as it inhibits the cleavage of the pro-apoptotic pro-caspase 9 and its subsequent activation (**Rigamonti et al., 2001**).

Interestingly, studies whereby Htt was knockdown by RNA interference in various models showed that decreased expression of Htt in the absence of mHtt was sufficient to alter cellular transport of trophic factors and organelles (**Cattaneo et al., 2005**). In Drosophila expressing a small interfering RNA against *Htt* (siHtt) and in $Hdh^{-/-}$ neurons, the transport of vesicles and mitochondria was reduced. Similarly, the vesicular transport of BDNF was impaired with siHtt in cell culture (**Cattaneo et al., 2005**). Indeed, one of the well-known functions of Htt is its role in the regulation of BDNF transcription

and vesicular transport (**Zuccato et al., 2010**). BDNF is a trophic factor, highly expressed in cortical neurons and transported along microtubules towards the striatum. BDNF increases striatal neuron survival and supports cortico-striatal synapse function (**Zuccato et al., 2010**). An elegant study from E.Catteneo's team showed that Htt sequestrated the transcription factor RE1-silencing transcription factor (REST) in the cytoplasm, which prevented the inhibition of *bdnf* transcription (**Zuccato et al., 2003**). Htt also promotes the transport of BDNF along cortical axons to striatal neurons through its interaction with Huntingtin associated protein 1 and the p150 subunit of dynactin, allowing the association to molecular motor and the vesicular transport along the microtubules (**Gauthier et al., 2004**).

This function of Htt is lost in the presence of mHtt (**Figure 15**). Indeed, patients with HD and mouse models display decreased levels of BDNF in the striatum, which results in the alteration of trophic support to MSNs (**Zuccato et al., 2010**). There is compelling evidence that mHtt impairs *bdnf* transcription. Indeed, by contrast to Htt, mHtt does not sequestrate REST in the cytoplasm. Indeed, nuclear accumulation of REST was detected in cultured cells, mouse models and in patients with HD (**Zuccato et al., 2010**). This dysfunction was associated with decreased expression of genes controlled by REST, encoding ions channels, transporters, growth factors or other transcription factors (**Zuccato et al., 2003; Bruce et al., 2004**). MHtt impairs BDNF transport by disrupting the assembly of the transport scaffold on microtubules (**Cattaneo et al., 2005**). Furthermore, mHtt impairs the trafficking of BDNF receptor at MSN dendrites, which results in the impairment of BDNF signaling (**Sepers and Raymond, 2014**).

In conclusion, Htt has crucial roles in neuron survival and cellular processes that may be lost in HD. Alternatively, Htt polyQ track confers a toxic gain of functions that contribute to neuronal dysfunction.

c) Mechanisms of neurodegeneration in HD

i) Protein aggregation and protein degradation pathways

MHtt is cleaved by caspases and calpains. The resulting N-terminal fragments of mHtt form aggregates (**Scherzinger et al., 1997**). Indeed, intracellular aggregates containing polyubiquitinated N-terminal fragments of mHtt are found in the brain of patients with HD and in various mouse models of HD, both in the cytoplasm and the nucleus (**Roze et al., 2008**). However, the contribution of aggregates to mHtt toxicity is controversial. In favor of a toxic role for mHtt aggregates, it was shown in culture systems that mHtt aggregation often precedes neuronal cell death (**Cooper et al., 1998**). Further evidence suggests that mHtt aggregates might be toxic as they sequestrate normal Htt, transcription factors and transport proteins (**Roze et al., 2008**). This redistribution of proteins into aggregates prevents their normal functions. In transgenic mouse and monkey models of HD, the extent of aggregation of mHtt in the cortex and the striatum was correlated with the severity of symptoms (**Wang et al., 2008**).

By contrast, other studies reported that mHtt aggregates could be protective against neuronal dysfunction. For example, in primary culture, expression of N-terminal fragments of mHtt was toxic for neurons but this effect was not correlated with the formation of aggregates (**Saudou et al., 1998**). Accordingly, Arrasate et al. showed that in culture, neurons expressing N-terminal fragments of mHtt die progressively, many of which without forming mHtt aggregates. Interestingly, they found a positive correlation between the presence of large mHtt aggregates and neuron survival (**Arrasate et al., 2004**). In accordance with these *in vitro* data, a mouse model carrying the two first exons of Htt with a polyQ expansion displayed no behavioral abnormalities, striatal atrophy or neuronal death despite the presence of widespread mHtt aggregates in their brain (**Slow et al., 2005**). These results suggest that mHtt aggregates may not pathogenic in themselves and that soluble N-terminal fragments of mHtt containing the polyQ expansion might be more toxic for neurons (**Zuccato et al., 2010**).

Even if the role of aggregates in mHtt toxicity is still debated, they are a prominant feature of HD and it is important to understand the factors regulating their formation and clearance.

The two key pathways for protein degradation in the cell are autophagy (**Figure 13**) and the ubiquitin-proteasome system (UPS) (**Figure 14**). Autophagy defines the lysosomal degradation of long-lived proteins, macromolecules and organelles. UPS is involved in the degradation of short-lived and misfolded proteins. Dysfunction of both the UPS and autophagy are classically associated with mHtt toxicity and HD pathogenesis but some results are controversial (**Schipper-Krom et al., 2012**).

Alteration of autophagy was first proposed after the observation of increased autophagosome-like structures in the brain of HD patients (**Ravikumar and Rubinsztein, 2006**). However this was not associated with increased mHtt degradation by autophagy (**Cortes and La Spada, 2014**), and it was proposed that autophagy impairment in HD was responsible for the accumulation of autophagosomes in neurons (**Martinez-Vicente et al., 2010**). Actually, mHtt impairs different aspects of autophagy (**Figure 13**). For example, mHtt polyQ interacts with the chaperone protein Hsc70 and thus decreases chaperone-mediated autophagy (**Cortes and La Spada, 2014**). MHtt sequestrates and inactivates the mammalian target of rapamycin, a negative regulator of macroautophagy, which should stimulate protein degradation (**Cortes and La Spada, 2014**). However, this process does not function properly in the presence mHtt that prevents the recognition and loading of targeted proteins into autophagosomes for degradation (**Martinez-Vicente et al., 2010**). Finally, mHtt alters the transcription of many genes and interferes with peroxisome proliferator-activated receptor gamma coactivator 1-α, a transcriptional co-regulator that increases the transcription of lysosomal enzymes (**Cortes and La Spada, 2014**).

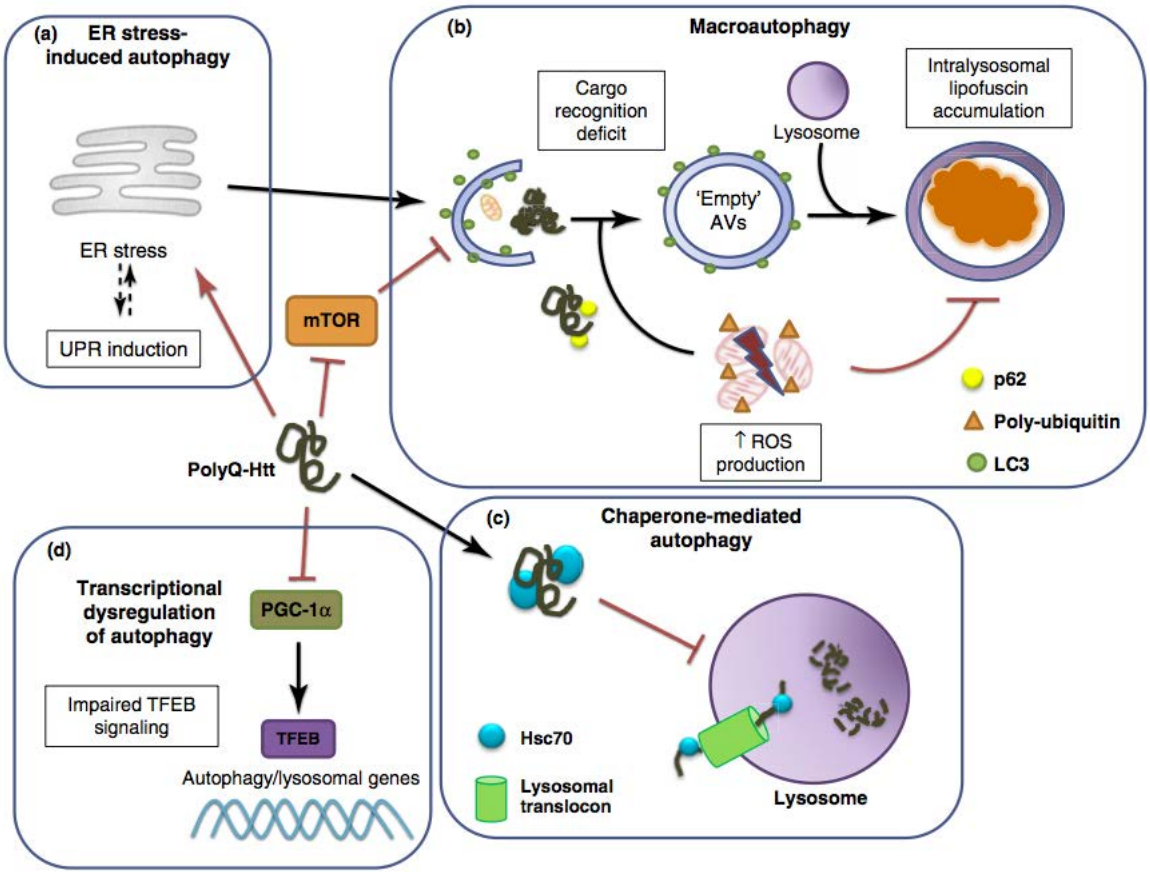

Figure 13. Several mechanisms of protein degradation by autophagy are altered in HD.
In HD, a polyglutamine-expanded huntingtin (polyQ- Htt) protein is produced and accumulates in cells. The misfolded polyQ-Htt elicits an endoplasmic reticulum (ER) stress response (a), and through direct inhibition of the ER-associated degradation pathway and impairment of ER-to-Golgi traffickin. PolyQ-Htt can sequester mammalian target of rapamycin (mTOR), resulting in disinhibition of macroautophagy; however, macroautophagy functions abnormally in HD, because the mutant polyQ-Htt protein prevents recognition and loading of cargo into developing autophagosomes, resulting in an accumulation of autophagic vesicles (AVs) that are relatively empty, in terms of substrates for degradation (b). Lysosomal enzyme activity is reduced in HD, possibly because of an increased burden of reactive oxygen species (ROS) (b). PolyQ-htt interacts excessively with Hsc70 and the lysosomal translocation machinery, resulting in diminished chaperone-mediated autophagy function in HD (c). As the amino-terminal fragment of polyQ-htt enters the nucleus, it has been shown to interfere with peroxisome proliferator-activated receptor gamma coactivator 1-α (PGC-1α), a transcriptional co-regulator, recently found to promote transcription factor E-B (TFEB) expression. Thus, polyQ-htt transcriptional dysregulation leads to impaired TFEB transactivation of its target genes, which encode the proteins and enzymes required for autophagosome assembly, autophagosome-lysosome fusion and lysosomal degradation (d). From (**Cortes and La Spada, 2014**)

The contribution of UPS dysfunction to HD pathogenesis is also controversial (**Ortega et al., 2007**). MHtt aggregates, found in the brain of patients and mouse models of HD, are positive for ubiquitin, suggesting that aggregated mHtt can be targeted to the proteasome (**Figure 14**) (**Davies et al., 1997; DiFiglia et al., 1997**). Early *in vitro* studies on purified proteasomes suggested that they were not able

to degrade polyQ-containing proteins (**Holmberg et al., 2004**). In accordance, a decreased activity of proteasome activity was detected with small fluorogenic peptides in brains of patients and in cells from the Hdh111 knock-in mouse model of HD (**Seo et al., 2004; Hunter et al., 2007**). Further evidence suggested that proteasome subunits were trapped in mHtt aggregates, contributing to UPS impairment (**Holmberg et al., 2004**) (**Figure 14**).

By contrast, *in vivo* studies in mouse models of HD found no global impairment of the UPS but an age-dependent decrease in the activity of proteasome enzymes (**Maynard et al., 2009**). Accordingly, in the Hdh140 knock-in model of HD, inhibition of the UPS resulted in a greater accumulation of N-terminal, but not full-length, mHtt, suggesting that the UPS is able to degrade mHtt (**Li et al., 2010**). In addition, a recent study using fluorescent polyQ peptides in cell culture, reported that proteasomes were not trapped but dynamically exchanged with mHtt aggregates and catalytically active (**Schipper-Krom et al., 2014**). Overall, these studies suggest that the UPS activity is impaired in HD, but still operational. Stimulating its activity could be efficient to decrease soluble mHtt levels.

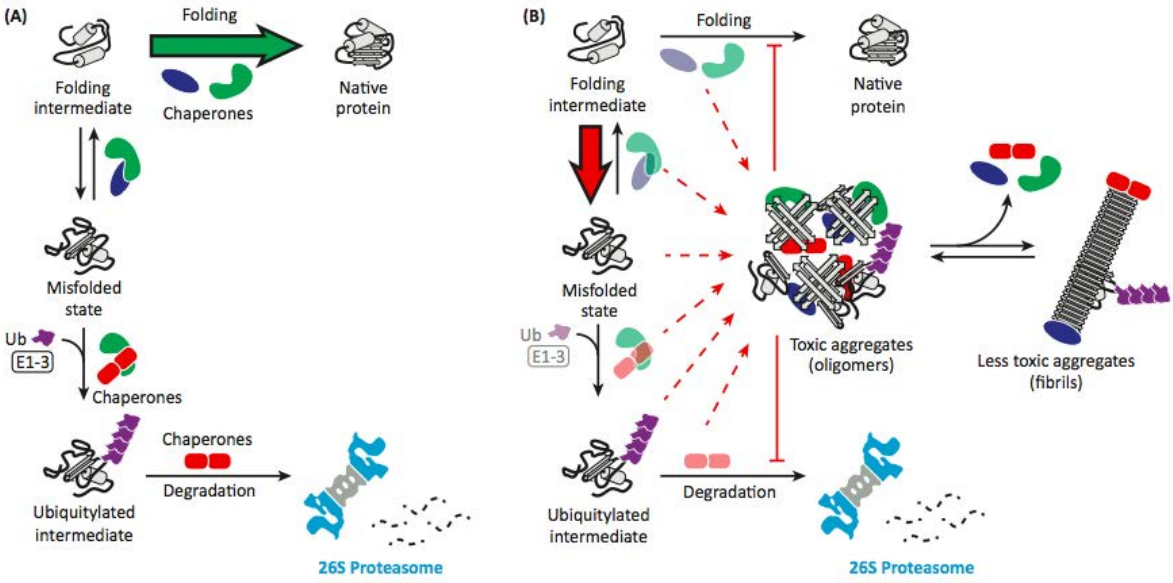

Figure 14. The ubiquitin-proteasome degradation pathway and its alteration in the presence of misfolded proteins.

A, In physiological conditions, there is an homeostasis between the formation of misfolded protein production and degradation through the ubiquitin proteasome system (UPS). Chaperones activity is sufficient to correctly fold most newly synthesized proteins. Alternatively, proteins that cannot be successfully folded after synthesis are degraded by the UPS. **B**, Protein degradation pathway is impaired in the presence of aggregates. Chaperone activity is altered by soluble and insoluble protein aggregates. This results in the accumulation of folding intermediates and misfolded proteins, which are polyubiquitylated and targeted for proteasomal degradation. When the accumulation of misfolded proteins exceeds the capacity of the UPS, additional protein aggregates containing ubiquitylated and nonubiquitylated protein molecules form. The role of aggregates is controversial as they can sequestrate functionally important proteins, therefore preventing them to fulfill their physiological functions. Alternatively, aggregation could represent a protective mechanism that secludes potentially toxic proteins into inclusions. From (**Hipp et al., 2014**).

ii) Transcription dysregulation

Dysregulation of gene transcription is a well-known feature of HD (**Figure 15**). The expression of hundreds of genes encoding receptors, enzymes and proteins involved in transport or synaptic function is disrupted by mHtt (**Moumne et al., 2013**). MHtt interacts with key transcription factors (cyclic AMP-response binding element (CREB), CREB-binding protein, p53, NF-κB or specificity protein 1) that are involved in the regulation of essential cellular functions including survival or control of cell proliferation. MHtt can result in both down or upregulation of gene expression (**Moumne et al., 2013**).

There is also evidence for interaction of mHtt with proteins involved in the epigenetic regulation of gene expression (**Moumne et al., 2013**). For example, mHtt interacts with CBP and p300/CBP complex and inhibits its histone acetyltransferase activity. This decreases histone phosphorylation and CBP-dependent gene transcription (**Moumne et al., 2013**). Because HD is characterized by transcriptional defects, histone deacetylase (HDAC) inhibitors have been tested as therapeutic strategies. In some studies, specific HDAC inhibitors improved HD pathology in mouse models of HD, primary culture of striatal neurons and in Drosophila (**Jia et al., 2012**). Epigenetic regulations also involve DNA methylation. In a recent study, Ng et al. showed that an important number of genes whose expression is altered in HD present abnormal DNA methylation (**Ng et al., 2013**).

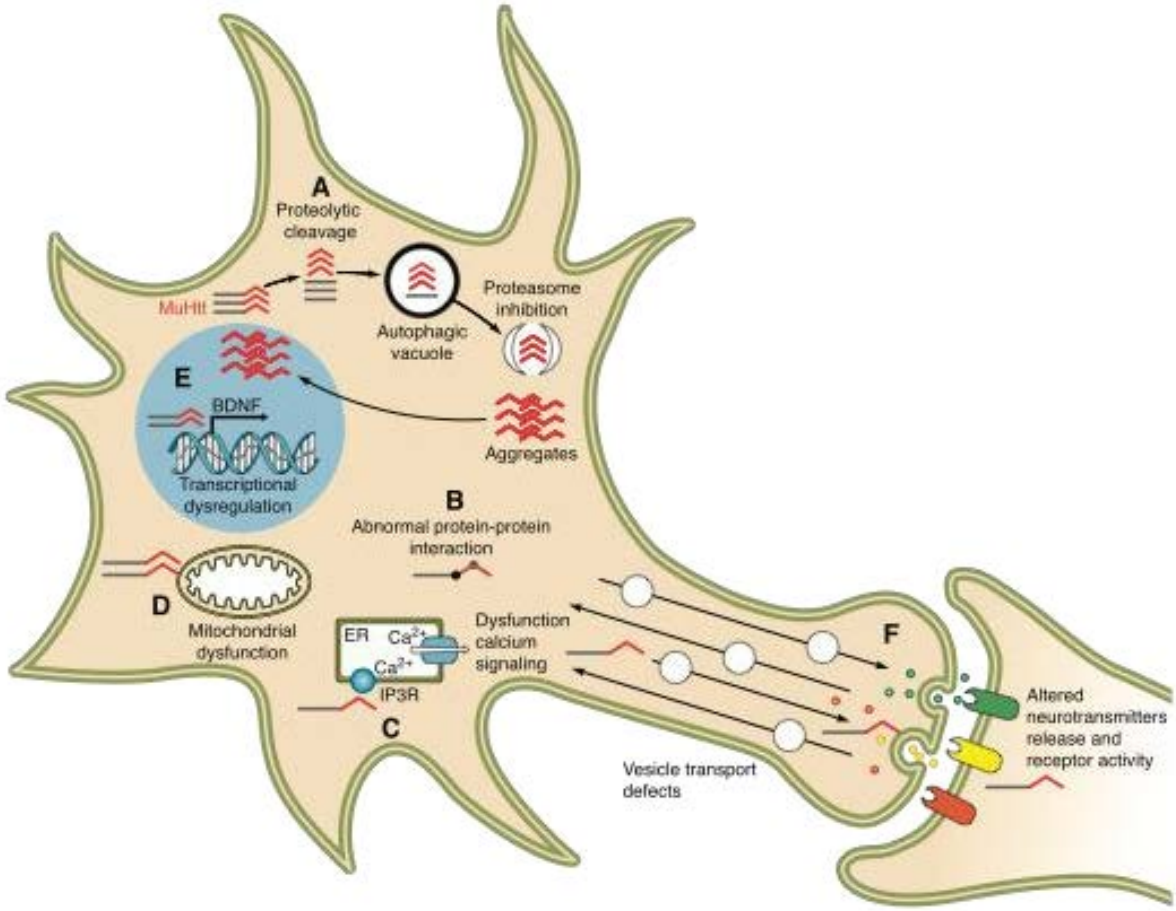

Figure 15. Cellular alterations and mechanisms of neurodegeneration in HD.
Several key cellular functions are altered in the presence of mHtt. MHtt is cleaved and N-terminal fragments containing the mutated polyQ expansion accumulate in the cell by forming nuclear and cytoplasmic aggregates. MHtt aggregates are not efficiently cleared because they impair autophagy and UPS degradation systems in neurons (A). Through its polyQ expansion, mHtt disrupts its interactions with a number of proteins or transcription factors, involved in trophic factor transport or regulation of gene expression (B). Neurons expressing mHtt also display abnormal Ca^{2+} signaling (C). HD pathogenesis involved the disruption of mitochondrial functions, through abnormal interactions of mHtt with the mitochondrial membrane. This dysfunction is associated with increased oxidative stress in neurons (D). MHtt alters the transcription of many genes, including *bdnf* (E). MHtt further disrupts BDNF vesicular transport in cortical neurons, therefore decreasing the trophic support of MSNs (F). At the cortico-striatal synapses, mHtt alters the release of neurotransmitter (glutamate) and trophic factors as well as disrupting the expression of their receptor on the post-synaptic element (F). From (**Zuccato et al., 2010**).

iii) Synaptic dysfunction and excitotoxicity

Excessive stimulation of glutamate receptors can lead to the excitotoxic cell death of neurons (**Figure 15**). There is a large body of evidence supporting the involvement of excitotoxicity in HD pathogenesis. Indeed, the observation that intrastriatal injection of kainate receptors and NMDAR agonists (kainate and quinolinate) resulted in acute death of striatal neurons and partly reproduced HD neuropathology strongly suggested the involvement of excitotoxicity in MSN death observed in HD (**Cepeda et al., 2010**). There is now compeling evidence, from electrophysiological studies, showing an alteration of the cortical-striatal glutamatergic signaling in HD models. In particular, it was shown that MSNs displayed an increased susceptibility to NMDA and glutamate through dysfunction of NMDARs in several transgenic mouse models of HD (**Cepeda et al., 2010**). In addition, change in expression of NMDARs subunits were found in the striatum of HD mouse models, including increased mRNA levels of NR1A and decreased expression of NR2B (**Zuccato et al., 2010**). NR2B-containing NMDARs are particularly enriched in the striatum. Therefore, alteration of NR2B-containind NMDARs functions could be involved in the selective vulnerability of the striatum in HD. Recently, Marco et al. showed that mHtt disrupted the synaptic retrieval of an NMDAR subunit, GluN3A by interfering with its endocytosis. Overexpression of GluN3A in WT mice reproduced synaptic deficits observed in HD. In addition, they showed that genetic deletion of GluN3A ameliorated synaptic, behavioral and neurodegenerative phenotypes in the YAC128 mouse model of HD (**Marco et al., 2013**).

Recent evidence implicates both synaptic and extra-synaptic NMDARs in the synaptic dysfunctions observed in HD. While synaptic NMDARs are associated with anti-apoptotic and pro-survival intracellular pathways (ERK), activation of extrasynaptic NMDARs activates apoptotic cascades and leads to Ca^{2+}-mediated mitochondrial dysfunction (**Parsons and Raymond, 2014**). For example, selective blockade of extrasynaptic NMDARs with low doses of memantine ameliorated behavioral phenotype (**Milnerwood et al., 2010**) and restored striatal atrophy in the YAC128 mouse model of HD (**Okamoto et al., 2009**).

iv) Mitochondrial dysfunction and oxidative metabolism

Energy deficit is a hallmark of HD (**Figure 15**). Patients with HD and even presymptomatic mHtt carriers show decreased cerebral and muscle glucose metabolism by PET imaging (**Grafton et al., 1992; Feigin et al., 2001**). Patients with HD as well as the majority of transgenic mouse models show significant weight loss with disease progression (**Chaturvedi and Beal, 2013**). NMR spectroscopy showed decreased levels of phosphocreatine and ATP in the cortex and the striatum of patients with HD (**Jenkins et al., 1993; Saft et al., 2005**). Deficits in energy metabolism suggest that mitochondrial dysfunction could be involved in HD. Indeed, mitochondrial complexes II and III expression are decreased in patients with HD. Furthermore, the toxin 3-nitropropionic acid that blocks the mitochondrial complex II succinate-dehydrogenase results in the selective degeneration of MSN, reproducing the main clinical feature of HD (**Brouillet et al., 1995**).

Different aspects of mitochondrial metabolism and energy production are modified in the presence of mHtt, which interacts directly with mitochondria. These defects include the alteration of energy production as well as mitochondrial fusion/fission, morphology, transport/trafficking and transcription (**Chaturvedi and Beal, 2013**).

HD is characterized by the apoptotic death of MSNs. Brains of patients with HD and in the R6/2 mouse model of HD showed increased levels of caspase 9 and cytosolic cytochrome C (**Kiechle et al., 2002**). Furthermore, mHtt promotes the phosphorylation of p53 and induces its dissociation with the apoptosis inhibitor iASPP. This increases the expression of apoptotic target genes (**Grison et al., 2011**). Finally, in the presence of mHtt, Huntingtin interacting protein 1 activates the extrinsic apoptotic pathway as it promotes the cleavage the pro-caspase 8 (**Gervais et al., 2002**). These results suggest that apoptosis and mitochondrial dysfunction are involved in MSNs death.

d) Non-cell autonomous mechanisms in HD

It is now well accepted that neuronal dysfunction that occurs in HD and in fact in any ND, is the result of alterations in both neurons and non-neuronal cells, referred to as 'non-cell autonomous' mechanisms (**Lobsiger and Cleveland, 2007**).

i) Reactive astrocytes

Many of the cellular alterations observed in HD involve neuronal functions that are regulated by neuron-astrocyte communication such as glutamate uptake, antioxidant defense, energy deficits or synaptic transmission. Importantly, astrocytes are reactive in the context of HD. Astrocyte reactivity is an early feature of HD since increase in GFAP staining can be detected in the striatum of presymptomatic mHtt carriers and increases with disease progression (**Faideau et al., 2010**). Thus, astrocytes are highly sensitive to early MSN dysfunction but there is also compelling evidence that some of their essential functions are disturbed in HD. First, astrocytes capacity to uptake glutamate is impaired in HD. GLT-1/EAAT2 mRNA and protein levels are decreased in patients with HD (**Faideau et al., 2010**) and mouse and fly models of HD (**Behrens et al., 2002; Lievens et al., 2005**) (**Figure 16**). Liévens et al. found a significant reduction of glutamate uptake in synaptosomal preparations that contained neuronal and astroglial processes from R6/2 HD mouse brains (**Lievens et al., 2001**). Importantly, a study carried out in our laboratory demonstrated that selective expression of mHtt by viral gene transfer in striatal astrocytes was sufficient to decrease GLT-1 expression, glutamate uptake and was associated with dysfunction of MSNs (**Faideau et al., 2010**). Using a transgenic mouse model, Bradford showed that mice carrying mHtt only in astrocytes developed motor abnormalities (**Bradford et al., 2010**). Evidence from an *in vitro* study suggested that while WT astrocytes protected neurons from mHtt-induced toxicity, HD astrocytes exacerbated MSN dysfunction when exposed to excitotoxic insults (**Shin et al., 2005**). Thus, alteration of glutamate uptake by reactive astrocytes contributes to the neuronal toxicity observed in HD.

Second, astrocytes contribute to functional synaptic transmission by buffering extracellular K^+ (**Figure 16**). Alteration of K^+ transmission is observed in mouse models of HD using electrophysiological recordings of MSNs (**Cepeda et al., 2010**). However, it was recently demonstrated that K^+ buffering capacity of astrocytes was altered in the R6/2 mouse model of HD and contributed to the synaptic dysfunction of MSNs. Kir4.1 is an inward rectifier K^+ channel, highly expressed in astrocytes that uptakes K^+ from synapses. In their elegant study, Tong et al. showed that Kir4.1 levels were decreased in R6/2 and Hdh150 mouse models of HD. This decrease was associated with increased extracellular K^+ *in vivo* and with altered electrophysiological properties of MSNs *in vitro*. Using a viral strategy, overexpression of Kir4.1 in striatal astrocytes improved some of the neurological features in R6/2 HD mice, suggesting that astrocyte K^+ buffering contributed to disease phenotype (**Tong et al., 2014**). However, it is not clear whether this alteration is due to the expression of mHtt in astrocytes or to disrupted neuron-astrocyte communication. It is to note that, in this study, Tong and colleagues did not evidence astrocyte reactivity in symptomatic R6/2 mice, based on GFAP expression and astrocyte morphology. Therefore, they showed that astrocytes could be dysfunctional without displaying a reactive phenotype.

Third, reactive astrocytes may provide less antioxidant support to vulnerable MSN in the context of HD (**Figure 16**). For example, evidence suggests that astrocyte antioxidant support to neurons through the release of ascorbic acid (AA) is altered in HD. AA is released by astrocytes; it protects neurons from oxidative damage and participates in the regulation of neuronal metabolism (**Castro et al., 2009**). AA release is coupled to glutamatergic synaptic activity and is transported into neurons by a neuronal-specific transporter. Interestingly, in the R6/2 mouse model of HD, AA concentration in the extracellular medium is lower than in age-matched WT mice but only during behavioral activity. In a recent study, Acuna et al. showed that this deficit was the result of an altered AA flux between astrocytes and neurons which involved different cellular mechanisms between presymptomatic and symptomatic phases of the disease. Indeed, *in vitro* and *ex vivo* experiments on slices, showed that presymptomatic R6/2 displayed a decrease in AA release from astrocytes whereas symptomatic HD mice showed an alteration of AA transport (**Acuna et al., 2013**).

Astrocytes also provide trophic support to neurons by releasing growth factors. Decrease production and release of such factors has been suggested to contribute to neuronal toxicity observed in HD (**Figure 16**). Recent evidence suggested that expression of mHtt in primary cultures of cortical astrocytes modified BDNF processing in astrocytes. Thus, HD astrocytes and their conditioned medium contained lower levels of mature BDNF. This was associated with decreased neurite development of primary cortical neurons (**Wang et al., 2012**). Consistent with these findings, viral-based delivery of BDNF by targeting astrocytes in the striatum delayed the onset of motor symptoms in the R6/2 mouse model of HD (**Arregui et al., 2011**). Conversely, transgenic mice overexpressing BDNF under the GFAP promoter displayed increased BDNF levels and enhanced neuroprotection after intrastriatal injection of quinolinate (**Giralt et al., 2010**).

In addition, astrocytes provide less trophic support for neurons by decreasing their release of the chemokine CCL5/RANTES (**Figure 16**). This chemokine is involved in neurite growth, neuronal migration and has neuroprotective properties. Importantly, CCL5/RANTES accumulates in the cytosol in patients with HD and in the R6/2 and Hdh150 mouse models of HD (**Chou et al., 2008**). It was recently shown that specific expression of mHtt in astrocytes decreased their ability to release CCL5/RANTES. Indeed, they found that mHtt inhibited the NF-κB pathway in astrocytes, which resulted in a decrease in *ccl5/rantes* transcription. In addition, CCL5/RANTES was retained in astrocytes due to a defective transport (**Chou et al., 2008**).

Overall, these results suggest that in HD, several supportive functions of astrocytes are impaired. This may participate in neuronal dysfunction and thus, contributes to HD pathogenesis. In most studies, the reactive phenotype of astrocytes was not observed or directly evaluated. Therefore, while these results suggest that astrocytes do not function normally in HD, whether there is a direct link between these alterations and their reactivity is not clear.

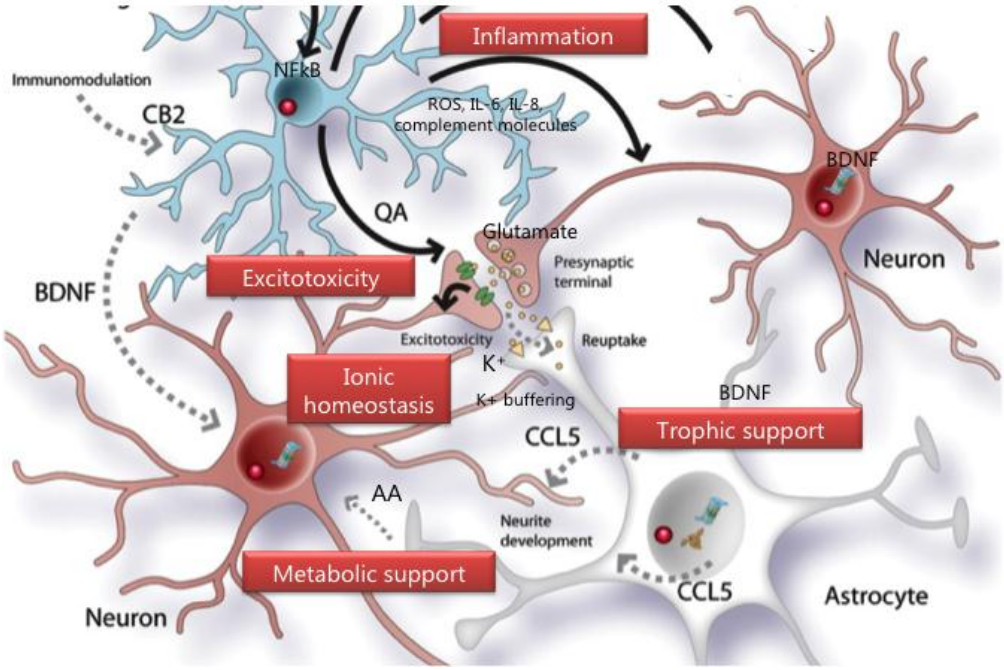

Figure 16. Reactive astrocytes display altered cellular functions and interactions with neurons in HD.
Several supporting functions of astrocytes are altered by mHtt expression and might enhance neuronal dysfunction in HD. Expression of mHtt in astrocytes is associated with decreased glutamate transporter levels and function, therefore enhancing excitotoxicity. Astrocytes display a decreased K^+ buffering capability, which contribute to the synaptic defects observed in HD. Expression of mHtt in astrocytes decreases the expression and secretion of chemokine (C-C motif) ligand 5 (CCL5), therefore attenuating its beneficial effects on neurite outgrowth and neuronal activity. Ascorbic acid (AA) synthesis and release from astrocytes is impaired in HD, thus decreasing AA-mediated antioxidant and metabolic support to neurons. Adapted from (**Cicchetti et al., 2011**).

ii) Activated microglia and immune cells

Microglial activation and recruitment of peripheral immune cells is a well-known feature of HD and is thought to contribute to neuronal toxicity. As astrocytes, microglial cells react at early stage in patients with HD, even in presymptomatic carriers (**Hsiao and Chern, 2010**). Importantly, microglial activation correlates with the severity of HD symptoms in an *in vivo* PET study and with neuronal death in HD brain samples (**Hsiao and Chern, 2010**). More generally, there is compelling evidence that mHtt expression alters the properties of peripheral immune system and enhances inflammatory processes. Indeed, the cerebrospinal fluid of HD patients showed increased levels of pro-inflammatory cytokines such as IL-6, IL-8 and TNF-α (**Silvestroni et al., 2009**). Furthermore, monocytes isolated from HD patients as well as microglia and macrophages from several HD mouse models were hyperactive in response to LPS stimulation (**Bjorkqvist et al., 2008**). Accordingly, Hsiao et al. compared the susceptibility of several transgenic mouse models of HD to inflammatory insult by systemic injection of LPS (**Hsiao et al., 2013**). They found that R6/2 and Hdh150 mice were particularly vulnerable to LPS whereas N171-82Q mice, expressing mHtt predominantly in neurons, did not show enhanced inflammatory response. This result suggests that expression of mHtt in glial cells might participate in the inflammatory phenotype in HD. In a recent and elegant work, Crotti et al. have studied mHtt-induced alteration of the transcriptome in a microglial cell line expressing mHtt. They found that expression of mHtt is sufficient to induce the expression of pro-inflammatory genes, some of which were also increased in the striatum and cortex of R6/2 mice and patients with HD. Importantly, in neuron-microglia co-culture, expression of mHtt in microglia increases the number of apoptotic neurons. In addition, to evaluate the specific contribution of mHtt expression in microglia, authors used Cx3cr1-Cre x Rosa-HD150 knock-in mice, which expressed mHtt only in microglia and not in other cells of the myeloid lineage. After LPS injection, mHtt expression in microglia led to higher neuronal death than in WT mice (**Crotti et al., 2014**).

Overall, these results suggest that both central and peripheral immune cells exhibit abnormal immune activation in HD.

In addition, alterations of specific metabolic pathways or receptor-mediated signaling in microglia might contribute to neuronal toxicity in HD. For example, evidence suggests that the kynurenine (KYN) pathway is involved in excitotoxic mechanisms observed in HD. Indeed, tryptophan degradation through the KYN pathway produces QA, a well-known inducer of excitotoxic lesions and used as a model of HD. In particular, dysregulation of the KYN pathway in microglia would contribute increased excitotoxicity in HD, as only microglia express the enzymes allowing the synthesis of QA by the KYN pathway such as tryptophan, KYN or 3- hydroxykynurenine (3-HK) (**Schwarcz et al., 2012**). In the brain of patients with HD, QA levels are particularly increased in the cortex and the striatum, the two vulnerable regions in HD. Similarly, levels of 3-HK are also increased in HD patients and mouse models, to concentrations that could trigger excitotoxic damage. Importantly, this increase in microglia-released molecules correlates with microglial activation (**Schwarcz et al., 2012**).

The endocannabinoid receptor signaling in microglia and immune cells has been involved in the pathogenesis of HD. Indeed, signaling through endocannabinoid receptor 2 (CB2) was shown to attenuate activation of the immune system. Deletion of CB2 receptor in microglia in the R6/2 mouse model of HD enhanced microglial activation and worsened disease phenotype (**Palazuelos et al., 2009**). In addition, genetic deletion of CB2 in peripheral immune cells in the BACHD mouse model of HD resulted in increased motor symptoms and disease onset (**Bouchard et al., 2012**). At the cellular levels, it decreases microglial activation and loss of synapses. Administration of a peripherally restricted CB2 receptor antagonist blocks these beneficial effects in R6/2 mice (**Bouchard et al., 2012**). These results suggest that signaling through CB2 receptor both microglial and peripheral immune cell contribute to the disease phenotype.

Taken together, these results suggest that alterations of the immune response both in the CNS and in the periphery actively contribute to HD pathogenesis. Especially, expression of mHtt in microglia or immune cells resulted in hyper-reactivity to inflammatory stimuli and potentiates mHtt toxicity on neurons.

The presence of reactive astrocytes, activated microglia and immune cells is a hallmark of HD. In fact, the role of this reactivity and its contribution to HD phenotype are poorly understood. In the case of astrocytes, this feature is not well reproduced in mouse models. Therefore, while astrocytes appear dysfunctional in HD, the contribution of their reactivity to the impairment of their functions is not known. In conclusion, while HD is mainly characterized by the selective vulnerability of MSNs, the ubiquitous expression of mHtt results in the impairment of cellular functions in various cell types, which contributes to the disease phenotype.

e) Therapeutic strategies

There is currently no available treatment for HD. The medication of patients with HD involves the symptomatic treatment of some of the psychologic and motor symptoms. Anti-depressants, neuroleptics and mood stabilizers are used to treat depression and some of the psychiatric symptoms. Anti-convulsant, benzodiazepines or DA-depleting agents are used for the treatment of motor symptoms (**Ross and Tabrizi, 2011**).

There are several ongoing clinical trials (phase 2-3) to assess the effect of therapeutic molecules including coenzyme Q10 and creatine in HD patients. Coenzyme Q10 (Q10) is an electron acceptor for the mitochondrial complex II-III, which has strong antioxidant properties. Early study showed that Q10 protected against mitochondrial dysfunction and oxidative stress in toxin and transgenic mouse models of HD (**Beal et al., 1994**). Q10 extended survival and delayed motor symptoms in the R6/2 and N171-82Q mouse models of HD (**Ferrante et al., 2002**). Later on, Smith et al. tested higher doses of Q10 in the R6/2 mouse model of HD. Q10-treated mice showed decreased weight loss, striatal atrophy and mHtt aggregates than non-treated animals (**Smith et al., 2006**). There is currently an

ongoing Phase 3 clinical trial (end 2017) to assess the safety, long-term tolerability and effectiveness of Q10 to slow HD symptoms.
Similarly, creatine is a promising therapeutic molecule for HD. There is compelling evidence from studies on animal models that creatine corrects energy deficits associated with HD. Creatine improved survival, delayed brain and MSN atrophy and reduced the formation of Htt aggregates in R6/2 mice (**Ferrante et al., 2000**). In patients with HD, creatine delayed cortical and striatal atrophy with a good tolerability at high doses (**Rosas et al., 2014**). There is currently a Phase 3 clinical trial (CREST-E) to assess the safety, tolerability and effectiveness of pharmaceutical creatine.

Several other therapeutic approaches are developed such as experimental strategies to decrease mHtt expression (gene silencing), targeting specific cellular dysfunction (mHtt degradation, apoptosis) or strategies to increase trophic support in the striatum and promote MSN survival.
For example, gene silencing can be achieved by the intracerebral injection of synthetic complimentary RNA such as short-hairpin RNA (shRNA), micro RNA (miRNA), small interfering RNA (siRNA) or antisense oligonucleotides. Following base-pairing, the target RNA is degraded by a specific machinery in the cell (**Ramaswamy and Kordower, 2012**). In the context of HD, miRNA, shRNA and antisense oligonucleotides against Htt have been developed. As mentioned previously, Htt is involved in a number of neuronal functions and thus, gene silencing must target mHtt and preserve Htt expression. A strategy is to design interfering RNA that target heterozygous single-nucleotide polymorphism (SNP) in the *htt* gene (**Schwarz et al., 2006**). In a study carried out in the laboratory, shRNA targeting *htt* SNP allowed the selective degradation of mHtt in a rat and mouse model of HD. Furthermore, *htt* silencing in human embryonic stem cells (hESC) was associated with functional recovery of BDNF transport (**Drouet et al., 2014**). However it may not even be necessary to only target mHtt and preserve WT Htt expression. In rhesus macaque monkeys, two studies showed that viral-delivery of shRNA and miRNA against total Htt decreased its expression and was well tolerated (**McBride et al., 2011; Grondin et al., 2012**).
An elegant study from D. Cleveland's laboratory showed that infusion in the CSF of antisense oligonucleotide directed against human Htt (HuASO) successfully reduced Htt levels in mouse models of HD and in non-human primates. Infusion of HuASO delayed disease progression reversed some symptoms and neuropathological features in several mouse models of HD (**Kordasiewicz et al., 2012**). A Phase 1 clinical trial is ongoing to assess the safety of antisense oligonucleotides in humans (**Schapira et al., 2014**).
Other strategies involve the stimulation of endogenous degradation pathways in cells to enhance the clearance of mHtt. Several studies showed that enhancing the UPS and autophagy degradation pathways cleared mHtt and were beneficial in models of HD (**Schapira et al., 2014**). Recently, a genetic screening for siRNA that regulate mHtt expression in a fly model of HD, allowed the identification of ubiquitin-like protein 1. It decreases mHtt levels by enhancing mHtt polyubiquitination and proteasomal degradation (**Lu et al., 2013**).

All these therapeutic approaches directly target neurons and for now, resulted in limited neuroprotective effects in patients with HD. In the laboratory, a model of CNTF overexpression in the striatum through lentiviral gene transfer showed drastic neuroprotective effects in models of HD (**Escartin et al., 2006**). Interestingly, CNTF is a potent activator of astrocytes and it was shown that the neuroprotective effects of CNTF were associated with increased efficiency of glutamate reuptake by activated astrocytes (**Escartin et al., 2006**). Therefore, CNTF represents a promising therapeutic molecule that stimulates astrocyte endogenous properties of support to promote MSN survival. The pre-clinical phase of a Phase I/II clinical study is ongoing in the laboratory to validate the safety of lentiviral vectors encoding CNTF in rodent and primate models of HD.

In conclusion, HD is characterized by the alteration of multiple cellular functions, both in neurons and other cell types in the CNS and the periphery. Therefore, while a hallmark of HD is the vulnerability of MSN, dysfunction of many other cell types and cell-cell interactions are likely to be altered to overall contribute to HD pathogenesis. Basic research has provided insights into the pathogenesis of HD but there are still controversial issues such as the role of mHtt aggregates or the contribution of reactive astrocytes. Expression of mHtt alters a number of essential cellular functions, especially in vulnerable neurons. Therefore, it might appear unrealistic to restore all these functions to develop a treatment for HD. Instead, the development of new approaches to influence astrocyte reactivity towards a neuroprotective phenotype would represent an alternative therapeutic strategy.

2) Reactive astrocytes in Alzheimer's disease

In this PhD project, we studied astrocyte reactivity and the activation of the JAK2/STAT3 pathway in reactive astrocytes in mouse models of HD and AD (Results, § III. A). We then assessed the consequences of manipulating astrocyte reactivity specifically in HD models (Results, § III. C). Therefore, I will only introduce key features of AD, which are relevant to understand the results section. The reader is invited to refer to recent and extensive reviews on the topic (**Giacobini and Gold, 2013; Reiman, 2014**).

AD is a neurodegenerative disorder and represents the most common form of dementia, characterized by cognitive deficits including learning impairment and memory loss (**Katzman, 1986**). The majority of AD cases are sporadic but approximately 1% of cases are associated with mutations in genes related to AD pathogenesis (amyloid precursor protein (APP), presenilin 1 and 2 (PS1, PS2)) (**Bertram et al., 2010**). At the cellular level, AD is characterized by extracellular accumulation of Aβ peptide forming amyloid depositions and neurofibrillary tangles formed by the accumulation of hyperphosphorylated Tau protein. AD is characterized by severe neuronal loss; primarly located in the hippocampus and the enthorinal cortex, the most vulnerable brain regions in AD (**Huang and Mucke, 2012**).

As for HD, astrocyte reactivity is detected in the brain of patients with AD before symptoms onset with imaging and proteomic techniques (**Owen et al., 2009; Carter et al., 2012**). Reactive astrocytes are found around amyloid plaques in patients with AD and in mouse models of AD (**Nagele et al., 2003; Wyss-Coray et al., 2003**). In addition to their apposition to amyloid depositions, reactive astrocytes can take up amyloid plaques and Aβ peptides (**Nagele et al., 2003**). In AD brains, double immunohistochemistry showed that reactive astrocytes internalize Aβ deposits (**Wyss-Coray et al., 2003**). In advanced AD cases, reactive astrocytes undergo cell lysis and form extracellular deposits that are $GFAP^+$ and contain neuronal-derived Aβ peptides (**Nagele et al., 2003**). Other studies showed that primary cultures of astrocytes from AD mouse were able to take up and degrade Aβ peptides and that this degradation was dependent upon the expression of apolipoprotein E (ApoE), a key player in AD pathogenesis (**Koistinaho et al., 2004**). This phenomenon also occurs *in vivo* as observed after the transplantation of GFP fluorescent astrocytes in the hippocampus in the APP/PS1dE9 mouse model of AD. Authors showed that astrocytes migrated towards amyloid plaques and internalized Aβ peptides (**Pihlaja et al., 2008**). Aβ peptides were degraded in reactive astrocytes lysosomes but this function is known to be altered in AD (**Wyss-Coray et al., 2003**). In a recent study, Xiao et al. showed that enhancement of the lysosomal biogenesis selectively in astrocytes can influence amyloid pathology in a mouse model of AD (**Xiao et al., 2014**). They used viral-mediated overexpression of transcription factor EB to enhance lysosome biogenesis and increase expression of lysosomal enzymes, cathepsins in the hippocampus of APP/PS1dE9 mouse model of AD. This resulted in the decrease of Aβ peptides and number of amyloid plaques in the hippocampus of AD mice (**Xiao et al., 2014**).

There are many lines of evidence suggesting that reactive astrocytes in AD display alterations of their functions (metabolism, oxidative stress, calcium signaling, connectivity ect…) that are deleterious for neighboring neurons. First, the metabolic support of astrocytes to neurons is likely to be altered in the context of AD. For example, in neuron-astrocyte co-culture, astrocyte internalization of Aβ peptides triggers intracellular changes that enhance glucose utilization, release of lactate, neurotoxic factors (oxygen peroxide) and glutathione (**Allaman et al., 2010**). These metabolic changes in astrocytes were associated with decreased neuronal survival *in vitro*. More importantly, in co-culture with no physical contact between neurons and astrocytes, Aβ-treated astrocyte medium decreased the viability of neurons (**Allaman et al., 2010**). Altogether, these results suggest that Aβ peptides can bind receptors and be internalized in astrocytes to increase clearance of the pathogenic molecule. In turn, this leads to alteration of astrocytic functions that are crucial for neuronal survival and thus contribute to AD pathogenesis.

Calcium signaling in astrocytes is also altered in mouse models of AD and *in vitro* when astrocytes are stimulated by Aβ. Reactive astrocytes in several mouse models of AD displayed hyperactive Ca^{2+} transients that were not observed WT mice using two-photon *in vivo* live imaging (**Takano et al., 2007; Kuchibhotla et al., 2009**).
The release of gliotransmitters by astrocytes is also modified in AD. Data from *in vitro* experiment reported that stimulation of primary astrocyte culture with Aβ induced the release of ATP. Exogenous but not astrocyte-released ATP restored Aβ-induced synaptic dysfunction in neuronal cultures (**Jung et al., 2012**). Very recently, two concomitant studies have provided evidence that reactive astrocytes release abnormal amounts of GABA that contribute to cognitive impairement in two mouse models of AD (**Jo et al., 2014; Wu et al., 2014**). They showed that reactive astrocytes abundantly released GABA, which resulted in a tonic inhibition of dentate gyrus granule cells in the hippocampus of AD mice. Inhibition of GABA synthesis or pharmacological blockade of GABA transporters restored synaptic plasticity and memory deficits in mouse models of AD (**Jo et al., 2014; Wu et al., 2014**).

Finally, as for many pathological conditions, neuroinflammation is a key feature of AD (**Birch et al., 2014**). Brains of patients with AD and mouse models displayed elevated levels of pro-inflammatory cytokines such as TNFα, IL-1β or COX2 (**Medeiros and LaFerla, 2013**). Several evidence points towards deleterious effects of neuroinflammation in AD pathogenesis. For example, blockade of TNFα interaction with its receptor prevented Aβ-induced synaptic loss and memory deficits in a mouse model of AD (**Medeiros et al., 2007; Medeiros et al., 2010**). Interestingly, AD transgenic mice appeared more susceptible to inflammatory insults than WT mice. For example, TNFα overexpression led to microglial activation and peripheral immune cell infiltration in the brain of 3xTg-AD but not WT mice (**Janelsins et al., 2008**). After intracerebral injection of recombinant Aβ in the rat cortex, reactive astrocytes upregulated pro-inflammatory cytokines (**Carrero et al., 2012**). This effect was associated with activation of the NF-κB pathway in reactive astrocytes. In addition, recent evidence showed that

Aβ increased the activity of the IKK complex resulting in the phosphorylation and degradation of IκBα. In turn, this led to the activation of NF-κB and subsequent increased expression of pro-inflammatory cytokines (**Medeiros et al., 2010**).

Taken together these results demonstrate that many astrocyte functions are altered in AD. Reactive astrocytes play a pivotal role and contribute to regulate various aspects to neuronal toxicity in AD. However, it is to note that a marjority of these studies have been performed in culture, whereby astrocytes and neurons are experimentally challenged with Aβ. Recent findings with transgenic mouse models, *ex vivo* and *in vivo* studies may provide a more integrated view of neuron-glia interactions to determine of the contribution of reactive astrocytes in AD.

3) Reactive astrocytes in other ND

a) Alexander disease

Alexander disease (AxD) is a rare genetic disorder characterized by leukoencephalopathy, psychomotor retardation and seizures. AxD is caused by heterozygous mutations in the *gfap* gene (**Brenner et al., 2001**). Indeed, overexpression of the human *gfap* gene is sufficient to trigger AxD-like phenotype in mice, displaying decreased lifespan and motor symptoms (**Messing et al., 1998**). At the cellular level, AxD is characterized by the presence of cytoplasmic aggregates in astrocytes, called Rosenthal fibers, which contain mutant GFAP associated and other proteins such as heat shock proteins. Brains of patients with AxD show extensive demyelination and neurodegeneration (**Sawaishi, 2009**). Interestingly, both in patients with AxD and in several mouse models, astrocytes are reactive. They strongly upregulate GFAP and show a marked hypertrophy of their primary processes (**Sosunov et al., 2013**). These morphological changes are associated with functional alterations of astrocytes and neuron-astrocyte interactions. For example, glutamate synthesis and glutamine transfer to neurons, measured by nuclear magnetic resonance spectroscopy, is altered in a mouse model of AxD (**Meisingset et al., 2010**). In addition, reactive astrocytes in AxD mouse models displayed alterations of GLT-1 expression and function, which impaired astrocyte ability to protect neurons from excitotoxicity (**Tian et al., 2010; Sosunov et al., 2013**). Reactive astrocytes also display altered coupling in the hippocampus suggesting a dysfunction of astroglial networks (**Sosunov et al., 2013**). Overall, AxD is the first example of a brain disorder primarly caused by astrocyte dysfunction, which as deleterious consequences on neighboring neurons and oligodendrocytes.

b) ALS

ALS is a fatal neurodegenerative disorder characterized by the progressive loss of upper motor neurons in the motor cortex and lower motor neurons in the brainstem and spinal cord. Most forms of ALS are sporadic but approximately 10% of patients have an inherited form. Mutations in four genes (*c9orf72, sod1, tardbp* and *fus/tls*) account for over 50% of the familial cases (**Ling et al., 2013**). Interestingly, the exanucleotide expansion in the *c9orf72* gene was found to be a common genetic

cause for ALS and frontotemporal dementia, which is another ND characterized by impairements of cognitive functions and language skills (**Lagier-Tourenne et al., 2013**). There is a growing body of evidence that ALS and FTD share early cellular dysfunctions that participate in the pathogenesis (**Ling et al., 2013**).

For ALS, many of the evidence on the pathogenic mechanisms come from the study of models carrying SOD1 mutations identified in familial forms of ALS. Pionnering work of D.Cleveland's laboratory clearly demonstrated that ALS pathogenesis involves non-cell autonomous mechanisms. Several studies on a transgenic mouse model of ALS, expressing the mutant Cu/Zn superoxide dismutase 1 (mSOD1) showed that disease onset depends mSOD1 expression in motor neurons whereas its expression in glial cells (microglia, astrocytes, oligodendrocytes and Schawnn cells) influenced disease progression (**Boillee et al., 2006; Lobsiger and Cleveland, 2007; Ilieva et al., 2009**).

In the case of astrocytes, there is compeling evidence from human brains and transgenic models that astrocyte dysfunction precede the appearance of symptoms and that they participate in disease phenotype. Indeed, GLT-1/ EAAT2 expression is decreased in patients with ALS as well as in mouse models (**Maragakis and Rothstein, 2006**). Restricted expression of mSOD1 in astrocytes induced their reactivity but was not sufficient to trigger ALS phenotype in transgenic mice, suggesting that astrocytes are not directly responsible for neuronal toxicity (**Gong et al., 2000**). More recently, Yamanaka et al. showed that deletion of mSOD1 selectively in astrocytes with the Cre-loxP system attenuated microglial activation and slowed the late stages of disease progression (**Yamanaka et al., 2008**). These results suggest that expression of mSOD1 in astrocytes is not sufficient to reproduce ALS phenotype but contributes to regulate disease progression. Evidence from *in vitro* experiments with hESC showed that expression of mSOD1 in astrocytes influenced motor neurons death by releasing of toxic factors (**Di Giorgio et al., 2007; Nagai et al., 2007; Marchetto et al., 2008**). For example, in human primary astrocytes expressing mSOD1, NOX2 activation led to the production of superoxide. This effect was toxic for hESC-derived motor neurons (**Marchetto et al., 2008**).

In addition, glial precursor cells carrying mSOD1 were grafted in the spinal cord of WT rats. After differentiation in astrocytes, mSOD1 expressing glial cells caused motor symptoms associated with motor neurons dysfunction and decreased GLT-1 expression (**Papadeas et al., 2011**). More recent evidence showed that astrocytes derived from progenitor cells of human spinal cord also displayed non-cell autonomous toxicity and promoted motor neuron death in co-culture experiments (**Haidet-Phillips et al., 2011**).

Overall, these results show a negative contribution of reactive astrocytes to ALS disease progression. Thus, targeting altered astrocytic functions is promising for developing therapeutic strategies for ALS. In this context, β-lactam antibiotics have been idenditied by high-throughput to enhance astrocyte-mediated glutamate uptake. This function was neuroprotective *in vitro* and *in vivo* in models of ALS

and excitotoxicity (**Rothstein et al., 2005**). Ceftriaxone, β-lactam antibiotic, has been used for the treatment of ALS in a clinical trial whose phase III has terminated this year (ClinicalTrials.gov NCT00349622).

c) PD

PD is a frequent neurodegenerative disorder characterized by motor symptoms such as resting tremor, bradykinesia and rigidity (**Jankovic, 2008**). Patients with PD also present with non-motor symptoms such as sleep disturbances, mood disorders and depression (**Jankovic, 2008**). As for many other ND, most of PD cases are sporadic and 3-5% of cases are familial. At the cellular level, PD is characterized by the selective loss of dopaminergic neurons in the substantia nigra pars compacta (SNpc), the presence of cytoplasmic inclusions of α-synuclein and neuroinflammation (**Hirsch et al., 2013**). Most of the pathogenic mechanisms involved in PD come from the study of the cellular alterations after 1-methyl-4-phenyl-1,2,3,6-tetrahydropyridine (MPTP) intoxication. This toxin induces a parkinsonian syndrome in humans, non- human primates and mice by causing the selective death of dopaminergic neurons in the SNpc (**Hirsch and Hunot, 2009**). PD pathogenesis involves many cellular alterations such as mitochondrial dysfunction, oxidative stress or altered proteolysis. A central feature in PD is neuroinflammation that involves microglia; peripheral immune cells but also astrocytes (**Hirsch and Hunot, 2009**). There is evidence that astrocyte participate in PD pathogenesis through the alteration of their support functions to neurons and their contribution to inflammatory processes. For example, restricted expression of mutated α-synuclein (A53T) in astrocytes caused motor symptoms, shortened lifespan in transgenic mice (**Gu et al., 2010**). At the cellular levels, expression of mutated α-synuclein in astrocytes resulted in enhanced microglial activation, expression of pro-inflammatory markers and neuronal loss in the mindbrain and spinal cord of PD mice (**Gu et al., 2010**).

While microglial contribution to pathogenesis is more studied in PD, there is also evidence for an influence of reactive astrocytes to disease phenotype. Thus, targeting specifically altered astrocytic functions might represent new therapeutic strategies to restore their functional support to neurons.

In conclusion, in patients with ND as well as in various animal models, reactive astrocytes display numerous changes in gene, protein expression or released molecules. Most of evidence points towards a deleterious role of these changes in reactive astrocytes on surrounding neurons. However, only few studies have directly evaluated the link between astrocyte reactivity and their deleterious effects on neurons. In particular, evidence showed that astrocytes could be dysfunctional without displaying a reactive phenotype. Therefore, it is important to dissect more precisely the functional changes and intracellular signaling pathways triggering astrocyte reactivity that are elicited in specific pathological conditions.

D. Are reactive astrocytes beneficial or detrimental for neurons?

Neuron-astrocyte interactions are essential for many brain functions. In addition, there is compelling evidence that reactive astrocytes can exert both beneficial and detrimental effects on neurons that influence disease progression (**Escartin and Bonvento, 2008; Sofroniew and Vinters, 2010 and see II.C**). Therefore, the role of reactive astrocytes in the pathological CNS is an ongoing debate. This issue is gaining more and more attention as most of the therapeutic strategies targeting exclusively neurons, have failed. Thus, understanding the contribution of reactive astrocyte to various CNS pathologies may help identify alternative therapeutic targets.

1) How specific astrocyte functions are modified when they are reactive? Evidence from experimentally activated astrocytes

In the first part of the introduction, I cited studies that have mainly described alterations of astrocyte functions in the context of specific pathological conditions. Here, I will present evidence highlighting an active role of reactive astrocytes in disease processes.

Reactive astrocytes can exert beneficial functions that support neurons through various functions including uptake of glutamate, release of trophic factors, antioxidant defense, metabolic support, degradation of aggregated proteins, BBB repair and glial scar formation. Alternatively, reactive astrocytes can also release pro-inflammatory molecules and thus exacerbate neuroinflammation. They can alter ionic homeostasis (K^+), releasing glutamate, produce ROS or contribute to cerebral oedema.

To study functional changes in reactive astrocytes and their impact on neurons, several studies have used various approaches (cytokines, growth factors or abnormal protein expression) to induce astrocyte activation and dissect their functional changes in a non-pathological context.

a) Metabolic and trophic support to neurons

Cytokines are known-inducers of astrocyte reactivity and can influence their metabolic status. Indeed, overexpression of CNTF in the rat striatum, through lentiviral gene transfer leads to robust astrocyte activation (**Escartin et al., 2006**). Furthermore, CNTF-activated astrocytes displayed rearrangement of their metabolic pathways, which provide them with increased resistance to metabolic insults. This was associated with neuroprotective effects of CNTF astrocytes after metabolic challenges *in vitro* (**Escartin et al., 2007**). In addition, stimulation of astrocytes with other cytokines resulted in changes in their metabolic pathways. For instance, pro-inflammatory cytokines such as IL-1β or TNFα stimulated glucose utilization, whereas anti-inflammatory cytokines IL-4 and IL-10 decreased the basal rate of glucose utilization in primary astrocyte cultures (**Gavillet et al., 2008; Belanger et al., 2011a**).

Cytokine-activated astrocytes have been shown to release various molecules that have trophic or toxic effects on neurons. For example, activation of cultured spinal cord astrocytes by CNTF or IL-1β

stimulated the release of FGF-2. This was associated with increased neuronal survival and neurite outgrowth *in vitro* (**Albrecht et al., 2002**). Conversely, IL-1, a known trigger of astrocyte activation, stimulated the release of pro- and anti-inflammatory molecules including cytokines (IL-6, IL-8, TNFα), chemokines (CCL5), NO, matrix metalloproteinases (MMP-9) and growth factors (NGF, CNTF, bFGF, PDGF) (**Pinteaux et al., 2009**). Similarly, cultured astrocytes stimulated with inflammatory mediators such as TGFβ 1, LPS or IFNγ alone or in combination upregulated various genes encoding cytokines, chemokines or growth factors (**Hamby et al., 2012**). This feature of reactive astrocytes was also reported *in vivo*, after MCAO and LPS injection (**Zamanian et al., 2012**).

Taken together, these results demonstrate the pivotal role of reactive astrocytes. Cytokine-stimulated astrocytes increased their metabolic support to neurons, which is neuroprotective *in vitro*. They can also release multiple anti-inflammatory cytokines or growth factors that favor neuronal survival. By contrast, reactive astrocyte can also increase their release of potentially neurotoxic molecules such as pro-inflammatory cytokines or NO.

b) Glutamate and excitotoxicity

Astrocytes reuptake glutamate from the synaptic cleft and thus prevent excitotoxic neuronal death in the brain. As previously mentioned, dysfunction of astrocyte glutamate transporters is observed in different pathological conditions such as ischemia or in ND (**Maragakis and Rothstein, 2006**).

Cytokine-stimulated astrocytes provided insights on the modulation of glutamate uptake by astrocytes. For example, CNTF-activated astrocytes strongly protected striatal neurons against excitotoxicity by QA (**Escartin et al., 2006**). This protection was associated with better handling of glutamate through a redistribution of glutamate transporters to lipid rafts at the plasma membrane (**Escartin et al., 2006**). In primary culture, astrocyte activation by cytokines (IL-1β, TNFα, IFNγ) induced variable effects on glutamate uptake by astrocytes and thus results are controversial (**Tilleux and Hermans, 2007; Namekata et al., 2008; Belanger et al., 2011b**). Nevertheless, cultured astrocytes stimulated with IL-1β and TNFα displayed increased glutamate uptake capacity that was associated with increased neuronal viability after excitotoxic insult (**Belanger et al., 2011b**).

c) Antioxidant defense

Astrocytes represent the main antioxidant defense of the brain. They synthetize and release antioxidant molecules that are in turn utilized by neurons as ROS scavengers (**Allaman et al., 2011**). Stimulation of cultured astrocytes with IL-1β and TNFα increased the release of GSH (**Gavillet et al., 2008; Belanger et al., 2011b**). These results suggest that reactive astrocytes, by releasing antioxidant molecules, might have neuroprotective effects on the surrounding neurons.

d) Water/ionic homeostasis

Astrocytes are key player in the regulation of water and ionic homeostasis because of the expression of specialized channels and transporters highly enriched at their perivascular endfeets. Vasogenic

edema consists in tissue swelling due to accumulation of extravascular fluid and is often observed in pathological conditions involving BBB disruption including brain injury, stroke or in the EAE model of MS. Reactive astrocytes can release molucules contributing to the BBB breakdown. Indeed, in culture, cytokine-stimulated astrocytes release metalloproteinases (MMP-9 and MMP-3) (**Cho et al., 2010; Hsieh et al., 2010**). MMP-9 was shown to degrade the BBB basal lamina following vasogenic odema (**Fukuda and Badaut, 2012**).

e) Synaptic transmission

Astrocytes regulate different aspects of the synaptic transmission. For example, astrocytes reuptake synaptically released glutamate and allow the replenishement of pre-synaptic vesicles through the glutamate-glutamine cycle involving the astrocytic enzyme, GS. Decreased GS expression is associated with an impaired inhibitory transmission. Indeed, decrease glutamine in the presynaptic element results in a decrease in GABA release at inhibitory synapses (**Clasadonte and Haydon, 2012**). In a recent study, Ortinski et al. used high-titer of viral vector encoding GFP to target hippocampal astrocytes and induce their activation. Astrocytes, activated with this non-specific approach, displayed decreased GS expression that was associated with altered GABAergic transmission in the hippocampus of mice (**Ortinski et al., 2010**).

Taken together, these results showed that numerous astrocyte functions are modified with their reactive status. Reactive astrocytes play a pivotal role and can exert both beneficial and detrimental effects on neurons. For example, cytokine-stimulated astrocytes are neuroprotective against excitotoxic or metabolic insults, increased neuronal antioxidant defense or promote neurite outgrowth. By contrast, activated astrocytes can also exert detrimental effects on neurons either by releasing of pro-inflammatory molecules or by change in astrocyte protein expression that impact neuron-astrocyte interactions. In any case, it is necessary to understand the functions of reactive astrocytes in order to manipulate these cells towards a neuroprotective phenotype.
In this context, several approaches have been developed to understand different aspects of astrocyte reactivity such as morphological changes, proliferation or more generally, intracellular targets.

2) Genetic ablation of astrocyte intermediate filaments

A hallmark of astrocyte reactivity is the upregulation of intermediate filament (IF) proteins such as GFAP and vimentin. In order to understand the role of IF in reactive astrocytes functions, transgenic mice simple KO for $GFAP^{-/-}$ or $Vim^{-/-}$ or double $GFAP^{-/-}Vim^{-/-}$ were developed. It is important to note, that IF upregulation is a terminal event in astrocyte reactivity process. Thus, the KO of these proteins might not be relevant to understand the effects of molecular trigger of astrocyte reactivity.
In the original paper, Pekny et al. showed that, after brain or spinal cord injury, simple KO $GFAP^{-/-}$ and $Vim^{-/-}$ mice display normal glial scars, similar to WT mice. By contrast, $GFAP^{-/-}Vim^{-/-}$ astrocytes were

not able to form a glial scar suggesting a synergistic effect of both intermediate filament proteins. Because of the lack of compensatory mechanism by other IF such as nestin, it was suggested that nestin required GFAP and vimentin expression to polymerize (**Pekny et al., 1999**). Thus, $GFAP^{-/-}Vim^{-/-}$ mice displayed attenuated astrocyte reactivity and glial scar formation in various models of brain injuries (**Pekny et al., 1999**). Later on, this model has been widely used to study the role of IF in reactive astrocytes in various acute injury models. After entorhinal cortex axon transection, $GFAP^{-/-}$ $Vim^{-/-}$ astrocytes displayed less hypertrophic primary processes while their overall volume was equivalent to those of WT astrocytes (**Wilhelmsson et al., 2004**). In this injury model, KO of IF was beneficial as $GFAP^{-/-}Vim^{-/-}$ astrocytes displayed higher synapse number than WT mice at 14 days post-lesion. It is to note, however, that this effect was not observed at earlier stages of the recovery process (**Wilhelmsson et al., 2004**).

Ablation of astrocyte IF was beneficial in other injury models including SCI (**Menet et al., 2003**), stroke (**Liu et al., 2014**), after retinal cell transplant (**Kinouchi et al., 2003**) or retinal detachment (**Nakazawa et al., 2007**). Following spinal cord hemisection, Menet et al. showed that $GFAP^{-/-}Vim^{-/-}$ mice displayed increased functional recovery with better motor performances. This functional recovery was associated with increased reinnervation of the lesioned area by supraspinal axon tracts (**Menet et al., 2003**). Recently, Berg et al. showed that $GFAP^{-/-}Vim^{-/-}$ mice displayed equivalent but delayed functional recovery compared with WT mice after peripheral sciatic nerve crush injury (**Berg et al., 2013**).

After medial cerebral artery (MCA) transection, a model of cerebral ischemia, $GFAP^{-/-}Vim^{-/-}$ mice displayed larger infarct volume than WT mice 7 days post-ischemia (**Li et al., 2008**). Conversely, in the Rose Bengal-induced cerebral cortical photothrombotic stroke, elicited in the forelimb motor area, Liu et al. showed that $GFAP^{-/-}Vim^{-/-}$ mice displayed impaired (or delayed) functional recovery (**Liu et al., 2014**). In this study, the stroke volume was similar in $GFAP^{-/-}Vim^{-/-}$ and WT mice but behavioral functional recovery was impaired in $GFAP^{-/-}Vim^{-/-}$ mice and associated with increased expression of chondroitin sulfate proteoglycan, a well-known inibibitor of axonal regeneration.

Taken together, these results highlight the complex contribution of astrocyte IF to functional recovery after CNS injury. Indeed, outcomes strongly depend on the type of injury (SCI, axonal transection, stroke, retinal detachment) and are even variable when considering different models of the same injury (spinal chord hemisection and peripheral sciatic nerve transection for SCI or MCA and Rose-bengal phototrombolysis for stroke).

Disruption of reactive astrocyte cytoskeleton was also studied in chronic pathological conditions such as in ND models. For example, In the SOD1H46R mouse model of ALS, genetic ablation of GFAP and vimentin led to shorter lifespan (**Yoshii et al., 2011**) while in the APP/PS1dE9 AD mice, it increased amyloid β load and the number of dystrophic neurites in the hippocampus (**Kraft et al., 2013**). These results suggest an essentially beneficial effect of reactive astrocytes IF in ND models.

Overall, the genetic ablation of IF in reactive astrocytes was used to determine their contribution in various injury or disease models. Results are heterogenous and suggest that the roles of IF upregulation in reactive astrocytes might be complex and context-depend. Furthermore, the functional consequences of cytoskeleton disruption on reactive astrocyte functions are difficult to assess in these models and knocking out intermediate filaments may impact multiple brain functions (**Shibuki et al., 1996**).

3) Ablation of scar-forming proliferating astrocytes

Another strategy used to evaluate the contribution of reactive astrocytes to CNS injury is the ablation of scar-forming proliferating astrocytes. This elegant model is based on the expression of the viral enzyme thymidine kinase (TK) in astrocytes in presence of ganciclovir (GFAP-TK) (**Bush et al., 1999**). Ganciclovir is metabolized in TK-expressing cells into a toxic product, which inhibits DNA polymerase and leads to cell death. Therefore, this system allows the selective ablation of cells expressing TK and undergoing proliferation (**Freeman et al., 1996**).

This model was initially developped to suppress proliferating enteric glia involved in the fulminant jejuno-ileitis (**Bush et al., 1999**). Later on, this approach was used in various CNS injury models including SCI and TBI and demonstrated multiple beneficial effects of proliferating astrocytes (**Bush et al., 1999; Faulkner et al., 2004; Myer et al., 2006**). Indeed, after SCI, disruption of glial scar formation led to increased infiltration of peripheral immune cells, enhanced neuronal death and demyelination. These effects were associated with worsened functional recovery of motor performances. Following controlled cortical impact lesion, a model of TBI, again, ablation of proliferating astrocytes exacerbated cortical neuron loss and inflammation (**Myer et al., 2006**). More recently, this strategy was used to determine the contribution of proliferating astrocytes in models of chronic pathological conditions such as ND. In the experimental autoimmune encephalopathy (EAE) model of MS, GFAP-TK mice also showed disrupted perivascular scars and increased leukocyte infiltration (**Voskuhl et al., 2009**). Overall, these convincing results showed that glial scar-forming reactive astrocytes are beneficial in a number of acute pathological conditions. These results are drastically opposed to the classical view of the glial scar especially after SCI (**Burda and Sofroniew, 2014**). In fact, glial-scar forming astrocytes act as a barrier to limit immune cell extravasation in the CNS parenchyma. These results are consistent with results obtained in the SOD1G93A mouse model of ALS, where astrocyte reactivity is diffused and progressive, without glial scar formation and immune cell infiltration. In this model, ablation of proliferating astrocytes had no effect on disease outcomes (**Lepore et al., 2008**). These results can furthermore be explained by the fact that proliferating astrocytes represents only a small fraction of reactive astrocytes in ND models (**Lepore et al., 2008; Sirko et al., 2013**).

4) Manipulation of intracellular signaling pathways to interfere with reactive astrocytes in pathological conditions

Several studies developed approaches to interfere with intracellular signaling pathways associated with astrocyte reactivity.

a) The NF-κB pathway

By overexpressing a dominant negative form of IkBα in $GFAP^+$ cells (GFAP-IkBα-dn), several studies have demonstrated that interfering with NF-κB pathway have effects on functional outcomes and inflammatory response after injury (**Brambilla et al., 2005; Bracchi-Ricard et al., 2013**). This model has been widely studied in a variety of acute disease models such as SCI, EAE, ischemia, axon transection or neuropathic pain.

In the initial paper, Brambilla et al. showed that GFAP-IκBα-dn prevents NF-κB activation following SCI. Eight-week post injury; $GFAP^+$ cells were still able to form a glial scar. However, the production of pro-inflammatory chemokines/cytokines such as CXCL10, CCL2 and TGFβ2 was decreased following SCI. GFAP-IκBα-dn mice displayed decreased lesion size and improved functional recovery associated with sparing of the white matter (**Brambilla et al., 2005**). However, in the context of a chronic ND like ALS, two independent studies have reported that inhibition of the NF-κB pathway in astrocytes does not influence disease phenotype in SOD1G93A mice (**Crosio et al., 2011; Frakes et al., 2014**). In an elegant study, Frakes et al. demonstrated that inhibition of the NF-κB pathway in reactive astrocytes did not influence disease progression, by two experimental strategies. First, they breeded mice deleted for Ikkb in astrocytes (GFAP-$Ikkb^{fl/fl}$) with SOD1G93A mice. Second, they overexpressed a dominant form of IκBα (AAV-IκB-SR) using viral gene transfer in astrocytes. They found that, overall, inhibition of the NF-κB pathway in reactive astrocytes did not influence motoneuron survival both in culture, whereby motorneurons were grown with WT or SOD1 G93A astrocytes or after injection in SOD1G93A mouse spinal cord.

Activation of the NF-κB pathway in reactive astrocytes was also studied in HD. In primary culture of astrocytes from R6/2 mouse model of HD, IKK activity was higher that in WT astrocytes (**Hsiao et al., 2013**). In this study, they used a lentiviral vector to overexpress a dominant negative form of IKKγ, to block NF-κB in the striatum of R6/2 mice. DN-IKKγ-injected ameliorated motor performances of R6/2 mice and prevented MSNs shrinkage (**Hsiao et al., 2013**). However, the lentiviral construct encoding DN-IKKγ infected astrocytes as well as neurons and microglia and thus the contribution of interfering with astrocytic NF-κB on disease phenotype cannot be ruled out.

It is to consider that, in most of the studies using GFAP-IkBα-dn transgenic mice, the cell-type specificity of both NF-κB activation and blockade of astrocyte reactivity by IkBα overexpression was not controlled. Because those mice display altered NF-κB signaling in $GFAP^+$ cells, developmental effects and/or alteration of NF-κB signaling in other cell types cannot be ruled out. Therefore, care is

needed when interpretating the consequences of the NF-κB signaling in reactive astrocytes on injury or disease outcomes.

b) The JAK/STAT pathway

As previously mentioned, activation of the JAK/STAT pathway is well correlated with astrocyte reactivity in many disease models. Several studies used transgenic mouse models to interfere with the JAK2/STAT3 pathway in reactive astrocytes. In this context, they found that reactive astrocytes mainly exert beneficial functions after injury. Because glial scar formation depends on STAT3 activation in reactive astrocytes, most of the studies have focused on acute injuries involving glial scar formation such as SCI (**Okada et al., 2006; Herrmann et al., 2008; Wanner et al., 2013**). As previously mentioned, STAT3 KO mice displayed disrupted glial scar formation, which was associated with increased neuronal death, infiltration of inflammatory cells and increased demyelination. In their study, Wanner et al. showed that $STAT3^{+}$ scar forming astrocytes displayed a distinct morphology and that they formed the core of the glial scar, along with fibrotic cells to separate the lesioned tissue from healthy parenchyma (**Wanner et al., 2013**). In all these studies, STAT3 KO mice displayed impaired functional recovery of motor performances after SCI. Very interestingly, Okada et al. demonstrated that deletion of *socs3*, the endogenous inhibitor of the JAK2/STAT3 pathway, in reactive astrocytes enhanced astrocyte reactivity, increased functional recovery and neuronal survival after SCI (**Okada et al., 2006**).

Similarly, after extracranial facial nerve transection in mice, astrocyte reactivity elicited in the facial nucleus was reduced in GFAP-STAT3 KO mice. This effect was associated with decreased neuronal survival and functional recovery of the synaptic inputs after axon transection (**Tyzack et al., 2014**). In the white matter injury model of neonatal brain injury, conditional deletion of *stat3* in astrocytes exacerbated white matter lesions and showed delayed maturation of oligodendrocytes (**Nobuta et al., 2012**). Furthermore, blocking the JAK2/STAT3 pathway either using astrocytes from STAT3 KO mice or by pharmacological inhibition resulted in an increase production of ROS as well as decreased GSH levels in cultured astrocytes (**Sarafian et al., 2010**).

Altogether, these results suggest that activation of the JAK2/STAT3 pathway in reactive astrocytes is beneficial effects on neuronal survival and ameliorated injury/disease phenotype.

c) The CN signaling pathways

CN is activated upon inflammatory stimulation and regulates gene expression through the activation of NFATs and NF-κB pathways (**Furman and Norris, 2014 and see B.2.d.i.**).

In cerebellar neuron-astrocyte co-culture experiments, transfection of astrocytes with a constitutively active form of CN protected neurons from inflammatory insults such as stimulation with TNFα and LPS (**Fernandez et al., 2007**). Interestingly, the same strategy in transgenic mice also protected neurons after acute brain injury or LPS injection (**Fernandez et al., 2007**). Expression of a constitutively active form of CN in the APP/PS1dE9 mouse model of AD resulted in decreased astrocyte and microglial

reactivity as well as decreased Aβ levels, amyloid plaques. These effects were associated with an amelioration of cognitive functions in AD mice (**Fernandez et al., 2012**). Interestingly, the beneficial effects of CN were mediated by the blockade of TNFα-mediated NF-κB activation and subsequent production of pro-inflammatory cytokines (**Fernandez et al., 2012**).

The opposite strategy was used to manipulate the CN pathway in reactive astrocytes in the APP/PS1dE9 mouse model of AD. In this study, authors used an adeno-associated viral vector encoding VIVIT, an inhibitor of NFATs to block CN/NFAT signaling in hippocampal astrocytes (**Furman et al., 2012**). It resulted in the improvement of cognitive functions, ameliorated synaptic plasticity and lowered amyloid levels in AD mice (**Furman et al., 2012**). Altogether, these results suggest that the CN pathway in reactive astrocytes is a double-edged component that can have strong anti-inflammatory and neuroprotective functions in acute injuries but has opposite effects in chronic pathological conditions such as AD.

d) The FGF signaling pathway

As previously mentioned, the FGF pathway has recently been proposed as a negative regulator of astrocyte reactivity (**Kang et al., 2014**). Indeed, they showed that *fgfr-1*$^{fl/fl}$ x *fgfr-2*$^{fl/fl}$ x *fgfr-3*$^{-/-}$ mice displayed increased astrocyte reactivity both in naive mice and after stab wound injury in the cortex. However, they showed that this disruption of the FGF signaling did not influence neuronal survival following brain injury (**Kang et al., 2014**).

Taken together, these data highlight that astrocyte reactivity is a complex mechanism, triggered by a variety of molecules. This intrinsic variability is further increased by the fact that these studies used different approaches (pharmacological inhibitors, transgenic mice and viral gene transfer) in a variety of injury or disease models (SCI, TBI, EAE, ND) that cannot be easily compared with one another. Furthermore, it is interesting to note that most of these studies used strategies to interfere with astrocyte reactivity to determine its effects on disease progression and neuronal survival. None of these studies have investigated reactive astrocytes “by themselves” to understand which and how their physiological functions are modified by their reactive status. Considering the number of essential functions that astrocytes fulfill in the healthy brain, it will be of great interest to decipher how these functions are modified with astrocyte reactivity. This would help identify new therapeutic targets to enhance neuroprotective functions of reactive astrocytes and decrease negative effects of neuroinflammation, especially in the context of ND, which remain incurable.

E. Objectives of the PhD project

Astrocytes are pleiotropic cells that display numerous support functions allowing the maintenance of brain homeostasis. Upon both acute and chronic pathological conditions, astrocytes become reactive. In particular, astrocyte reactivity is a hallmark of many ND, such as AD or HD. In ND, whether the multiple supportive functions of astrocytes are modified by their reactivity is a matter of intense debate. In particular, conflicting reports regarding the impact of reactive astrocytes on ND have been published recently (**Furman et al., 2012; Kraft et al., 2013; Frakes et al., 2014; Jo et al., 2014; Kang et al., 2014; Wu et al., 2014**). These discrepancies are usually explained by the fact that astrocyte reactivity is a heterogeneous response that encompasses multiple functional states depending on the disease, brain region or signalling cascade involved.

Therefore, in this study, we aimed at characterizing intracellular signaling pathways that specifically mediate astrocyte reactivity in multiple models of ND. By the development of original viral tools, we aimed at determining the contribution of astrocyte reactivity to disease progression in models of a prototypic ND, HD. Last, we aimed at modeling astrocyte reactivity in the absence of pathological condition to characterize reactive astrocyte functional features.

MATERIAL AND METHODS

II. MATERIAL AND METHODS

A. Viral vectors

1) Lentiviral vectors

Lentiviral vectors are derived from the human immunodeficiency virus-1. They are deleted for wild-type viral proteins and thus called “self-inactivating” (**Zufferey et al., 1998**). Lentiviral vector integrate their genetic material into the genome of infected cells, which allow stable transgene expression over time (**Deglon et al., 2000**).

The sequence of the gene of interest is placed under the control of the ubiquitous phosphoglycerate kinase (PGK) promoter. Furthermore, lentiviral vectors contain the Woodchuck hepatitis post-regulatory element allowing increased transgene expression through post-transcriptional regulation (**Zufferey et al., 1999**). Lentiviral vectors also carry the C-terminal polypurine track (**Zennou et al., 2001**) to enhance viral RNA retrotranscription.

Two types of vectors were used to express transgenes of interest either in neurons or astrocytes in the rodent and non-human primate brains. Lentiviral vectors targeting neurons are pseudotyped with the G protein of the vesicular stomatitis virus (VSV-G) (**Desmaris et al., 2001**). To target astrocytes, lentiviral vectors are pseudotyped with the G protein of the mokola lyssaviruses (MOK). MOK-lentiviral vectors transduce approximately an equal number of neurons and astrocytes in the mouse striatum. A “detargeting” strategy is thus used to restrict transgene expression to astrocytes (**Colin et al., 2009**). MOK-pseudotyped lentiviral vectors contain four copies of the target sequence of the neuronal miRNA124 (miR124T/MOK). Therefore, when the transgene is expressed into neurons, the mRNA is degraded through the microRNA degradation system. The remaining transgene expression is restricted at approximately 89% to astrocytes (**Colin et al., 2009**).

For the production of lentiviral vectors, HEK293T were transiently co-transfected with four plasmids (**Hottinger et al., 2000**). First, the transfer plasmid encodes the gene of interest. This plasmid contains the Ψ sequence necessary for the encapsidation of the viral genome. The transfer plasmid is deleted of regulatory sequences in the 3’-LTR region, which decreases the risk of formation of replicative vectors and prevents interference with the host cell promoter (**Zufferey et al., 1998**). Second, a plasmid encodes different viral proteins (capsid, reverse transcriptase, integrase etc…). Third, the regulator of expression of virion proteins (REV) plasmid encodes the rev gene. Finally, HEK 293T cells are transfected with a plasmid encoding the vector envelope, either VSV-G to transduce neurons or MOK-G to transduce astrocytes.

Viral proteins are synthetized and assemble around the viral RNA. Virions are then released in the extracellular medium. Forty-eight hours after transfection, HEK293T culture medium is collected; filtered and viral vectors are concentrated by ultracentrifugation. They are then resuspended in 0.1M PBS with 1% bovine albumine serum (BSA). The absence of replicative viral vectors is verified for each batch and the viral titer of infectious protein is determined using ELISA detection of the viral capsid protein p24.

2) Adeno-associated viral vectors

Adeno-associated viral vectors are derived from an adeno-associated virus (AAV), a nonpathogenic human parvovirus. AAV are non-integrative, thus the viral genome remains as an extrachromosomal episome in the host cell nucleus (**Flotte and Carter, 1995**). AAV are characterized by their serotype that determines their tropism in the CNS, due to the binding of the viral capsid to specific receptors (**Wu et al., 2006**). In the CNS, AAV-9 transduces astrocytes *in vivo* but also neurons and other cell types (**Cearley and Wolfe, 2006**). To express transgenes of interest in astrocytes, a truncated form of the gfap promoter was used (gfaABC1D) (**Lee et al., 2008**).

AAV vectors are produced by transient co-transfection of HEK293T cells with three plasmids. First, the AAV cis-plasmid carries the sequence of the gene of interest, under the control of the gfaABC1D promoter sequence. The transgene is flanked by two long inverted terminal repeats necessary for AAV genome replication. Second, the AAV trans-plasmid, which contains sequences encoding proteins necessary for AAV replication and capsid structure. Third, the adenovirus helper plasmid encoding the E1, E2A, E4, and VA proteins, is necessary for AAV vector replication.

Twenty-four hours after transfection, the HEK293T culture medium containing AAV particles is collected. The purification and concentration of AAV is performed using iodixanol gradient ultracentrifugation. The viral titer is determined using qPCR amplification of the viral genome (VG).

B. Mouse models of ND

1) Transgenic and lentiviral mouse models of ND

The table below summarizes the main characteristics of transgenic and lentiviral-based models of AD and HD that we used in this project.

Mouse model	Disease model	Genetic constructs	Promoter	Initial strain	Sex	Lifespan (months)	Genotype	Symptoms	Histopathological features	vulnerable brain region	Age of analysis	Primary paper
APP/PS1dE9	AD	Mo/hu APPswe and PS1-dE9	Two independent mouse protein prion promoters, transgenes integrated at the same locus, co-segregation	C57BL/6J	F	normal	+/Tg	Impairement Morris water maze (12 months) Impaired electrophysiological properties (basal and LTP) (16 months)	Intracellular amyloid and extracellular amyloid depositions, decreased synaptophysin staining	hippocampus, cortex	8 months	Jankowsky et al. (2004)
3xTg-AD	AD	knock-in PSEN1 (PS1M146V) embryos injected with human APPswe and tauP301L transgenes	Mouse Thy1.2	Mixed 129Sv and C57BL/6J	F	normal	Tg/Tg	Impaired electrophysiological properties (basal and LTP) (6 months) Memory and cognitive deficits (8 months)	Intracellular amyloid and extracellular amyloid depositions, tau pathology, dendritic spine alteration	subiculum, hippocampus (CA1), enthorinal cortex	12 months	Oddo et al., (2003)
N171-82Q	HD	Truncated exon 1 of human Htt with 82 polyQ	Prion	Mixed C57BL/6 and C3H/HeJ	M and F	4.5-6	+/Tg	Deficits at the rotarod test (4 months) Altered gait, grip strenght, locomotor activity (4.5-6 months)	Htt cytoplasmic and nuclear inclusions	striatum, motor cortex	22 months (endstage)	Schilling et al. (2004)
Hdh140	HD	Mo/hu exon 1 Htt with 140 CAG	Endogenous mouse Htt promoter	Mixed 129Sv and C57BL/6J	M	normal	+/Tg	hypolocomotion (4 months), impaired gait (12 months)	Htt cytoplasmic and nuclear inclusions	striatum, motor cortex	17 months	Menalled et al. (2003)
Lenti-Htt82Q	HD	Truncated exon 1 of human Htt with 82 polyQ- lentiviral vector	PGK	C57BL/6J	M	normal		no behavioral alterations	Htt cytoplasmic and nuclear inclusions	striatum	6 weeks	De Almeida et al. (2002)

Table 1 Transgenic and lentiviral mouse models of ND

Abbreviations: Mo/hu: chimeric mouse/human gene, Htt: Huntingtin, polyQ: polyglutamine; +/Tg: hemizygous, Tg/Tg: homozygous, LTP: long-term potentiation

2) Genotyping of transgenic mouse lines

Genotyping by polymerase chain reaction was performed at 4-6 weeks of age for N171-82Q, Hdh140 and APP/PS1dE9 mice. The Kappa Genotyping Kit (Kappa biosystems, Wilmington, MA) was used for genotyping. DNA was extracted from tail samples using Kappa protease and amplified using Polymerase Chain Reaction (PCR). 2% agarose gel was used to migrate samples and verify amplicon size. The following oligonucleotide sequences were used for genotyping:

N171-82Q mice: N171-82Q-gen-F GAACTTTCAGCTACCAAGAAAGACCGTGT; N171-82Q-gen-R GTGGATACCCCCTCCCCCAGCCTAGACC; N171-82Q-pos-F CAAATGTTGCTTGTCTGGTG; N171-82Q -pos-RGTCAGTCGAGTGCACAGTTT.

APP/PS1dE9 mice: APP-F AGGACTGACCACTCGACCAG; APP-R CGGGGGTCTAGTTCTGCAT.

Hdh140 mice: Hdh-F CATTCATTGCCTTGCTGCTAAG; Hdh-R CTGAAACGACTTGAGCGACTC.

C. Stereotaxic injections

Mice and rats were anesthetized with a mixture of ketamine and xylazine (**Table 2**). Lidocaine was injected subcutaneously on the skull 5 min before the beginning of surgery (**Table 2**). Animals received stereotaxic injections of diluted viral vectors in the striatum, the subiculum or the CA1 region of hippocampus using a 10 µl Hamilton syringe via a 34 gauge blunt needle. The stereotaxic coordinates were determined using Bregma and the ventral coordinate measured from the dura (**Table 2**).

For lentiviral vectors injections, mice received a total of 2.5, 3 or 3.5 µl per injection site at a rate of 0.2 µl/min. Rats received a total of 3.5 µl per injection site at a rate of 0.25 µl/min. For AAV injections, mice received a total of 2 µl per injection site at a rate of 0.2 µl/min. At the end of the injection, the needle was left in place for 5 min before being slowly removed. The skin was sutured and mice were allowed to recover.

Anesthetic	Dose (mg/kg)	
	Mice	**Rats**
Ketamine	150	75
Xylazine	10	10
Lidocaine	5	5

Injection site	Mice			Rats
	striatum	**subiculum**	**hippocampus**	**striatum**
Stereotaxic coordinates	*mm*	*mm*	*mm*	*mm*
Tooth bar	0	0	0	-3.3
Ear bars	4	4	4	6
Antero-posterior	1	-2.92	-2	+0.5
Lateral	+/- 2	+/- 1.5	+/- 1.5	+/-3
Ventral	- 2.5	-1.5	-1.3	-4

Tabl **otaxic injections of viral vectors in the rode**

Mice ine and Xylazine. Lidocaine is injected subc experiment, mice were either injected in the ted in the striatum. Ventral stereotaxic coor

Lentiviral vectors were diluted in 0.1 M PBS with 1% BSA at a final concentration of 100 ng p24/µl. AAV were diluted in 0.1M PBS with 0.001% pluronic acid. The table below summarizes the characteristics of all viral vector injections performed for this project.

Specie	Model/ Mice	Brain Region	Injections				Experiment
			Lentiviral vectors	*Dose (ng p24)*	Volume (µl)	Injections/ hemisphere	
mouse	C57BL/6	striatum	STAT3C+ GFP	200 + 50	2,5	bilateral	Selection of STAT3 and JAK2 constructs to induce astrocyte activation
			STAT3C opt + GFP	200 + 50	2,5	bilateral	
			JAK2WT+ GFP	200 + 50	2,5	bilateral	
			JAK2Y570F+ GFP	200 + 50	2,5	bilateral	
			JAK2T875N+ GFP	200 + 50	2,5	bilateral	
			GFP	250	2,5	bilateral	
rat	CNTF model	striatum	CNTF+SOCS3+GFP	50+200+ 50	3	right	Inhibition of astrocyte activation in the CNTF model
			CNTF+GFP	50+250	3	left	
mouse	C57BL/6	striatum	Htt18Q+JAK2ca+ GFP	100+150+ 50	3	left	Modulation of astrocyte reactivity in the lentiviral-based HD model
			Htt82Q +JAK2ca+ GFP	100+150+ 50	3	right	
			Htt18Q+SOCS3+ GFP	100+150+ 50	3	left	
			Htt82Q+ SOCS3+ GFP	100+150+ 50	3	right	
			Htt18Q+GFP	100+ 200	3	left	
			Htt82Q+ GFP	100+ 200	3	right	
			Htt82Q+ SOCS3+ GFP	150+150+ 50	3,5	right	Inhibition of astrocyte reactivity in HD
			Htt82Q+ GFP	150+ 200	3,5	left	
mouse	3xTg-AD and B9129Sv controls	subiculum	SOCS3+ GFP	200+ 50	2,5	right	Inhibition of astrocyte reactivity in AD
			GFP	250	2,5	left	Inhibition of astrocyte reactivity in AD
			AAV vectors	*Dose (VG/site)*	*Volume (µl)*	*Injections/ hemisphere*	
mouse	N171-82Q and B6C3 controls	striatum	SOCS3+GFP	$4.10^9 + 1.10^9$	2	bilateral	Effect of reactive astrocytes on N171-82Q mice phenotype
			GFP	5.10^9	2	bilateral	
			JAK2ca+GFP	$4.10^9 + 1.10^9$	2	bilateral	
mouse	C57BL/6	striatum	JAK2ca+GFP	$4.10^9 + 1.10^9$	2	bilateral	characterization of activated: microarray
			Tomato+ GFP	$4.10^9 + 1.10^9$	2	bilateral	characterization of activated: microarray
			GFP	5.10^9	2	bilateral	characterization of activated: microarray
mouse	C57BL/6	Hippocam-pus (CA1)	JAK2ca+GFP	$4.10^9 + 1.10^9$	2	bilateral	characterization of activated astrocytes: electrophysiology
			GFP	5.10^9	2	bilateral	

Table 3 List of experiments with stereotaxic injections of lentiviral and AAV vectors

D. Behavioral analysis

Behavioral tests were performed on N171-82Q HD transgenic and B6C3 (WT) control mice. Prior to any behavioral task, mice were habituated to the experimenter during 2 minutes per animal during 3 consecutive days. N171-82Q and WT mice were weighted once a week from 8 weeks of age and two times a week from 15 weeks of age.

1) Rotarod

The rotarod test is used to assess motor coordination in N171-82Q and WT mice. Mice were trained for 2 min on the rotating rod (Med-associates, St. Albans, VT) at a constant speed of 4 rpm. During the test, mice (up to 5 mice/ assay) were placed on the rod, accelerating from 4 to 40 rpm. The latency to fall and the speed at fall was automatically measured for each mouse. Three tests were performed during three consecutive days. Animals were only manipulated by the experimenter during the week of the experiment.

2) Open field

The open field test is used to assess spontaneous locomotor activity, exploratory behavior and anxiety in rodents. Animals were allowed to explore an arena, placed in a lighted room (30 lux), during 10 min. Mice movements were recorded by a camera and analyzed using EthoVision XT software (Noldus, Netherlands). The software automatically calculated the total distance moved during the trial. In addition, several parameters were manually assessed: the number of rearing, grooming and defecations.

E. Histology

1) Fixation protocol and slicing

All animals were euthanized with sodium pentobarbital overdose. According to the experiment, they were either transcardially perfused with 4% paraformaldehyde (PFA) or their brains post-fixed 24h in 4%PFA. Brains were then cryoprotected in a 30% sucrose solution. Coronal brain sections (mouse: 30 µm; rats and non-human primates: 40 µm) were cut on a freezing microtome, collected serially. 8 series for mice and 10 for rats were generated and stored at -20°C in storage solution until further analysis.

2) Immunohistochemistry and histochemistry stainings

Slices were rinsed in 0.1M PBS and incubated in 0.3% H_20_2 to inactivate endogenous peroxidases. For ubiquitin labeling, slices were incubated 1h in phenyhydrazine solution (1:1000) to further block peroxidase activity. For EM48 staining on brain slices from N171-82Q mice, slices were pretreated 20 min in TBS 0.05M, 0.05% Tween-20, pH=9 at 95°C. After rinsing, non-specific binding sites were

blocked by incubation of slices in Normal Goat Serum (NGS) (10% for ubiquitin staining and 4.5% otherwise) in 0.1M PBS/ 0.2% Triton X-100 1 hour at room temperature. Slices were then incubated with primary antibodies (**Table 4**) 48h or overnight at 4°C under agitation. Slices were rinsed and incubated with secondary biotinylated antibodies (anti-mouse or anti-rabbit, Vector laboratories, Burlingame, United-Kingdom) for 1h at room temperature under agitation. After rinsing, slices were incubated with the ABC complex (Vector laboratories) containing the avidine-biotin complex coupled to a peroxidase (HRP). Brain slices were then rinsed and the revelation was performed with either DAB or VIP reagents (Vector laboratories). For cytochrome C oxidase (COX) histochemistry, brain slices were incubated for 6 h at 37°C in PB 0.1M, 4% sucrose, 50 mg DAB and 30mg COX (Sigma, St.Louis, MO).

After rinsing, brain slices were mounted on superfrost slices and dried. For DAB revelation, slices were dehydrated using alcohol and toluene whereas for VIP revelation, slices were dehydrated using acetone and toluene. Coverslips were mounted using Eukitt (Sigma).

3) Immunofluorescence stainings

Antigen retrieval protocols were used for STAT3, phospho-STAT3, 4G8 and BrdU stainings. For STAT3 and phospho-STAT3 immunofluorescence, slices were pretreated in 100% methanol at -20°C for 20 min to permeabilize cell membranes. For 4G8 staining, slices were pretreated in 70% formic acid for 5 min to retrieve epitopes in amyloid depositions. For BrdU labeling, slices were incubated in 2N HCl 30 min at 37°C to denaturate DNA. Brain sections were blocked in 0.1M PBS, 0.2% Triton-X100 and either 1% BSA for STAT3 or 4.5% NGS otherwise. Slices were then incubated with primary antibodies 36h for STAT3 and phospho-STAT3 antibodies and overnight at 4°C otherwise (**Table 4**). After rinsing, brain slices were incubated for 1h at room temperature with fluorescent secondary Alexa fluor-conjugated antibodies (anti-mouse Alexa 488, 594; anti-rabbit Alexa 488, 594, 546 and 633; anti-chicken Alexa 594 and 633; anti-rat Alexa 594, Life technologies, Carlsbad, CA). Slices were stained with DAPI (1:2000, Life technologies) and were mounted using FluorSave reagent (Calbiochem, San Diego, CA).

For NeuN and S100β immunofluorescence protocols, the Mouse on mouse (MOM) kit (Vector laboratories) was used to reduce the non-specific background staining when using primary antibodies produced in mice. Sections were rinsed in 0.1M PBS and incubated in the MOM Mouse Ig Blocking Reagent. After rinsing, brain slices were incubated 5 minutes in working solution of MOM Diluent and 30 min at room temperature in the primary antibody diluted in the MOM Diluent. Sections were rinsed and incubated 1h at room temperature with anti-Mouse Alexa fluor 594 secondary antibody. Brain slices were then mounted using FluorSave reagent.

Antibody	Specie	Reference	Antibody dilution		
			IHC	IF	WB
4G8	mouse	Signet Covance		1:1000	
Actin	rabbit	Sigma			1:5000
BrdU	rat	Serotec		1:100	
DARPP32	rabbit	Santa-cruz	1:1000	1:1000	1:1000
EM48	mouse	Chemicon	1:500-1000		
GAPDH	mouse	Abcam			1:4000
GFP (biotinylated)	rabbit	Vector labs		1:500	
GFAP	rabbit	Dako	1:1000	1:1000	1:1000
GFAP-Cy3		Life sciences		1:1000	
GLT-1	rabbit	Frontiers	1:5000		
GS	rabbit	Sigma		1:1000	
IBA1	rabbit	Wako		1:1000	
IκBα	mouse	Cell signaling			1:500
JAK2	rabbit	Cell signaling			1:200
MBP	rabbit	Chemicon		1:500	
MAP2	mouse	Sigma		1:1000	
Nestin	mouse	BD bioscience		1:1000	
NeuN	mouse	Chemicon	1:500	1:500	
NG2	rabbit	Millipore		1:200	
Phospho-JAK2 (Tyr1007/1008)	rabbit	Cell signaling			1:200
Phospho-STAT3 (Tyr705)	rabbit	Cell signaling			1:200
S100β	mouse	Sigma		1:500	
STAT3α	rabbit	Cell signaling		1:500	1:200
Tom20	rabbit	Santa Cruz			1:3000
Ubiquitin	rabbit	Dako	1:1000		
Vimentin	chicken	Abcam		1:1000	
Vimentin	mouse	Calbiochem	1:2000	1:2000	

Table 4 List of antibodies and their concentrations for different applications.
Abbreviations: IHC, immunohistochemistry; IF: immunofluorescence and WB: western blot

F. Quantification of immunostainings

Labeled brain sections were analyzed using brightfield, epifluorescence (DM6000, Leica, Nussloch, Germany) or confocal microscopy (LSM 510; Zeiss, Thornwood, NY and TCS SPE or SP8, Leica).

1) Volume quantification

The quantification of parameters relative to the injected area was performed on 2.5x, 5x or 10x mosaic images, acquired using an epifluorescence microscope (DM6000, Leica) with fluorescence (Retiga, Qimaging, Canada) or brightfield (Microflire, Olympus, Melville, NY) cameras and Morphostrider acquisition software (Explora nova, France). Images were processed using Image J software (http://imagej.nih.gov/ij/, Bethesda, MA). Lesion (loss of DARPP32, NeuN, COX) or injected areas (GFP^+, $GFAP^+$, $EM48^+$, $ubiquitin^+$) were manually segmented on each slice and corresponding volumes were estimated using the Cavalieri method:

$$V = \Sigma (A \times n \times k)$$

Where A is the segmented area on each slice; n is the number of slice series and k is the slice thickness. Alternatively, the $GFAP^+$ volume was quantified on confocal images (see § III.F.2).

2) Quantification of double labeling and thresholding

Quantifications at the cellular level were were performed on stacked confocal images (13-18 steps, Z-step: 1 µm, maximum intensity stack) acquired with the 40x objective on three slices per animal and three fields on each slice. The $GFAP^+$ area was measured on each 40x Z-stack image using the threshold function of Image J software. It was divided by the area of the image and expressed as a percentage.

The average number of $GFAP^+$ cells expressing STAT3 in the nucleus ($nSTAT3^+/GFAP^+$ cells) was quantified on these images. In lenti-GFP-injected mice, we also quantified the average number of GFP^+ infected astrocytes co-expressing STAT3 ($GFP^+/STAT3^+$ cells), S100β (GFP^+/ $S100\beta^+$ cells) or GFAP ($GFP^+/GFAP^+$ cells). Finally, astrocyte soma was manually segmented and the corresponding mean gray value for STAT3 staining was measured with Image J. We also determined the number of cells with a mean gray value for STAT3 over a fixed threshold for each experiment. These cells were considered as cells expressing high levels of STAT3. Unfortunately, the presence of autofluorescent puncta in the subiculum, made it impossible to quantify reliably the intensity of STAT3 staining in WT and 3xTg-AD mice. Microscope settings and Image J thresholds were identical for all images and mice, within each experiment.

The number of $NeuN^+$ cells and of $EM48^+$ aggregates were quantified on histological stainings with DAB amplification with the threshold function of Morphostrider software (Explora Nova). The number of $NeuN^+$ cells was determined on three slices, anatomically corresponding to the injected area. For EM48 staining, the injected area was manually segmented and threshold applied to this region.

G. Cell culture

HEK293T cells were cultured in DMEM (Life technologies) supplemented with 10% fetal bovine serum (Sigma) and 1% penicicilin/streptomycin antibiotic cocktail (Sigma), at 37˚C with 5% CO_2. 20-30% confluent HEK293T cells (density 750 000 cells/ well) were transfected with 5 µg of plasmids encoding *stat3c, stat3copt, jak2, jak2 Y570F* and *jak2 T875N* in 0.5M $CaCl_2$ and HEPES buffer saline 2X. Non-transfected cells were used as controls. Cultured medium was changed 4-6 hours after transfection. Transgenes were expressed during 48h prior to cell lysis and protein extraction for western blot analysis (see § II. H.1).

H. Biochemistry

1) Protein extraction

Animals were euthanized by pentobarbital overdose. Brains were rapidly collected and sliced into 1mm-thick coronal sections using a brain matrix (Ted Pella, Redding, CA). The GFP^+ area was dissected on each slice using 1 mm (mice) or 1.5 mm (rats) diameter punches (Ted Pella) under a fluorescence macroscope (Leica Macrofluo, Leica). Alternatively, brain structure (striatum, dorso-anterior hippocampus) was dissected. Collected brain tissue was manually homogenized in a glass-glass potter (20 times) in lysis buffer containing 50 mM Tris, 100 mM NaCl, 1% sodium dodecyl sulfate, 1X protease and 1/100 phosphatase cocktail inhibitors. Samples (punches) were homogenized in 50 µl/ punch of buffer for mice and 75 µl/ punch for rats. Brain structures were homogenized in 200-300 µl of lysis buffer. The protein concentration was determined using the BCA protein assay (Thermo Fisher Scientific, Rockford, IL) on separate aliquots (16-20 µl), stored at -80°C. Aliquots of 30 to 90 µl were directly diluted in NuPAGE LDS sample buffer (4X) with NuPAGE® Sample Reducing agent (10X) (Life technologies) and stored at -20°C. The remaining volume was stored at -80°C.

2) Western blotting

Prior to gel migration, samples were heated 10 minutes at 75°C to denaturate proteins. Diluted samples (15-25 µg) were loaded onto 4-12% Novex NuPage Bis-Tris gel (Life technologies) along with the Kaleidoscope or spectra (8 µl) molecular weight marker (BioRad, Hercules, CA). Migration was set at a constant voltage of 200mV. The transfer onto nitrocellulose membrane was performed using the iBlot transfer system (Life technologies). Membranes were then colored with Ponceau red to control sample migration, quality of the transfer and absence of protein degradation. Membranes were rinsed in 25 mM Tris-HCl pH=7.4, 150 mM NaCl and 0.1% Tween-20 (TBS-T) and blocked with 5% BSA for the detection of phosphorylated proteins. Membranes were incubated with primary antibodies (**Table 4**) overnight at 4°C. After rinsing, membranes were incubated with horse raddish peroxidase (HRP)-coupled secondary antibodies (anti-mouse, cell signaling 1:500; vector laboratories 1:5000; anti-rabbit: cell signaling 1:500; vector laboratories 1:2000; anti-goat: 1:1000, sigma). Membranes were rinsed

and proteins revealed by chemiluminescence using the Enhanced chemiluminescence reagent (ECL, GE Healthcare) or the Clarity reagent (BioRad). Light emission was detected using the Fusion X2 camera (Thermo Fisher Scientific).

For the detection of phospho-protein levels, antibody stripping was performed after incubation with the phospho-antibody. Anti-phospho-protein antibodies were stripped off the membrane by incubation in 1X Re-blot plus solution for 15 min at RT (Millipore, Germany). Antibody stripping allows the subsequent incubation with the total protein antibody without contaminating signal. Stripping was controlled by incubation in secondary antibody for 1h at RT and revelation with ECL or clarity reagents.

Actin or glyceraldehyde-3-phosphate dehydrogenase (GAPDH) were used as loading controls. Positive controls for NF-κB pathway activation were included, they were prepared from HeLA cells treated with TNFα (Cell signaling, Danvers, MA).

I. Molecular biology

1) RNA extraction

Mice and rats were euthanized with an overdose of sodium pentobarbital. Animal brains were rapidly collected and sliced into 1mm-thick coronal sections using a brain matrix. The GFP^+ area was dissected on each slice using 1 mm (mice) or 1.5 mm (rats)- diameter punches under a fluorescence macroscope (Leica). Punches were stored in RNA later (Sigma) at -80°C until further processing. Total RNA was isolated from punches with TRIzol (Life sciences) according to the manufacturer's instructions. RNA quantity was determined using the Nanodrop-1000 spectrophotometer (Labtech France).

2) cDNA synthesis

To eliminate potential contamination of extracted RNA with genomic DNA, RNA was treated with RQ1 DNase I (0.1 u/µl, Promega, Madison, WI). Total RNA was diluted in RNA buffer containing TE pH7.6 RNA grade, DTT 0,1M and RNAse Inhibitor (0.001 u/µl, Promega). cDNA was synthetized with the Superscript VILO cDNA synthesis kit (Life Technologies) from 0.2 µg of RNA. For each experiment, an aliquot of RNA was incubated with without the reverse transcriptase as a control for genomic DNA contamination (RT-).

3) Real time quantitative Polymerase Chain Reaction (qRT-PCR)

qRT-PCR allows the quantitative measurement of mRNA levels of gene of interest. For each sample, diluted cDNA (0.15- 0.3 ng/µl) was incubated with the qRT-PCR mix containing gene-specific oligonucleotide sequences and the Platinum SYBR Green qPCR SuperMix UDG (Life Technologies). Each sample was assessed in triplicate. The following protocol was used for qRT-PCR:

- Polymerase activation: 10 min at 95°C

- Cycles (40 x): melting: 15 sec at 95°C
  elongation: 1min at 59°C
- Dissociation: 60°C to 95°C with 0.5°C steps.

In parallel, housekeeping gene sequences were amplified in order to normalize mRNA levels between groups. Three housekeeping genes *cyclophilin A*, *hprt1* and *gapdh* were used. According to the experiment, the housekeeping with the less variable mRNA levels was used for normalization. The abundance of each gene was normalized to the abundance of housekeeping genes using the ΔΔCt method. Distilled water and RT- RNA were used as negative controls.
For each gene, the melting curve and melting temperature were verified to confirm the presence of a unique amplicon and were used to control the absence of genomic DNA amplification with the RT-control. Each set of primer was validated using standards of diluted samples (3.5 to 0.028 ng/µl range) from control animals and qRT-PCR efficiencies were determined. They were comprised between 85 and 110% for each set of primers.
The number of animal per experiment was frequently too high to allow the quantification of both housekeeping gene and gene of interest on the same qPCR. Thus, we controlled inter-plate variability by the repeated quantification of *cyclophilin A*, *hprt1* and *gapdh* housekeeping genes from a unique control sample on all processed plates. Primers of housekeeping genes and control cDNA samples were processed identically on each plate. The variation coefficient of the measure of housekeeping gene quantity between plates was less than 2%.

J. Flow cytometry and cell sorting

1) Tissue dissociation

We used fluorescence activated cell sorting (FACS) to sort AAV-infected astrocytes based on their expression of fluorescent proteins. We used mice injected in the striatum with AAV-tdtomato + AAV-GFP, AAV-JAK2ca + AAV-GFP or AAV-GFP alone (**Table 3**). The GFP fluorescent area from four injected mice were pooled for each FACS session in order to collect enough material for microarray analysis.
Mice were euthanized, brains rapidly collected and sliced into 1mm-thick coronal sections using a brain matrix. The GFP^+ or $tdTomato^+$ area was dissected on each slice using 1 mm-diameter punches under a fluorescence macroscope (Leica). Punches were collected in 1 ml ice-cold Ca^{2+}, Mg^{2+} Hank's Balanced Salt Solution (HBSS). Brain tissue was dissociated using the Neural Tissue Dissociation Kit protocol (Miltenyi Biotec, Germany). Brain punches were incubated in pre-warmed solution containing papain and DNAse for 15 min at 37°C. They were manually dissociated using fire-polished Pasteur pipettes. After several incubations/dissociation cycles, the homogenate was filtered through a 40 µm-filter and diluted in 10 ml of ice-cold HBSS. Samples were then centrifuged 10 min at 300 g, the supernatant was discarded and the dissociated cells resuspended in 1 ml of HBSS.

2) Flow cytometry and FACS

FACS was performed at the Flow cytometry and cell-sorting platform (CEA, DSV, I2BM, iRCM, in collaboration with J. Baier and N. Deschamps) with an Influx biohazard cell sorter (BD Biosciences, San Jose, CA).

The population of interest was determined using SSC and FSC parameters to exclude myelin debris, aggregated cells or doublets. Sample from a non-injected C57BL/6 control mouse was used to evaluate basal autofluorescence. Gates were determined on a control sample (GFP^+) and were similar for all samples. Fluorescent cells were separated in different tubes: two tubes (tubes 1 and 2) containing infected astrocytes and one tube (tube 3) containing debris, non-infected astrocytes and other cell types. The number of GFP^+ cells collected in the tube 1 was constant for all conditions (approximately 6300 cells) in order to normalize the amount of total RNA to be extracted between samples. Similarly, the number of GFP- cells collected in the tube 3 was set at 100 000.

For each sample, sorting was performed within 1 hour. Sorted cells were centrifuged 5 min at 300 g, supernatant removed and cell lysis was immediately performed by addition of 800 µl of TRIzol reagent (Life Technologies). Samples were stored at -80°C until further processing.

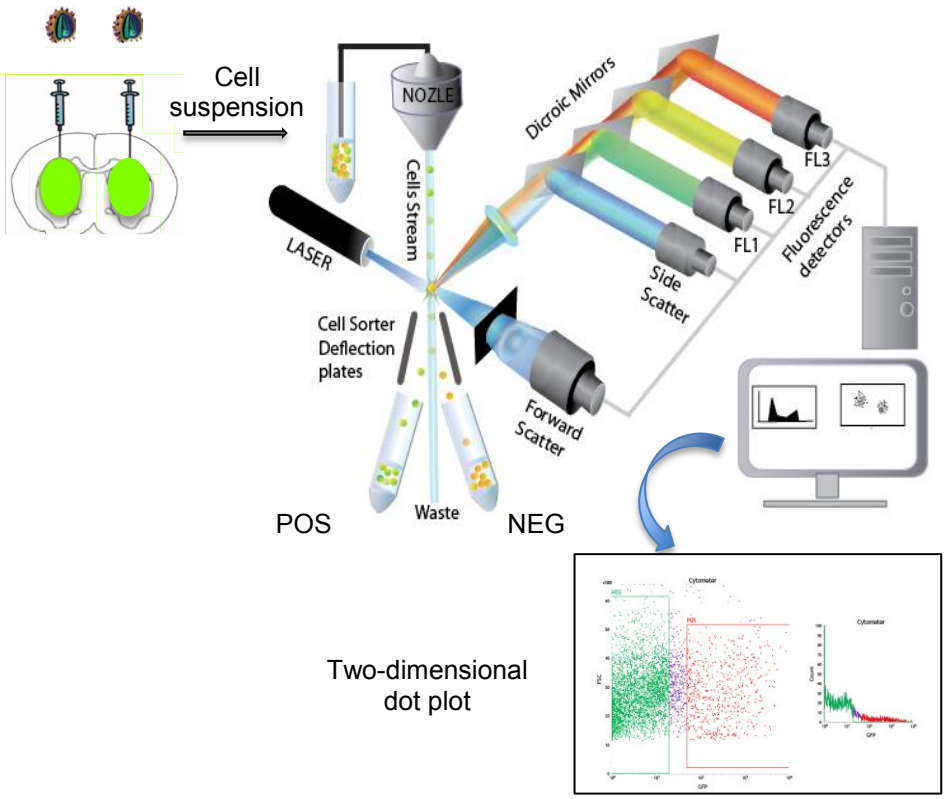

Figure 17 Fluorescence activated cell sorting of GFP-expressing astrocytes from mouse brain. GFP fluorescent punches are dissected from injected mouse brains. After tissue dissociation, the cell suspension is injected in an isotonic fluid stream inside the cytometer. Fluid pulses align droplets containing one cell each to the interrogation point where they cross the 488 laser. Emitted light is reflected on wavelength-selective dichroic mirrors towards fluorescence detectors. Fluorescence is measured for individual cell and results are represented as two-dimensional dot plots. Cell-containing drops are charged either positively or negatively and are separated by electrostatic deflection in specific tubes corresponding to the GFP^+or GFP^-.

K. Transcriptional analysis

This experiment was performed in collaboration with R. Olaso and Céline Derbois at the Centre National de Genotypage (CEA Evry).

1) RNA extraction

For microarray transcriptomic analysis, RNA extraction was performed using RNeasy micro kit (Qiagen, Netherlands). RNA was extracted by adding 200 µl of isopropanol, centrifuged at 12000 g during 15 min at 4°C. The aqueous phase was then transferred onto a fresh tube and an equivalent volume (350 µl) of freshly made 70% ethanol was added. RNA extraction was performed using RNeasy MinElute column according to the manufacturer's instructions (Qiagen). To eliminate potential DNA contamination, DNAse treatment was performed directly onto the column. In the final step, total RNA was eluted in RNAse-free water by heating at 70°C for 5 min. RNA quality and integrity was evaluated using using a Pico chip on the Agilent 2100 Bioanalyzer (Agilent Technologies, Santa Clara, CA) and RNA Integrity Number (RIN) determined for each samples. RIN were comprised between 5.4 and 8.7 for the samples in which RNA was detectable.

2) RNA amplification

Extracted RNA concentration was below (150 ng/µl), the recommended input amount to perform microarray analysis. Thus, RNA was amplified using the Ovation PicoSL VTA system V2 kit (Nugene). Kit steps consisted in 1) the first strand cDNA synthesis (RT), 2) Second strand cDNA synthesis, 3) Purification of cDNA 4) Amplification of Single Primer Isothermal Amplification (SPIA) cDNA. This amplification technique uses chimeric DNA/RNA primers (SPIA primers), DNA polymerase and RNAse H. Single strand DNA and SPIA cDNA were purified using Agencourt RNAClean XP magnetic beads (Nugen Technologies, San Carlos, CA). cDNA concentration was measured using Nanodrop-1000 spectrophotometer (Labtech France).

3) cDNA labeling

The Encore biotiNL kit (Nugen Technologies) was used for the fragmentation and labeling of the purified SPIA cDNA prior to hybridization on the Ilumina BeadChip. cDNA was fragmented in products ranging from 50 to 100 bp. Then, fragmented cDNA were linked in 3'-hydroxyl terminus to a biotin-labeled oligonucleotide. Labeled cDNA (0.56 to 2 µg) were purified using the MinElute Reaction cleanup kit (Qiagen). cDNA concentration was measured using Nanodrop-1000 spectrophotometer prior to the hybridization step.

4) Hybridization

Labeled probe hybridization to Illumina BeadChips mouse WG-6v2 was carried out using Ilumina's beadChip WG-6v2 protocol (Illumina, San Diego, CA). These beadchips contain 48,701 unique 50-

mer oligonucleotides in total, with hybridization to each probe assessed at 30 different beads on average. 22, 403 probes (46%) are targeted at ReferenceSequence (RefSeq) transcripts and the remaining 26,298 (54 %) are for other transcripts, generally less well characterized (including predicted transcripts).

BeadChips were scanned on the Illumina Iscan using IluminaIscan control software. Illumina GenomeStudio software was used for preliminary data analysis. Several quality control procedures were used to assess the quality metrics of each run. Total RNA control samples were analyzed with each run.

The recommended quantity of cDNA to load onto Illumina BeadChips is 1.5 µg cDNA in 10µl according to the manufacturer's instructions. The samples we used had very low RNA concentrations. Even after the Ovation kit amplification, cDNA quantities were below this specification. The concentration of hybridized cDNA was normalized at 537 ng for all samples. Two samples were too poorly concentrated and the hybridized with a cDNA concentration of 384 and 435 ng, respectively. Despite this experimental limitation, we were able to detect the signal of 409 probes significantly modulated in reactive astrocytes.

5) Microarray analysis

For the transcriptomic analysis of FACS-isolated astrocytes, we used mice injected with AAV-JAK2ca + AAV-GFP or AAV-GFP alone, in the striatum, at the same total virus load (**Table 3**). We performed two types of comparisons:

1/ we compared GFP^+ cells (i.e. infected astrocytes) with GFP^- cells (i.e. non infected astrocytes and all other cell types) within the same control group (mice injected with AAV-GFP). This first analysis allowed us to evaluate the enrichment in astrocyte markers in the GFP^+ cell population and to validate the sorting procedure. For clarity, these two cell populations are referred to as POS and NEG respectively.

2/ we then compared GFP^+ cells from mice injected with AAV-GFP (controls) with mice injected with AAV-JAK2ca. These two cell populations are referred to as GFP and JAK2ca respectively. This analysis aimed at evaluating the transcriptional changes in reactive astrocytes.

The control summary report was generated by the GenomeStudio software (Illumina), which evaluates the performance of the built-in controls of the BeadChips across particular runs. Variation in signal intensity, hybridization signal, background signal, and the background/noise ratio were controlled for all the samples analyzed in a run. We applied a quantile normalization (without background subtraction) for each comparison (POS vs NEG, N = 4 vs 2 and GFP vs JAK2ca, N = 4 vs 4) with GenomeStudio Software. The normalized hybridization value for each probe and sample were then analyzed with Microscoft Excel.

The objective of this transcriptional analysis was to identify functions or pathways that are altered in reactive astrocytes. This data set will then be used to select a few genes of interest and study their

role in reactive astrocytes by biochemical or functional analysis. Therefore, we decided to analyze the microarray dataset without corrections for multiple testing or false discovery rate in order to obtain the most comprehensive list of altered genes. For each comparison, difference in the average signal between the two groups was tested by a bilateral t-test.

POS vs NEG:

The list of genes significantly enriched in POS or NEG cells were compared with previous publications on the transcriptome of astrocytes (**Cahoy et al., 2008; Doyle et al., 2008; Orre et al., 2014b**), microglia (**Orre et al., 2014b**), neurons (**Doyle et al., 2008**), oligodendrocytes (**Cahoy et al., 2008; Okaty et al., 2011**).

GFP vs JAK2ca :

We first generated a list of 409 genes with a $p < 0.05$ with a bilateral Student's t-test. We supplemented the first list with another list of genes for which the t-test p value could not be calculated because the beadchip signal was undetectable in one group. We considered that it could happen when JAK2ca induced a strong down-regulation (genes undetectable in the JAK2ca group, but well expressed in the GFP group) or, on the opposite, when JAK2ca strongly induced gene expression (genes undetectable in the GFP group, but detected in the JAK2ca group). Probes with undetectable signal in 3 or 4 out of the 4 samples in the GFP or JAK2ca groups were selected. We then applied objective criteria to remove false positive genes. We only kept genes whose expression was both high enough (>170 fluorescent signal) and not too variable within samples of the same group (CV<50%). To further remove false positives from this list, we only selected genes with more than 20% difference between the GFP and JAK2 groups. This second list contained 170 genes. We then combined these two probe sets and used the Database for Annotation, Visualization and Integrated Discovery (DAVID) with KEGG analysis to identify enriched pathways.

L. Electrophysiological recordings

These experiments were performed in collaboration with S. Oliet, A. Panatier and J. Veran at the Neurocentre Magendie, Bordeaux.

1) Slice preparation

Transverse hippocampal slices (350 µm) were prepared from adult C57BL/6 mice (12-17 weeks old) as described previously (**Panatier et al., 2011**), in accordance with the French National Code of Ethics on Animal Experimentation and approved by the Committee of Ethics of Bordeaux (No. 50120110-A). Mice were anesthetized with isoflurane (5%) and euthanized. The brain was rapidly excised and placed in ice cold artificial cerebrospinal fluid (ACSF) saturated with 95% O2 and 5% CO2 and

containing (in mM): 125 NaCl, 2.5 KCl, 1.25 NaH_2PO_4, 1.3 $MgSO_4$, 2 $CaCl_2$, 26 $NaHCO_3$ and 10 glucose (pH 7.3; 300-305 mosmol/kg). A block of tissue containing the hippocampus was prepared and sagittal hippocampal slices were cut on a vibratome (Leica, Nussloch, Germany). Slices were incubated 30 min at 32°C and then allowed to recover for at least one hour at room temperature. Then, they were transferred to a recording immersion chamber where they were perfused (3 ml/min) with ACSF at room temperature.

2) Field recordings

A cut in between CA3 and CA1 was made to avoid epileptiform activity, due to the presence of picrotoxin (50µM) in the ACSF just before the recording. CA3-CA1 areas were identified with differential interference contrast microscopy (Olympus BX50). Field excitatory postsynaptic potentials (fEPSPs) were recorded with a Multiclamp 700B amplifier (Axon Instruments, Inc.) using pipettes (2-3 MΩ) filled with ACSF and placed in the vicinity of fluorescent astrocytes, in the stratum radiatum of CA1 area. Synaptic responses were evoked at 0.033 Hz by orthodromic stimulation (100 µs) of Schaffer collaterals using a glass pipette, filled with ACSF and placed in the stratum radiatum >200 µm away from the recording electrodes. LTP was induced by applying a high-frequency stimulation (HFS) protocol consisting of a 100 Hz train of stimuli for 1 s repeated three times at 20 s intervals in current clamp mode. Signals were filtered at 2 kHz and digitized at 10 kHz via a DigiData 1322 interface (Axon Instruments Inc., Orleans Drive Sunnyvale, CA).

3) Data analysis

Data were collected and analyzed using pClamp 9 software (Axon Instruments, Inc.). Average fEPSPs traces were obtained from at least 10 min of stable recordings. Data are reported as mean ± SEM. Significance was assessed at $p < 0.05$.

M. Statistical analysis

Results are expressed at mean ± sem. Statistical analysis was performed using Statistica software (Statsoft, Tulsa, OK). A Student's t-test was used to compare two experimental groups (example: WT versus transgenic mice) and a Student's paired t-test for left-right comparisons. The fraction of cells expressing high levels of STAT3 was normalized by the arcsine transformation, before applying a Student's t-test. A one-way ANOVA test and Scheffé post-hoc tests were used when comparing more than two groups. A repeated measure ANOVA and Bonferonni post-hoc test was used for analysis of the rotarod test. The significance level is set at $p < 0.05$.

RESULTS

III. RESULTS

The results will be divided in four parts: first, we studied the JAK2/STAT3 pathway in reactive astrocytes in various models of ND. Second, we developed new viral tools to manipulate the JAK2/STAT3 pathway in reactive astrocytes. Third, we used these newly developped tools to determine the influence of reactive astrocytes on neuronal dysfunction in two models of HD. Last, we studied the impact of astrocyte reactivity on astrocyte transcriptome and on astrocyte modulation of synaptic activity.

A. The JAK2/STAT3 pathway is activated in reactive astrocytes in various neurodegenerative disease models

In this first part, we studied the JAK2/STAT3 pathway, a well-known signaling pathway, involved in acute CNS injuries (**Sofroniew, 2009**). We aimed to determine whether this pathway was also associated with astrocyte reactivity observed in chronic pathological conditions such as ND.

1) Astrocyte activation is observed in vulnerable brain regions in AD and HD mouse models

Astrocyte reactivity occurs both in acute and progressive pathological conditions and is a hallmark of multiple ND (**Sofroniew and Vinters, 2010**). Astrocyte reactivity develops in vulnerable regions in early stages of ND and progresses along with neurological symptoms and cell death. Reactive astrocytes are observed in close proximity to amyloid depositions in both patients with AD and mouse models of AD (**Mitani and Tanaka, 2003; Lobsiger and Cleveland, 2007**). They are also found in the striatum and cortex of patients with HD and some mouse models of HD (**Vonsattel et al., 1985; Yu et al., 2003; Faideau et al., 2010**).

a) Astrocyte reactivity in AD models

We studied astrocyte reactivity in two transgenic models of AD. APP/PS1dE9 mice carry mutated forms of the human APP and PS1, associated with familial forms of AD (**Jankowsky et al., 2004**). 3xTg-AD mice harbor mutated APP, PS1 and a mutation of the microtubule-associated protein Tau (TauP301L) that reproduces the tau pathology observed in patients with AD (**Oddo et al., 2003a**). Reactive astrocytes overexpressing GFAP were found around $4G8^+$ amyloid depositions in both the APP/PS1dE9 and the 3xTg-AD transgenic mouse models of AD, consistent with previous findings (**Oddo et al., 2003b; Ruan et al., 2009**). APP/PS1dE9 mice develop amyloid plaques from 7-8 months of age, thus we decided to study 8 month-old animals. In these mice, astrocytes overexpressed GFAP and displayed hypertrophic processes in the stratum lacunosum moleculare and the dentate gyrus (**Figure 19A**, see also **Figure 22A, B**). We quantified this phenomenon by counting the number of pixels that were positive for GFAP staining on confocal images of the hippocampus. The $GFAP^+$ area was four times larger in APP/PS1d9 mice than in WT mice ($p < 0.001$, n = 3-4 mice/

group, Student's t-test; **Figure 19B**). Astrocytes in APP/PS1dE9 mice also strongly expressed vimentin (**Figure 22B**).

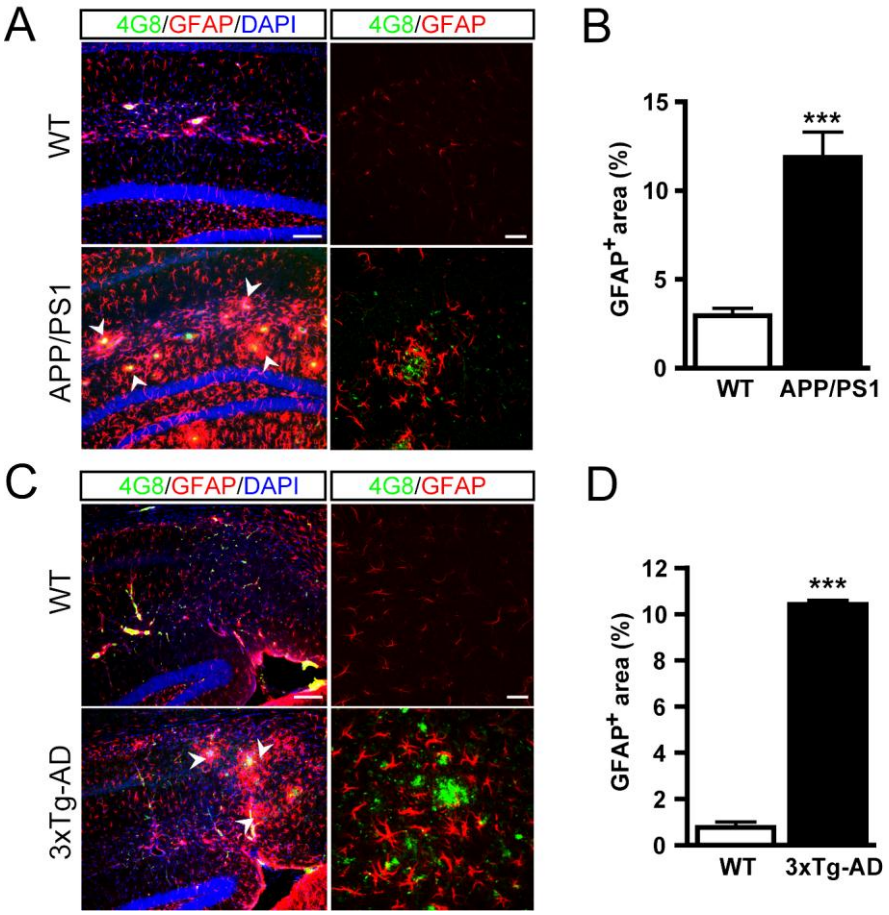

Figure 19. Mouse models of AD display astrocyte reactivity the hippocampus.
A-C, Images of double stainings for amyloid plaques (4G8, green) and astrocytes (GFAP, red) on AD mouse brain sections. **A,** In 8-month-old APP/PS1dE9 mice, hippocampal astrocytes strongly up-regulate GFAP and display a reactive morphology around amyloid depositions (arrowheads) in the stratum lacunosum moleculare and the dentate gyrus compared with age-matched controls. **B,** Quantification of the $GFAP^+$ area in the hippocampus of APP/PS1dE9 and WT mice. **C,** In the subiculum, 3xTg-AD mice display amyloid depositions that are surrounded by $GFAP^+$ reactive astrocytes (arrowheads). **D,** Quantification of the $GFAP^+$ area in the subiculum of 12-month-old 3xTg-AD mice and age-matched WT mice. Data are mean ± sem. N= 3-6/ group. *** $p < 0.001$, Student's t-test. Scale bars: 100 µm, 20 µm.

The APP/PS1dE9 mouse is a quickly evolving model of AD, with substantial deposits of amyloid at 6 months of age (**Jankowsky et al., 2004**). We thus analyzed astrocyte reactivity in 3xTg-AD mice, a more progressive model of AD. These mice develop amyloid depositions from 12 months of age. Therefore, we analyzed 3xTg-AD mouse brains at this age. We observed astrocyte reactivity around amyloid depositions primarily in the subiculum in female 3xTg-AD mice at 12 months of age (**Figure 19C**, see also **Figure 23A, B**). In this region, the $GFAP^+$ area was 13-fold larger in 3xTg-AD mice than in age-matched controls ($p < 0.0001$, n = 3-5 mice/ group, Student's t-test; **Figure 19D**). Furthermore,

astrocytes displayed a reactive morphology with enlarged soma and processes and overexpressed vimentin, which was nearly undetectable in WT mice (**Figure 23B**).

b) Astrocytes reactivity in HD models

We also studied astrocyte reactivity in HD mouse models. We used two transgenic mouse models of HD: the N171-82Q mice and the Hdh140 knock-in HD mice. N171-82Q mice express a truncated N-terminal fragment of the human Htt with 82 polyglutamine repeats (**Schilling et al., 1999**). The Hdh140 model is a knock-in mouse model, carrying a human/mouse chimeric *Htt* sequence with 140 CAG repeats (**Menalled et al., 2003**).

In the first cohort of N171-82Q mice that we studied, we observed reactive astrocytes overexpressing GFAP in the cortex and striatum of endstage HD mice, at 18 weeks of age (**Figure 20A**). However, this increase in GFAP was only detectable using immunostaining with DAB amplification. Indeed, we could not detect GFAP upregulation by immunofluorescence. In addition, we did not evidence upregulation of vimentin, another marker for reactive astrocytes.

In the Hdh140 model of HD, reactive astrocytes were detected in a 17 month-old mouse compared with an age-matched control mouse using GFAP staining (**Figure 20B**). While interesting, we had no other samples from old Hdh140 mice to quantify this phenomenon. It is to note, however, that in the Hdh140 model of HD, astrocyte reactivity was not observed at earlier stages of the disease (12 month-old).

Thus, these results suggest that HD transgenic mice show limited or very late astrocyte reactivity as recently described in other models of HD (**Tong et al., 2014**).

We thus focused on a lentiviral-based model of HD that has been extensively used in the laboratory (**Ruiz and Deglon, 2012**). This model reproduces both the neuronal death and strong astrocyte reactivity that are observed in HD patients (**Faideau et al., 2010**). C57BL/6 mice were injected in the striatum with lentiviral vectors encoding either the N-terminal fragment of the human Htt with 18 glutamine repeats (lenti-Htt18Q) or a mutated Htt carrying 82 glutamine repeats (lenti-Htt82Q). Overexpression of Htt82Q in neurons led to the formation of intraneuronal $EM48^+$ aggregates 6 weeks post-injection (**Figure 20C**). In the lenti-Htt82Q-injected area, astrocytes strongly up regulated both GFAP and vimentin compared with control conditions (lenti-Htt18Q), in which GFAP was expressed at basal levels and vimentin expression was undetectable (**Figure 20C**). In addition, the $GFAP^+$ area within the injected area was increased 6-fold in the Htt82Q-side compared with Htt18Q ($p < 0.001$, n = 6, Student's paired t-test; **Figure 20D**).

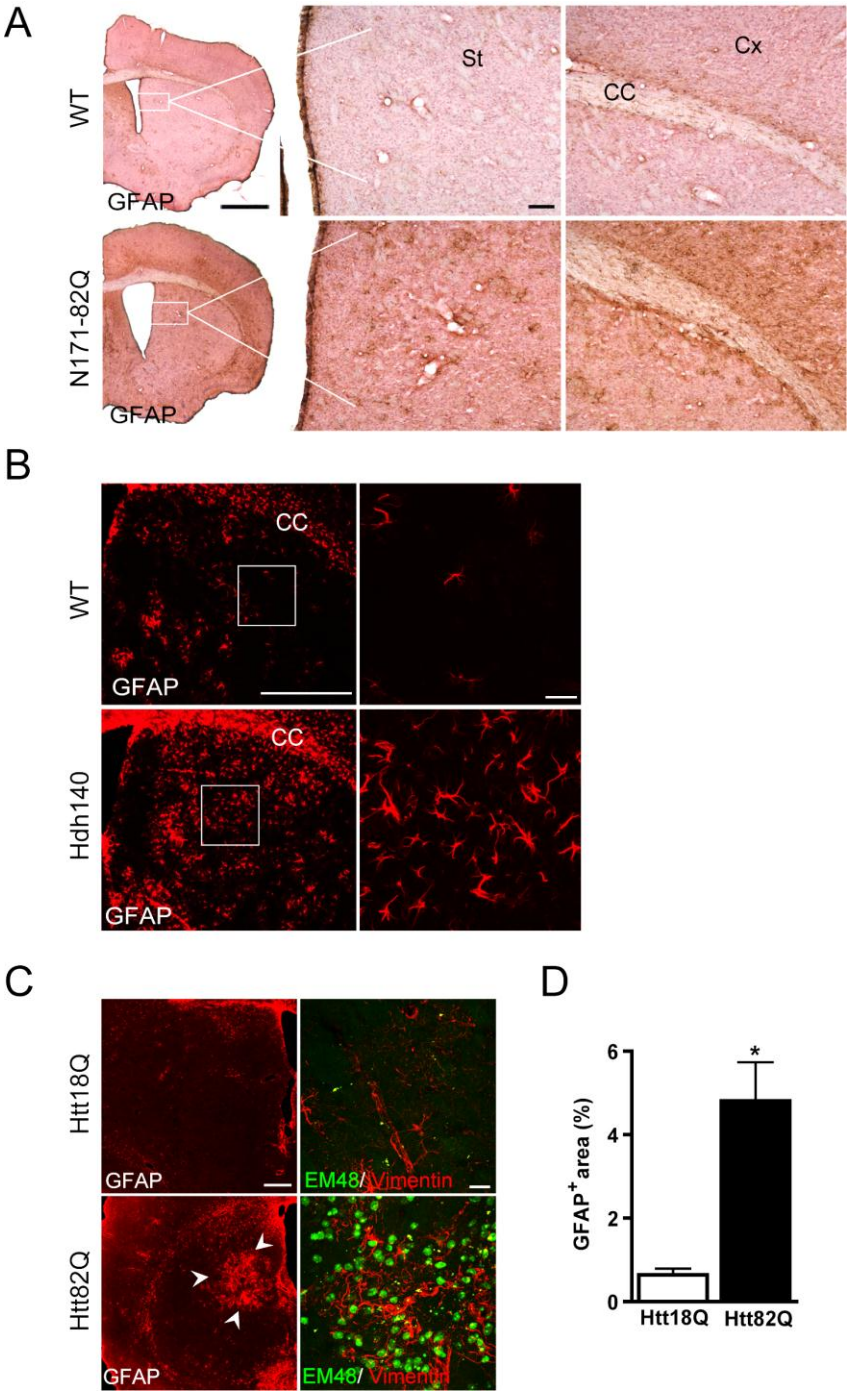

Figure 20. Mouse models of HD display astrocyte reactivity in the striatum.
A, Astrocyte reactivity in the striatum and cortex in end-stage N171-82Q mice compared with WT mice. **B,** A 17-month-old Hdh140 mouse displays reactive astrocytes in the striatum compared with age-matched control mouse. **C,** Mice injected in the striatum with lenti-Htt82Q display EM48^{+} aggregates of mutated Htt (green). Expression of mutated Htt in striatal neurons leads to astrocyte reactivity (arrowhead) as shown with increased GFAP and vimentin staining (red). Data are mean ± sem**.** N = 6 mice. * $p < 0.05$, paired Student's t-test. Scale bars: 100 µm, 20 µm.

These results show that astrocytes become reactive in both AD and HD models. Thus, these ND models are suitable to study intracellular signaling pathways that are involved in astrocyte reactivity *in vivo*.

2) Activation of the JAK2/STAT3 pathway in reactive astrocytes is a common feature in multiple ND models

The JAK2/STAT3 pathway is involved in astrocyte activation in various acute disease models (**Sofroniew, 2009; Hamby and Sofroniew, 2010**). However, it is largely unknown whether this pathway is also activated in reactive astrocytes in more chronic pathological conditions such as ND.

a) The JAK2/STAT3 pathway is activated in reactive astrocytes in mouse models of AD

The phosphorylated form of STAT3 (pSTAT3) was undetectable by immunofluorescence or western blotting in these progressive models of ND. Following activation, pSTAT3 translocates to the nucleus where it stimulates the transcription of a set of target genes including the *stat3* gene itself (**Campbell et al., 2014**). We were able to detect pSTAT3 by immunofluorescence in the striatum of lenti-CNTF-injected mice that was used as a positive control (**Figure 21**).

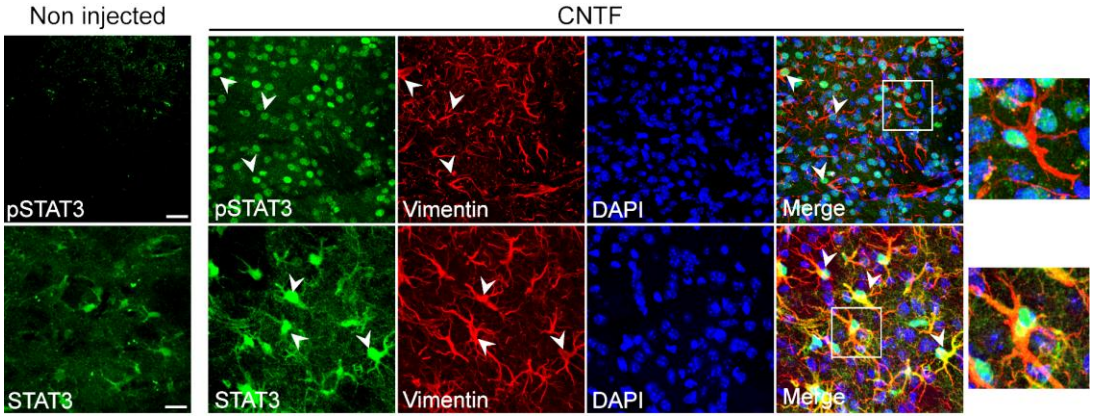

Figure 21. CNTF activates astrocytes through the JAK2/STAT3 pathway in the mouse striatum. Images of brain sections from lenti-CNTF or non-injected mice double-stained for pSTAT3 (green, upper panel), STAT3 (green, lower panel) and reactive astrocytes labeled with vimentin (red). Intrastriatal injection of lenti-CNTF induces astrocyte activation as astrocytes express vimentin and display an activated morphology. Vimentin$^+$ reactive astrocytes display increased pSTAT3 staining, located in the nucleus (arrowhead) compared to undetectable levels in the striatum of non-injected mice. STAT3 accumulates in the nucleus of vimentin$^+$ reactive astrocytes with CNTF (arrowhead). Scale bars: 20 µm.

Indeed, in this model, CNTF strongly activates astrocytes through the JAK2/STAT3 pathway (**Escartin et al., 2006**). PSTAT3 was detected in the nucleus of vimentin$^+$ reactive astrocytes, whereas it was undetectable in non-injected WT mice (**Figure 21**). Interestingly, STAT3 staining was strongly upregulated in the nucleus of reactive astrocytes after lenti-CNTF injection, compared with STAT3

signal in the striatum of non-injected WT mice (**Figure 21**). Therefore, we considered STAT3 nuclear localization and increased immunoreactivity as indexes of JAK2/STAT3 pathway activation, as reported in previous publications (**Escartin et al., 2006; Tyzack et al., 2014**). This also enabled us to identify cell types displaying an active JAK2/STAT3 pathway.

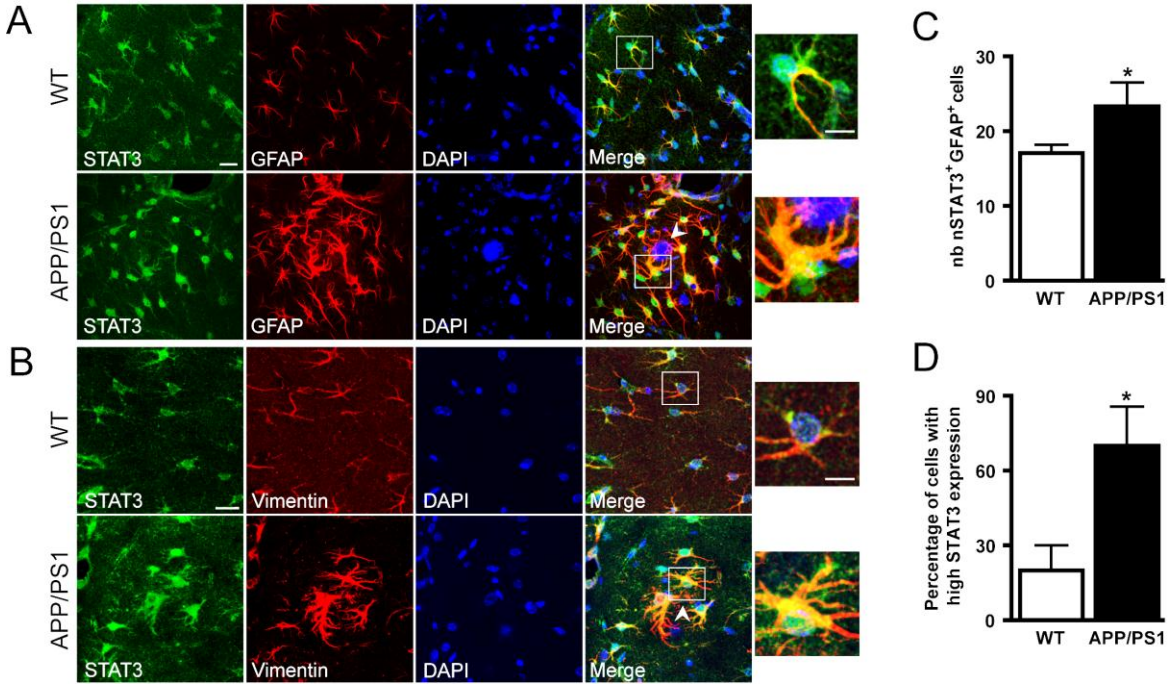

Figure 22. The JAK2/STAT3 pathway is activated in reactive astrocytes in APP/PS1dE9 mice. **A-B,** Images of brain sections from 8-month-old APP/PS1dE9 mice showing double staining for STAT3 (green) and reactive astrocyte markers (**A**: GFAP, **B**: vimentin). **A-B,** APP/PS1dE9 mice display reactive astrocytes that over-express GFAP, vimentin and STAT3, around amyloid plaques (arrowhead) in the hippocampus. STAT3 accumulates in the nucleus of reactive astrocytes (see enlargement). **C,** The number of $GFAP^+$ astrocytes co-expressing STAT3 in the nucleus ($nSTAT3^+/GFAP^+$ cells) is significantly higher in APP/PS1dE9 mice than in WT mice. **D,** The percentage of cells showing strong staining for STAT3 is higher in APP/PS1dE9 mice than in WT mice. N = 3-4/ group. * $p < 0.05$. Scale bars: 20 µm and 5 µm.

Interestingly, STAT3 staining was predominantly observed in astrocytes in all models. In 8 month-old female APP/PS1dE9 mice, there was an accumulation of STAT3 in the nucleus of $GFAP^+$ and $vimentin^+$ reactive astrocytes, whereas in age-matched WT mice, STAT3 was expressed at basal level throughout astrocyte cytoplasm (**Figure 22A, B**). The number of $GFAP^+$ astrocytes expressing STAT3 in the nucleus ($nSTAT3^+/GFAP^+$ cells) was higher in APP/PS1dE9 mice than in age-matched WT mice (p <0.05, n = 3-4 mice/ group, Student's t-test; **Figure 22C**). We also measured STAT3 immunoreactivity in astrocyte cell bodies. The percentage of cells with high STAT3 expression was more than 3 fold higher in APP/PS1dE9 mice than in WT mice, reflecting STAT3 activation in this mouse model of AD ($p < 0.05$, n = 3-4 mice/ group, Student's t-test; **Figure 22D**).

In the subiculum of 12 month-old female 3xTg-AD mice, there was also a strong increase in STAT3 immunoreactivity in the nucleus of reactive astrocytes overexpressing GFAP and vimentin (**Figure 23A, B**). The number of astrocytes co-expressing GFAP and STAT3 in the nucleus was more than 10 fold higher in 3xTg-AD mice than in age-matched WT mice ($p < 0.0001$, n = 3-5 mice/ group, Student's t-test; **Figure 23C**).

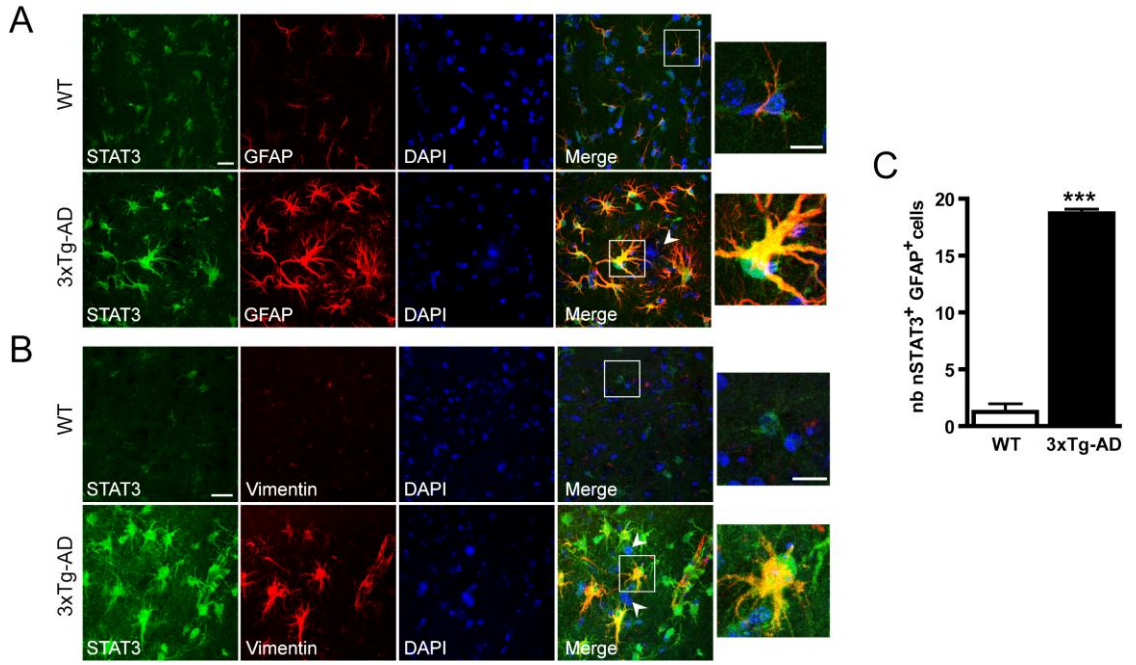

Figure 23. The JAK2/STAT3 pathway is activated in reactive astrocytes in 3xTg-AD mice.
A-B, Images of brain sections from the subiculum of 12-month-old 3xTg-AD mice. STAT3 (green) accumulates in the nucleus of reactive astrocytes labeled with GFAP (**A**, red) or vimentin (**B**, red), especially around amyloid plaques (arrowheads). **C,** The number of $nSTAT3^+/GFAP^+$ cells is significantly higher in 3xTg-AD mice than in age-matched WT controls. N = 3-5/ group. *** $p < 0.001$. Scale bars: 20 µm and 5 µm.

b) The JAK2/STAT3 pathway is activated in reactive astrocytes in models of HD

i) Mouse models

To investigate whether the JAK2/STAT3 pathway was also activated in other ND models, we studied HD mouse models. In the 17-month old heterozygous male Hdh140 mouse that displayed significant astrocyte reactivity in the striatum, STAT3 was upregulated in $GFAP^+$ reactive astrocytes (**Figure 24A**). STAT3 displayed a nuclear localization, reflecting its activation. Unfortunately, we did not have additional samples to perform quantification.

We then investigated whether the JAK2/STAT3 pathway was activated in the lentiviral-based mouse model of HD. STAT3 staining was strongly upregulated in reactive astrocytes found in the lenti-Htt82Q-injected striatum (**Figure 24B**). Indeed, there were four times more $nSTAT3^+/GFAP^+$

astrocytes in the Htt82Q striatum than in the Htt18Q striatum ($p < 0.001$, n = 6, Student's paired t-test; **Figure 24C**). Cells expressing high levels of STAT3 were also more abundant in the Htt82Q striatum than in the Htt18Q striatum ($p < 0.01$, n = 6, Student's paired t-test; **Figure 24D**).

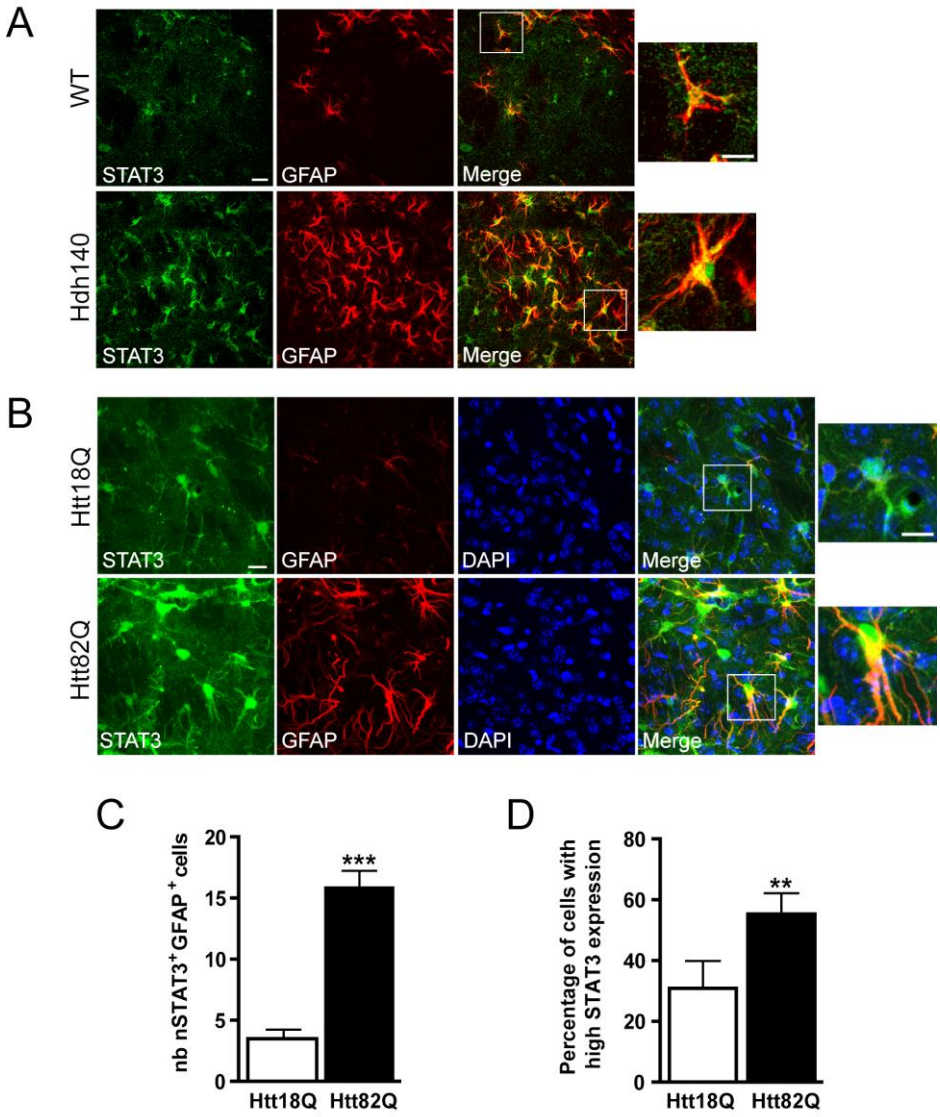

Figure 24. The JAK2/STAT3 pathway is activated in reactive astrocytes in mouse models of HD. **A-B,** Images of double stainings for STAT3 (green) and GFAP (red) on mouse brain sections. **A,** A 17 month-old Hdh140 mouse displays hypertrophic and highly GFAP$^+$ reactive astrocytes in the striatum compared with an age-matched control. STAT3 accumulates in the nucleus of reactive astrocytes in Hdh140 mouse compared to its low basal expression in the control animal. **B,** Six weeks after the infection of striatal neurons with lenti-Htt18Q or lenti-Htt82Q, astrocytes in the Htt82Q striatum are hypertrophic and express higher levels of STAT3 in their nucleus relative to resting astrocytes in the Htt18Q striatum. **C-D,** The number of nSTAT3$^+$/GFAP$^+$ cells (**C**) and the percentage of cells displaying strong staining for STAT3 (**D**) are significantly higher in the Htt82Q striatum than in the Htt18Q striatum. N = 6. * $p < 0.05$. Scale bars: 20 µm and 5 µm.

ii) Non-human primate model

We sought to evaluate whether the JAK2/STAT3 pathway was also activated in reactive astrocytes in other species. Therefore, we took advantage of the fact that lentiviral vectors can be used in several animal species, including non-human primates. Injection of lenti-Htt82Q in the macaque putamen leads to the formation of Htt aggregates, neuronal death and motor symptoms (**Palfi et al., 2007**). We found that the injection of lenti-Htt82Q into the macaque putamen induced the formation of $EM48^+$ aggregates of Htt and led to strong astrocyte reactivity (**Figure 25**). In addition, there was a prominent accumulation of STAT3 in the nucleus of $GFAP^+$-reactive astrocytes. In contrast, at a distance from the injection area, resting astrocytes of the same animal expressed nearly undetectable levels of both GFAP and STAT3 (**Figure 25**).

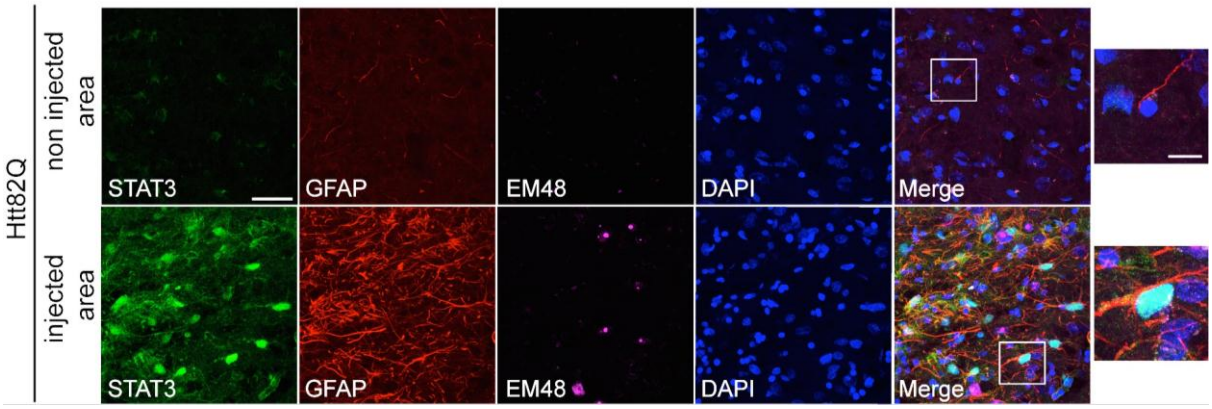

Figure 25. The JAK2/STAT3 pathway is activated in reactive astrocytes in the primate model of HD.
Images of brain sections from macaques injected with lenti-Htt82Q in the putamen showing triple staining for STAT3 (green), GFAP (red) and EM48 (magenta). Seventeen months after infection with lenti-Htt82Q, $EM48^+$ aggregates of Htt are observed in the putamen, as well as prominent astrocyte reactivity. The immunoreactivity for STAT3 is much stronger in $GFAP^+$ reactive astrocytes than in resting astrocytes found outside the injected area in the same animal. Images are representative of all three macaques. Scale bars: 40 µm and 10 µm.

c) The JAK2/STAT3 pathway is activated in reactive astrocytes in other ND models

Because of the apparent universality of the activation of the JAK2/STAT3 pathway in ND models, we sought to investigate astrocyte reactivity in additional ND models. We used samples from the 1 - methyl 4 - phenyl 1,2,3,6-tétrahydro pyridine (MPTP) mouse model of PD.

Astrocyte reactivity is observed in the substancia nigra of patients with PD (**Forno et al., 1992**). This feature is reproduced in the MPTP model (**Maragakis and Rothstein, 2006**). Systemic injection of MPTP causes a selective degeneration of dopaminergic neurons in the substantia nigra par compacta and astrocyte reactivity (**Hirsch and Hunot, 2009**). Consistent with these findings, we found that, seven days post-intoxication, MPTP mice displayed reactive astrocytes upregulating GFAP in the

substantia nigra *pars compacta* and *pars reticulata* (**Figure 26A**) and the striatum (**Figure 26B**). STAT3 signal was upregulated in the nucleus of reactive astrocytes in both regions, compared to its expression in saline-injected controls, illustrating activation of the JAK2/STAT3 pathway.

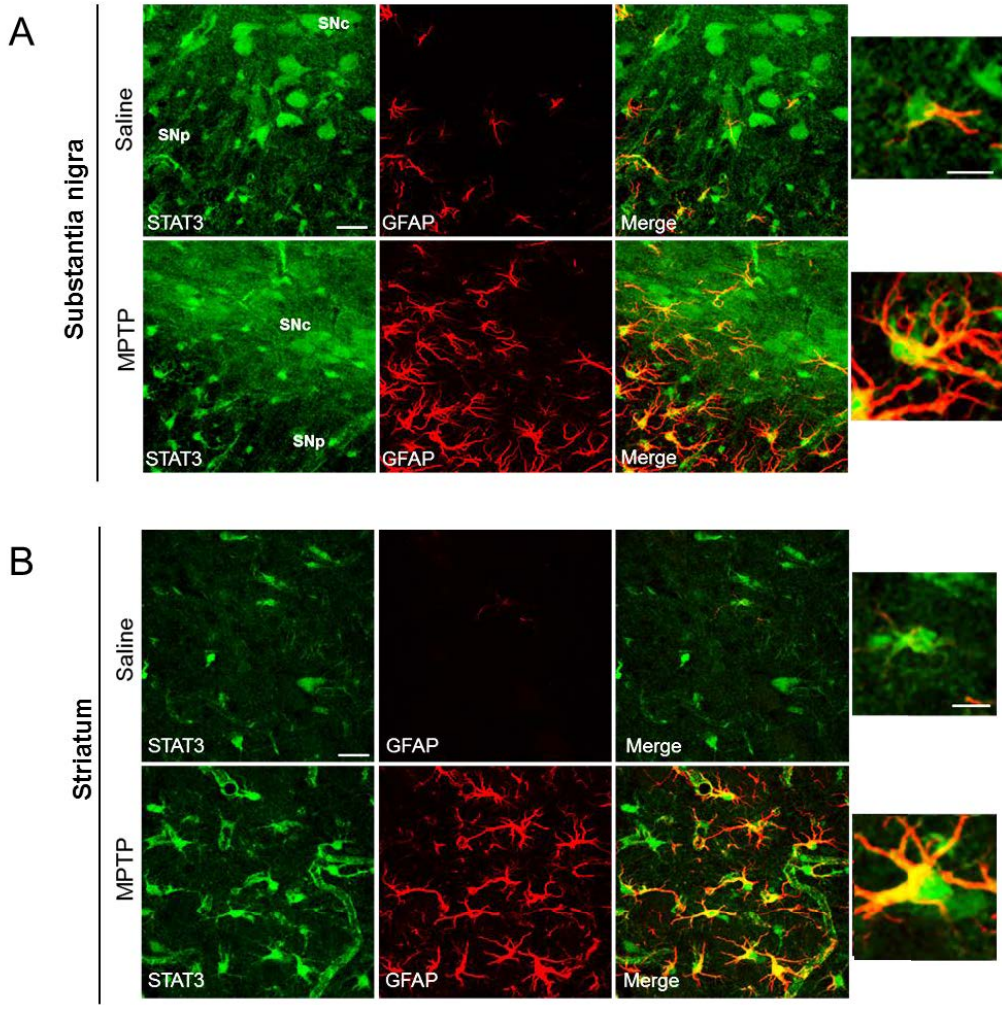

Figure 26. The JAK2/STAT3 pathway is activated in reactive astrocytes in the MPTP model of PD.
A-B, Images of double stainings for STAT3 (green) and GFAP (red) on brain sections from MPTP-intoxicated mice. Seven days after MPTP injection, astrocytes are hypertrophic and strongly upregulate GFAP in the substantia nigra pars compacta (SNc), pars reticulata (SNr) (**A**) and in the striatum (**B**). Reactive astrocytes show increased STAT3 expression in the nucleus, reflecting its activation. Note the presence of $STAT3^{+}$ neurons in the SNc of saline mice that have degenerated after MPTP intoxication. Scale bar: 40 µm, 5 µm.

Interestingly, STAT3 expression was different among brain regions. In the hippocampus, STAT3 was expressed at higher level in astrocytes. By contrast, in the striatum, some astrocytes and large round cells- most likely cholinergic interneurons- displayed a weak STAT3 expression although detectable by immunofluorescence labeling. In the substantia nigra, DA neurons were labeled with STAT3 as well as astrocytes. Furthermore, we observed a robust correlation between STAT3 and GFAP expression in all the brain regions of the mouse brain.

3) The NF-κB pathway is not activated in 3xTg-AD mice and in the HD lentiviral-based model

Other pathways such as the NF-κB pathway have been associated with astrocyte reactivity (**Kang and Hebert, 2011**). We thus investigated whether this cascade could be activated, in addition of the STAT3 pathway in ND models. We measured by western blotting the protein levels of IκBα, the inhibitor of the NF-κB pathway, which is degraded upon pathway activation (**Hayden and Ghosh, 2008**).

We performed this experiment on samples from 3xTg-AD mice and lenti-Htt82Q injected mice, as they displayed the strongest astrocyte reactivity. In 3xTg-AD mice, the abundance of IκBα normalized to GAPDH were similar to WT mice (p = 0.4037, n = 4-6 mice/ group, Student's t test; **Figure 27A**), while the positive control of cells treated with the cytokine TNFα displayed the expected decrease in IκBα expression (**Figure 27A, B**). Similarly the level of expression of IκBα normalized to GAPDH was not different between mice injected with lenti-Htt18Q or Htt82Q (p = 0.8062, n = 6 mice/ group, Student's paired t test; **Figure 27B**).

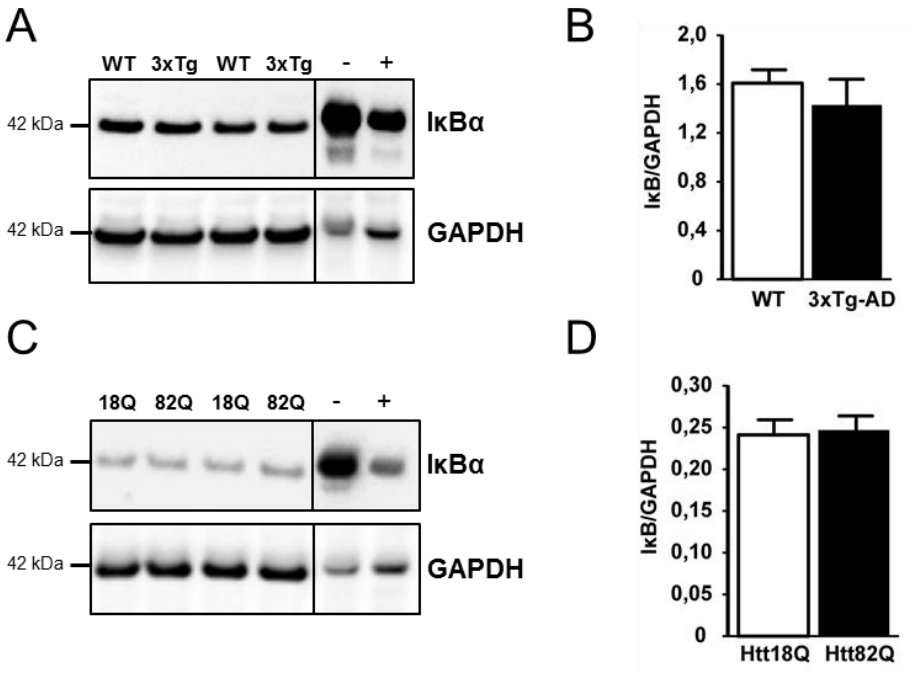

Figure 27. The NF-κB pathway is not activated in 3xTg-AD mice and the lentiviral-based model of HD.
Western blots (**A**, **C**) and quantification (**B**, **D**) for IκBα and GAPDH in (**A**) 3xTg-AD mice (3xTg) or their age-matched WT controls (WT) or (**C**) mice injected in the left striatum with lenti-Htt18Q (18Q) and in the right striatum with lenti-Htt82Q (82Q). IκBα expression is similar between 3xTg-AD mice and WT mice (**B**) and between the left and right striatum of mice injected with lenti-Htt (**D**). The abundance of IκBα is lower in HeLA cells treated with TNFα (positive control, +) than in untreated cells (negative control, -). N = 4-6 mice/group.

Taken together, these results show that the JAK2/STAT3 pathway is activated in reactive astrocytes in multiple models of ND. Interestingly, this phenomenon is highly conserved between brain regions and animal species despite the variety of pathological mechanisms involved. Therefore, the JAK2/STAT3 pathway is a universal feature of astrocyte reactivity in ND models.

B. Development of new viral vectors targeting the JAK2/STAT3 pathway to modulate astrocyte reactivity *in vivo*

The JAK2/STAT3 pathway was previously shown to be involved in astrocyte activation in acute injury models (**Sofroniew, 2009 and see § II.B.2.c**). We showed here that the JAK2/STAT3 pathway is also activated in ND models. Thus, it appears as a potent and universal molecular target to study astrocyte reactivity in chronic pathological conditions. Therefore, we aimed at developing viral vectors allowing the manipulation of the JAK2/STAT3 pathway specifically in astrocytes *in vivo*.

1) Lentiviral and adeno-associated viral vectors allow the selective targeting of astrocytes in the adult rodent brain

a) Lentiviral vectors

Lentiviral vectors allowing selective transgene expression in astrocytes were previously developed in the laboratory (**Colin et al., 2009**). They are pseudotyped with the MOK envelope and carry the miR124T sequence (MOK/miR124T). Lentiviral vectors encoding the green fluorescent protein (lenti-GFP) were injected in the striatum of 8 week-old C57BL/6 mice at a dose of 250 ng p24 in 2,5 µl. Six weeks post-injection, mouse brains were analyzed by immunofluorescence staining to characterize these vectors. The volume transduced by lenti-GFP was 0.82 ± 0.07 mm^3. Co-labeling with cell-type specific markers was used to study viral vector tropism and transgene expression. GFP expression was detected in $GFAP^+$ astrocytes and did not co-localize with $IBA1^+$-microglia, $NeuN^+$-neurons, MBP^+-mature oligodendrocytes or $NG2^+$-oligodendrocyte progenitors (**Figure 28**).

In some experiments performed for the project, we used co-injection of two MOK/miR124T vectors. Thus, to evaluate the percentage of cells co-infected with two vectors, C57BL/6 males were co-injected in the striatum with lenti-GFP and with a lentiviral vector encoding the blue fluorescent protein (lenti-BFP). One month later, post-mortem analysis was performed and the direct fluorescence of GFP and BFP was assessed using epifluorescence microscopy. Quantification showed that 88.7 ± 2 % of cells co-expressed GFP and BFP.

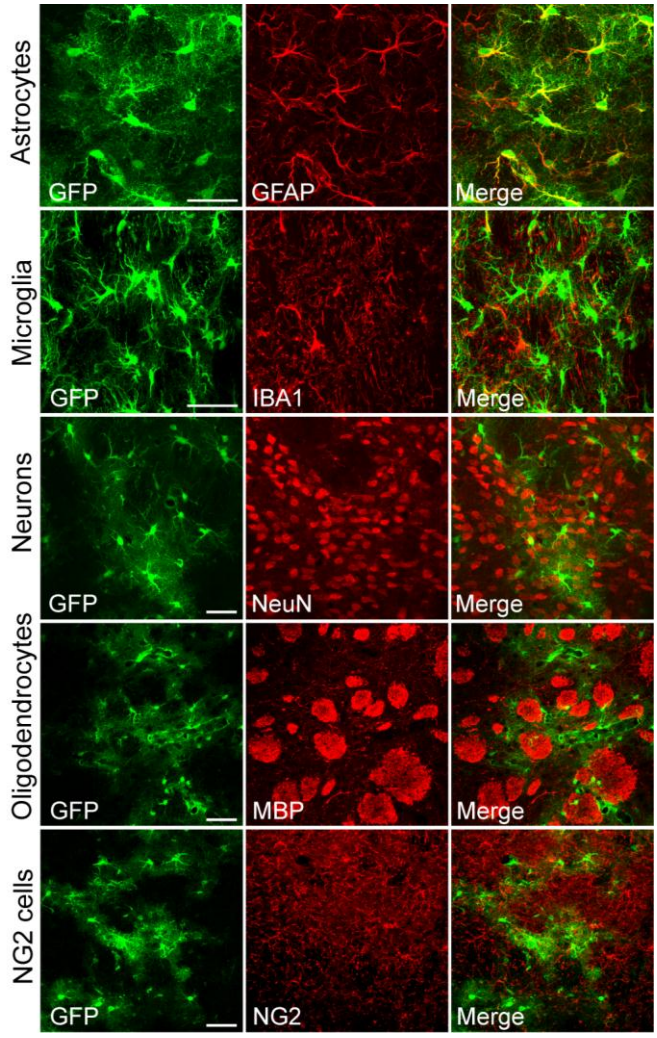

Figure 28. Mokola/miR124T lentiviral vectors lead to transgene expression specifically in astrocytes.
Images of double labelings for lentiviral vector encoded-GFP (green) and cell-type specific markers (red). GFP is expressed in $GFAP^+$ astrocytes but not in $IBA1^+$-microglia, $NeuN^+$-neurons, MBP^+-myelinating oligodendrocyte or $NG2^+$-oligodendrocyte progenitors. Scale bar: 40 µm

We also controlled that lentiviral vectors encoding GFP did not elicit inflammatory response at the viral titer we used. Indeed, for most of the mouse strains, injection of lenti-GFP did not trigger increase in GFAP staining in the injected volume, except at the needle track. However, lenti-GFP triggered astrocyte reactivity in the B6C3 (C57BL/6 x C3H) mouse strain, as determined by an increase in GFAP staining in the striatum of those mice.

In addition to their non-specific inflammatory effects in B6C3 mice, MOK/miR124T lentiviral vectors have a poor efficiency in the hippocampus and only few astrocytes express the transgene. Thus, AAV vectors were subsequently developed for the project.

b) Adeno-associated viral vectors (AAV)

AAV vectors are small viral particles (20 nm) allowing large diffusion in the brain and they are poorly immunogenic (**Sun et al., 2003**).

AAV that transduce astrocytes were developed in the laboratory. We used AAV2/9-serotyped-AAV carrying the gfa-ABC1D promoter (**Lee et al., 2008**). A dose-response experiment was performed to determine the optimal virus load to inject in the mouse brain without eliciting astrocyte reactivity using the control vector encoding GFP (AAV-GFP). Ten-week-old B6C3 mice were injected in the striatum with either 4 doses of AAV 3.10^8 VG, 1.10^9, 5.10^9 VG and 1.10^{10} VG in 2 µl. One month post-injection, immunofluorescence staining was performed to evaluate transgene expression levels, AAV spreading and inflammation (**Figure 29**). The overall transduction volume was comparable between doses (**Figure 29B**). However, GFP fluorescence in the injected area was increased with the highest doses compared to lowest doses (**Figure 29C**). We evaluated the dose-effect on astrocyte reactivity with GFAP staining to identify reactive astrocytes. GFAP fluorescence intensity was comparable between groups with a tendency to increase in the highest dose although results showed more variability with this viral titer (**Figure 29A, C**). Thus, we decided to use the second higher dose (5.10^9 VG) for all experiments involving AAV injections.

Double immunofluorescent staining with cell-type specific markers was performed to control the tropism of AAV vectors in the striatum and the hippocampus. AAV-GFP transduced mainly S100β$^+$-astrocytes, but not IBA1$^+$-microglia, NeuN$^+$-neurons or MBP$^+$-oligodendrocytes (**Figure 30A**).

We quantified the co-infection percentage of two AAV 2/9- gfaABC1D vectors encoding for GFP and tdTomato, a red fluorescent protein. C57BL/6 mice were co-injected in the striatum with AAV-tdTomato+ AAV-GFP or AAV-GFP alone. One month post-injection, mouse brains were collected and the fluorescent injected-area was dissected out and processed for FACS analysis (**Figure 30B, C**). In AAV-GFP mice, fluorescent cells were only GFP$^+$ and did not express tdTomato whereas cells isolated from AAV-tdTomato+ AAV-GFP mice were GFP$^+$ and tdTomato$^+$ (**Figure 30B**). Quantification showed that 99.3% of GFP$^+$ cells co-expressed tdTomato and GFP. In addition, we confirmed the co-expression of the two fluorescent proteins in striatal astrocytes by confocal microscopy (**Figure 30C**).

Thus, we developed both lentiviral and AAV vectors allowing highly selective expression of transgenes in astrocytes *in vivo*, without eliciting non-specific inflammatory reaction.

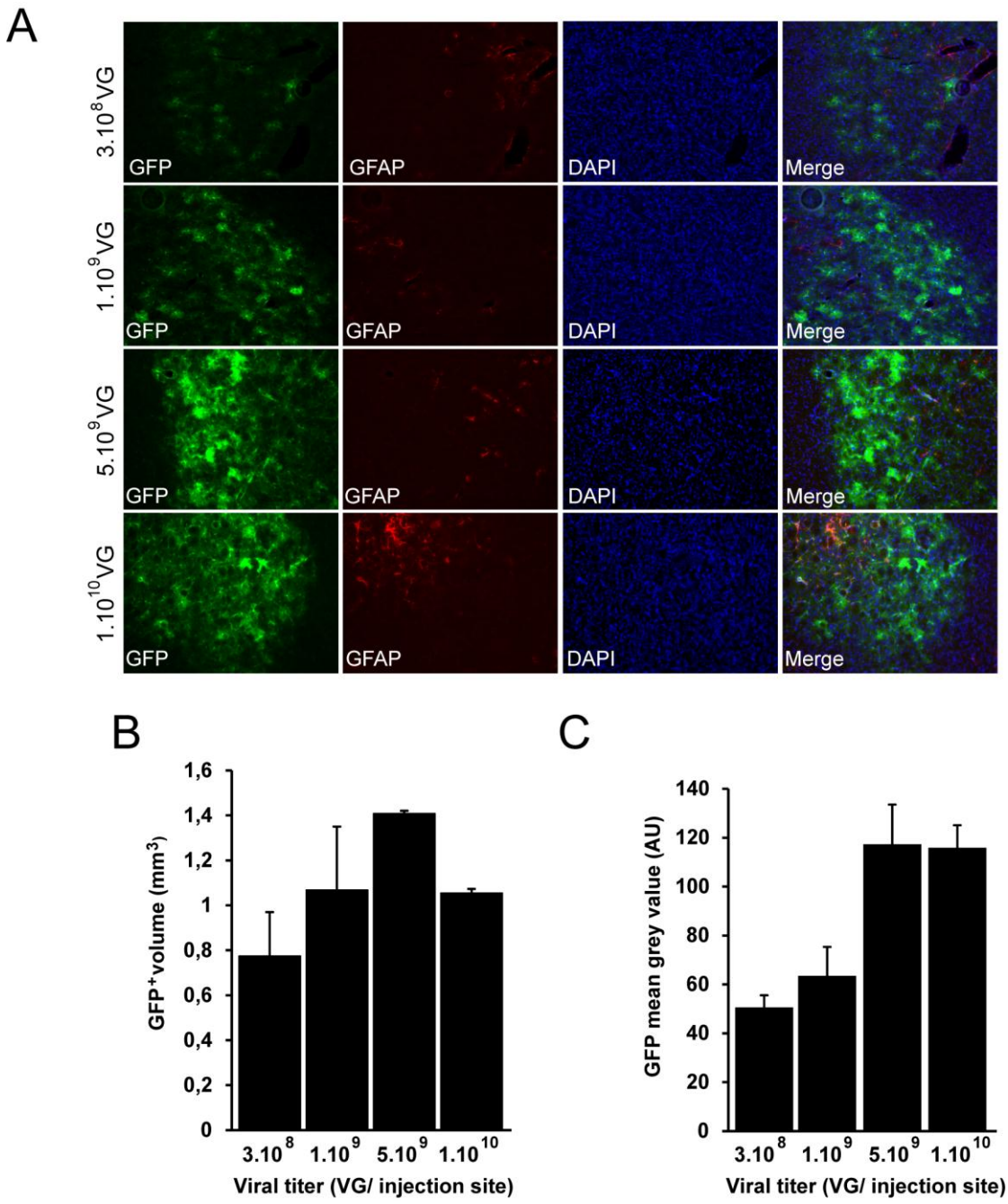

Figure 29. Dose response of GFP expression and spreading using AAV-GFP in the mouse striatum.

A, Immunofluorescent detection of GFP (green), GFAP (red) in mice injected with AAV-GFP in the striatum. **B,** The GFP^+ volume in the striatum is highest with a viral titer of 5.10^9 VG/ injection site. **C,** The GFP fluorescence intensity within the injected volume increases with the two highest viral titers. Data are mean ± sem. N=4/ group. Ns, one-way ANOVA. Scale: 60µm.

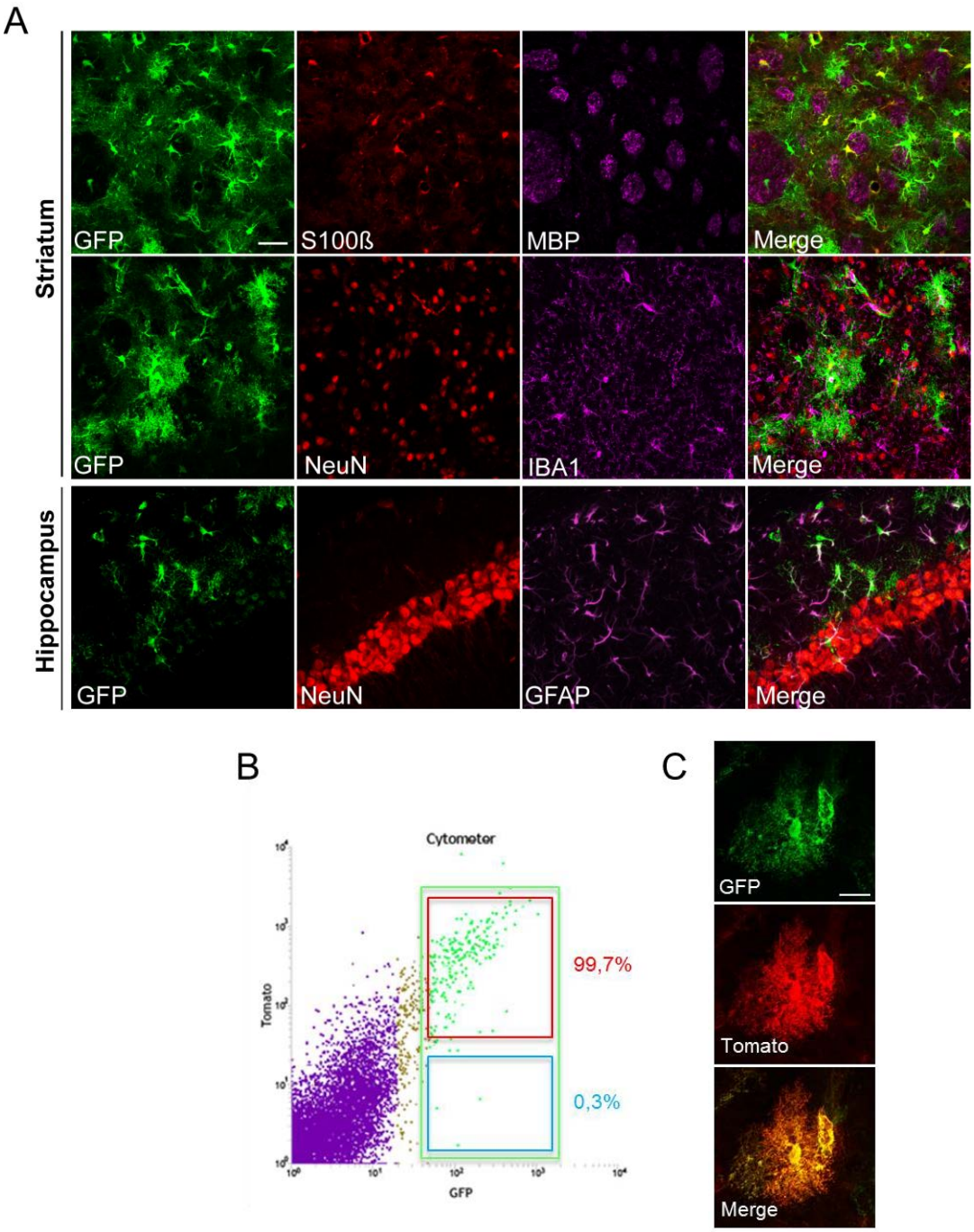

Figure 30. AAV-GFP vectors transduce astrocytes in the mouse brain.
A, Images of immunofluorescent labelings for GFP (green) and cell-type specific markers (red and magenta) in mice injected with AAV-GFP in the striatum (upper) and the hippocampus (bottom). GFP co-localizes with S100β^{+} astrocytes but not with MBP^{+} oligodendrocytes, NeuN^{+} neurons or IBA1^{+} microglia. **B-C**, FACS analysis of dissociated cells from mice injected with AAV-GFP (**B**) and AAV-tdTomato+ AAV-GFP (**C**) in the striatum. Most of the GFP^{+} cells (99%) analyzed by FACS co-expressed tdTomato (**C**). **D**, Direct fluorescence detection of AAV-encoded GFP and tdTomato. Both fluorescent proteins co-localize in striatal astrocyte. Scale: 40 µm

2) Overexpression of a constitutively active form of JAK2 successfully activates astrocytes in the mouse brain

We decided to target the JAK2/STAT3 pathway to manipulate reactive astrocytes *in vivo*. We developed new viral tools to activate the JAK2/STAT3 pathway in astrocytes and induce their reactivity. We used viral vectors to overexpress wild-type or mutant forms of JAK2 and STAT3 proteins.

a) Lentiviral-mediated expression of wild-type and mutated forms of JAK2 and STAT3 proteins differentially activate astrocytes

We used the lentiviral vectors described in the previous paragraph to express WT or mutants forms of STAT3 and JAK2 in astrocytes. We used two mutant constructs of STAT3: STAT3C encodes a mutated form of STAT3 carrying a substitution of two cysteine residues in the SH2 domain that leads to spontaneous dimerization and nuclear translocation of the mutant protein (**Bromberg et al., 1999**). STAT3Copt is a codon-optimized sequence of STAT3C leading to increased transgene expression (produced by Geneart). We also used a construct encoding the wild-type JAK2 protein (JAK2WT) and two constitutively active mutant of JAK2. JAK2Y570F lacks an inhibitory phosphorylation at the residue 570 (JAK2Y570F) (**Robertson et al., 2009**) and JAK2T875N has a constitutively active kinase domain (**Haan et al., 2009; Zou et al., 2011**).

First, we transfected HEK293T with plasmids encoding STAT3, STAT3Copt, JAK2WT, JAK2Y570F and JAK2T875N to validate these constructs. Twenty-four hours post-transfection, western blot analysis was performed to detect STAT3 and JAK2 protein levels in HEK293T cells (**Figure 31A**). Both JAK2 and STAT3 proteins were detected in all conditions at the expected molecular weight (160kDa for JAK2 and 86 kDa for STAT3). In addition, STAT3Copt led to higher protein expression than STAT3C, as expected with the codon-optimized sequence. JAK2WT appeared more expressed than the JAK2Y570F and JAK2T875N mutant constructs (**Figure 31A**). This result showed that all wild-type and mutant constructs of JAK2 and STAT3 were efficiently expressed *in vitro*.

We then co-injected C57BL/6 mice in the striatum with lentiviral vectors encoding STAT3 (lenti-STAT3) and JAK2 (lenti-JAK2) wild-type or mutant constructs (250 ng p24) and with lenti-GFP (50 ng p24). To visualize infected cells, we performed co-injection of the different constructs with lenti-GFP. In addition, we used several control groups to evaluate the effect of control lentiviral vector injection and surgery on astrocyte reactivity. Mice were injected with lenti-GFP alone (250 ng) or with the vehicle used to dilute lentiviral vectors (PBS/BSA). We also used non-injected (NI) mice as additional controls for the basal expression of the markers we studied. Post-mortem analysis was performed 1.5 month after injection.

We first detected GFAP by immunohistochemistry to determine if the overexpression of JAK2 and STAT3 constructs would induce astrocyte reactivity in the mouse striatum. In NI mice, GFAP expression was undetectable whereas it was locally up regulated in PBS and lenti-GFP-injected

controls at the level of the needle track (**Figure 31B**). We observed that STAT3 and JAK2 constructs led to variable increase in GFAP signal intensity (**Figure 31B, C**). We thus measured the optical density (OD) of GFAP staining in the striatum for each group. GFAP OD was increased in the lenti-JAK2 WT and lenti-JAK2T875N groups compared with other mutants and control groups although it did not reach significance due to the limited number of mice per group (**Figure 31C**).

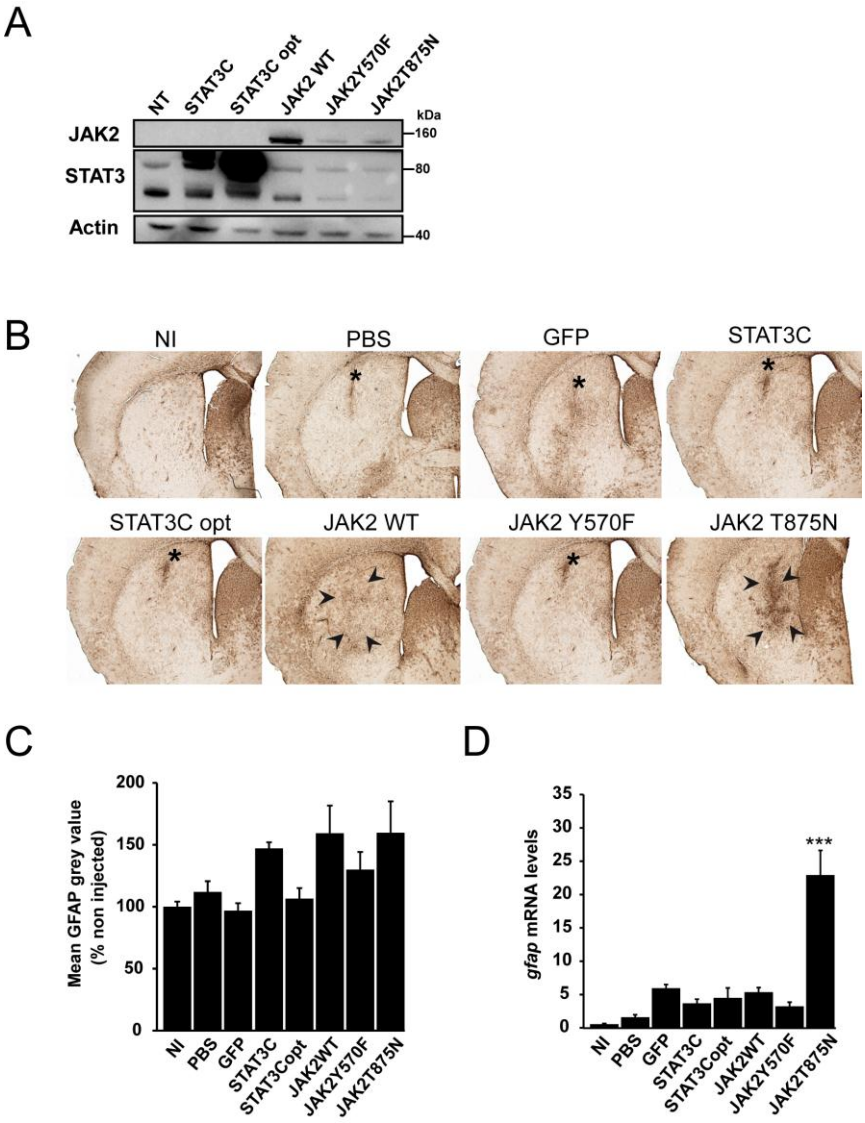

Figure 31. Overexpression of wild-type and mutant forms of STAT3 and JAK2 activates astrocytes in the mouse striatum.
A, Detection by western blotting of STAT3 and JAK2 proteins after transfection of HEK293T cells with plasmids encoding STAT3 and JAK2 constructs. **B**, Detection of reactive astrocytes using GFAP staining in mice injected in the striatum with lentiviral vectors encoding WT and mutants constructs of STAT3, JAK2 and co-injected with GFP or controls. GFAP is expressed at basal levels in non-injected (NI) control mice and upregulated at the level of the needle track (*) in the PBS and lenti-GFP-injected control groups. GFAP expression is strongly increased in the injected area in the lenti-JAK2 WT + lenti-GFP and lenti-JAK2 T875N + lenti-GFP mice. **C**, The mean GFAP grey value is higher in STAT3C, JAK2WT and JAK2 T875N groups than in other groups and controls. **D**, *gfap* mRNA levels are detected by qRT-PCR. They are increased in the lenti-JAK2 T875N + lenti-GFP group. Data are mean ± sem. N= 4/ group. ***, p <0.001, One-way ANOVA and Scheffé tests. Scale bar: 500 µm.

The JAK2/STAT3 pathway regulates the transcription of a set of target genes including the *gfap* gene. Thus, we used qRT-PCR for the quantification of *gfap* mRNA levels in lenti-STAT3 and lenti-JAK2-injected groups. All mice were co-injected with lenti-GFP hence the GFP^+ area was dissected out and analyzed by qRT-PCR. Lenti-JAK2T875N led to the strongest induction in *gfap* mRNA compared with all other groups ($p < 0.001$, n = 3-4 mice/ group, one-way ANOVA and Scheffé tests; **Figure 31D**).

Taken together, histological and qRT-PCR results suggest that JAK2T875N is the best construct to achieve robust astrocyte activation in the mouse striatum. Viral constructs encoding JAK2T875N will be named as constitutively active JAK2 (JAK2ca) in the following paragraphes.

b) JAK2ca leads to selective and robust astrocyte activation in the mouse brain

i) Lenti-JAK2ca

Lenti-JAK2ca encodes a constitutively active form of JAK2 and thus should activate STAT3. One month post-injection, we detected STAT3 using immunofluorescence staining in JAK2ca and GFP mice. For all injection experiments, we co-injected lenti-JAK2ca with lenti-GFP (lenti-JAK2ca + lenti-GFP in figure legends). Therefore, infected astrocytes were visualized by their expression of GFP in both groups. STAT3 expression was higher in $GFAP^+$ reactive astrocytes in the JAK2ca group compared to the GFP controls (**Figure 32A**). Furthermore, STAT3 staining was increased in the nucleus of JAK2ca astrocytes, reflecting STAT3 pathway activation (enlargement, **Figure 32A**). We used immunofluorescence staining and confocal microscopy to characterize the phenotype of lenti-JAK2ca astrocytes. They expressed vimentin in contrast to GFP astrocytes (**Figure 32B**). Moreover, JAK2ca astrocytes displayed a reactive morphology, with enlarged primary processes compared with lenti-GFP astrocytes.

We detected *jak2* overexpression in lenti-JAK2ca mice compared with lenti-GFP controls by qRT-PCR (**Figure 32C**). JAK2ca induced mRNA levels of *serpina3n* and *vimentin*, two markers of reactive astrocytes ($p < 0.05$, n = 4-7 mice/ group, Student's t-test; **Figure 32D and E**, respectively). Upon important stimulation of the pathway, STAT3 induces the transcription of *socs3* as a feedback regulatory mechanism (see II.B.2.c.i). We thus detected *socs3* mRNA levels as additional index of JAK2/STAT3 pathway activation with JAK2ca. Indeed, *socs3* mRNA levels were higher in the JAK2ca group than in GFP controls ($p < 0.05$, n = 4-7 mice/ group, Student's t-test; **Figure 32F**). We then detected the expression of genes that are not directly related to astrocyte reactivity and which encode functionally important astrocyte proteins. We found that mRNA levels of *glt-1* and *cx43* were not significantly different between the JAK2ca and GFP groups (n = 4-7 mice/ group, Student's t-test; **Figure 32G** and **H**, respectively). These results demonstrate that JAK2ca overexpression activates the JAK2/STAT3 pathway in astrocytes and selectively induces the expression of reactive astrocyte markers.

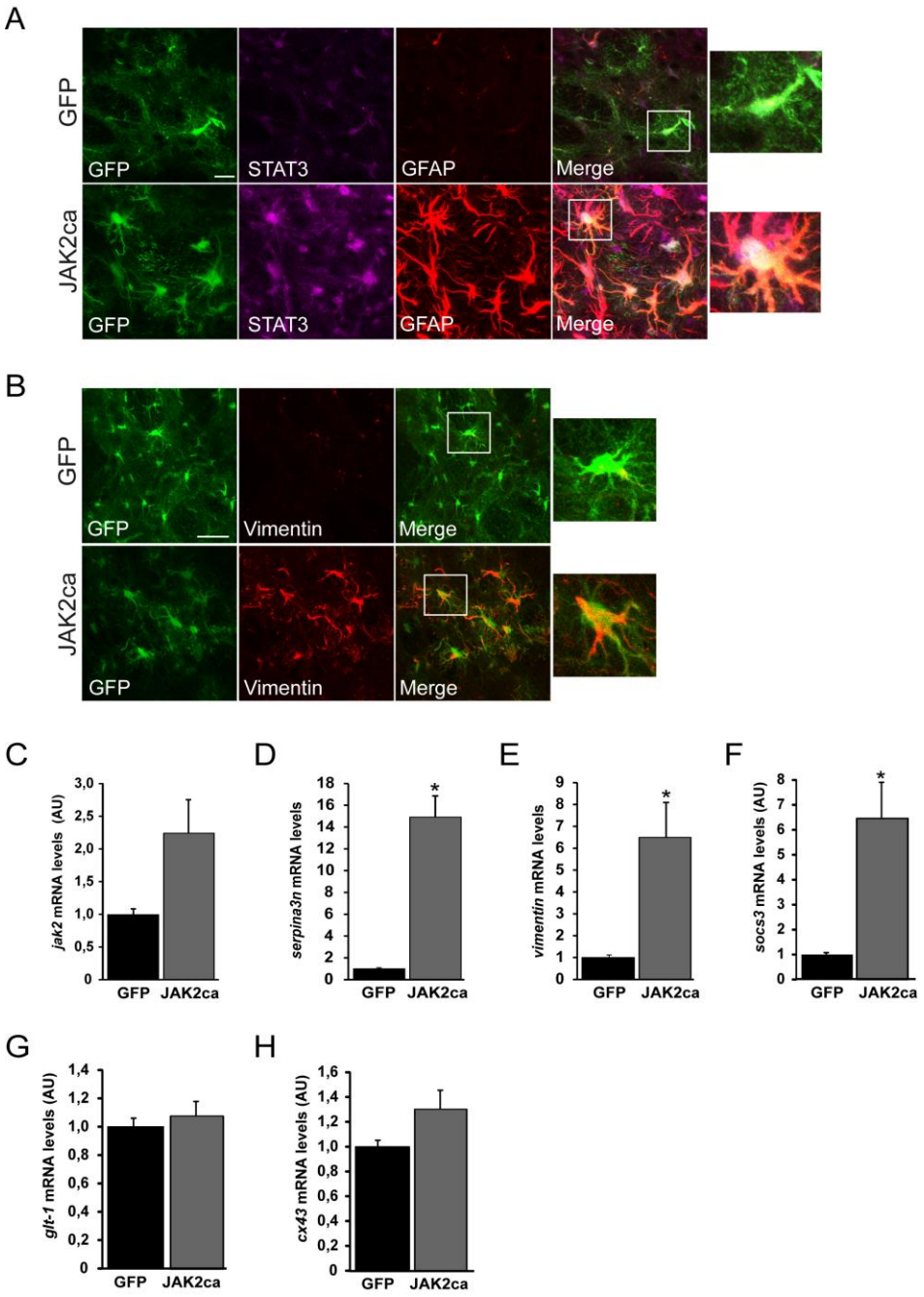

Figure 32. Lenti-JAK2ca activates astrocytes in the mouse striatum.
A, Images of triple labeling of GFP (green), STAT3 (red) and GFAP (red). Mice were injected with lenti-JAK2ca + lenti-GFP in one striatum and with the control lenti-GFP in the other. Infected astrocytes are dectected by their expression of GFP. JAK2ca astrocytes are hypertrophic and up regulate GFAP whereas it is undetectable in lenti-GFP controls. Along with GFAP, lenti-JAK2ca astrocytes show increased STAT3 reactivity with a strong nuclear localization compared with controls. **B**, JAK2ca overexpression in striatal astrocytes induces vimentin+ expression. By contrast, GFP astrocytes display undetectable vimentin levels. **C-H**, qRT-PCR analysis on mice injected with lenti-JAK2ca or lenti-GFP in the striatum. **C**, *Jak2* mRNA levels show a tendency to increase in the JAK2ca group. **D-E**, Reactive astrocyte markers *serpina3n* (**D**) and *vimentin* (**E**) are induced by JAK2ca. **F**, *Socs3* mRNA levels are increased with JAK2ca overexpression. By contrast, astrocyte-specific markers *glt-1* (**G**) and *cx43* (**H**) display similar mRNA levels between the JAK2ca and GFP groups. Data are mean ± sem. N= 4/ group. * $p < 0.05$, Student's t-test. Scale bar: 40µm.

We then evaluated the effects of lenti-JAK2ca-mediated astrocyte activation on striatal neurons. They were detected by immunofluorescence using the classical neuronal marker NeuN and with dopamine- and cAMP-regulated neuronal phosphoprotein (DARPP32), specifically expressed in the medium-sized spiny neurons (MSN) in the striatum. DARPP32 expression in the striatum was similar in the lenti-GFP and lenti-JAK2ca groups (**Figure 33A**). Similarly, NeuN staining was comparable in the injected area in lenti-GFP and lenti-JAK2ca mice (**Figure 33B**). In addition, mRNA levels of *d2r*, which is highly expressed in MSNs, were not different between GFP and JAK2ca groups (n = 4 mice/ group, Student's t-test; **Figure 33C**). Taken together, these results suggest that astrocyte activation though JAK2ca overexpression in striatal astrocytes does not induce any detectable neuronal toxicity.

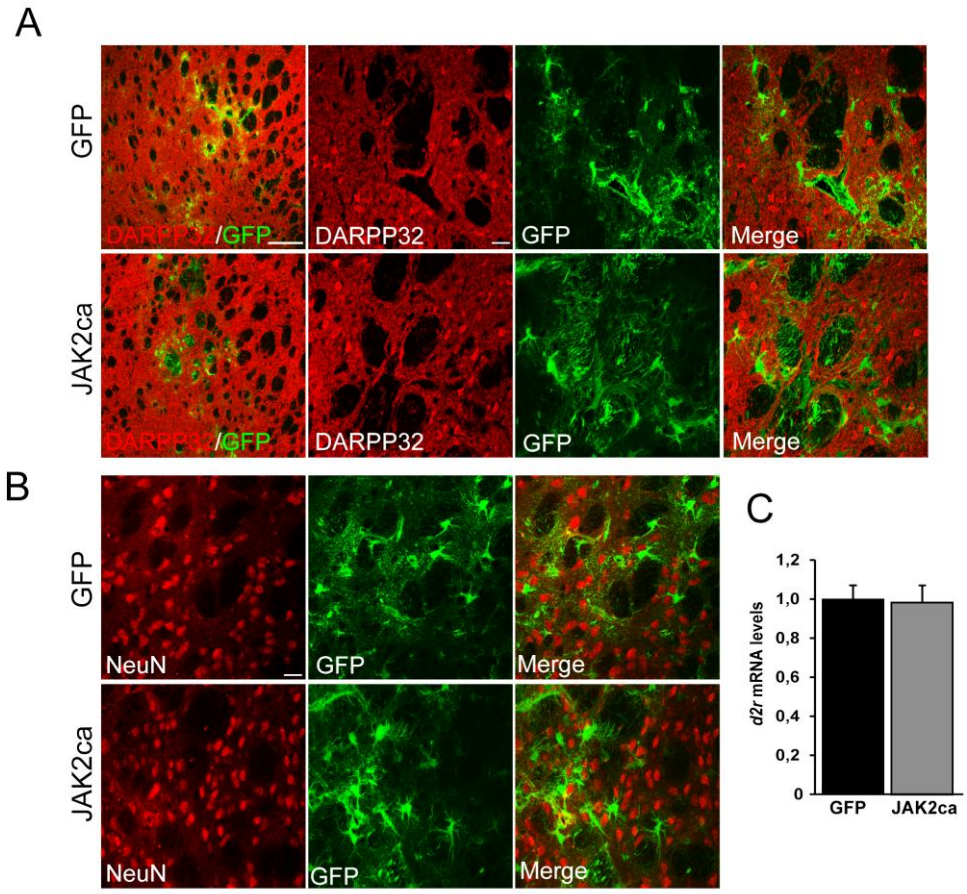

Figure 33. Lenti-JAK2ca does not lead to detectable neuronal death or toxicity.
A-B, Images of double labeling of GFP (green) and neuronal markers (**A**, DARPP32 and **B**, NeuN (red)) in lenti-GFP and lenti-JAK2ca + lenti-GFP-injected mice. **A**, Expression of DARPP32, a marker of striatal neurons, is similar between the two groups. At high magnification, DARPP32^{+} neurons have a similar morphology in the JAK2ca and GFP groups. **B**, NeuN staining is comparable between JAK2ca and GFP groups. **C**, qRT-PCR analysis of *d2r* mRNA levels in lenti-JAK2ca + lenti-GFP and lenti-GFP-injected mice. *d2r* expression is not altered following lenti-JAK2ca-injection in the striatum. Data are mean ± sem. N= 4/ group. Scale bar: 200 µm, 40 µm.

We next evaluated the effect of JAK2ca-mediated astrocyte activation on microglia. The density of IBA1^{+} microglial cells was measured in the striatum in the NI, GFP and JAK2ca groups. IBA staining in

NI mice was used as baseline to evaluate the effect of viral vector injection on microglial activation (**Figure 34A**). The density of IBA1$^+$ cells was increased in the JAK2ca group compared with NI controls (p < 0.05, n = 4 mice/ group, one-way ANOVA and Scheffé tests; **Figure 34B**). Importantly, IBA1$^+$ cell density was not significantly different between JAK2ca and GFP groups, suggesting that JAK2ca has only a limited effect on microglial cells. Consistently, mRNA levels of *cd11b*, a marker of activated microglia, were not significantly different between JAK2ca and GFP groups (n = 4 mice/ group, Student's t-test; **Figure 34C**). These results suggest that activation of the JAK2/STAT3 pathway specifically in astrocytes led to limited microglial activation in the mouse striatum.

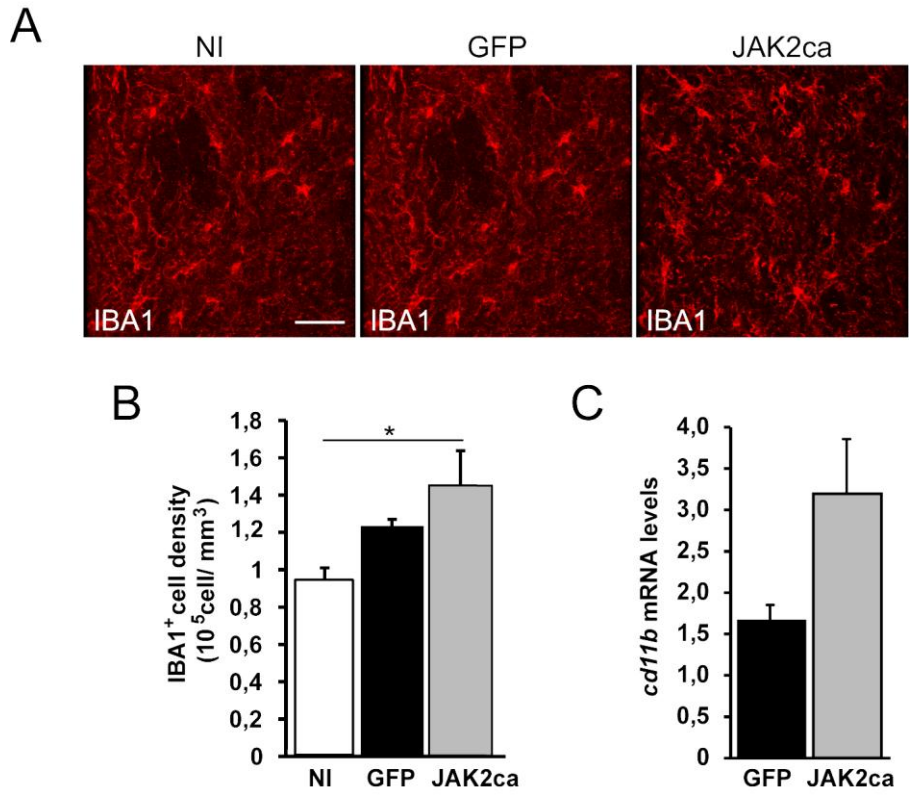

Figure 34. Lenti-JAK2ca induces moderate microglial activation in the mouse striatum.
A, Images of microglial cells using IBA1 staining (red) in the striatum of NI, lenti-GFP and lenti-JAK2ca + lenti-GFP-injected mice. **B**, The density of IBA1$^+$ cells is increased in GFP and JAK2ca virus-injected groups compared with NI mice. There is no difference in the density of microglial cells in the GFP and JAK2ca groups. **C**, *cd11b* mRNA levels, detected by qRT-PCR are not different between lenti-JAK2ca + lenti-GFP and lenti-GFP controls. Data are mean ± sem. N= 4/ group; * p <0.05, One-way ANOVA and Scheffé tests or Student's t-test. Scale bar: 40 µm.

JAK2T875N mutant has been identified as an oncogene (**Haan et al., 2009; Zou et al., 2011**). Thus, mice were injected with Bromo-2-deoxyuridine (BrdU) to evaluate the effect of JAK2ca overexpression on cellular proliferation. BrdU incorporation was detected by immunofluorescence on mouse brain sections (**Figure 35**). We did not observe BrdU$^+$ astrocytes in the injected area after lenti-JAK2ca-injection. Cellular proliferation in the SVZ served as a control for BrdU injection and labeling. The

number of BrdU$^+$ cells in the SVZ does not appear to be qualitatively different between the GFP and JAK2ca groups (**Figure 35**).

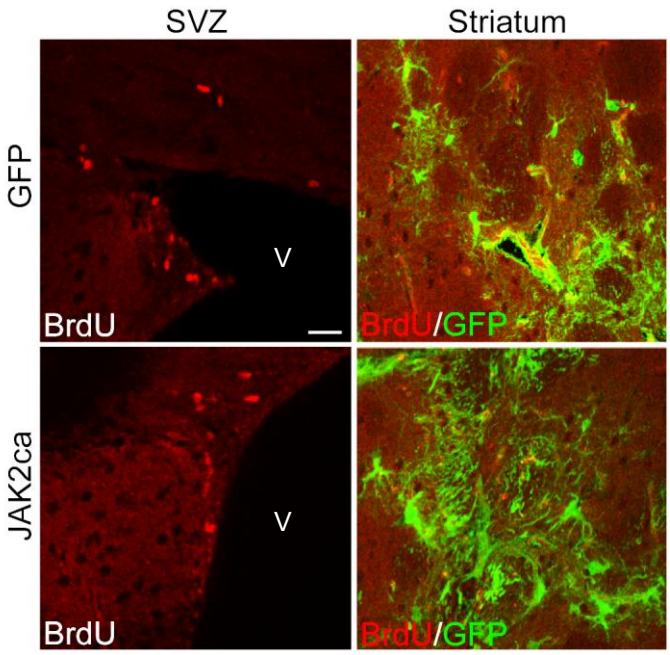

Figure 35. Absence of abnormal cellular proliferation in lenti-JAK2ca-injected mice.
Images of double stainings for BrdU (red) and GFP (green) in the SVZ (V, ventricle) and striatum in lenti-GFP and lenti-JAK2ca + lenti-GFP-injected mice. The number of BrdU-positive cells in the SVZ is comparable in between both groups. No BrdU-labeled astrocyte is observed in the injected area. N= 4/ group. Scale bar: 40 µm.

Overall, these results show that injection of lentiviral vector encoding JAK2ca specifically induces astrocyte activation in the injected area. JAK2ca causes mild microglial activation and does not lead to detectable neuronal toxicity or cellular proliferation in the mouse striatum.

Lentiviral vectors elicited a non-specific inflammatory reaction in the B6C3 mouse strain (N171-82Q mice). Therefore, to overexpress JAK2ca in N171-82Q mice, we had to use AAV vectors.

ii) AAV-JAK2ca

We used AAV vectors encoding JAK2ca to functionally characterize reactive astrocytes in the striatum and the hippocampus. AAV encoding JAK2ca were systematically co-injected with AAV-GFP (AAV-JAK2ca + AAV-GFP in figure legends). Therefore, infected cells are detected with GFP in JAK2ca and GFP groups. Again, we controlled that JAK2ca overexpression led to activation of the JAK2/STAT3 pathway in infected astrocytes. C57BL/6 mice were injected in the striatum or in the CA1 region of the hippocampus with AAV-JAK2ca or AAV-GFP. One month post-injection, immunofluorescence staining for STAT3 and GFAP was performed in both groups. STAT3 staining was increased in mice injected with AAV-JAK2ca compared to GFP controls both in the striatum (**Figure 36A**) and the hippocampus (**Figure 36B**).

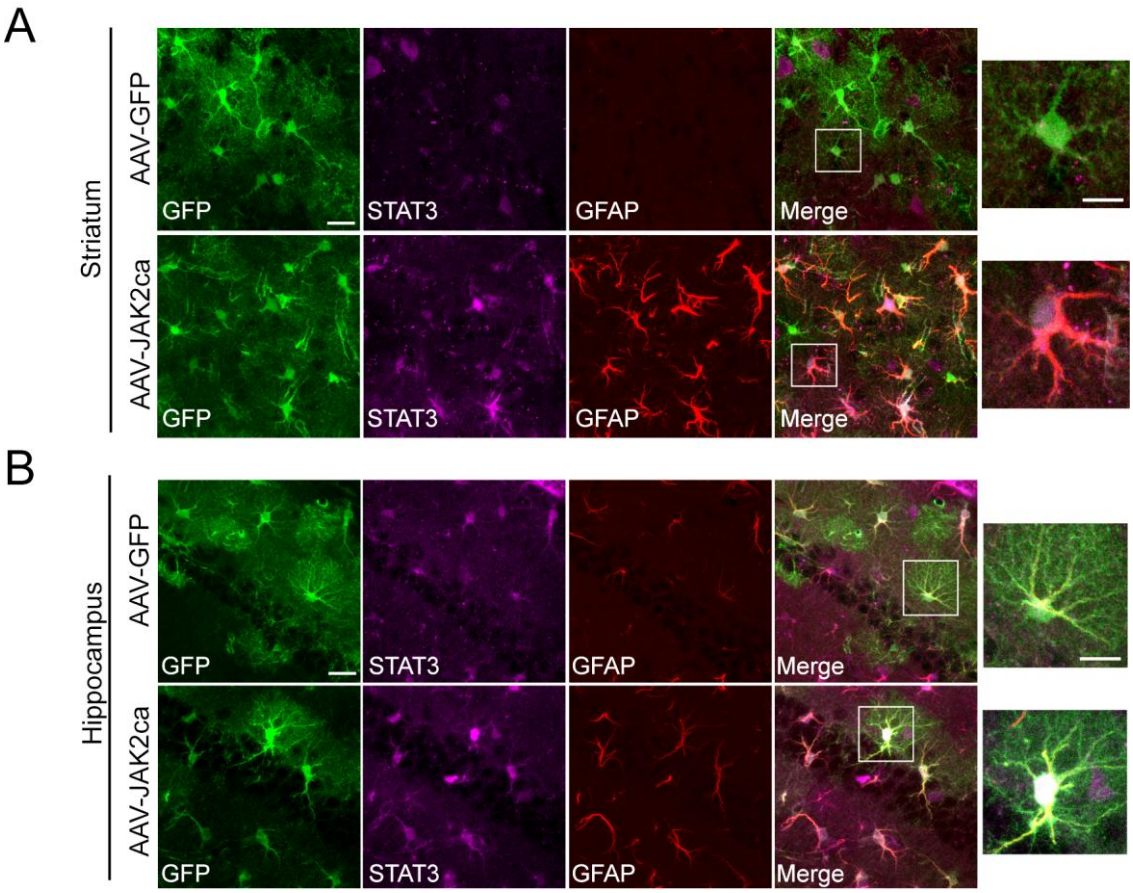

Figure 36. AAV-JAK2ca activates astrocytes and the JAK2/STAT3 pathway in the mouse striatum and hippocampus.
A-B, Images of triple immunolabeling for GFP (green), STAT3 (magenta) and GFAP (red) on mouse brain sections injected with AAV-GFP or AAV-JAK2ca + AAV-GFP in the striatum (**A**) or the CA1 region of the hippocampus (**B**). AAV-JAK2ca-infected astrocytes display higher GFAP staining than AAV-GFP controls in the striatum (**A**) and the hippocampus (**B**). Reactive astrocytes up regulate STAT3 in the JAK2ca-group in both brain regions. N= 4/ group. Scale bar: 40 µm.

We then evaluated the effect of JAK2ca overexpression on both astrocytes and neurons in the mouse striatum and hippocampus. In the striatum, injection of AAV-JAK2ca led to increased expression of the reactive astrocyte marker vimentin. DARPP32^{+} striatal neurons displayed similar staining and morphology in the JAK2ca and GFP groups (**Figure 37A**). Equally, in the CA1 region of the hippocampus, AAV-JAK2ca-injected mice showed increased vimentin staining compared with AAV-GFP mice. Furthermore, neurons labeled with microtubule associated protein 2 (MAP2) displayed equivalent expression between the two groups (**Figure 37B**).

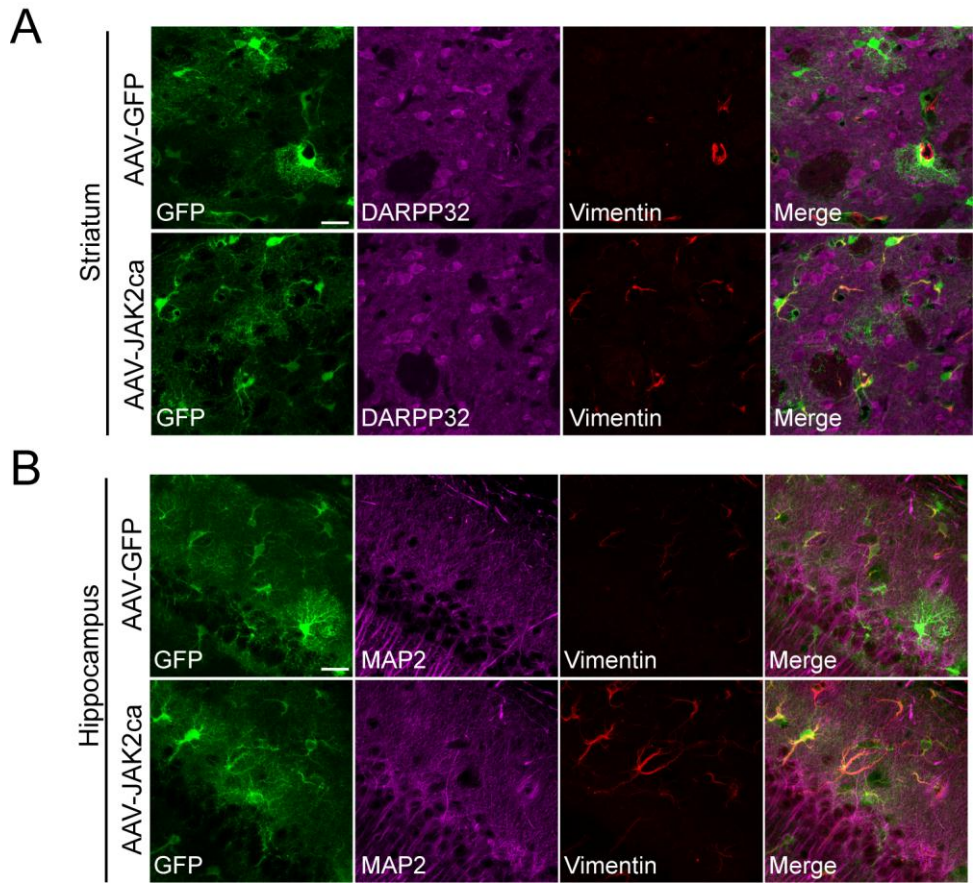

Figure 37. AAV-JAK2ca does not lead to detectable neuronal toxicity in the mouse striatum and hippocampus.
A-B, Images of triple immunolabeling for GFP (green), neuronal markers (striatum: DARPP32; hippocampus: MAP2; magenta) and vimentin (red) on mouse brain sections injected with AAV-GFP or AAV-JAK2ca + AAV-GFP in the striatum (**A**) the CA1 region of the hippocampus (**B**). AAV-JAK2ca-infected astrocytes display increased vimentin staining compared with AAV-GFP controls in the striatum (**A**) and the hippocampus (**B**). **A**, In the striatum, expression of the neuronal marker DARPP32 is similar between AAV-GFP and AAV-JAK2ca. $DARPP32^{+}$ neurons display normal morphology and density. **B**, In the CA1 region of the hippocampus, MAP2 staining of the neuronal cytoskeleton is comparable in AAV-GFP and AAV-JAK2ca groups. N= 4/ group. Scale bar: 40 µm.

Taken together, these data show that JAK2ca overexpression using AAV vectors activates astrocytes through the JAK2/STAT3 pathway. In addition, AAV-JAK2ca does not lead to detectable neuronal loss or toxicity both in the striatum and the hippocampus.

In conclusion, we have developed and validated two potent viral tools that selectively activate astrocytes through the JAK2/STAT3 pathway *in vivo*. These tools allow robust and stable effects and can be easily used in different models, brain regions or animal species.

3) SOCS3 prevents astrocyte activation in multiple models and species

a) SOCS3 prevents CNTF-mediated astrocyte activation in the rat striatum

The JAK2/STAT3 pathway is regulated through a feedback mechanism involving SOCS3, its endogenous inhibitor (see II.B.2.C.ii). Thus, we took advantage of this regulation and overexpressed SOCS3 to block astrocyte reactivity *in vivo*. We used a model of astrocyte activation based on the lentiviral gene transfer of the CNTF (lenti-CNTF), previously developed in the laboratory. Lenti-CNTF strongly activates astrocytes in the rat striatum by activation of the JAK2/STAT3 pathway (**Escartin et al., 2006**).

Rats received bilateral injection of lenti-CNTF. They were co-injected with lenti-SOCS3 + lenti-GFP in one striatum and with lenti-GFP in the other, at the same total virus load. Co-injection with lenti-GFP was used to visualize the morphology of infected cells.

SOCS3 overexpression was detected by qRT-PCR. *Socs3* mRNA levels were increased from approximately 2 fold in lenti-SOCS3-injected striatum compared with GFP controls (**Figure 38A**). It is to note that CNTF already induces *socs3* expression (data not shown from C. Escartin). However, this moderate increase in *socs3* mRNA levels was sufficient to elicit a significant physiological effect at the protein level. By western blotting analysis, we showed that lenti-CNTF increased levels of pSTAT3 compared to NI controls. Interestingly, SOCS3 restored pSTAT3 expression to a similar level as NI controls (**Figure 38B**). Thus, SOCS3 efficiently prevents the JAK2/STAT3 pathway activation in lenti-CNTF-injected rats.

We then ask whether blockade of the JAK2/STAT3 pathway would prevent astrocyte activation in the CNTF model. We detected GFAP and vimentin (**Figure 38C**) by immunohistochemistry. Both markers of reactive astrocyte were strongly increased by lenti-CNTF in the control striatum (**Figure 38C and 39A, B**). By contrast, this increase was completely prevented in the SOCS3 striatum (**Figure 38C and 39A, B**). Lenti-SOCS3 led to a significant decrease in the $GFAP^+$ and $vimentin^+$ volumes after lenti-CNTF-injection in the rat striatum (20,9% and 18,5%, respectively, $p<0,01$, n = 6 rats, paired Student's t-test). In accordance with these data, mRNA levels of *gfap* and *vimentin* were decreased in the lenti-SOCS3 striatum compared with lenti-GFP control ($p < 0,05$, n = 6 rats, Student's t-test; **Figure 38D**).

These results suggest that SOCS3 is able to prevent CNTF-mediated astrocyte activation by blocking the JAK2/STAT3 pathway and subsequent transcriptional regulation of reactive astrocyte markers.

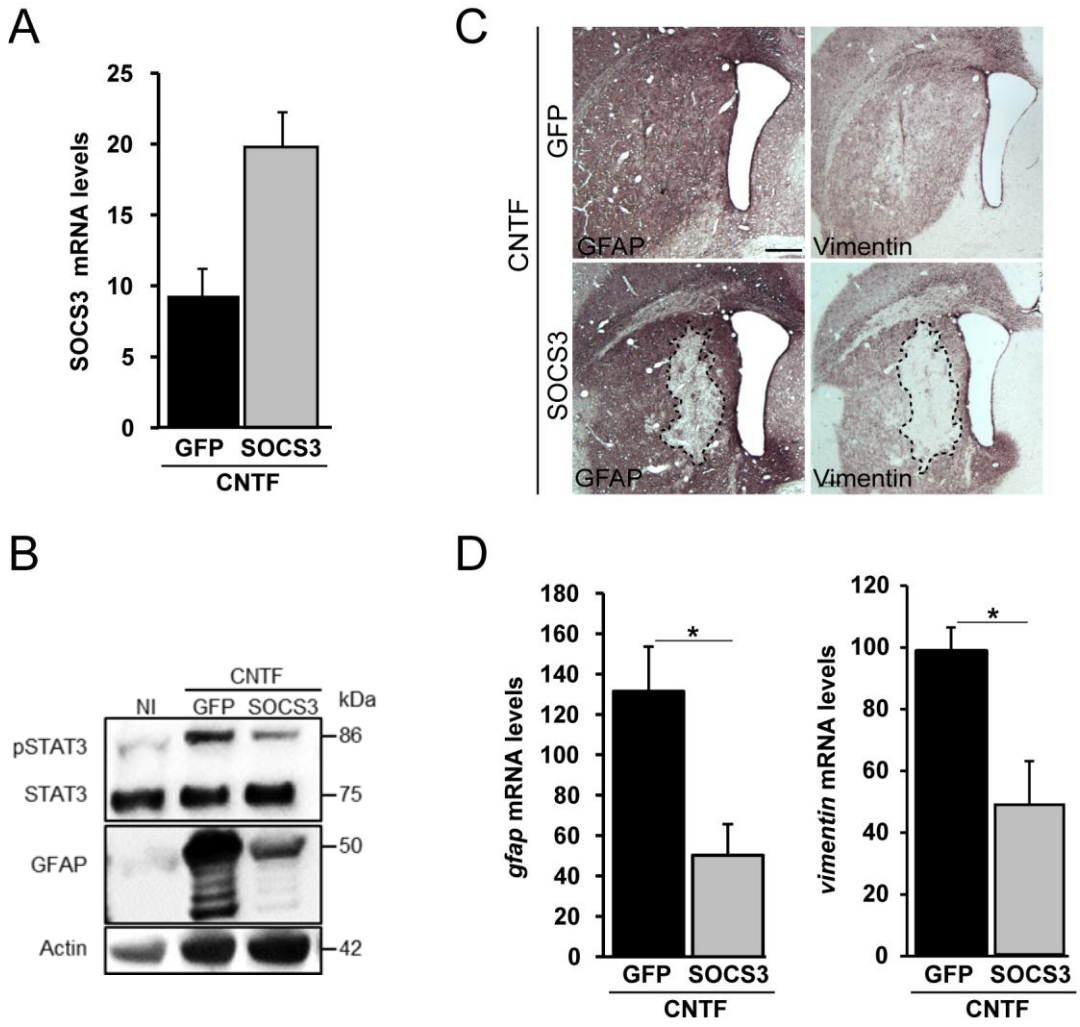

Figure 38. Lenti-SOCS3 prevents CNTF-mediated astrocyte activation in the rat striatum.
A, qRT-PCR analysis of socs3 mRNA levels in rats after striatal injection of lenti-CNTF+ lenti-GFP in the left striatum and lenti-CNTF+ lenti-SOCS3 + lenti-GFP in the right striatum. *Socs3* mRNA levels are doubled after lenti-SOCS3 injection. **B**, Western blot detection of pSTAT3, STAT3 and actin in GFP, SOCS3 and NI striata. Lenti-CNTF increases pSTAT3 levels compared with its expression in NI striatum. Lenti-SOCS3 reduces pSTAT3 and GFAP. The housekeeping protein actin is used as a loading control. **C**, Images of GFAP and vimentin stainings in rat injected with lenti-CNTF+ lenti-GFP in one striatum and with lenti-CNTF+ lenti-SOCS3 in the contralateral hemisphere. Lenti-CNTF leads to robust increase in GFAP and vimentin expression. Both markers are decreased in the lenti-SOCS3-injected area. **D**, *gfap* and *vimentin* mRNA levels are decreased in lenti-SOCS3 group compared to GFP controls. N= 4, * $p < 0.05$, Student's t-test. Scale bars: 2 mm.

b) SOCS3 restores basal astrocyte protein expression

To assess the phenotype of SOCS3 astrocytes, we analyzed the expression of other astrocyte-specific proteins by confocal microscopy. In contrast to GFAP and vimentin, S100β and GLT-1 levels were similar in the lenti-SOCS3 and lenti-GFP-injected striata (**Figure 39A and B**). Furthermore, mRNA levels of *glt-1*, *cx43* and *aqp4* were not significantly altered by SOCS3 overexpression (n = 6 rats/ group, Student's t-test; **Figure 39C**).

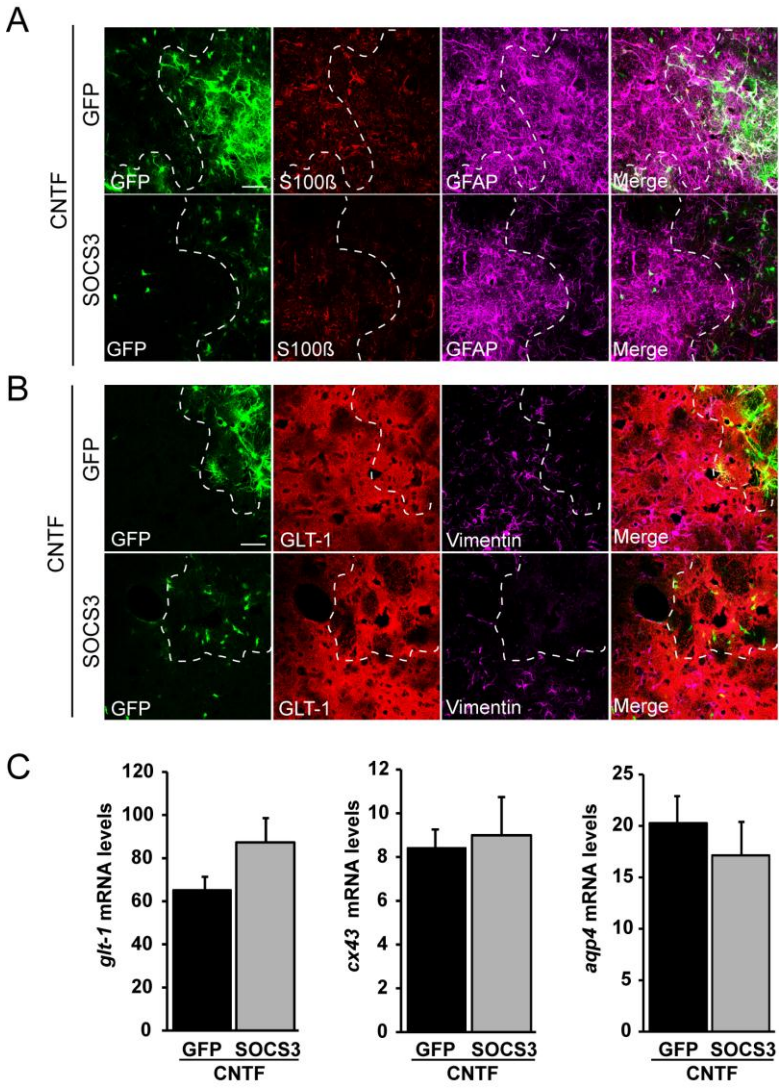

Figure 39. Lenti-SOCS3 does not alter all astrocyte markers.
A-B, Images of immunofluorescent stainings for GFP (green), astrocytes (A, S100β and B, GLT-1, red) and reactive astrocytes (A, GFAP and **B**, vimentin, magenta) on rat brain sections after striatal injection of lenti-CNTF+ lenti-GFP in the left striatum and lenti-CNTF+ lenti-SOCS3 + lenti-GFP in the right striatum. Expression of the astrocyte markers S100β (**A**) and GLT-1 (**B**) is not different between lenti-SOCS3 and lenti-GFP striata. By contrast, GFAP (**A**) and vimentin (**B**) are strongly downregulated in lenti-SOCS3-injected area. **C**, qRT-PCR analysis of *glt-1*, *cx43* and *aqp4* mRNA levels. The expression of these three genes is not altered by lenti-SOCS3 injection (at the right of white dashes lines). N= 4, Student's t-test. Scale bar: 40 µm. The injected area is delimited by white dashes.

c) The STAT3 pathway triggers astrocyte reactivity in ND models

i) The JAK2/STAT3 pathway is responsible for astrocyte reactivity in 3xTg-AD mice

In the first part of the manuscript, we showed that the JAK2/STAT3 pathway was a universal feature of astrocyte reactivity in ND models. However, the instrumental role of this pathway in mediating astrocyte reactivity has not been directly evaluated. Thus, we aimed to determine the requirement of the JAK2/STAT3 pathway for mediating astrocyte reactivity in ND models. As shown in the previous paragraph, lenti-SOCS3 is a powerful tool that selectively prevents astrocyte activation through selective blockade of the JAK2/STAT3 pathway in a rat model.

Viral vectors are versatile tools and can be used in different animal species as well as brain regions. We thus used lenti-SOCS3 to evaluate whether blockade of the JAK2/STAT3 pathway would prevent astrocyte reactivity in ND mouse models, in two brain regions: in the subiculum of 3xTg-AD mice and in the striatum in the lentiviral-based model of HD.

We injected lenti-SOCS3 + lenti-GFP or lenti-GFP alone into the subiculum of 7 to 8 month-old 3xTg-AD mice and analyzed them 4.5 months later. We first tested whether SOCS3 overexpression in astrocytes was able to inhibit the JAK2/STAT3 pathway *in situ*. SOCS3 strongly decreased STAT3 expression in astrocytes from 3xTg-AD mice (**Figure 40A**). The number of GFP^+-astrocytes showing STAT3 immunoreactivity in the nucleus was significantly lower in mice co-infected with lenti-SOCS3 than in those infected with lenti-GFP alone ($p < 0.05$, n = 3-5 mice/ group, Student's t-test; **Figure 40B**). Furthermore, GFAP expression was 73% lower in the SOCS3 group than in the GFP controls, although this difference was not statistically significant ($p = 0.0827$, n = 3-5 mice/ group, Student's t-test; **Figure 40 D**). There were significantly fewer GFP^+-astrocytes co-expressing GFAP in the SOCS3 group than in the control (- 94%, $p < 0.05$, n = 3-5 mice/ group, Student's t-test; **Figure 40E**). GFP expression in infected astrocytes allowed us to visualize their morphology in both groups. Astrocytes in the subiculum of 3xTg-AD mice displayed a morphology characteristic of reactive astrocytes with enlarged soma and large $GFAP^+$ primary processes (**Figure 40A, C**). By contrast, SOCS3-infected astrocytes displayed complex ramifications composed of thin cytoplasmic processes radially organized around the soma, typical of resting astrocytes of the mouse brain (Wilhelmsson et al., 2006 and **Figure 40A, C**). We also performed immunostaining for S100β, a ubiquitous marker of astrocytes, to verify that SOCS3 did not globally impair protein expression in astrocytes. The abundance of S100β was similar between 3xTg-AD mice injected with lenti-SOCS3 or lenti-GFP (**Figure 40F**).

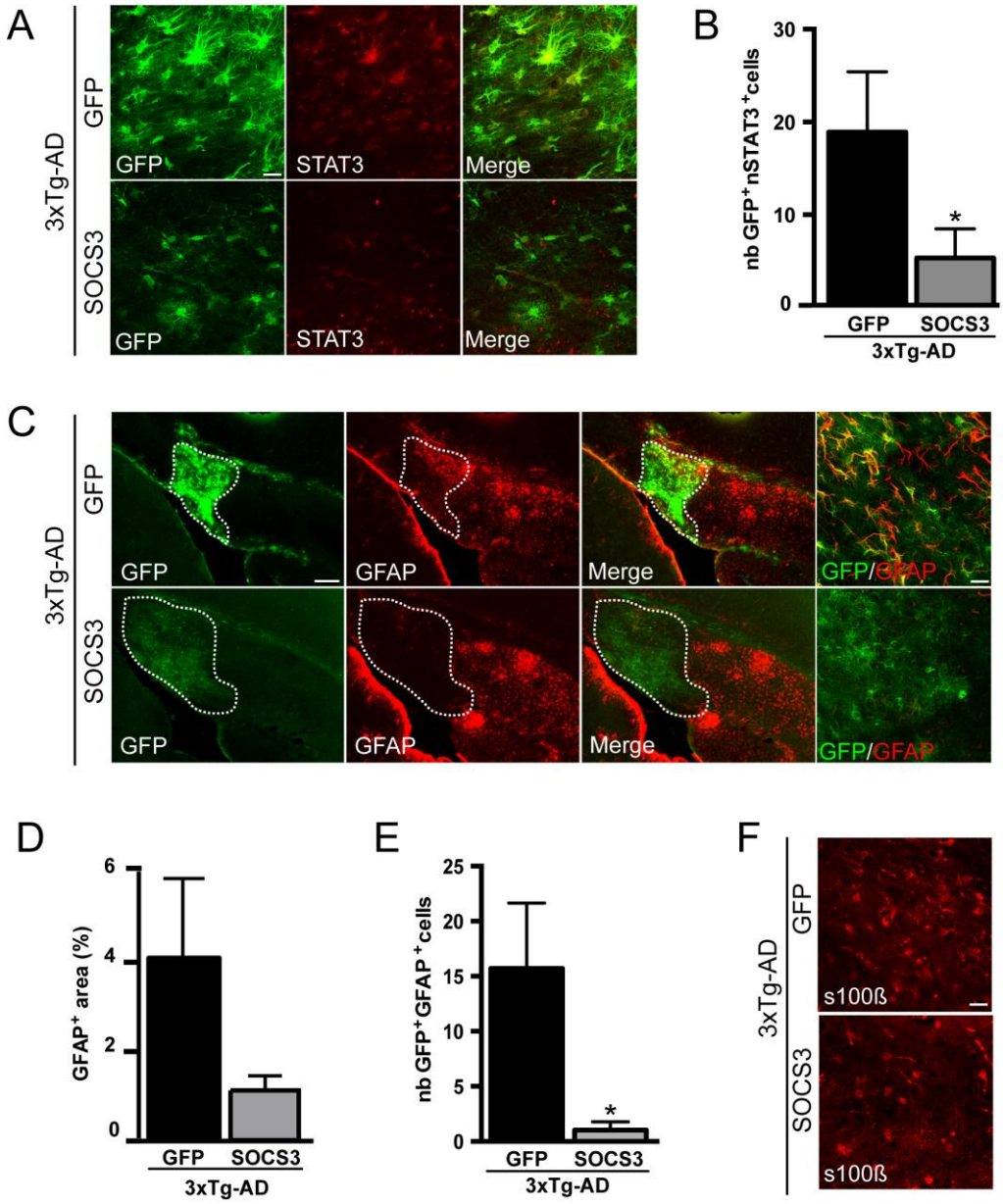

Figure 40. The JAK2/STAT3 pathway is responsible for astrocyte reactivity in 3xTg-AD mice.
A, Immunofluorescent staining of GFP (green) and STAT3 (red) in 7-8 month-old 3xTg-AD mice injected in the *subiculum* with lenti-GFP or lenti-SOCS3 + lenti-GFP (same total virus load). SOCS3 expression in astrocytes reduces STAT3 expression to undetectable levels compared with control astrocytes only infected with lenti-GFP. **B,** The number of GFP^+ infected astrocytes co-expressing STAT3 in the nucleus ($GFP^+/nSTAT3^+$ cells) is significantly decreased in the SOCS3 group compared with GFP controls. **C,** Images of GFAP (red) and GFP (green) stainings on 3xTg-AD mouse brain sections after hippocampal injection of lenti-GFP or lenti-SOCS3. Lenti-SOCS3 injection in 3xTg-AD mice strongly reduces GFAP expression in the injected area (delimited by white dots). Note that GFP^+, infected astrocytes in the SOCS3 group have a bushy morphology compared with those in the control group, which are hypertrophic with enlarged primary processes. **D,** Quantification of the $GFAP^+$ area in 3xTg-AD mice injected with lenti-SOCS3 or lenti-GFP. **E,** The number of GFP^+ infected astrocytes co-expressing GFAP is significantly decreased in the SOCS3 group compared with GFP controls. **F,** Immunofluorescent labeling for the astrocyte marker S100β shows that its expression is not altered by SOCS3. N = 3-5/ group. * $p < 0.05$, Student's t-test. Scale bars: 500 µm, 20 µm. Infected astrocytes in both groups are identified by their expression of GFP.

ii) The JAK2/STAT3 pathway is responsible for astrocyte reactivity in the lentiviral-based model of HD.

We performed the same experiment with the lentiviral-based model of HD. C57BL/6 mice were injected with lenti-Htt82Q and lenti-GFP in the left striatum and with lenti-Htt82Q, lenti-SOCS3 and lenti-GFP in the right hemisphere, at the same total virus load. Again, SOCS3 efficiently prevented the activation of the JAK2/STAT3 pathway in astrocytes (**Figure 41A**). The number of infected cells co-expressing STAT3 was 87% lower in the striatum injected with lenti-SOCS3 than in the control striatum (p <0.001, n = 4, Student's paired t-test; **Figure 41B**). In addition, the percentage of cells highly fluorescent for STAT3 was strongly reduced by SOCS3 (p < 0.05, n = 4, Student's paired t-test; **Figure 41C**). SOCS3-expressing astrocytes displayed a bushy morphology with thin cytoplasmic processes and numerous ramifications whereas reactive astrocytes in the control striatum showed enlarged and tortuous primary processes (**Figure 41D**). Inhibition of the JAK2/STAT3 pathway by SOCS3 prevented the increase of GFAP expression in the lenti-Htt82Q-injected area (**Figure 41D**). The $GFAP^+$ area was 86% smaller in the striatum injected with lenti-SOCS3 than in the control striatum (p = 0.0035, n = 4, Student's paired t-test; **Figure 41E**). In addition, the number of $GFP^+/GFAP^+$ cells was significantly decreased by SOCS3 (p < 0.001, n = 4, Student's paired t-test, **Figure 41F**). On the contrary, the abundance of the ubiquitous astrocyte marker S100β was not altered by SOCS3 (**Figure 41G**).

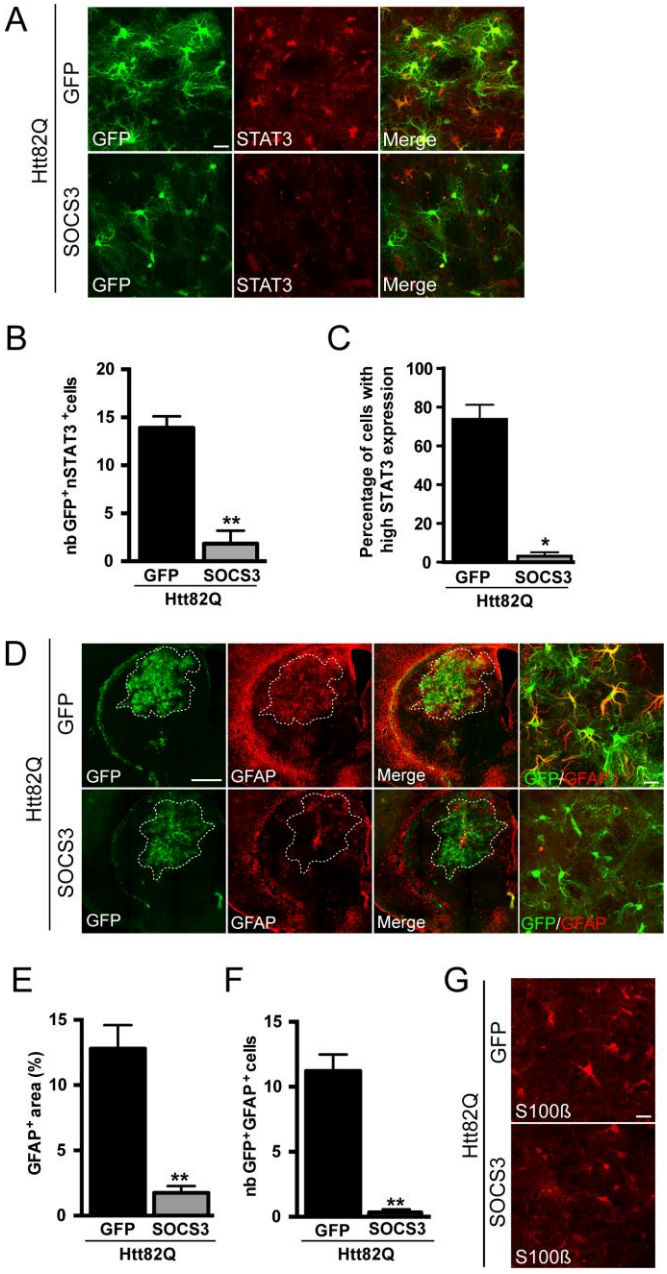

Figure 41. The JAK2/STAT3 pathway is responsible for astrocyte reactivity in the lentiviral-based HD mouse model.

A, Immunofluorescent staining of GFP (green) and STAT3 (red) in mice injected in one striatum with lenti-Htt82Q + lenti-GFP and the contralateral striatum with lenti-Htt82Q + lenti-SOCS3 + lenti-GFP. SOCS3 expression in astrocytes reduces STAT3 expression to undetectable levels compared with control astrocytes in the GFP group. **B,** The number of $GFP^+/nSTAT3^+$ astrocytes is significantly decreased in the SOCS3 group compared with GFP controls. **C,** The number of highly fluorescent $STAT3^+$ cells is significantly decreased by SOCS3. **D,** SOCS3 expression strongly reduces GFAP expression (red) in the injected area (GFP^+, green). Infected astrocytes in the SOCS3 group display thin processes and complex ramifications compared with reactive astrocytes in the control group. **E,** Quantification confirms that the $GFAP^+$ area is significantly decreased with lenti-SOCS3. **F,** The number of GFP^+ infected astrocytes co-expressing GFAP is significantly decreased in the SOCS3 group compared with GFP controls. **G,** Immunofluorescent staining for the astrocyte marker S100β (red). N = 4. ** $p < 0.01$, paired Student's t-test. Scale bars: 500 µm, 20 µm.

We studied the mRNA abundance of reactive astrocyte markers to further characterize the effect of SOCS3. We only used the lentiviral-based HD model, because the infected area in the subiculum of 3xTg-AD mice was too small to be dissected out for qRT-PCR analysis.

Socs3 mRNA levels were strongly induced in lenti-SOCS3 compared with lenti-Htt18Q and Htt82Q ($p < 0.001$, n = 3-5 mice/ group, ANOVA and Scheffé's test; **Figure 42A**). The abundance of *gfap* and *vimentin* mRNA was more than 2 fold higher in the Htt82Q striatum than in the Htt18Q striatum, consistent with immunofluorescence results (**Figure 42B, C**). Expression of SOCS3 in astrocytes normalized the expression of these two genes to levels comparable to controls ($p < 0.05$ versus Htt82Q, n = 3-5 mice/ group, ANOVA and Scheffé's test; **Figure 42B, C**). We also studied the mRNA abundance of some markers of neuroinflammation. The expression of the microglial marker *iba1* and the chemokine *ccl2* were increased 2.3 and 4.1-fold respectively by Htt82Q and reduced to Htt18Q control levels by SOCS3 ($p < 0.05$ and 0.001 versus Htt82Q, respectively, n = 3-5 mice/ group, ANOVA and Scheffé's test; **Figure 42D, E**). These results suggest that inhibition of the JAK2/STAT3 pathway in reactive astrocytes restores a resting-like status to astrocytes and reduces the neuroinflammatory response.

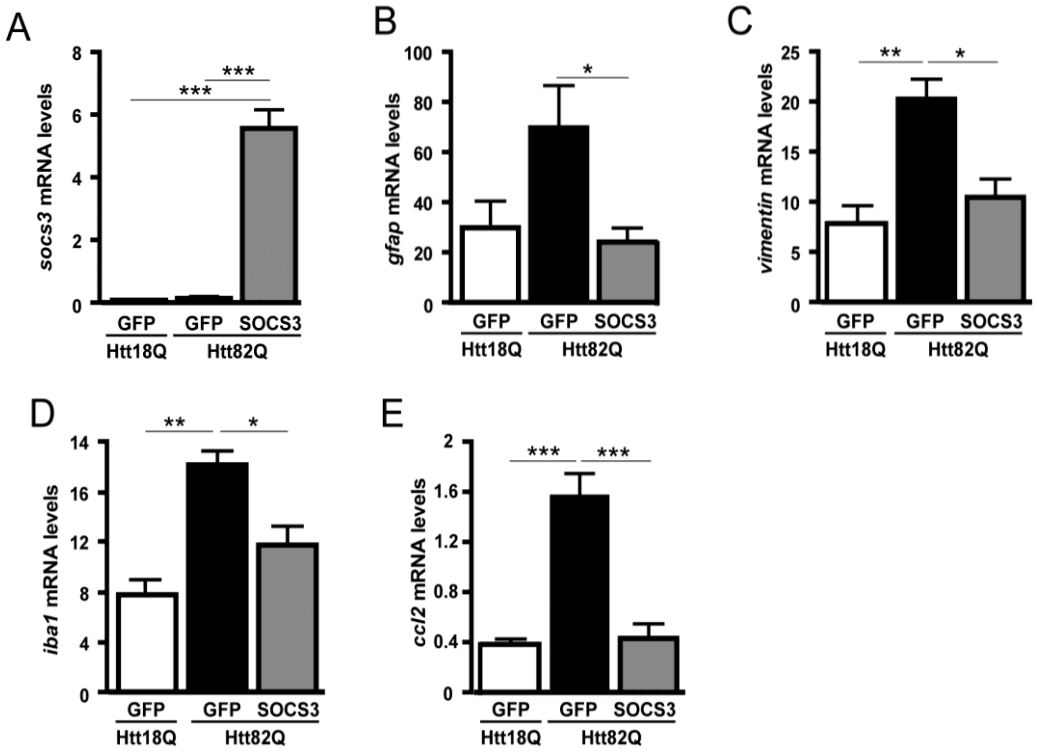

Figure 42. SOCS3 normalizes the expression of markers of astrocyte reactivity and neuroinflammation.

qRT-PCR analysis on mice injected in the striatum with lenti-Htt18Q + lenti-GFP; lenti-Htt82Q + lenti-GFP; or lenti-Htt82Q + lenti-SOCS3 + lenti-GFP (same total virus load). **A,** *Socs3* mRNA is overexpressed after lenti-SOCS3 injection. The expression of *gfap* (**B**)**,** *vimentin* (**C**), *iba1* (**D**) and *ccl2* (**E**) is induced by lenti-Htt82Q and is restored to levels observed in the Htt18Q control by the expression of SOCS3. N = 3-5/group. * $p < 0.05$, ** $p < 0.01$; *** $p < 0.001$.

In addition to lentiviral vectors, we developed AAV vectors encoding SOCS3 that were used to modulate astrocyte reactivity in the N171-82Q HD mouse model (see § C.2). The table below summarizes the different applications of these newly validated viral tools. They allow the selective induction (JAK2ca) or inhibition (SOCS3) of astrocyte reactivity *in vivo*. We have already validated their use in a number of experimental paradigms including different species (mice and rats) and models (wild-type and transgenic mouse models of AD and HD).

INDUCTION OF ASTROCYTE REACTIVITY BY JAK2ca

Species	Animals	Age	Disease model	Lentiviral-based models	Brain region	Viral vector	Results
rat	Sprague-Dawley	8 weeks		CNTF-mediated astrocyte activation	striatum	AAV	no induction of astrocyte reactivity *
mouse	C57BL/6	8 weeks			striatum	lentiviral	astrocyte activation
mouse	C57BL/6	8 weeks			striatum and hippocampus (CA1)	AAV	astrocyte activation
mouse	C57BL/6	8 weeks	HD	LV-Htt18Q(G)/ LV-Htt82Q(D)	striatum	lentiviral	Increased astrocyte reactivity
mouse	N171-82Q	13 weeks	HD		striatum	AAV	Increased astrocyte reactivity
mouse	Hdh140	12 months	HD		striatum	lentiviral	Increased astrocyte reactivity
mouse	APP/PS1dE9	12 months	AD		hippocampus (CA1)	AAV	Increased astrocyte reactivity #

INHIBITION OF ASTROCYTE REACTIVITY BY SOCS3

Species	Animals	Age	Disease model	Lentiviral-based models	Brain region	Viral vector	Results
rat	Sprague-Dawley	8 weeks		lenti-CNTF	striatum	lentiviral	prevention of CNTF-mediated astrocyte activation
rat	Sprague-Dawley	8 weeks		CNTF-mediated astrocyte activation	striatum	AAV	prevention of CNTF-mediated astrocyte activation
mouse	C57BL/6	8 weeks	HD	LV-Htt18Q(G)/ LV-Htt82Q(D)	striatum	lentiviral	Prevention of LV-Htt82Q-induced astrocyte reactivity
mouse	APP/PS1dE9	12 months	AD		hippocampus (CA1)	AAV	Prevention of astrocyte reactivity #
mouse	3xTg-AD	12 months	AD		subiculum	lentiviral	Prevention of astrocyte reactivity

Table 5. Summary of injections experiments to induce or prevent astrocyte reactivity in various models. * data from M-A.Carrillo de Sauvage, # data from K.Ceyzeriat.

In conclusion, we have validated a lentiviral vector encoding SOCS3 that enables the specific and almost complete abolition of astrocyte reactivity in several models *in vivo*. SOCS3 efficiently prevented CNTF-mediated astrocyte activation in the rat striatum. Furthermore, we used this powerful tool to demonstrate, for the first time, the instrumental role of the JAK2/STAT3 pathway in the induction of astrocyte reactivity mouse models of AD and HD, in different brain regions.

C. Manipulation of the JAK2/STAT3 pathway to determine the contribution of reactive astrocytes to neuronal dysfunction in HD models

It is widely discussed that reactive astrocytes may influence disease outcomes in many pathological conditions, including ND (**Maragakis and Rothstein, 2006**). However, the direct contribution of reactive astrocytes to HD is largely unknown. Therefore, we took advantage of our newly developed viral tools to evaluate the impact of reactive astrocytes to disease progression in two HD models: the lentiviral-based model and the N171-82Q mouse model of HD.

1) SOCS3 prevents astrocyte reactivity and influences the number of Htt aggregates in the lentiviral-based model of HD

We first decided to modulate astrocyte reactivity in the lentiviral-based model of HD. All mice were injected in the striatum with lentiviral vectors leading to the expression of Htt18Q or Htt82Q in neurons. They were co- injected with astrocyte-targeted lentiviral vectors encoding either JAK2ca to over-activate astrocyte, SOCS3 to prevent astrocyte activation or GFP as control.

Six weeks post-injection, mice were perfused for histological analysis. First, we evaluated the effect of JAK2ca and SOCS3 overexpression on astrocytes in the lenti-Htt18Q and the lenti-Htt82Q-injected striata. We controlled that injection of lenti-Htt18Q did not induce astrocyte reactivity in the lenti-GFP control group by double immunofluorescence staining for GFP and GFAP. Indeed, in the Htt18Q striatum, GFAP levels were nearly undetectable. This was also the case in the SOCS3 group. By contrast, JAK2ca activated astrocytes in the lenti-Htt18Q striatum, as they upregulated GFAP in the GFP^+ injected area.

In comparison, in the Htt82Q striatum, astrocytes were reactive as they upregulated GFAP in the GFP group (as already presented in § III.B.3.c.ii and **Figure 43A**). Even if GFAP levels were not further increased, vimentin expression was induced by JAK2ca overexpression (**Figure 43C**). These results suggest that JAK2ca was able to activate astrocytes in the control Htt18Q striatum, and it only led to a limited increase of astrocyte reactivity in the Htt82Q striatum.

By contrast, SOCS3 overexpression successfully prevented astrocyte reactivity in the Htt82Q striatum (**Figure 43A, B** and also shown in **Figure 41D**). Indeed, the $GFAP^+$ volume was decreased by 80% in lenti-SOCS3-injected mice compared with GFP controls ($p < 0{,}001$, n = 9-11mice/ group, one-way ANOVA and Scheffé tests; **Figure 43B**).

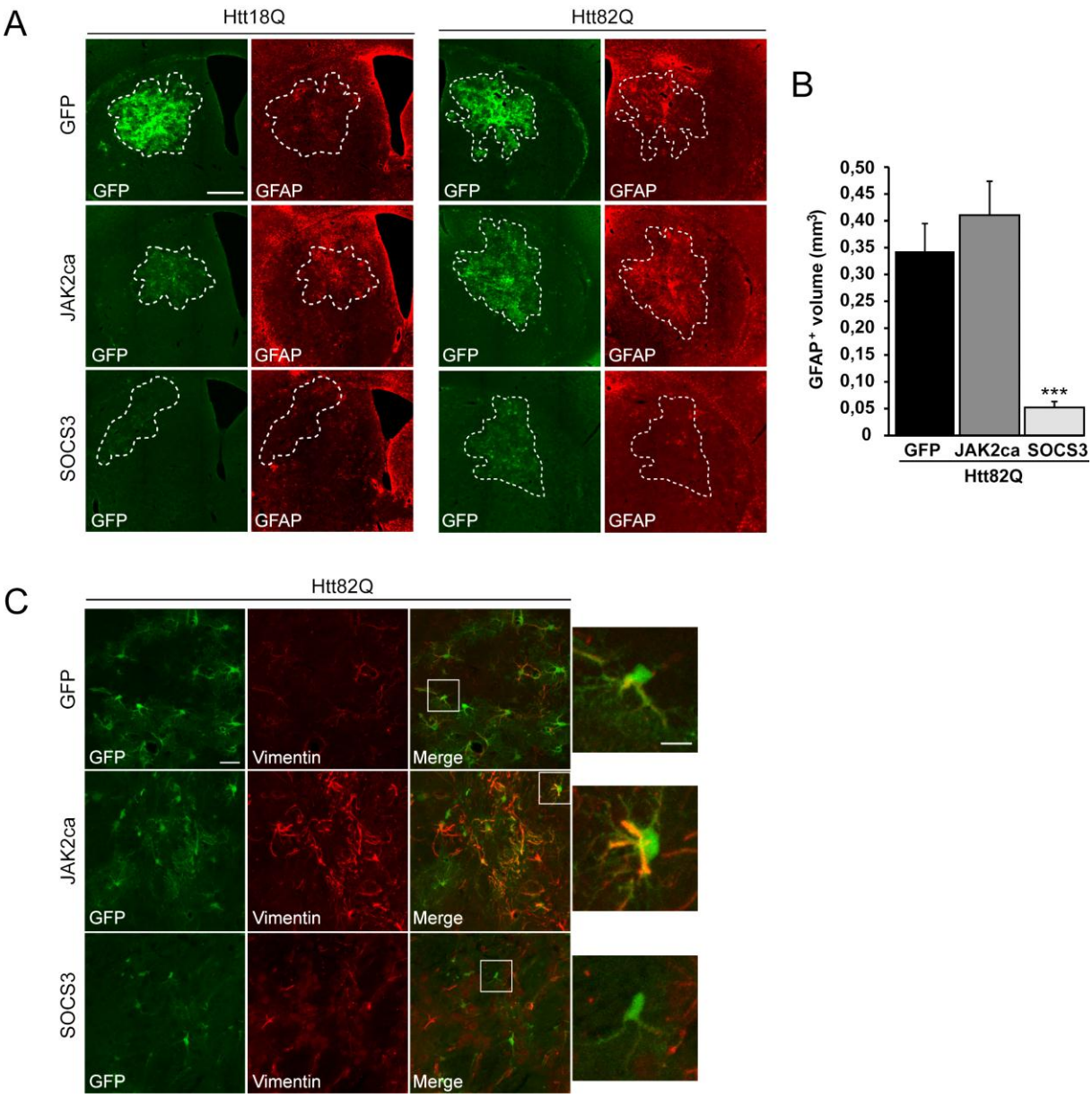

Figure 43. Positive and negative modulation of astrocyte reactivity in the lentiviral-based model of HD.

A-C, Immunofluorescent stainings for GFP (green) and reactive astrocyte markers (**A,** GFAP and **C,** vimentin, red) in mice injected in one striatum with lenti-Htt18Q and in the contralateral striatum with lenti-Htt82Q. Mice are bilaterally co-injected with either lenti-GFP, lenti-JAK2ca+ lenti-GFP or lenti-SOCS3+ lenti-GFP. **A,** Six weeks post-infection, expression of Htt82Q (right) leads to increased GFAP expression in the GFP^+ injected area compared with Htt18Q control (left). Co-injection with lenti-JAK2ca shows a tendency to increase Htt82Q-induced astrocyte reactivity. Co-injection with lenti-SOCS3 completely inhibits astrocyte reactivity following Htt82Q-injection. **B,** Quantification of the $GFAP^+$ volume in the GFP^+ injected striatum. Lenti-SOCS3 decreases $GFAP^+$ volume induced by Htt82Q expression in striatal neurons. **C,** High magnification of immunofluorescent stainings for GFP (green) and vimentin (red). Following Htt82Q-injection, astrocytes in the GFP group weakly express vimentin whereas lenti-JAK2ca leads to a strong induction of vimentin expression. In lenti-SOCS3-injected mice, vimentin is nearly undetectable in the striatum after Htt82Q-injection. N = 9-11/ group. *** $p < 0.001$, one-way ANOVA and Scheffé post-hoc test. Scale bars: 500 µm, 40 µm, and 5 µm.

Injection of lenti-Htt82Q in the mouse striatum leads to neuronal distress and death 6 weeks post-injection (**Galvan et al., 2012**). We quantified the striatal lesion by detecting loss of DARPP32 and NeuN staining by immunohistochemistry (**Figure 44A**). Overall, the lesion volume measured with both markers was not different between GFP, JAK2ca and SOCS3 groups (n= 9-11 mice/ group, one-way ANOVA test, **Figure 44A, B**).

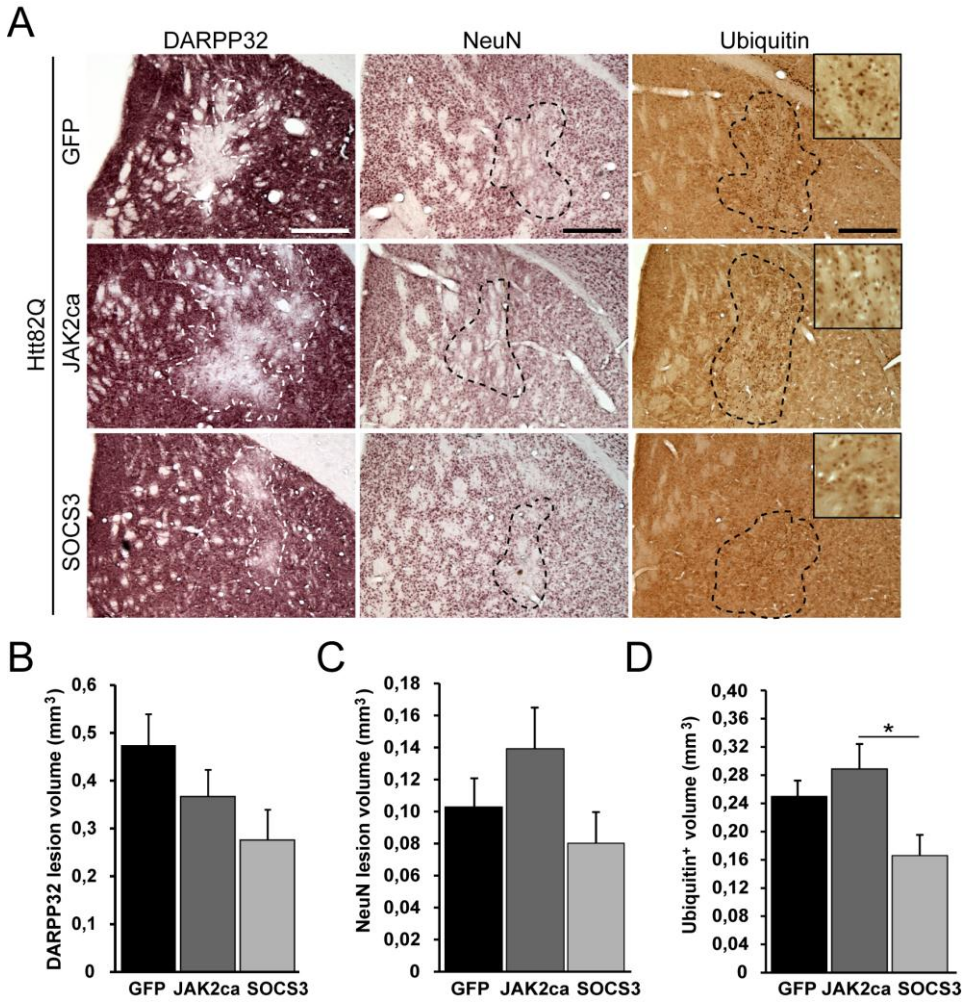

Figure 44. Modulation of astrocyte reactivity has no effect on striatal neuron dysfunction but lenti-SOCS3 decreases the number of ubiquitin-positive aggregates in the lentiviral-based model of HD.

A, Detection of neuronal markers DARPP32, NeuN and of ubiquitin^{+} aggregates by immunohistochemistry on mouse brain sections after striatal injections with lenti-Htt82Q. Mice were co-injected with lenti-GFP, lenti-JAK2ca+ lenti-GFP or lenti-SOCS3+ lenti-GFP. Htt82Q-expression in the mouse striatum leads to local loss of DARPP32 (white dashes) and NeuN (black dashes) stainings and to the formation of ubiquitin^{+} aggregates 6 weeks post-infection. **B-C,** Quantification of the lesion volumes using DARPP32 (**B**) and NeuN (**C**) stainings in the striatum. Co-injection with lenti-JAK2ca or lenti-SOCS3 has no effect on the lesion volumes. **D,** Quantification of the ubiquitin^{+} volume in the striatum after Htt82Q expression. Lenti-SOCS3 decreases the number of ubiquitin^{+} aggregates following Htt82Q-injection. N = 9-11/ group. * $p < 0.05$, one-way ANOVA and Scheffé post-hoc test. Scale bars: 100 µm.

Overexpression of Htt82Q led to the formation of ubiquitin$^+$ mHtt aggregates, mainly in striatal neurons (**Figure 44A**). The ubiquitin$^+$ volume was decreased with SOCS3 ($p < 0.05$, n = 9-11 mice/ group, one-way ANOVA and Scheffé post-hoc tests, **Figure 44D**). In addition, the number of ubiquitin$^+$ aggregates, quantified by stereology, was significantly decreased by SOCS3 (data not shown).
In conclusion, in the lentiviral-based of HD, overexpression of JAK2ca in astrocytes only resulted in a limited increase of astrocyte reactivity. Indeed, in this acute model, astrocytes are already strongly activated in response to neuronal death. By contrast, SOCS3 almost completely prevented astrocyte reactivity in this model. Blockade of astrocyte reactivity did not influence neuronal loss but decreased the number of ubiquitin$^+$ aggregates following Htt82Q injection in the mouse striatum.

Because SOCS3 effets on ubiquitin$^+$ aggregates were small and only different form the JAK2ca group, we decided to perform another experiment whereby SOCS3 effects are directly tested against Htt82Q within the same animal. C57BL/6 mice were bilaterally injected in the striatum with lenti-Htt82Q and with lenti-GFP in one striatum and lenti-SOCS3 + lenti-GFP in the other. As for the first experiment, we found that the lesion volumes, measured with DARPP32 and NeuN stainings, were not different between the GFP and SOCS3 groups (**Figure 45A and B**). Surprinsingly, we found that the number of mHtt aggregates, labeled with EM48, was significantly increased by SOCS3 ($p < 0.05$, n = 12 mice, paired Student's t-test; **Figure 45C**).

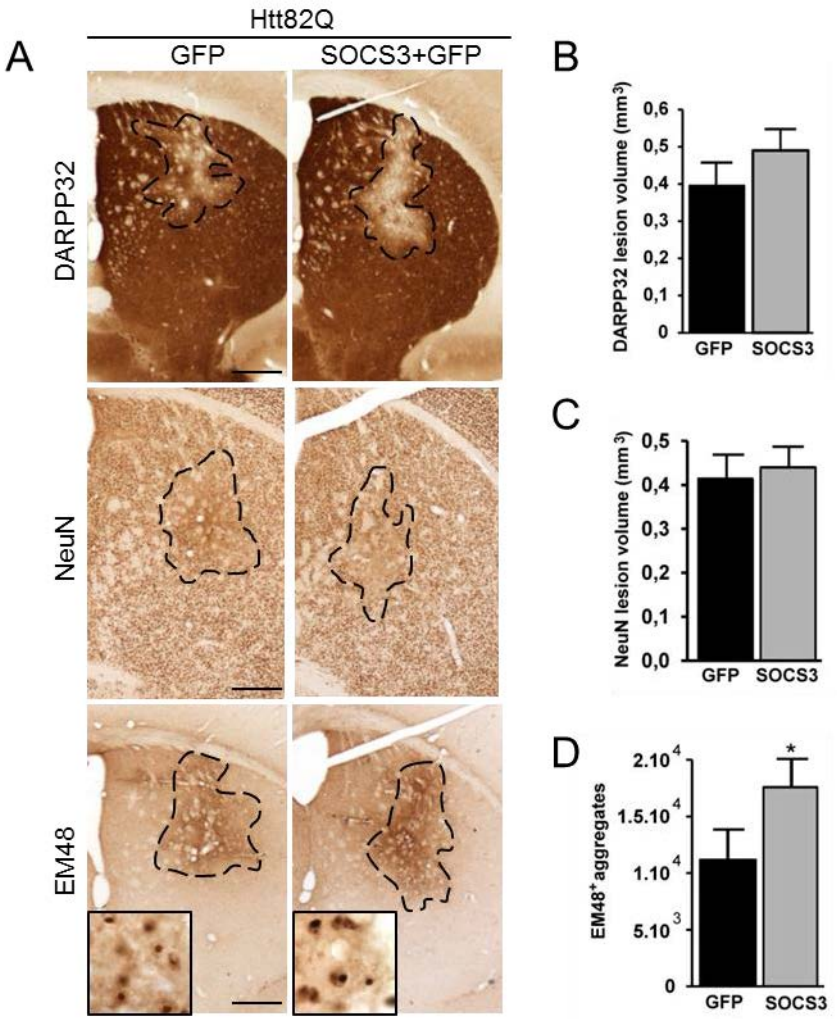

Figure 45. Lenti-SOCS3 increases the number of Htt aggregates in the lentiviral-based HD mouse model.
A, Immunohistological detection of neuronal markers DARPP32, NeuN and EM48$^+$ aggregates on mouse brain sections after injection with lenti-Htt82Q in the striatum. Mice were co-injected with lenti-GFP in the left striatum and with lenti-SOCS3+ lenti-GFP in the right striatum. **B-D,** Quantification of the Htt82Q-induced lesion volume in the striatum using DARPP32 (**B**) and NeuN (**C**) staining (black dashes). Lenti-SOCS3 has no effect on Htt82Q-induced neuronal dysfunction 6 weeks post-infection. **D,** Quantification of the number of EM48$^+$ aggregates. Lenti-SOCS3 increases the number of mHtt aggregates after Htt82Q injection. N = 12. * $p < 0.05$, paired Student's t-test. Scale bars: 500 µm.

In conclusion, these data demonstrate that modulating the astrocytic JAK2/STAT3 pathway in the lentiviral-based model of HD does not influence neuronal death. However, preventing astrocyte reactivity with SOCS3 influence the number of Htt aggregates.

2) Deciphering the contribution of reactive astrocyte to chronic neuronal dysfunction in the N171-82Q HD mouse model

We then aimed at evaluating the role of reactive astrocytes in a transgenic mouse model of HD, the N171-82Q mouse model, that reproduce some of the behavioral and histological alterations observed in patients with HD. First, we wanted to reproduce, in our experimental conditions, the behavioral deficits and histological alterations previously described in this model (**Schilling et al., 1999; Yu et al., 2003**).

a) Characterization of the N171-82Q HD mouse model

We studied a first cohort of N171-82Q and WT male mice, obtained from the Jackson laboratory (n = 8 mice/ group). Lifespan was comprised between 16 and 18 weeks. N171-82Q mice were not able to gain weight from 8 weeks of age and started to lose weight from 14 weeks of age (**Figure 46A**). N171-82Q mice displayed abnormal motor behavior at the rotarod test as early as 8 weeks of age compared to age-matched WT ($p < 0,01$, n = 8 mice/ group, repeated measure ANOVA test and Bonferonni post-hoc test; **Figure 46B**). These motor defecits worsened with time. However, both N171-82Q and WT mice displayed normal motor learning as their performances increased with the number of trials (**Figure 46B**). Tremor, decreased locomotion and abnormal gait were observed in mouse cage from 11 weeks of age in HD mice. However, alteration of the locomotor activity was not detectable with the open-field test at this age. By contrast, 18 week-old N171-82Q mice performed less rearings than age-matched WT mice (**Figure 46C**). Interestingly, the total distance moved and grooming behavior were not different between N171-82Q and WT mice (data not shown). Thus, on this first cohort of animals, we were able to reproduce the behavioral deficits described in the N171-82Q model.

We then performed post-mortem analysis on these mice, at 18 weeks of age (endstage). We labelled the striatal marker DARPP32 to measure the striatal volume in endstage N171-82Q and age-matched WT mice (**Figure 47A**). HD mice showed striatal atrophy and ventricle enlargment compared with WT mice ($p < 0.01$, n = 8 mice/ group, Student's t-test; **Figure 47A and B**). They also displayed numerous $EM48^+$ Htt aggregates throughout the cortex and the striatum, which were not present in WT mice, (**Figure 47A**). Expression of DARPP32, was slightly reduced by approximately 20% in HD compared with age-matched WT mice, as measured by western blotting (**Figure 47C**). Furthermore, *d2r* mRNA levels were decreased by 50% in N171-82Q mice ($p < 0.01$, n = 8 mice/ group, Student's t-test; **Figure 47D**).

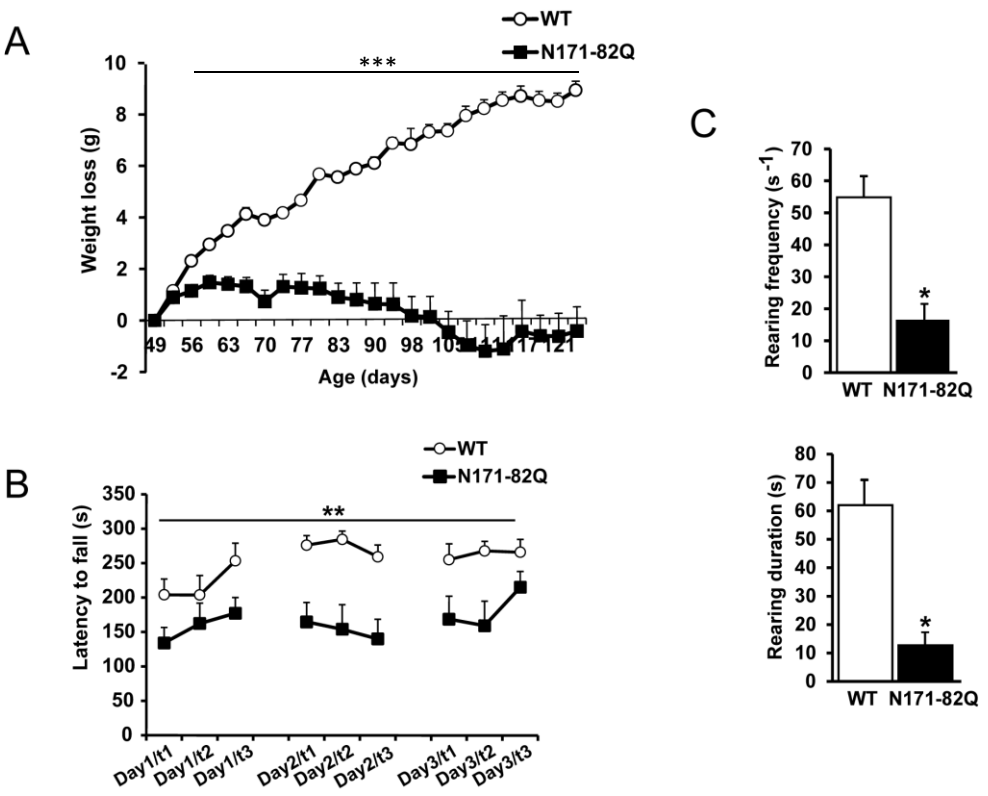

Figure 46. Characterization of behavioral alterations in the N171-82Q mouse model of HD.
A-C, Behavioral characterization of N171-82Q HD mice and WT littermates. **A**, N171-82Q mice start losing weight from 14 weeks of age. **B**, Eight week-old HD mice display abnormal motor coordination on the rotarod. **C**, 17-week-old N171-82Q mice show altered rearing duration and frequency at the open field test. N= 8/ group; * $p<0.05$, ** $p < 0.01$, *** $p < 0.001$ repeated measure ANOVA and Bonferronni post-hoc tests (**B**) or Student's t-test (**C**).

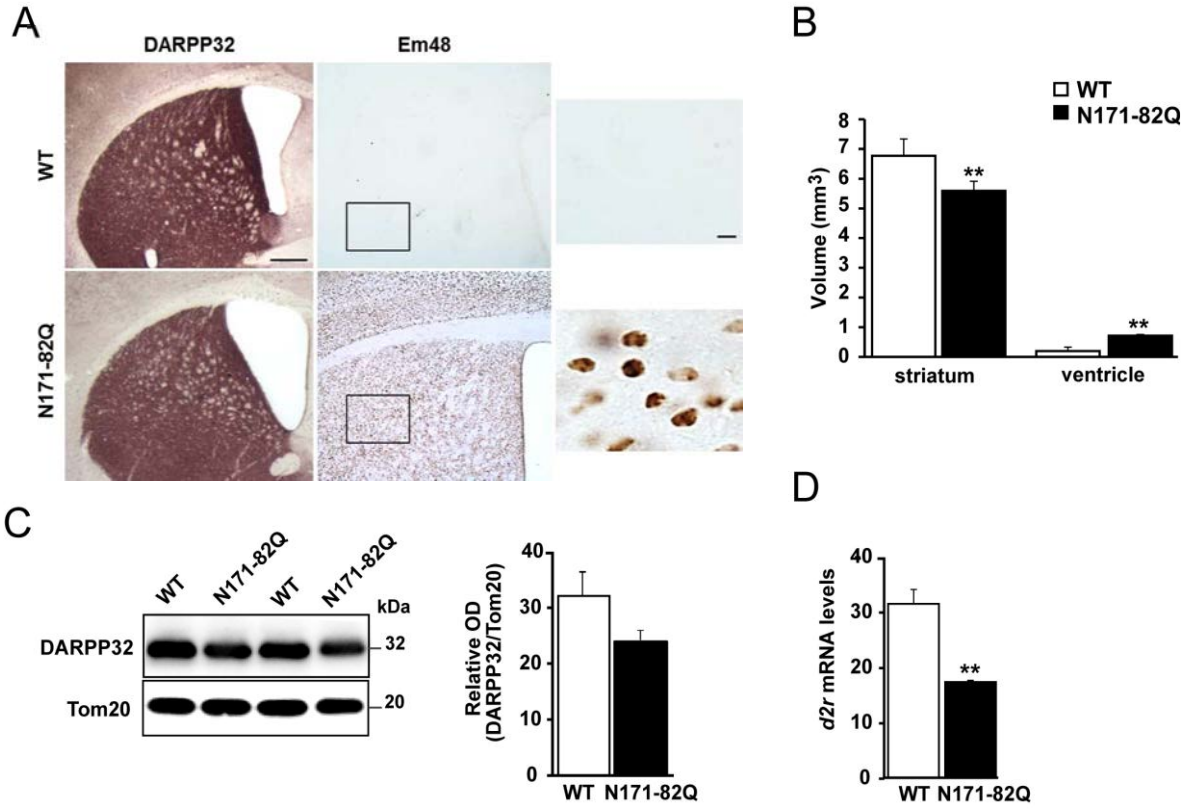

Figure 47. Post-mortem analysis of the N171-82Q mouse model of HD.
A-D, Analysis was performed on 18-week-old endstage N171-82Q mice and age-matched controls. **A**, DARPP32 and EM48 immunostainings on N171-82Q HD and WT mice. DARPP32 staining is comparable between N171-82Q and WT mice. HD mice show EM48^{+} Htt aggregates throughout the cortex and the striatum compared with WT, where Htt aggregates were not detected. **B**, N171-82Q mice display striatal atrophy and ventricle enlargement (see DARPP32 staining in **A**). **C**, Western blot analysis of the striatal marker DARPP32. DARPP32 protein levels are slightly decreased in HD mice compared with age-matched controls. **D**, qRT-PCR analysis of *d2r* mRNA levels. *d2r* expression is reduced in N171-82Q mice. N= 8/ group; ** $p < 0.01$, Student's t-test (**B**, **C** and **D**).

In conclusion, we were able to detect behavioral, histological and molecular alterations previously described in these mice. This characterization allowed us to evidence several parameters altered in HD mice (motor performances at the rotarod test, striatal volume and expression of striatal markers). We then used these parameters as outcomes to evaluate the effects of modulating astrocyte reactivity in the N171-82Q model of HD.

b) Modulation of astrocyte reactivity does not influence chronic neuronal dysfunction in N171-82Q mice

We used AAV vectors to modulate astrocyte reactivity in the N171-82Q mouse model of HD. For this experiment, we used mice from our own colony and performed a pilot study on the small number of animals available at that time.

Six to eight week-old male and female N171-82Q and age-matched controls were distributed in three groups. WT or N171-82Q mice were injected in the striatum with AAV-GFP (WT-GFP and N171-GFP mice). N171-82Q mice were injected with AAV-JAK2ca and AAV-GFP (N171-JAK2ca) or with AAV-SOCS3 and AAV-GFP (N171-SOCS3), at the same total virus load.

Five weeks post-injection, we assessed motor coordination on these mice with the rotarod test. Females displayed high anxiety levels despite the habituation protocol. Their performances at the rotarod test were too variable for interpretation, thus we only analyzed the performances of male mice (**Figure 48**).

Unexpectedly, we observed that WT-GFP mice displayed abnormal performances at the rotarod test compared with non-injected mice from the first cohort, which stayed longer than 250 sec on the rotarod (see §C.2.a, **Figure 46A**). In fact, in this experiment, we were not able to evidence any difference in motor performances between WT-GFP and N171-GFP mice. They both displayed very low mean latencies to fall of the rod (82.5 ± 6.9 and 78.0 ± 5.0 sec, respectively) (**Figure 48**). N171-JAK2ca mice also poorly performed at the rotarod test, as they showed a mean latency to fall of approximately 60 sec. Interestingly, N171-SOCS3 showed a tendency to perform better at the rotarod. The mean latency to fall in the SOCS3 group was 107.6 ± 6.9 (**Figure 48**).

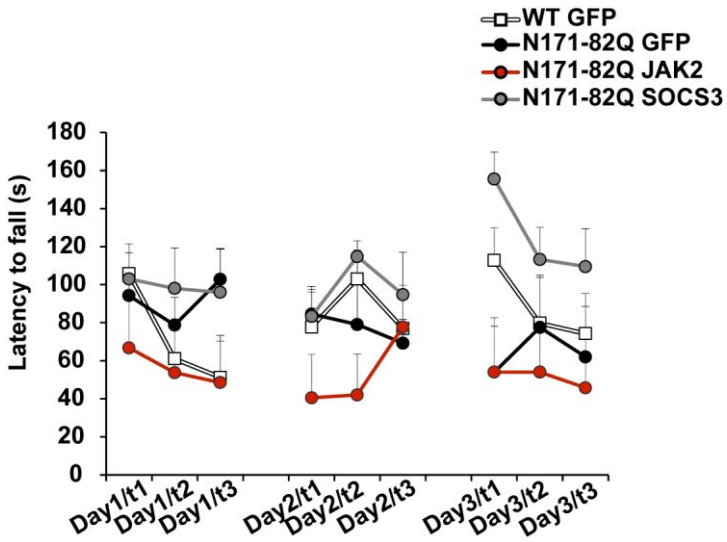

Figure 48. AAV-injected WT and N171-82Q poorly perform at the rotarod test.
Motor performances at the rotarod test of WT and N171-82Q male mice injected in the striatum with AAV-GFP, AAV-JAK2ca or AAV-SOCS3. 5 weeks post-injection, both WT and N171-82Q mice poorly perform at the rotarod test. At the third day of testing, N171-SOCS3 mice tend to perform better than the other groups. N= 4/ group. Ns, repeated measure ANOVA.

Mice were euthanized at 3-3.5 months of age, one brain hemisphere was used for histological analysis and the other for qRT-PCR. We first controlled transgene overexpression in the different groups. As JAK2ca and SOCS3 cannot be detected by histology due to the lack of specific antibodies, we detected *jak2* and *socs3* mRNA levels by qRT-PCR. *Jak2* mRNA was upregulated 10-fold in N171-JAK2ca mice, and *socs3* mRNA was upregulated approximately 150-fold in N171-SOCS3-injected

mice compared with other groups (p < 0.00, n = 7 WT-GFP, 5 N171-GFP, 6 N171-JAK2ca and 3 N171-SOCS3 mice, one-way ANOVA and Scheffé tests; **Figure 49A**). This result suggests that mice were correctly injected and that AAV led to significant overexpression of *jak2* and *socs3* mRNA in the appropriate groups.

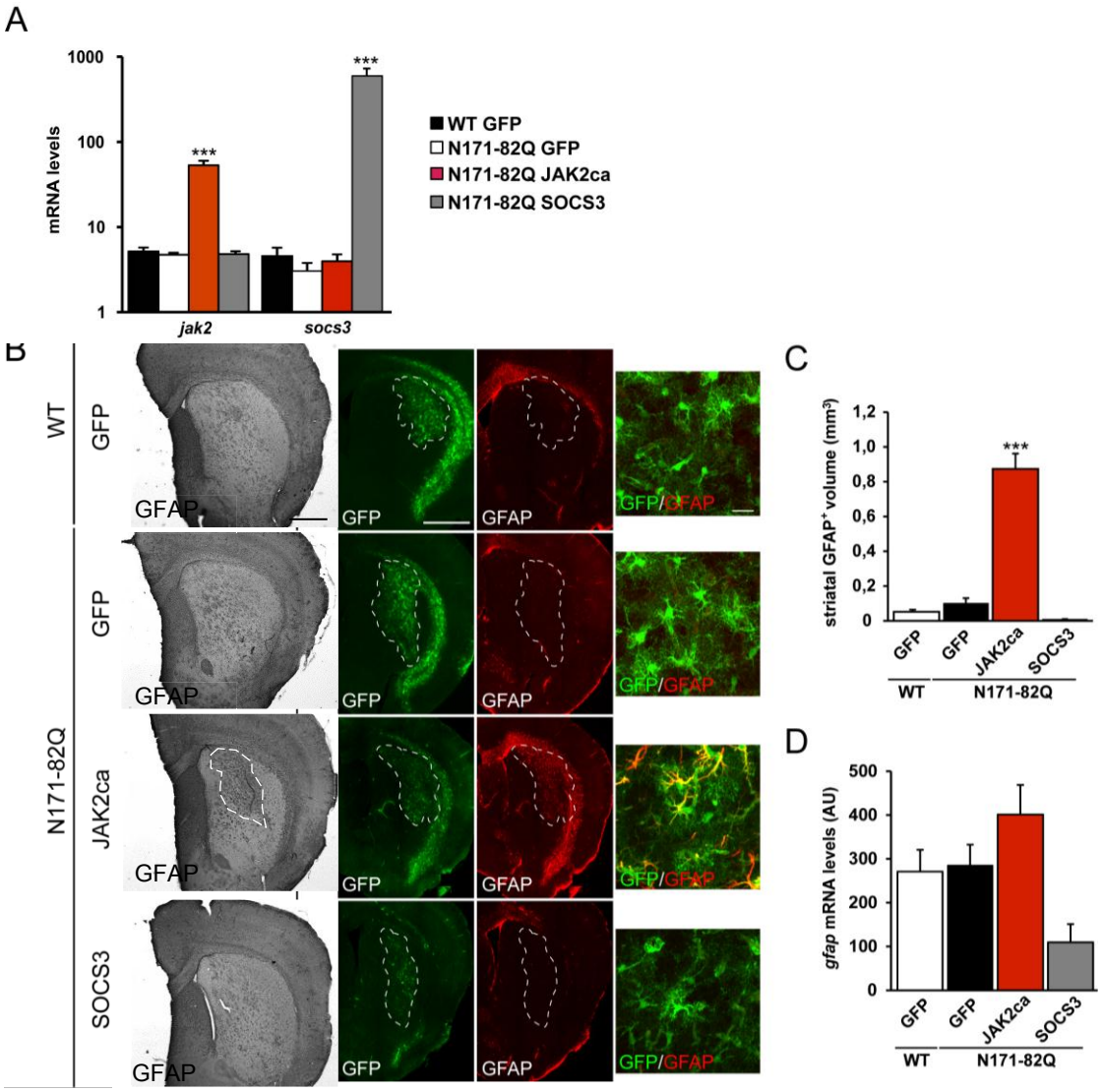

Figure 49. Positive and negative modulation of astrocyte reactivity in the N171-82Q model of HD.

A, qRT-PCR analysis of *jak2* and *socs3* mRNA levels in WT and N171-82Q mice injected in the striatum with AAV vectors encoding GFP, JAK2ca or SOCS3, 8 weeks post-injection. *jak2* and *socs3* are highly overexpressed in the N171-JAK2ca and N171-SOCS3 groups, respectively. **B,** Images of immunodetection of GFAP (left) and immunofluorescent stainings for GFP (green) and GFAP (red) (right). N171-JAK2ca-mice show GFAP$^+$ reactive astrocytes compared with other groups. **C,** The GFAP$^+$ volume is increased in N171-JAK2ca mice. **D,** *gfap* mRNA levels were detected by qRT-PCR. *Gfap* mRNA levels show a tendency to increase in the N171-JAK2ca and to decrease in the N171-SOCS3 group compared with WT GFP and N171-GFP control groups. N= 3-9/ group, *** p < 0.001, Two-way ANOVA and Scheffé post-hoc test. Scale bar: 1 mm, 40 µm.

We then controlled AAV injection site and spreading as well as astrocyte reactivity by immunolabeling for GFAP. We detected GFAP by DAB immunohistochemistry, as in the first cohort, we had to amplify the signal to evidence reactive astrocytes in the striatum of N171-82Q mice (see III.B.1.b and **Figure 20A**). Surprisingly, GFAP staining was not different between WT-GFP and N171-GFP groups. We also performed a double labeling for GFP and GFAP by immunofluorescence to measure the GFAP signal in the GFP^+ injected area. As expected, the $GFAP^+$ volume was not significantly different between the WT-GFP and N171-GFP groups (**Figure 49B and C**). By contrast, N171-JAK2ca mice displayed increased $GFAP^+$ volume in the injected area as compared with the other groups ($p < 0.001$, (n = 9 WT-GFP, 6 N171-GFP, 6 N171-JAK2ca and 3 N171-SOCS3, one-way ANOVA and Scheffé tests, **Figure 49B and C**). GFAP staining and volume in N171-SOCS3 mice was comparable to WT-GFP and N171-GFP mice (**Figure 49B and C**). In addition, we observed by qRT-PCR that *gfap* mRNA levels showed a tendency to be increased with JAK2ca and decreased by SOCS3, although it did not reach significance (**Figure 49D**). These results suggest that N171-82Q mice from our colony did not display the mild astrocyte reactivity observed in the first cohort. Therefore, we could not demonstrate SOCS3 effects on astrocyte reactivity; however JAK2ca was able to activate astrocytes in these mice.

In either case, manipulating the JAK2/STAT3 pathway in astrocytes could still influence neuronal dysfunction in N171-82Q mice. Thus, we investigated the status of striatal neurons by detecting DARPP32 and NeuN by immunohistochemistry in these mice. As observed in the first cohort, DARPP32 staining was comparable in N171-GFP and WT-GFP mice (**Figure 50A**). Unexpectedly, the striatal volume was not different between N171-GFP and WT-mice and N171-GFP mice did not displayed ventricle enlargement (**Figure 50A and B**). We also detected NeuN as an additional marker for neurons and the staining was also comparable between the two groups. The number of $NeuN^+$ cells in the injected area was also similar between WT-GFP and N171-GFP (**Figure 50A, C**). Last, we detected Htt aggregates by performing EM48 immunohistochemistry. Surprisingly, N171-GFP mice displayed fewer aggregates in the striatum than N171-82Q mice from the first cohort (compare **Figure 50A** and **47A**). Again, these unexpected results show that N171-82Q mice from our colony did not reproduce the symptoms and histological alterations observed in the first cohort and in the literature.

Despite these surprising results, we analyzed the effect of JAK2/STAT3 pathway modulation in astrocytes by JAK2ca and SOCS3 overexpression. We found that the striatal volume and the number of $NeuN^+$ cells in the injected area were not different between the four groups (**Figure 50A, B and C**). Similarly, we observed no visible change in the number or size of $EM48^+$ aggregates in the striatum between the N171-GFP, N171-JAK2ca and N171-SOCS3 groups (**Figure 50A**). However, we observed interesting tendencies when measuring *d2r* and *darpp32* mRNA levels by RT-qPCR (**Figure 50D and E**). Indeed, mRNA levels of these striatal markers showed a tendency to decrease in N171-GFP compared with WT-GFP mice. Intriguingly, N171-SOCS3 mice displayed higher mRNA levels for both *d2r* and *darpp32* than N171-GFP controls, although it did not reach significance (**Figure 50D and E**).

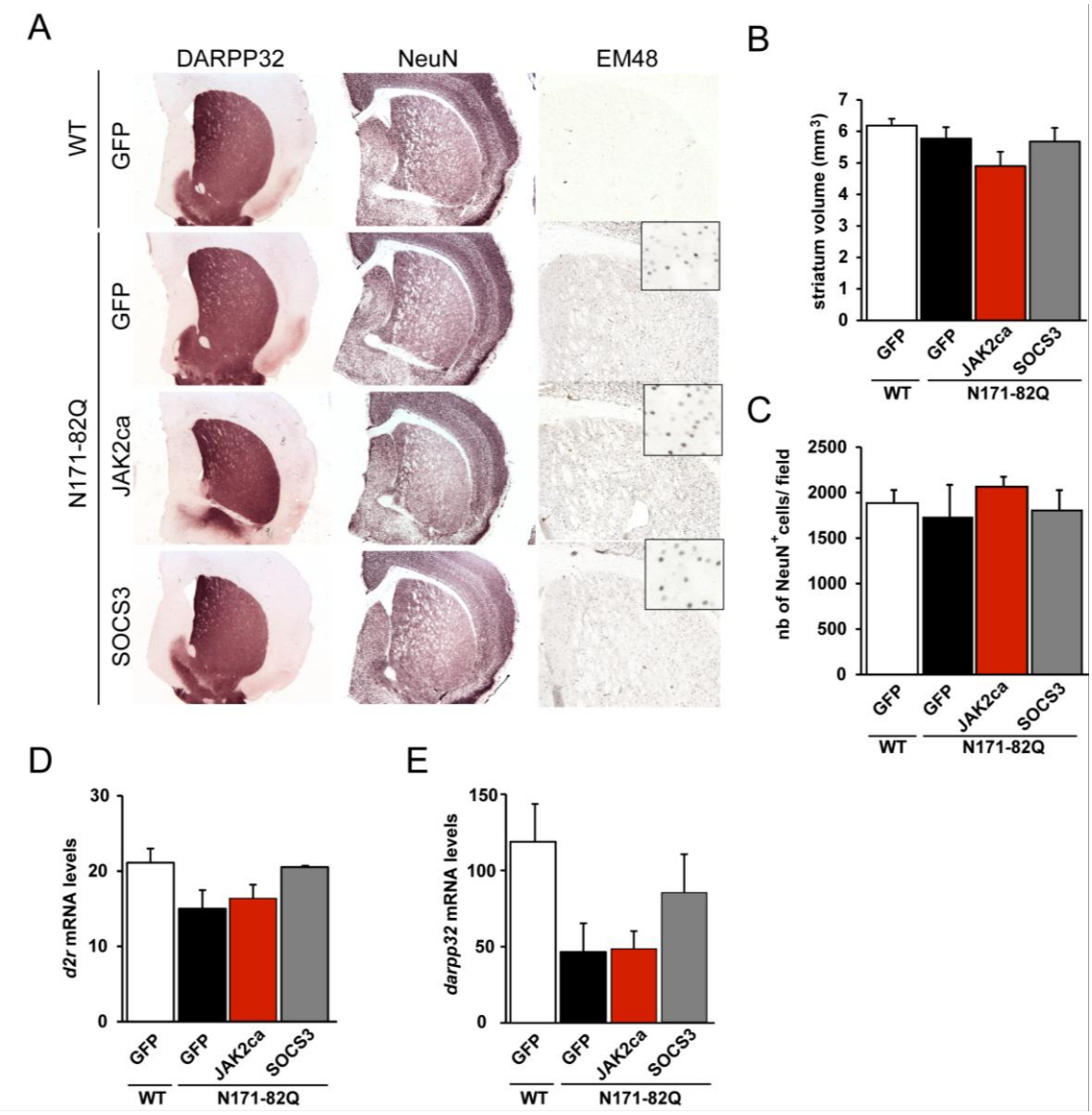

Figure 50. Modulation of astrocyte reactivity has no effect on striatal neurons in the N171-82Q HD mice.

A, Immunohistochemical detection of the neuronal markers DARPP32, NeuN and of mHtt aggregates with EM48 in WT or N171-82Q mice injected with AAV vectors encoding GFP, JAK2ca or SOCS3 in the striatum. **B,** Quantification of the striatal volume which is similar between WT GFP and N171-GFP mice. JAK2ca and SOCS3 overexpression have no effect on the striatal volume 8 weeks post-injection. **C,** Quantification of the number of $NeuN^+$ neurons in the injected area. The total number of neurons is not different between the four groups in the AAV-injected area. **D-E,** qRT-PCR analysis of the striatal neuron markers *d2r* and *darpp32* mRNA levels. Both *d2r* (**D**) and *darpp32* (**E**) mRNA levels tend to be decreased in N171-GFP mice in comparison with WT-GFP. SOCS3 shows a tendency to restore the expression of *d2r* and *darpp32*. N= 3-9/ group, One-way ANOVA, ns. Scale bar: 1 mm. Abbreviations: St, striatum; CC, corpus callosum.

These results show that manipulating astrocyte reactivity did not cause histological alterations in the N171-82Q mouse model of HD. Indeed, inducing astrocyte reactivity with AAV-JAK2ca had no

detectable toxic effects on striatal neurons in N171-82Q mice. By contrast, SOCS3 showed a tendency to restore mRNA levels of two striatal markers in these mice.

Overall, in two models of HD, our results suggest that reactive astrocytes do not play a major role in the disease and that modulating their reactivity only moderately impact disease outcomes.

D. Manipulation of the JAK2/STAT3 pathway to characterize astrocyte reactivity

1) Selective activation of the JAK2/STAT3 pathway leads to changes in astrocyte transcriptome

In the previous part of the manuscript, we showed that JAK2ca overexpression selectively activates astrocytes in the mouse striatum, by the JAK2/STAT3 pathway (see III.B.2.b.i and ii). As previously mentioned, the JAK2/STAT3 pathway regulates the expression of hundreds of genes, which, however, were mainly studied in cell lines. Therefore, we were interested in studying the transcriptional changes associated with activation of the JAK2/STAT3 pathway in astrocytes. We used mice injected with AAV-JAK2ca or AAV-GFP in the striatum. One month post-injection, the GFP^+ infected area was dissected out and dissociated for FACS analysis. GFP^+ infected astrocytes were sorted and their RNA extracted. RNA was then processed for microarray analysis in collaboration with Dr. R. Olaso and C. Derbois at the Institut de Génomique, Centre National de Génotypage in Evry.

FACS was used to sort GFP^+ cells (POS) and GFP^- cells (NEG) to evaluate the enrichment in astrocyte markers in POS cells. We found hundreds of probes differentially expressed between the NEG and the POS cell populations. First, we controlled that GFP was detected in POS cells. Indeed, *gfp* expression was detected in the POS but not in the NEG population (1846.35 ± 98.68 versus 0.65 ± 0.65, n = 4 POS, 2 NEG, $p < 0.001$, Student's t-test). We then confirmed that POS isolated cells yielded to a relatively pure population of astrocytes. We analyzed the gene expression of cell-type specific genes on the Beadchip data set by comparing the NEG and the POS sorted cell populations. The POS population expressed higher levels of astrocyte-specific genes (*Cx30*, *Glt-1*, *Glast* and *Cx43*) than the NEG population and thus corresponds to purified astrocytes (**Figure 51A**). The POS population was also highly enriched in genes associated with important astrocyte functions, and previously described as astrocyte markers. For example, glypican 5 (*Gpc5*) was enriched 36 fold in the POS population compared with NEG cells ($p < 0.01$, n = 4 POS, 2 NEG, Student's t-test). It belongs to a family of astrocyte proteins involved in synapse formation during development (**Allen, 2013**). Similarly, glutathione-S-transferase (GST) (*Gstm1*) was enriched 13 fold in POS cells compared with NEG cells ($p < 0.05$, n = 4 POS, 2 NEG, Student's t-test). GST is a key astrocytic protein involved in their antioxidant defense function (**Johnson et al., 1993**).

By contrast, POS cells expressed low levels of microglial markers (*P2ry12, C1q and Aif1*) compared with the NEG population (**Figure 51A**). A majority of probes for neuronal genes were not detectable in the Beadchip data set (**Cahoy et al., 2008**). This was possibly due to low expression levels of neuronal transcripts or degradation during the dissociation process. However, for the few neuronal-specific markers that we were able to detect (*Mal2, Sv2 and Snap25*), we found that they were more abundant in the NEG than the POS population (**Figure 51A**). This was also the case for several oligodendrocyte markers (*mbp, mobp and ugt8a*) and the NG2 marker of oligodendrocyte progenitors.

Taken together, these results showed that we successfully isolated astrocytes from AAV-GFP injected mouse brains using FACS.

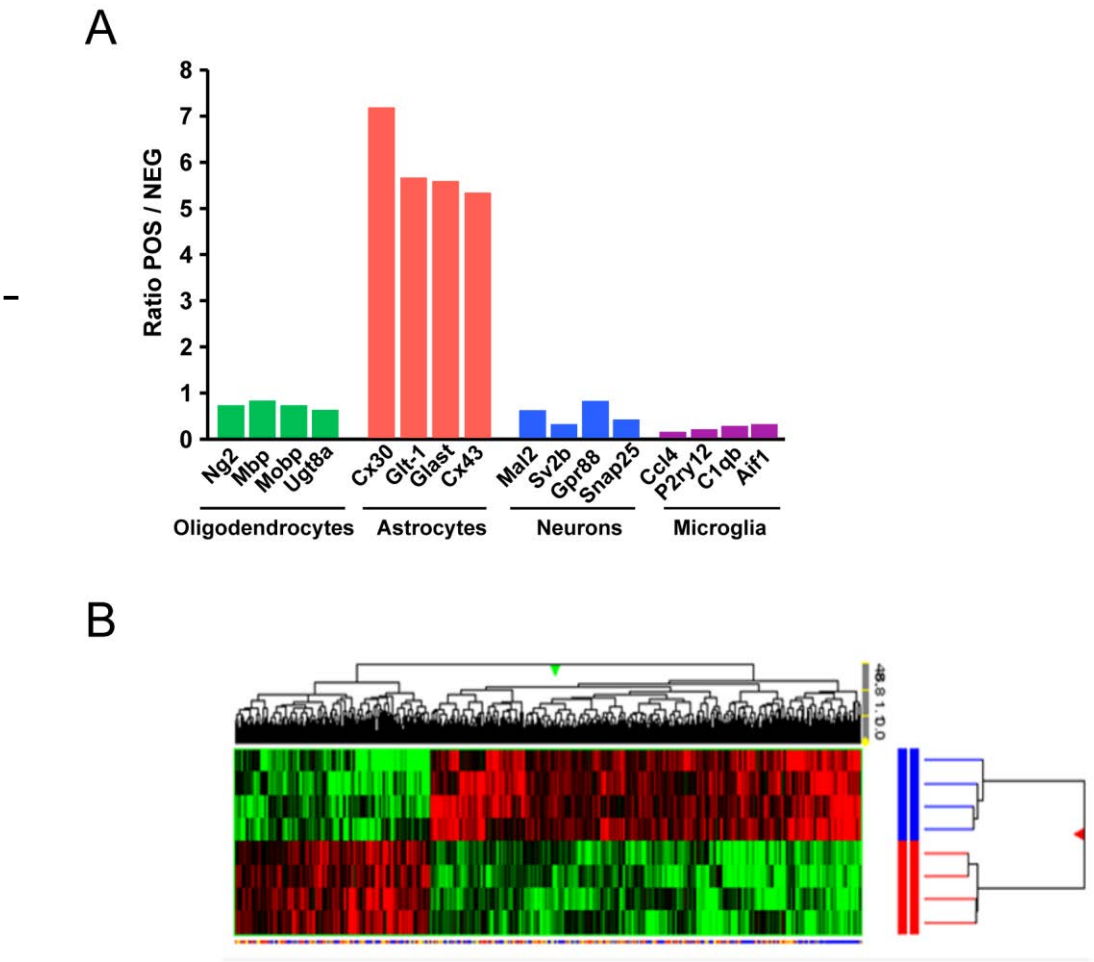

Figure 51. FACS isolation of GFP$^+$ cells from AAV-injected mice are composed of astrocytes. **A-B**, Expression profile of FACS isolated GFP$^+$ or GFP$^-$ cells from AAV-GFP-injected mice. GFP$^+$ population is highly enriched in astrocyte-specific markers (red) but not for markers of oligodendrocytes (green), neurons (blue), microglia (purple). **B**, Hierarchical clustering of probes differentially expressed in sorted astrocytes between astrocytes from AAV-GFP (blue) and AAV-JAK2ca + AAV-GFP- injected mice (red). Astrocyte activation by AAV-JAK2ca + AAV-GFP in the adult mouse striatum results in multiple transcriptional changes.

This microarray analysis was considered as a first screen to evaluate the effects of JAK2ca on astrocyte transcriptome. Thus, we analyzed the gene expression between the POS cells from the GFP and JAK2ca groups. We first controlled that we could detect transgene overexpression in infected astrocytes. Indeed, *gfp* was detected in both GFP and JAK2ca astrocytes (1731.44 ± 94.37 and 1028.36 ± 122.90 respectively). Furthermore, *jak2* levels were increased 5-fold in JAK2ca astrocytes compared with GFP controls ($p < 0.001$, n = 4/ group, Student's t-test). We next evaluated the expression of genes encoding reactive astrocyte markers in isolated astrocytes. *Gfap* levels were higher in JAK2ca astrocytes compared with GFP controls (2.7-fold increase, $p < 0.001$, n = 4/group,

Student's t-test). Another marker of reactive astrocytes, *serpina3n* showed a tendency to increase in the JAK2ca group, although it did not reach significance (**Figure 52**). We also evaluated the effects of JAK2ca on genes encoding other functionally important astrocyte proteins. Interestingly, GLT-1 (*slc1a2*) levels were significantly induced by approximately 50% in JAK2ca astrocytes ($p < 0.01$, n = 4/group, Student's t-test). By contrast, other transcripts encoding astrocyte proteins were not significantly modified by JAK2ca expression such as Kir4.1 (*Kcnj10*), GS (*Glul*), Aqp4, Cx43 and Cx30 (**Figure 52**). Thus, using this method, we were able to detect changes in gene expression indicative of the activated status of astrocytes in the JAK2ca group and to evaluate the effects of JAK2ca overexpression on several astrocyte transcripts.

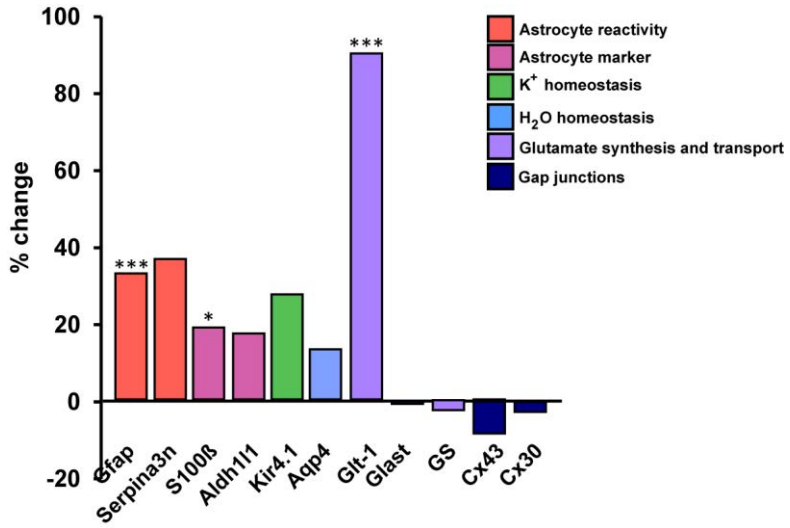

Figure 52. Activation of the JAK2/STAT3 pathway in striatal astrocytes modulates expression of functionally important genes. Expression of several astrocyte-specific genes expressed as fold change percentage between GFP and JAK2ca astrocytes.

In addition to astrocyte-specific markers, hundreds of genes displayed altered expression with JAK2ca in the striatum. We identified a total of 266 genes upregulated and 861 downregulated by JAK2ca (**Figure 51B**).

Interestingly, we found that JAK2ca modified the expression of genes involved in other signaling pathways related to astrocyte reactivity. Inhibitors of the NF-κB pathway such as IκBζ (*Nfkbiz*) and IκBα (*Nfkbia*) were strongly upregulated by JAK2ca, from 3.5 and 4.6 fold, respectively (**Table 5**). It is to note that *Nfkbia* is the second most upregulated gene by JAK2ca, suggesting that this effect is particularly robust. Furthermore, fibroblast growth factor 2 (*Fgfr2*) was downregulated whereas fibroblast growth factor binding protein 3 (*Fgfbp3*) was upregulated by JAK2ca (**Table 5**). These results are particularly relevant in the context of astrocyte reactivity. Indeed, FGF2 was shown to maintain astrocytes in a resting state under physiological conditions (**Kang et al., 2014**) and FGFBP3 is an inhibitor of FGF2 (**Hanneken et al., 1994**).

We used the Database for Annotation, Visualization and Integrated Discovery (DAVID) with KEGG enrichment to evaluate if these genes were part of known cellular pathways (**Table 5**). Several cellular functions were identified including lysosome and ubiquitin proteasome degradation pathways, antigen presentation and oxidative metabolism. Strikingly, most of the genes that were downregulated by JAK2ca were associated with alterations observed in ND (HD, AD, PD), which was particularly interesting in the context of this project. These genes mainly encode for proteins involved in oxidative metabolism, whose dysfunction is a common feature in ND. Indeed, an important number of genes was significantly downregulated by JAK2ca. For example, a striking result was the downregulation of 28 genes involved in oxidative metabolism (*Cox17, Cox6a1, Sdhb, Uqcrc2, Cycs, Ndufs, 1, 2, 6, 8*) and related to the TCA cycle (*Dlst, Idh3g, Dld, Mdh1*) (**Table 5**). Overall, JAK2ca astrocytes displayed reduced oxidative metabolism (**Figure 53**).

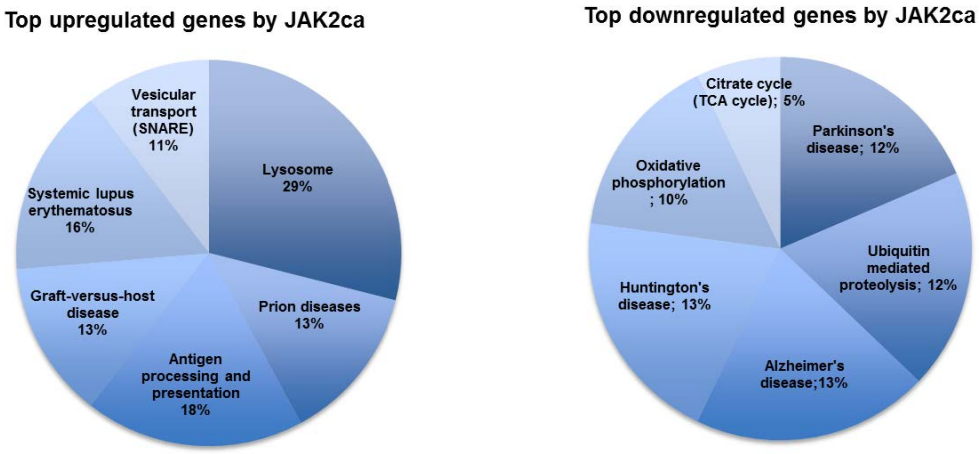

Figure 53. Activation of the JAK2/STAT3 in astrocytes modulates the expression of genes involved in key cellular functions. Pie charts show the DAVID categorization from JAK2ca up- or downregulated gene sets. The percentage corresponds to the proportion of genes from the dataset that are related to a given pathway in DAVID.The lysosome degradation and immune response are prominently induced whereas oxidative metabolism and mitochondrial function related to ND are downregulated.

Of particular interest in the context of HD, several genes encoding proteins of the ubiquitin-proteasome system were downregulated by JAK2ca in the mouse striatum (**Figure 53, 54 and Table 5**). These genes encode for ubiquitin-conjugating proteins (*Ube2d1, Ube2l3, Ube2h, Ube2o, Ube2q2*) and E3 ubiquitin-ligase proteins (*Keap1, Map3k1, Itch*) (see **Figure 56**).

Finally, we found that a number of genes related to lysosomal metabolism were upregulated by JAK2ca from approximately 1.5 fold to 5 fold. These genes included cathepsins (*Ctss, Ctsz, Ctsb* and *Ctsc*), lysosomal transmembrane proteins (*Laptm5, Atp6v0a1*) and antigen proteins (*Cd63, Cd68*). The antigen presentation pathway was also upregulated in JAK2ca astrocytes including class I MHC molecules (*H2-D1, H2-T23, H2Q6-8*) and β2-microglobulin (*B2m)* were upregulated from 1.3 fold to 3.6 fold in JAK2ca astrocytes (**Figure 53, 54 and Table 5**). These data are consistent with previous

findings from gene expression analysis on isolated astrocytes from LPS-injected mice (**Zamanian et al., 2012**).

PROBE ID	GENE SYMBOL	GENE NAME	P VALUE	FOLD CHANGE	DAVID
Interaction with other pathways (FGF, NFKB)					
1218605	*Nfkbia*	nuclear factor of kappa light polypeptide gene enhancer in B cells inhibitor, alpha	7,50E-03	4,6	no
2755008	*Nfkbiz*	nuclear factor of kappa light polypeptide gene enhancer in B cells inhibitor, zeta	8,40E-04	3,5	no
1238326	*Nkiras1*	NFKB inhibitor interacting Ras-like protein 1	1,30E-02	0,5	no
2515081	*Trim59*	tripartite motif-containing 59, RING finger protein 1	8,40E-04	0,2	no
1225071	*Fgfr2*	fibroblast growth factor receptor 2	1,19E-03	0,5	no
2841593	*Fgfbp3*	fibroblast growth factor binding protein 3	1,30E-02	1,5	no
Uquitin-proteolysis					
1258406	*Keap1*	kelch-like ECH-associated protein 1, NRF2 cytosolic inhibitor	N/A		yes
2993267	*Keap1*	kelch-like ECH-associated protein 1, NRF2 cytosolic inhibitor	N/A		yes
2595091	*Nhlrc1*	NHL repeat containing 1, E3 ubiquitin-protein ligase NHLRC1	N/A		yes
2870688	*Anapc7*	anaphase promoting complex subunit 7	N/A	0,7	yes
2754636	*LOC639931*		4,66E-03	0,5	yes
2435025	*Ube2d1*	ubiquitin-conjugating enzyme E2D 1	N/A		yes
2471793	*Ube2l3*	ubiquitin-conjugating enzyme E2L 3	N/A		yes
2628258	*Syvn1*	synovial apoptosis inhibitor 1, synoviolin	N/A		yes
2614380	*Map3k1*	mitogen-activated protein kinase kinase kinase 1, E3 ubiquitin protein ligase	N/A	0,9	yes
2451035	*Ube2h*	ubiquitin-conjugating enzyme E2H	N/A	1,9	yes
1245815	*Ube2o*	ubiquitin-conjugating enzyme E2O	N/A		yes
2826027	*Ube2q2*	ubiquitin-conjugating enzyme E2Q family member 2	N/A	1,6	yes
2569275	*Itch*	itchy E3 ubiquitin protein ligase	N/A		yes
2869312	*Fbxo4*	F-box protein 4	N/A	1,2	yes
2655066	*Ube2k*	ubiquitin-conjugating enzyme E2K	3,93E-03	1,6	yes
2959247	*Ube2b*	ubiquitin-conjugating enzyme E2B	8,00E-03	2,0	yes
2430374	*Uba1*	ubiquitin-like modifier activating enzyme 1	2,20E-02	1,5	yes
Lysosome					
2491670	*Sgsh*	N-sulfoglucosamine sulfohydrolase	2,00E-02	2,4	yes
1217849	*Laptm5*	lysosomal protein transmembrane 5	1,33E-03	2,0	yes
1246861	*Ctss*	cathepsin S	9,00E-03	2,9	yes
2839569	*Ctsz*	cathepsin Z	1,76E-02	1,6	yes
2666007	*Ctsz*	cathepsin Z	1,01E-02	1,6	yes
2683316	*Ctsb*	cathepsin B	1,89E-02	1,3	yes
3008858	*Ctsc*	cathepsin C	5,60E-03	4,9	yes
2661971	*Gm2a*	GM2 ganglioside activator	2,39E-02	1,4	yes
3128907	*Cd63*	CD63 molecule, lysosomal-associated membrane protein 3	3,69E-03	1,3	yes
2689785	*Cd68*	macrophage antigen CD68	N/A	1,7	yes
1247682	*Atp6v0a1*	ATPase, H+ transporting, lysosomal V0 subunit a1	7,00E-03	1,5	yes
1253049	*Hyal1*	hyaluronoglucosaminidase 1	N/A		yes
2762823	*Npc1*	Niemann-Pick type C1	N/A		yes
Antigen processing and presentation and inflammation					
1216746	*B2m*	beta-2 microglobulin	1,50E-04	3,6	yes
2739999	*B2m*	beta-2 microglobulin	3,80E-04	3,5	yes
1246861	*Ctss*	cathepsin S	9,00E-03	2,9	yes
2683316	*Ctsb*	cathepsin B	1,89E-02	1,3	yes
2462745	*H2-D1*	histocompatibility 2, D region locus 1	7,00E-03	2,1	yes
2777471	*H2-T23*	histocompatibility 2, T region locus 23	7,00E-03	2,4	yes
2777474	*H2-T23*	histocompatibility 2, T region locus 23	8,00E-03	2,4	yes
2771182	*H2-Q8*	histocompatibility 2, Q region locus 8	1,40E-02	2,0	yes
2675337	*H2-Q6*	histocompatibility 2, Q region locus 6	1,40E-02	1,6	yes
2607675	*LOC641240*		N/A		yes
1226525	*H2-Ab1*	histocompatibility 2, class II antigen A, beta 1	N/A		yes
1238221	*Hsp90ab1*	heat shock protein 90kDa alpha (cytosolic), class B member 1	2,10E-02	0,6	yes
2878071	*Lyz*	lysozyme	4,33E-04	3,7	no
2939681	*Lyzs*	lysozyme s	9,99E-04	2,7	no
2939681	*Lyzs*	lysozyme s	3,27E-03	2,8	no
2619620	*C1qb*	complement component 1 q	2,19E-02	2,3	no
2777498	*Il1b*	interleukin 1 beta	#DIV/0!	#DIV/0!	no
1232041	*Klf6*	Kruppel-like factor 6	#DIV/0!	#DIV/0!	no
2619408	*Atf3*	activating transcription factor 3	#DIV/0!	2,2	no
3133448	*Mfge8*	milk fat globule-EGF factor 8 protein	0,03747875	1,1	no
2689931	*Megf10*	multiple EGF-like-domains 10	0,01405585	0,4	no
Oxidative metabolism					
3160517	*Cox17*	COX17 cytochrome c oxidase copper chaperone	2,00E-02	0,6	yes
2842572	*Ndufs6*	NADH dehydrogenase (ubiquinone) Fe-S protein 6, 13kDa (NADH-coenzyme Q reductas	9,80E-03	0,7	yes
2702704	*Ndufv1*	NADH dehydrogenase (ubiquinone) flavoprotein 1, 51kDa	1,80E-02	0,5	yes
2638875	*Cox6a1*	cytochrome c oxidase subunit VIa polypeptide 1	2,95E-03	0,6	yes
2435140	*Uqcrc2*	ubiquinol-cytochrome c reductase core protein II	1,83E-02	0,6	yes
1224781	*Ndufs2*	NADH dehydrogenase (ubiquinone) Fe-S protein 2, 49kDa (NADH-coenzyme Q reductas	N/A	1,1	yes
2704165	*Ndufs2*	NADH dehydrogenase (ubiquinone) Fe-S protein 2, 49kDa (NADH-coenzyme Q reductas	N/A	1,2	yes
2691936	*Ndufs1*	NADH dehydrogenase (ubiquinone) Fe-S protein 1, 75kDa (NADH-coenzyme Q reductas	N/A	1,3	yes

2878071	*Lyz*	lysozyme	4,33E-04	3,7	no
2939681	*Lyzs*	lysozyme s	9,99E-04	2,7	no
2939681	*Lyzs*	lysozyme s	3,27E-03	2,8	no
2619620	*C1qb*	complement component 1 q	2,19E-02	2,3	no
2777498	*Il1b*	interleukin 1 beta	#DIV/0!	#DIV/0!	no
1232041	*Klf6*	Kruppel-like factor 6	#DIV/0!	#DIV/0!	no
2619408	*Atf3*	activating transcription factor 3	#DIV/0!	2,2	no

PROBE ID	GENE SYMBOL	GENE NAME	P VALUE	FOLD CHANGE	DAVID
Interaction with other pathways (FGF, NFKB)					
1218605	*Nfkbia*	nuclear factor of kappa light polypeptide gene enhancer in B cells inhibitor, alpha	7,50E-03	4,6	no
2755008	*Nfkbiz*	nuclear factor of kappa light polypeptide gene enhancer in B cells inhibitor, zeta	8,40E-04	3,5	no
1238326	*Nkiras1*	NFKB inhibitor interacting Ras-like protein 1	1,30E-02	0,5	no
2515081	*Trim59*	tripartite motif-containing 59, RING finger protein 1	8,40E-04	0,2	no
1225071	*Fgfr2*	fibroblast growth factor receptor 2	1,19E-03	0,5	no
2841593	*Fgfbp3*	fibroblast growth factor binding protein 3	1,30E-02	1,5	no
Uquitin-proteolysis					
1258406	*Keap1*	kelch-like ECH-associated protein 1, NRF2 cytosolic inhibitor	N/A		yes
2993267	*Keap1*	kelch-like ECH-associated protein 1, NRF2 cytosolic inhibitor	N/A		yes
2595091	*Nhlrc1*	NHL repeat containing 1, E3 ubiquitin-protein ligase NHLRC1	N/A		yes
2870688	*Anapc7*	anaphase promoting complex subunit 7	N/A	0,7	yes
2754636	*LOC639931*		4,66E-03	0,5	yes
2435025	*Ube2d1*	ubiquitin-conjugating enzyme E2D 1	N/A		yes
2471793	*Ube2l3*	ubiquitin-conjugating enzyme E2L 3	N/A		yes
2628258	*Syvn1*	synovial apoptosis inhibitor 1, synoviolin	N/A		yes
2614380	*Map3k1*	mitogen-activated protein kinase kinase kinase 1, E3 ubiquitin protein ligase	N/A	0,9	yes
2451035	*Ube2h*	ubiquitin-conjugating enzyme E2H	N/A	1,9	yes
1245815	*Ube2o*	ubiquitin-conjugating enzyme E2O	N/A		yes
2826027	*Ube2q2*	ubiquitin-conjugating enzyme E2Q family member 2	N/A	1,6	yes
2569275	*Itch*	itchy E3 ubiquitin protein ligase	N/A		yes
2869312	*Fbxo4*	F-box protein 4	N/A	1,2	yes
2655066	*Ube2k*	ubiquitin-conjugating enzyme E2K	3,93E-03	1,6	yes
2959247	*Ube2b*	ubiquitin-conjugating enzyme E2B	8,00E-03	2,0	yes
2430374	*Uba1*	ubiquitin-like modifier activating enzyme 1	2,20E-02	1,5	yes
Lysosome					
2491670	*Sgsh*	N-sulfoglucosamine sulfohydrolase	2,00E-02	2,4	yes
1217849	*Laptm5*	lysosomal protein transmembrane 5	1,33E-03	2,0	yes
1246861	*Ctss*	cathepsin S	9,00E-03	2,9	yes
2839569	*Ctsz*	cathepsin Z	1,76E-02	1,6	yes
2666007	*Ctsz*	cathepsin Z	1,01E-02	1,6	yes
2683316	*Ctsb*	cathepsin B	1,89E-02	1,3	yes
3008858	*Ctsc*	cathepsin C	5,60E-03	4,9	yes
2661971	*Gm2a*	GM2 ganglioside activator	2,39E-02	1,4	yes
3128907	*Cd63*	CD63 molecule, lysosomal-associated membrane protein 3	3,69E-03	1,3	yes
2689785	*Cd68*	macrophage antigen CD68	N/A	1,7	yes
1247682	*Atp6v0a1*	ATPase, H+ transporting, lysosomal V0 subunit a1	7,00E-03	1,5	yes
1253049	*Hyal1*	hyaluronoglucosaminidase 1	N/A		yes
2762823	*Npc1*	Niemann-Pick type C1	N/A		yes
Antigen processing and presentation and inflammation					
1216746	*B2m*	beta-2 microglobulin	1,50E-04	3,6	yes
2739999	*B2m*	beta-2 microglobulin	3,80E-04	3,5	yes
1246861	*Ctss*	cathepsin S	9,00E-03	2,9	yes
2683316	*Ctsb*	cathepsin B	1,89E-02	1,3	yes
2462745	*H2-D1*	histocompatibility 2, D region locus 1	7,00E-03	2,1	yes
2777471	*H2-T23*	histocompatibility 2, T region locus 23	7,00E-03	2,4	yes
2777474	*H2-T23*	histocompatibility 2, T region locus 23	8,00E-03	2,4	yes
2771182	*H2-Q8*	histocompatibility 2, Q region locus 8	1,40E-02	2,0	yes
2675337	*H2-Q6*	histocompatibility 2, Q region locus 6	1,40E-02	1,6	yes
2607675	*LOC641240*		N/A		yes
1226525	*H2-Ab1*	histocompatibility 2, class II antigen A, beta 1	N/A		yes
1238221	*Hsp90ab1*	heat shock protein 90kDa alpha (cytosolic), class B member 1	2,10E-02	0,6	yes
2878071	*Lyz*	lysozyme	4,33E-04	3,7	no
2939681	*Lyzs*	lysozyme s	9,99E-04	2,7	no
2939681	*Lyzs*	lysozyme s	3,27E-03	2,8	no
2619620	*C1qb*	complement component 1 q	2,19E-02	2,3	no
2777498	*Il1b*	interleukin 1 beta	#DIV/0!	#DIV/0!	no
1232041	*Klf6*	Kruppel-like factor 6	#DIV/0!	#DIV/0!	no
2619408	*Atf3*	activating transcription factor 3	#DIV/0!	2,2	no
3133448	*Mfge8*	milk fat globule-EGF factor 8 protein	0,03747875	1,1	no
2689931	*Megf10*	multiple EGF-like-domains 10	0,01405585	0,4	no
Oxidative metabolism					
3160517	*Cox17*	COX17 cytochrome c oxidase copper chaperone	2,00E-02	0,6	yes
2842572	*Ndufs6*	NADH dehydrogenase (ubiquinone) Fe-S protein 6, 13kDa (NADH-coenzyme Q reductas	9,80E-03	0,7	yes
2702704	*Ndufv1*	NADH dehydrogenase (ubiquinone) flavoprotein 1, 51kDa	1,80E-02	0,5	yes
2638875	*Cox6a1*	cytochrome c oxidase subunit VIa polypeptide 1	2,95E-03	0,6	yes
2435140	*Uqcrc2*	ubiquinol-cytochrome c reductase core protein II	1,83E-02	0,6	yes
1224781	*Ndufs2*	NADH dehydrogenase (ubiquinone) Fe-S protein 2, 49kDa (NADH-coenzyme Q reductas	N/A	1,1	yes
2704165	*Ndufs2*	NADH dehydrogenase (ubiquinone) Fe-S protein 2, 49kDa (NADH-coenzyme Q reductas	N/A	1,2	yes
2691936	*Ndufs1*	NADH dehydrogenase (ubiquinone) Fe-S protein 1, 75kDa (NADH-coenzyme Q reductas	N/A	1,3	yes
2914507	*Ndufb6*	NADH dehydrogenase (ubiquinone) 1 beta subcomplex, 6, 17kDa	N/A	1,9	yes
2682019	*Ndufa8*	NADH dehydrogenase (ubiquinone) 1 alpha subcomplex, 8, 19kDa	N/A		yes
2769064	*Sdhb*	succinate dehydrogenase complex, subunit B, iron sulfur (Ip)	N/A	0,8	yes
2769065	*Sdhb*	succinate dehydrogenase complex, subunit B, iron sulfur (Ip)	N/A	0,9	yes
3155380	*Cycs*	cytochrome c, somatic	N/A	1,2	yes
1243149	*Atp6v0b*	ATPase, H+ transporting, lysosomal 21kDa, V0 subunit b	N/A	1,1	yes
1237507	*Dlst*	dihydrolipoamide S-succinyltransferase (E2 component of 2-oxo-glutarate complex)	N/A		yes

or in NI control mice. This study was performed in collaboration with Drs. S. Oliet, A. Panatier and J. Veran, at the Neurocentre Magendie, in Bordeaux.

First, we recorded extracellular field excitatory post-synaptic potentials (fEPSPs) to study basal glutamatergic synaptic transmission at hippocampal CA3-CA1 synapses (**Figure 54A**), on acute hippocampal slices, in the GFP_+ injected area. The efficacy of glutamatergic transmission was quantified by measuring the fEPSPs slope for a given stimulation. We observed that the basal synaptic strength was not different between GFP and NI mice, suggesting that surgery and AAV injection did not altered basal synaptic activity in itself (n = 6 NI, 8 GFP, ns, two-way ANOVA and Bonferonni post-hoc tests, **Figure 54 B and C**). By contrast, glutamatergic synaptic transmission was altered in JAK2ca mice as fEPSP displayed smaller amplitudes than in GFP (n = 8 mice, $p < 0.05$; 60 - 70V; $p < 0.01$, 80 - 90V, two-way ANOVA and Bonferonni post-hoc) and NI controls (n = 8 mice, $p < 0.05$, 60 - 70V; $p < 0.01$ 80 - 90V, two-way ANOVA and Bonferonni post-hoc tests, **Figure 54 B and C)**. This unexpected result shows that overexpression of JAK2ca in hippocampal astrocytes is able to influence basal glutamatergic synaptic transmission.

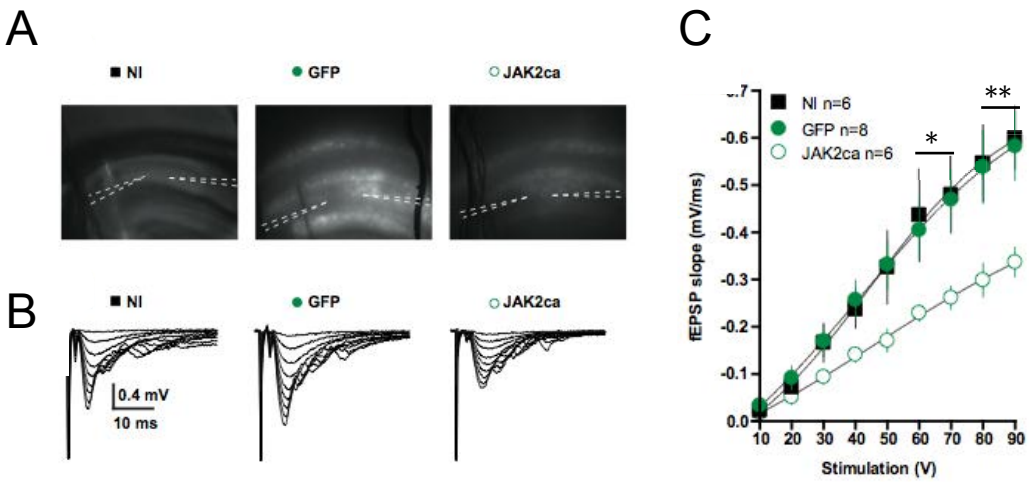

Figure 54. Activation of the JAK2/STAT3 in astrocytes decreases basal synaptic transmission in the mouse hippocampus.
A-C, Basal synaptic transmission was evaluated by measuring evoked fEPSPs within the stratum lacunosum moleculare of the CA1 region of the hippocampus in non-injected (NI), AAV-GFP control or AAV-JAK2ca-injected mice. **A**, fEPSPs were recorded in the GFP^+ injected area. **B**, Representative responses from NI, GFP and JAK2ca mice, show a reduction in fEPSPs in the JAK2ca group. **C**, Average fEPSP slopes of JAK2ca mice (open circles), GFP control mice (green circles) and NI mice (black squares) and plotted as a function of the stimulus intensity. Basal synaptic transmission is impaired in JAK2ca mice. * $p < 0.05$, ** $p < 0.01$, Two-way ANOVA and Bonferonni post-hoc tests.

Synaptic plasticity and long-term potentiation (LTP) are thought to underlie learning and memory in the brain (**Malenka and Bear, 2004**). LTP was successfully induced in NI and GFP mice while JAK2ca mice displayed LTP deficits (**Figure 55**). Indeed, 30-50 min after LTP induction, an increase of more than 150% in the average fEPSP slope was observed in GFP (159.4 ± 6.4 %, n = 10 mice) and NI

mice (152.7 ± 6.8 %, n = 7 mice, ns, Mann-Whitney test) whereas only a 119% increase was observed in JAK2ca mice (119.7 ± 8.1, n = 9 mice, $p < 0.01$ vs NI and $p < 0.001$ vs GFP) (**Figure 55**). Interestingly, the fEPSPs response immediately after LTP stimulation showed that synapses could be potentiated in JAK2ca mice but that the maintenance of the potentiated state was altered.

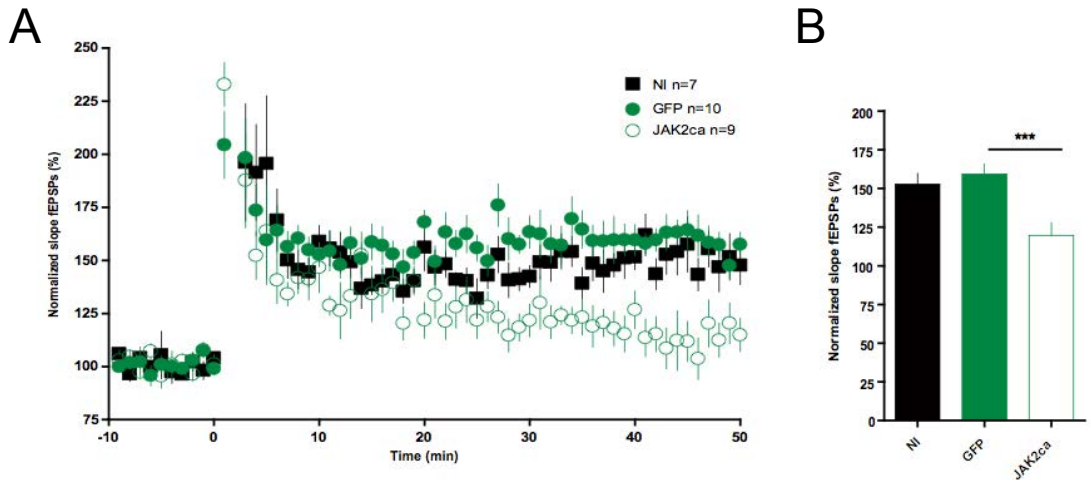

Figure 55. Activation of the JAK2/STAT3 in astrocytes decreases synaptic plasticity in the mouse hippocampus.
A-B, LTP protocol in the CA1 region of the hippocampus in non-injected (NI), AAV-GFP control or AAV-JAK2ca-injected mice. **A**, Average time course of LTP in JAK2ca mice (open circles) and GFP controls (green circles) compared with NI (black squares). LTP in JAK2ca mice was significantly lower compared with controls. **B**, Cumulative probability distribution of LTP measured as the percentage of potentiation 30-50 min after tetanus compared with baseline period. LTP in JAK2ca mice was significantly lower than GFP or NI controls. *** $p < 0.001$, Two-way ANOVA and Mann-Whitney tests.

Taken together, these interesting results show that activation of the JAK2/STAT3 pathway specifically in hippocampal astrocytes is able to alter basal synaptic transmission and plasticity. Experiments are ongoing to increase the number of mice per group and decipher the molecular mechanisms involved.

In conclusion, we used a viral vector to induce the activation of the JAK2/STAT3 pathway specifically in astrocytes, in the WT mouse brain. We showed that the JAK2/STAT3 pathway regulates the expression of a number of genes involved in several important cellular functions in the mouse striatum. In addition, we showed that activating astrocytes by the JAK2/STAT3 pathway impacts synaptic transmission and plasticity in the mouse hippocampus. Therefore, these results validate that the JAK2/STAT3 pathway in astrocytes is a key regulatory cascade and represents a powerful target to study functional changes in reactive astrocytes.

DISCUSSION

V. DISCUSSION

In this study, we have investigated the role of the JAK2/STAT3 pathway in reactive astrocytes. We showed that this pathway is a universal signaling cascade that mediates astrocyte reactivity in several mouse models of ND. By the development of new viral tools, we have manipulated this pathway in two different and complementary mouse models of HD. We found that, in both models, manipulating astrocyte reactivity does not influence neuronal dysfunction. However, preventing astrocyte reactivity in the lentiviral-based model of HD influences the accumulation of Htt aggregates. Finally, we conducted experiments to characterize functional changes occuring in reactive astrocytes. We found that activation of the JAK2/STAT3 pathway in reactive astrocytes causes profound changes in their gene expression profile and could impact synaptic transmission. These interesting results raise questions about the universality of astrocyte reactivity, the functional changes that characterize reactive astrocytes and their consequences on neurons. These points will be discussed in the following part of the manuscript.

A. Astrocyte reactivity is a universal feature of pathological conditions in the CNS

Astrocyte reactivity is a hallmark of both acute and progressive pathological conditions in the CNS. We have studied astrocyte reactivity in multiple ND models of AD, HD and PD. We found that the JAK2/STAT3 pathway, a well-known inducer of astrocyte reactivity in acute models, is also activated in reactive astrocytes in a variety of ND models. Thus, the JAK2/STAT3 pathway is a common feature of astrocyte reactivity to virtually all pathological conditions in the CNS.

1) Identification of reactive astrocytes

Reactive astrocytes as compared with resting astrocytes are mainly identified by morphological changes. They become hypertrophic and upregulate several markers including intermediate filaments. Astrocyte reactivity is a hallmark of any pathological condition in the CNS, either acute or chronic. While reactive astrocytes have received a substantial attention in the context of acute injury involving the formation of a glial scar, in chronic pathological conditions, astrocyte reactivity is much less studied. The study of reactive astrocytes is dampened by the lack of specific markers to detect their reactive state. Thus, upregulation of GFAP and vimentin are considered as gold standards to label reactive astrocytes. In acute pathological conditions or when astrocytes are experimentally activated (e.g by cytokines, growth factors or toxic molecules), nestin, a marker of radial glial cells, can also be re-expressed by mature astrocytes. A recent study involving the study of transcriptional changes in reactive astrocytes after LPS injection or in a model of ischemia has identified two proteins that are highly upregulated by reactive astrocytes, serpina3n and lcn2 (**Zamanian et al., 2012**). Upon

inflammatory conditions, reactive astrocytes upregulate proteins such as iNOS or various cytokines (**Sofroniew and Vinters, 2010**). Changes in the expression of other proteins have been associated with astrocyte reactivity. For example, N-myc downregulated gene 2 (NDRG2) has recently been described as a protein expressed in astrocytes, throughout the brain in various species. Furthermore, following acute injury in the cortex, NDRG2 expressed is decreased in vimentin$^+$ reactive astrocytes (**Flugge et al., 2014**). Decreased expression of GS has also been reported in different studies either in experimentally activated astrocytes or in pathological conditions (**Ortinski et al., 2010; Eid et al., 2012; Tong et al., 2014**). In this study, like others in the field, we used morphological changes and increase GFAP expression to identify reactive astrocytes, but there is a lack for reactive astrocyte markers that are functionally related to their reactive state. Transcriptomic studies from B. Barres's lab and others have provided useful information but additional efforts are needed to identify more universal and functional markers for reactive astrocytes.

2) Astrocyte reactivity in ND models

In this work, we studied astrocyte reactivity in mouse models of AD, HD and PD. We observed that GFAP was strongly upregulated around amyloid depositions in the hippocampus of APP/PS1dE9 and the subiculum of 3xTg-AD mouse models of AD, consistent with previous findings (**Oddo et al., 2003b**) (**Ruan et al., 2009**). By contrast, in these models, only few GFAP$^+$ astrocytes also expressed vimentin and GFAP$^+$/Vim$^+$ astrocytes were mainly found in direct contact with amyloid plaques. In the lentiviral-based model of HD, intrastriatal injection of lenti-Htt82Q resulted in the death of striatal neurons as well as the formation of Em48$^+$ Htt aggregates, 6 weeks post-injection. In addition, we observed many reactive astrocytes in the injected area. Both the expression of both GFAP and vimentin was induced in astrocytes with Htt82Q in the mouse striatum. These results suggest that GFAP and vimentin may be differentially regulated depending on the pathological stimulus (amyloid plaques, Htt aggregates or neuronal death) or brain region.

Interestingly, we found that astrocyte reactivity was differentially induced in different ND models. Indeed, it was strongly induced in the APP/PS1dE9 and 3xTg-AD mouse models of AD and in the MPTP model of PD. By contrast, transgenic mouse models of HD displayed limited or late astrocyte reactivity. Indeed, we examined astrocyte reactivity in two transgenic mouse models of HD: N171-82Q mice and Hdh140 mice. Both models displayed behavioral abnormalities and striatal atrophy at the age of post-mortem analysis. However, we did not observe substantial astrocyte reactivity in end-stage N171-82Q mice (18 weeks) or before 17 months of age in Hdh140 mice. This limited astrocyte reactivity in HD transgenic mice is consistent with the literature (**Tong et al., 2014**), but differs greatly from what is observed in HD patients (**Faideau et al., 2010**). Indeed, by contrast to mice, in humans, even pre-manifest HD patients display astrocyte reactivity in the striatum years before symptoms onset and neuronal death. This discrepancy may be related to regional specificity of astrocytes in the mouse striatum and/or to the absence of massive neuronal death in HD mouse models.

3) The JAK2/STAT3 pathway is a universal feature of astrocyte reactivity

Astrocyte reactivity can be triggered by hundreds of molecules including cytokines, chemokines, aggregated proteins or infectious agents, released by various cell types and that activate multiple intracellular signaling pathways (**Kang and Hebert, 2011 and see § II.B.1**). Among these pathways, the JAK2/STAT3 cascade has been shown to trigger astrocyte reactivity in various acute pathological conditions (**Sofroniew, 2009; Kang and Hebert, 2011**). By contrast, its role in mediating astrocyte reactivity in chronic pathological conditions was not known.

Thus, in this study, we aimed to decipher the role of the JAK2/STAT3 pathway in astrocyte reactivity in the context of ND. To this end, we detected STAT3 by immunofluorescence in several ND models of AD and HD. Because the JAK2/STAT3 pathway is ubiquitous, immunofluorescence detection of STAT3 was performed to identify in which cell type it was expressed by double labeling with cell-type specific markers. Surprisingly, the majority of $STAT3^+$ cells also expressed astrocyte markers such as GFAP or S100β both in ND models but also in their respective age-matched controls as well as in WT mice. The most striking example is the lenti-CNTF model that we used as a positive control in our experiments. CNTF activates astrocytes through the JAK2/STAT3 pathway. Following lenti-CNTF injection, CNTF is produced by neurons and released in the extracellular space. The CNTF receptor is expressed by neurons as well as reactive astrocytes. Thus, in lenti-CNTF-injected animals, CNTF should bind to its neuronal receptor and activate the JAK2/STAT3 pathway in those cells. Very surprisingly, the majority of $STAT3^+$ cells also expressed reactive astrocyte markers. These results showed that, upon various conditions, in resting astrocytes as well as when they are reactive (CNTF or ND), the JAK2/STAT3 pathway is primarily detectable in astrocytes suggesting a higher activity of this cascade in astrocytes than in other brain cells.

Upon cytokine binding on their cognate receptors, STAT3 is recruited to the receptor and phosphorylated by JAK2. Two phosphorylated STAT3 dimerize and translocate to the nucleus to regulate gene expression (**Levy and Darnell, 2002 and see Figure 9**). Thus, the phosphorylation of STAT3 (pSTAT3) is classically used as a marker of activation of the JAK2/STAT3 pathway. PSTAT3 could not be detected by immunofluorescence in the ND models we studied. This was not unexpected, however, given the number of publications that also reported undetectable pSTAT3 staining, even in more severe and acute injury models (**Sriram et al., 2004; Nobuta et al., 2012; Tyzack et al., 2014**). The absence of pSTAT3 immunoreactivity was not due to a technical problem as we successfully detected pSTAT3 in the lenti-CNTF positive control. Therefore, in our study, we used increased STAT3 expression and nuclear localization as alternative indicators of pathway activation, as previously used by our group and others (**Sriram et al., 2004; Escartin et al., 2006; Tyzack et al., 2014**). We showed that the JAK2/STAT3 pathway is activated in reactive astrocytes present in specific vulnerable brain regions according to the disease model. Thus, we found that the JAK2/STAT3 pathway was activated in reactive astrocytes around amyloid depositions in the hippocampus and the

cortex (data not shown) of APP/PS1dE9 and in the subiculum of 3xTg-AD models of AD. Activation of the JAK2/STAT3 pathway was observed in reactive astrocytes the striatum of mice and NHP in the lentiviral-based model of HD and in an old Hdh140 mouse. Similarly, the JAK2/STAT3 pathway was activated in reactive astrocytes in the substantia nigra and in the striatum in the MPTP mouse model of PD. In all models, STAT3 and GFAP expression were concomitantly increased in reactive astrocytes. This correlation was highly robust and thus, the detection of STAT3 can basically serve as a marker of reactive astrocytes in itself. Consistent with these findings, in the striatum of endstage N171-82Q mice, astrocyte reactivity was mild or absent and no STAT3 immunoreactivity was detected.

In our study, we detected STAT3 by immunofluorescence staining. This technique offers several advantages. First, as compared to biochemical techniques such as WB or ELISA, immunofluorescence allows to perform co-stainings to identify the cell-type specific expression of STAT3. Second, we were able to carefully quantify the absolute number of $STAT3^+$ cells as well as fluorescence intensity in their soma. However, this histological technique obviously depends on the quality of the tissue on which the staining is performed. STAT3 staining did not appear to be sensitive to the fixation process on mice, as we obtained the same results on both perfused or post-fixed mouse brains. However, we encountered some trouble with stainings on 3xTg-AD mice and age-matched WT mice (B6129Sv). Brain slices from these mice displayed autofluorescent puncta, mainly in neurons. The presence of these puncta was not due to the immunostaining process of as they were observed on unstained slices. This phenomenon prevented the quantification of STAT3 fluorescence intensity in this model.

We have also generated samples for western blotting of the GFP^+ injected area in the lentiviral-based model of HD and of the dorsal- hippocampus in 3xTg-AD mice and age-matched controls. PSTAT3 was not detectable by western blotting in those samples. Again, this was not due to a technical issue because pSTAT3 was successfully detected in the lenti-CNTF positive control by western blotting. Instead, it may be due to the models of ND themselves, which are progressive and may involve low, transient or asynchronous phosphorylation of STAT3. Indeed, in several studies that successfully detected an increase in pSTAT3 levels in naive or treated mice (methamphetamine or MPTP), they were sacrificed by focused microwave irradiation to preserve the phosphorylated state of proteins (**Hebert and O'Callaghan, 2000; O'Callaghan and Sriram, 2004; Sriram et al., 2004**).

Phosphoproteins can be detected with alternative techniques with higher sensitivity such as ELISA or with cell cytometry by the phosphoflow assay (**Krutzik et al., 2008**). We have generated samples to measure pSTAT3 and STAT3 levels by ELISA in ND models; these experiments are ongoing.

In this study, we reported that activation of the JAK2/STAT3 pathway occurs in reactive astrocytes of many ND models (AD, HD, PD) and is also conserved between species (mouse and NHP). Importantly, the etiology of these ND models is very different and involves specific vulnerable brain regions (striatum, hippocampus, substantia nigra). Thus, activation of the JAK2/STAT3 pathway appears to be a universal feature of astrocyte reactivity in ND, which is conserved across disease

models, brain regions and animal species despite different pathological mechanisms and molecular triggers.

B. Manipulating the JAK2/STAT3 pathway through viral gene transfer reveals its instrumental role in astrocyte reactivity in ND models

1) The JAK2/STAT3 pathway is instrumental for mediating astrocyte reactivity in ND models

Histological and biochemical techniques have shown that the JAK2/STAT3 pathway is activated in reactive astrocytes in several models of acute injury (**Justicia et al., 2000; Xia et al., 2002**) and in ND (**Shibata et al., 2010, Ben Haim et al. under revision**). However the requirement for the JAK2/STAT3 pathway to mediate astrocyte reactivity was not demonstrated in most of these studies. Experiments involving pharmacological inhibitors of JAKs suggested that this pathway was needed for astrocyte reactivity, including in the MPTP model of PD (**Sriram et al., 2004**). However, the JAK2/STAT3 pathway is active in all brain cells; therefore, it is possible that such inhibitors affect other cell types besides astrocytes. More recently, genetic approaches have been developed to KO the expression of STAT3 specifically in astrocytes with the Cre-LoxP system. STAT3 conditional KO strongly reduces astrocyte reactivity following acute injuries of the brain (**Tyzack et al., 2014**) and spinal cord (**Okada et al., 2006; Herrmann et al., 2008; Wanner et al., 2013**). However, in all these studies *stat3* was deleted in nestin^{+} or GFAP^{+} cells using non-inducible Cre recombinase expression. *Nestin* and *gfap* promoters are expressed in radial glial cells during embryonic development (**Han et al., 2013**) and the JAK2/STAT3 signaling pathway plays a central role during development. Particularly in the CNS, it controls the developmental switch between neurogenesis and astrogliogenesis in radial glial cells (**Kamakura et al., 2004; He et al., 2005; Kanski et al., 2014**). Thus, the specific deletion of *stat3* might have triggered non-specific developmental effects, including alteration of the establishment of neuronal networks, neuron-glia interactions or compensatory mechanisms. These effects could be confounding for result interpretation. This issue could be overcome by several approaches allowing the temporal control of Cre expression with the inducible expression of Cre (CreER^{T2}) or the Tet ON/Tet OFF system (**Pfrieger and Slezak, 2012**). In any case, gene deletion is a rather drastic approach compared to the overexpression of dominant negative form of the protein of interest or overexpression of its inhibitor. By contrast, we used lentiviral vectors to selectively overexpress SOCS3 in astrocytes in the adult rodent brain. We first validated this approach *in vivo*, in a model whereby astrocytes are strongly activated by CNTF in the rat striatum. When a lentiviral vector expressing SOCS3 was co-injected in astrocytes, it completely prevented their activation by CNTF. We controlled that SOCS3 was able to blunt the strong phosphorylation of STAT3

induced by CNTF, suggesting that SOCS3 effects are indeed mediated by the blockade of the JAK2/STAT3 pathway.

Furthermore, we showed that SOCS3 overexpression was able to prevent the accumulation of STAT3 in the nucleus of reactive astrocytes in the 3xTg-AD mouse model of AD and in the lentiviral-based model of HD. This selective strategy allowed us to demonstrate that the JAK2/STAT3 pathway was responsible for astrocyte reactivity in ND models. Indeed, SOCS3 overexpression strongly decreased GFAP expression in reactive astrocytes. In addition SOCS3-expressing astrocytes displayed a bushy morphology with thin distal processes as compared with GFP control astrocytes both in the 3xTg-AD mouse model of AD and in the lentiviral-based model of HD. Although we did not quantify these morphological changes, they were consistently observed. A morphometric method such as the Scholl analysis could be used to quantify these morphological changes, as described in the literature (**Tong et al., 2014**).

Further evidence suggesting a central role of the JAK2/STAT3 pathway is that overexpression of *jak2* and *stat3* was sufficient to trigger astrocyte reactivity *in vivo,* in C57BL/6 mice, in the absence of any pathological condition. Indeed, we overexpressed WT or constitutively active mutants of JAK2 and STAT3 by lentiviral gene transfer in the striatum of C57BL/6 mice. All JAK2 and STAT3 constructs resulted in increased GFAP and vimentin immunoreactivity in the injected area, although to various extent. We determined that the mutant construct JAK2T875N (JAK2ca), encoding a mutated JAK2 with a constitutively active kinase domain was the most efficient to induce astrocyte reactivity. Thus, we validated that JAK2ca overexpression activated the STAT3 pathway and resulted in astrocyte reactivity in various brain regions (see IV.B.2). Altogether, our results extend the data from the literature to show that the JAK2/STAT3 pathway is a central player in astrocyte reactivity both in acute and chronic pathological conditions.

2) What about other intracellular cascade associated with astrocyte reactivity?

It is intriguing that despite multiple molecular triggers and intracellular pathways, the JAK2/STAT3 pathway ultimately mediates astrocyte reactivity. Indeed, several other signaling cascades have been associated with reactive astrocytes (**Sofroniew, 2009; Kang and Hebert, 2011**). In particular, the NF-κB pathway is associated with astrocyte reactivity in acute disorders such as spinal cord and peripheral nerve injury (**Kang and Hebert, 2011**). However, in ND conditions, evidence for an activation of the NF-κB in reactive astrocytes is sparse. In ALS, the NF-κB pathway is activated mainly in microglial cells in the spinal cord (**Frakes et al., 2014**). In AD and HD mouse models, NF-κB signaling was reported to be active in astrocytes (**Hsiao et al., 2013; Medeiros and LaFerla, 2013**) but it is better demonstrated in peripheral immune cells of HD patients and it is altered in neurons (**Granic et al., 2009; Khoshnan and Patterson, 2011**).

The NF-κB, was specifically targeted to interfere with astrocyte reactivity, in both acute and chronic pathological conditions, *in vivo* (**Brambilla et al., 2005; Crosio et al., 2011; Furman et al., 2012;**

Frakes et al., 2014; Kang et al., 2014). However, it is interesting to note that astrocyte reactivity was unaltered or attenuated but not abrogated by interfering with this pathway. For example, blockade of the NF-κB pathway in astrocytes did not alter the reactive phenotype of astrocytes after SCI (**Brambilla et al., 2005**) and only reduced astrocyte reactivity slightly and transiently in the SOD^{G93A} mouse model of ALS (**Crosio et al., 2011**).

Confirming a minor role of this pathway in the context of ND, we did not observe any evidence for an activation of the NF-κB pathway in the striatum of lenti-Htt82Q-injected mice or in the hippocampus of 3xTg-AD mice. By contrast, we found that blockade of the JAK2/STAT3 pathway nearly abolished the upregulation of intermediate filaments and hypertrophy in reactive astrocytes in mouse models of AD and HD. Therefore, our results suggest that even though other signaling cascades might be activated in reactive astrocytes in ND, the JAK2/STAT3 pathway ultimately controls the reactive phenotype of astrocytes.

There are multiple levels of crosstalk between the NF-κB and the JAK2/STAT3 pathways, at least in immune cell lines *in vitro* (**Fan et al., 2013**). Therefore, it is possible that the NF-κB pathway secondarily activates the JAK2/STAT3 pathway or that STAT3 inhibits the NF-κB pathway (**Yu et al., 2002**). Very interestingly, our data suggest that, when the JAK2/STAT3 pathway is activated in astrocytes, the expression of several genes involved in the regulation of the NF-κB and FGF pathways is modified. Indeed, expression of *Nfkbia* encoding IκBα, a subunit of the IκB complex, the master regulator of NF-κB, is the second most upregulated gene in the transcriptomic analysis of JAK2ca astrocytes. Similarly, *Nfkbiz*, another component of the IκB complex is strongly upregulated by JAK2ca along with a downregulation of *Nkiras1*, which inhibits the degradation of IκB. These results strongly suggest that activation of the JAK2/STAT3 pathway concomitantly inhibits NF-κB signaling. Consistent with this hypothesis, a recent study showed that overexpression of IL-32 activates astrocytes and induces a concomitant increase in pSTAT3 levels and decrease in NF-κB levels (**Hwang et al., 2014**). This result suggests that activation of the JAK2/STAT3 pathway in reactive astrocytes results in NF-κB pathway inhibition.

In addition to the NF-κB pathway, we also found that mRNA levels of *Fgfr2*, which has been recently shown to maintain the resting state of astrocytes in the healthy brain, are decreased upon activation of the JAK2/STAT3 pathway. Thus, these data show, for the first time, that activation of the JAK2/STAT3 pathway within astrocytes is able to regulate parallel signaling cascades in reactive astrocytes.

Last, it is to note that the JAK/STAT pathway itself is composed of several JAK, STAT and SOCS proteins. Several JAK/STAT/SOCS proteins interact preferentially. For example, it was recently shown that SOCS3 specifically inhibits the substrate-docking site on JAK2. We showed that SOCS3 overexpression in astrocytes prevents their reactivity in models of AD and HD. However, although SOCS3 mainly inhibits JAK/STAT signaling by blocking JAK2, it is possible that JAK2 could activate other STATs such as STAT1 and STAT5. Thus, we cannot exclude that SOCS3 could still have additional blocking effects (**Kershaw et al., 2013b**). It would be interesting to detect STAT1 and STAT5 in these models of ND to evaluate their activation in reactive astrocytes.

In conclusion, although other signaling pathways might be active in reactive astrocytes in ND, our experiments based on the specific inhibition by SOCS3, show that the JAK2/STAT3 pathway is ultimately responsible for triggering astrocyte reactivity in these ND models. Taken together, these results suggest that activation the JAK2/STAT3 pathway in reactive astrocytes may trigger transcriptional regulation that induces 1) astrocyte reactivity and 2) inhibition of parallel signaling cascades.

3) Manipulating the JAK2/STAT3 pathway through viral gene transfer

By contrast with previous approaches to interfere with the JAK2/STAT3 pathway in astrocytes, we used viral vectors to either overexpress a constitutively active form of JAK2 (JAK2ca) or SOCS3, specifically in astrocytes, in the adult rodent brain. With this strategy, we found that overexpression of JAK2ca in astrocytes induces their reactivity. Conversely, SOCS3 overexpression prevents astrocyte reactivity in various models, through efficient inhibition of the JAK2/STAT3 pathway. Therefore, with this elegant strategy, we demonstrate that the JAK2/STAT3 pathway plays a central role in mediating astrocyte reactivity.

a) Viral vectors allow selective transgene expression in astrocytes

We used lentiviral vectors that were previously developed in the laboratory (**Colin et al., 2009**). These lentiviral vectors are pseudotyped with the MOK envelope and, when injected in the mouse striatum, transduce equally neurons and astrocytes. Transgene expression is under the control of the ubiquitous PGK promoter, thus the cell-specificity is mainly determined by the detargeting strategy with MOK lentiviral vectors. This is achieved by the presence of a sequence encoding the target of a microRNA (miR124T), preferentially expressed in neurons. Thus, when MOK/miR124T lentiviral vectors are injected in the mouse striatum, they will infect both neurons and astrocytes but the presence of the miR124T will lead to transgene degradation in neurons. Therefore, transgene will mainly be expressed in astrocytes.

We have validated transgene expression with lentiviral vectors encoding GFP with cell-type specific markers for astrocytes, neurons, microglia, NG2 cells and oligodendrocytes, in the mouse and the rat striatum. In all our experiments with MOK/miR124T lentiviral vectors, we observed only a few cells (<5%, mainly neurons, NG2 and microglia cells) transduced besides astrocytes either based on morphological identification or with co-staining with cell-type specific markers by immunofluorescence.

We also transduced astrocytes in the adult rodent brain with AAV vectors of serotype 9. In the CNS, AAV-9 transduces astrocytes *in vivo* but also neurons and other cell types (**Cearley and Wolfe, 2006**). By contrast with lentiviral vectors, the promoter used to control transgene expression in AAV vectors mainly dictates vector tropism. Thus, to achieve transgene expression in astrocytes, we used a truncated form of the *gfap* promoter (gfaABC1D) that was shown to be active predominantly in astrocytes compared to other cell types in the mouse brain (**Lee et al., 2008**). Again, we validated

transgene expression with AAV vectors encoding GFP with cell-type specific markers for astrocytes, neurons, microglia and oligodendrocytes in the mouse striatum and hippocampus.

Unfortunately, we could not detect JAK2ca and SOCS3 transgenes in the rodent brain, by immunostaining or western blotting, using different antibodies. We were able to detect transgene overexpression at the mRNA levels by qRT-PCR in samples from injected animals and to detect JAK2 overexpression after transfection of HEK293T cells. This result suggests that the level of expression achieved with viral vectors might not be sufficient to be detected by western blotting. In addition, available antibodies may not recognized fixed epitopes on brain sections. In the case of SOCS3, we have tested several antibodies on several tissue samples, none of which worked. However, despite the fact that we could not detect overexpression at the protein level of JAK2 and SOCS3, we did observe significant biological effects.

To overcome this issue, we systematically co-injected the vector encoding the transgene of interest with a vector encoding GFP. In all experiments, we used a 4 : 1 ratio (transgene : GFP) in terms of viral particle load. We conducted careful experiments to validate that a majority of cells co-expressed two transgenes encoded by two different viral vectors, both with lentiviral and AAV vectors (see § IV.B.1). Indeed, we found that following intrastriatal injection with two MOK/mir124T lentiviral vectors encoding GFP and BFP, 95% of cells co-expressed both fluorescent proteins. Similarly, we found that a majority of cells (99%) co-expressed GFP and tdTomato, when mice were co-injected in the striatum with AAV-GFP and AAV-tdTomato.

This co-injection strategy has two additional assets. First, co-injection with a viral vector encoding GFP allows the visualization of the injected brain area (GFP^+). This infected area can then be dissected out for molecular biology or biochemistry experiments, in order to study only the area efficiently infected by the viral vectors. In addition, we can visualize infected cells and their morphology including their fine processes, as cells are “filled” with GFP.

b) Advantages/ limitations of viral vectors to study astrocyte reactivity

Viral vectors are useful tools: they can be used in mice, rodents and non-human primates with a great versatility; they can be injected at any time of the postnatal life, including in adult and old animals. The fact that they only transduce limited areas of the brain is also an advantage to study the vulnerability of neuronal populations in specific brain regions as in ND or the regional heterogeneity of cellular processes. Indeed, by targeting a limited number of cells in a specific brain area with a viral vector, the rest of the brain parenchyma is unaltered, decreasing the probability of non-specific effects. Experimentally, this property is very useful, because the same animal can be injected independently with viral vectors in different parts of its two hemispheres. For example, we often inject the viral vector encoding the gene of interest in one striatum, and the control in the other. This paradigm is very practical as each animal serves as its own control to take into account inter-individual variability.

Furthermore, viral vectors allow stable transgene expression (**Lowenstein and Castro, 2002; McCown, 2011; Delzor et al., 2013**). Our results showed that transgene expression in the striatum of

mice injected with MOK/mir124T vectors is stable for at least 6 months. For AAV vectors, data from the literature showed that AAV vectors targeting astrocytes led to stable transgene expression at least after 9 months post-injection (**Furman et al., 2012**). Unpublished data from the team confirm that our AAV vectors are stable for at least 5 months. Last, because we inject viral vectors in adult animals, it is unlikely that the viral transduction affect cerebral development.

It could appear paradoxical to modulate astrocyte reactivity with viral vectors that could intrinsically elicit an inflammatory response and glial reactivity when injected in the brain. We addressed this issue by performing dose-response experiments to determine the viral titer that was sufficient to trigger a biological effect but that did not elicit non-specific effects (astrocyte and microglial activation) on any of the control groups (injection of vehicle or injection of control vector GFP). In this context of studying astrocyte reactivity and neuroinflammation, it is to note that the injection of viral vectors itself results in the formation of a glial scar at the needle track. Therefore, in all our experiments, quantification of immunostainings was performed on fields outside of this area. Moreover, our results show that the transduced volume increases with the viral titer. Therefore, as we could not use high viral titers when studying neuroinflammation, we could not transduce large brain areas. Thus, at the titer used for both vectors, the volume of injection was rather small, approximately an average of 1/8th of the total striatal volume and 1/10th of the hippocampal volume.

In fact, this kind of viral-based approach might not be adapted to assess the effect of transgene expression on integrated cerebral functions with behavioral tests or for other techniques that require large amounts of tissue such as transcriptomic or proteomic studies. Nevertheless, we were able to perform a transcriptomic analysis on infected astrocytes even if it required the pooling several mouse samples and RNA amplification.

4) Universality of the JAK2/STAT3 pathway versus heterogeneity of reactive astrocytes

Both resting and reactive astrocytes are now considered as highly heterogeneous cells in terms of their morphological or functional features (**Matyash and Kettenmann, 2010; Anderson et al., 2014**). Because of the variety of molecular triggers, intracellular signaling cascades and effectors that have been associated with astrocyte reactivity, this phenomenon is intrinsically heterogeneous. On the opposite, results from our group and others have identified the JAK2/STAT3 pathway as a universal cascade in reactive astrocytes. How can we explain these discrepancies? It is important to consider different points. First, the large repertoire of molecular signals and pathways that trigger astrocyte activation comes from *in vitro* studies, whereby astrocytes are experimentally stimulated with various molecules (cytokines, growth factors or toxins). While these studies are essential to dissect precise molecular mechanisms, several caveats have to be taken into account especially when studying reactive astrocytes. Indeed, cultured astrocytes do not have the same morphology, molecular profile and cellular interactions than their *in vivo* counterparts (**Eddleston and Mucke, 1993; Foo et al., 2011**). Furthermore, microglial contamination is not always controlled both in primary astrocyte and

neuron-astrocyte co-cultures. This contamination might play a role in the molecular profile of astrocytes upon stimulation (**Saura, 2007**).

Second, most of the signaling pathways associated with reactive astrocytes have been detected in experimentally activated astrocytes or toxic insults. These studies are important to formulate hypothesis about the functional features of astrocyte reactivity, but may not correspond to what occurs in pathological conditions, even acute (**Sofroniew, 2009**). Thus, the apparent heterogeneity of astrocyte reactivity might also partly be due to the variety of experimental strategies, injury models and molecular targets that have been studied. By contrast, we have studied a single intracellular signaling cascade in endogenous reactive astrocytes, in lentiviral-based and transgenic models of ND *in vivo*. Our results suggest that the molecular cascades involved in their reactivity are in fact, highly conserved between disease states, species and brain regions.

The JAK2/STAT3 pathway is involved in the regulation of key intracellular processes both during development and in the adult life. Activation of the JAK2/STAT3 pathway is strongly associated with the regulation of inflammation in the peripheral immune system. Of importance, the majority of *stat, jak* and *socs* null mice are embryonically or perinatally lethal due to defects in cell survival, erythropoiesis, immune system and placental development. Genes involved in cell survival (*Bcl-xl, Bcl-2, Fas*) and proliferation (*Cyclin D1, p53*) are regulated by the JAK2/STAT3 pathway. In the CNS, the JAK2/STAT3 pathway has a key role in the switch that determines astrogliogenesis onset. Thus, one hypothesis is that the JAK2/STAT3 pathway controls intracellular programs that are necessary for cell survival and thus, this pathway could be favored in pathological conditions.

Last, the JAK2/STAT3 pathway differentially regulates gene expression in a cell-type specific manner. Therefore, while this pathway is conserved in reactive astrocytes, it could be possible that the expression of genes that it modulates varies according to the pathological condition or brain region, contributing to the heterogeneity of astrocyte reactivity.

In conclusion, we have extended previous data of the literature showing that the JAK2/STAT3 pathway is activated in several mouse models of ND: AD, HD and PD. Furthermore, we have demonstrated that this pathway is responsible for astrocyte reactivity *in vivo*, in the 3xTg and APP/PS1dE9 mouse models of AD, in the lentiviral-based model of HD. Thus, the JAK2/STAT3 pathway is a highly conserved, powerful target to study astrocyte reactivity in ND.

C. Reactive astrocytes have a limited contribution to neuronal dysfunction in HD models

It is widely discussed whether reactive astrocytes influence disease outcomes in many pathological conditions, including ND (**Maragakis and Rothstein, 2006**). In HD, alterations of specific astrocyte functions have been evidenced including decreased glutamate reuptake (**Lievens et al., 2001; Behrens et al., 2002**), GABA release (**Wojtowicz et al., 2013**), K^+ buffering (**Tong et al., 2014**) and

release of anti-inflammatory cytokines (**Chou et al., 2008**) or antioxidant factors (**Acuna et al., 2013**). Only few studies mentioned or investigated how alterations of these functions or expression of mHtt influenced astrocyte reactivity. For example, a study carried in our laboratory clearly showed that lentiviral-mediated expression of Htt82Q specifically in striatal astrocytes was associated with GFAP upregulation and hypertrophic morphology (**Faideau et al., 2010**). By contrast, in two studies, Bradford et al. have investigated the consequences on mouse phenotype to overexpress mHtt in astrocytes, alone or in combination with a neuronal expression of mHtt (**Bradford et al., 2009; Bradford et al., 2010**). In these studies, authors did not mention whether astrocytes acquired a reactive phenotype upon expressing mHtt.

In our study, we aimed at targeting the JAK2/STAT3 pathway to globally modulate the reactive phenotype of astrocytes and to evaluate its consequences on disease outcomes. We manipulated the JAK2/STAT3 pathway to induce or prevent astrocyte reactivity in two models of HD: the lentiviral-based model and the transgenic N171-82Q model of HD. In both models we found that, despite a successful manipulation of the astrocytic JAK2/STAT3 pathway and astrocyte reactivity, it only had limited effects on neuronal dysfunction observed in these models. Therefore, at least in these two models of HD, reactive astrocytes do not participate in a significant extent to neuronal dysfunction.

1) SOCS3 overexpression in astrocytes interferes with Htt aggregation in the lentiviral-based model of HD

a) Effects of SOCS3 overexpression on astrocyte reactivity and neuroinflammation

We studied the lentiviral-based model of HD whereby neurons express either the WT (Htt18Q) or mutated (Htt82Q) Htt protein. This model reproduces the loss of MSN and induction of astrocyte reactivity observed in patients with HD. The viral vector used to overexpress Htt (VSV-Htt18Q or 82Q) mainly drives transgene expression into neurons. Thus, in this model, astrocytes do not or very weakly express mHtt and become reactive in response to neuronal dysfunction and death.

Six weeks post-injection, overexpression of Htt82Q led to neuronal death and dysfunction as well as the formation of $EM48^+$ and $Ubiquitin^+$ Htt aggregates, in surviving striatal neurons. While Htt82Q is expressed mainly in neurons, we co-injected lentiviral vectors to modulate the JAK2/STAT3 pathway specifically in astrocytes. Thus, we showed that overexpression of SOCS3 almost completely prevented Htt82Q-mediated astrocyte reactivity. By contrast, overexpression of a constitutively active form of JAK2 led to a limited increase in astrocyte reactivity. This result could be expected, as astrocytes are highly reactive with Htt82Q in the control group.

Interestingly, we found that SOCS3 overexpression in astrocytes decreased the expression of inflammatory markers such as *iba1* and *ccl2.* Importantly, SOCS3 decreased the expression of the microglial marker iba1; we are currently analyzing the effect of SOCS3 overexpression in astrocytes on reactive microglia in lenti-Htt82Q mice, by immunofluorescence and by detecting additional

markers of inflammation by qRT-PCR. These results suggest that preventing astrocyte reactivity in the lentiviral-based model of HD decreases neuroinflammation and microglial activation in the injected area despite similar Htt82Q-mediated neuronal death. Therefore, it seems that astrocyte reactivity might be triggering microglial activation in this model.

b) Effects of SOCS3 overexpression on neuronal dysfunction

We investigated the consequences of manipulating the JAK2/STAT3 pathway on neuronal survival after lenti-Htt82Q injection. We found that astrocyte reactivity does not contribute to a significant extent to neuronal death in this model of HD. Indeed, activation or blockade of the JAK2/STAT3 pathway in astrocytes has no detectable effect on the lesion volume evaluated by immunolabeling of DARPP32 and NeuN. Although these markers do not appear very sensitive, other neuroprotective studies carried out in the laboratory found significant neuroprotection or neurotoxicity with these indexes. In these studies, neurons were co-infected with viral vectors encoding Htt and the protective protein. Here, we investigated whether targeting a signaling cascade in astrocytes would influence neuronal death caused by the overexpression of Htt82Q in neurons. Therefore, in this particular model, neuronal dysfunction and subsequent death observed 6 weeks post-injection appears to be mainly neuron-autonomous.

However, we did not perform a time-course or dose-response study, and we cannot exclude that modulation of reactive astrocytes influences neuronal death onset, time-course or when the lesion is milder. We decided to perform post-mortem analysis at 6 weeks post-injection for mice to fully recover from surgery. It is possible that early change in neuron-astrocyte communication occurs as transgenic proteins start to be synthetized in both cell types. Our data suggest that transgenes are expressed within the same time frame in neurons and astrocytes. Moreover, we observed that SOCS3 overexpression even reduces the formation of the glial scar at the needle track following stereotaxic injections. This phenomenon occurs typically in less than a week-following stab wound injury in the cortex (**Bardehle et al., 2013**). This suggests that SOCS3 most likely prevents the establishment of astrocyte reactivity both due to the injection itself and to the expression of Htt82Q in neurons. Thus, it is possible that the JAK2/STAT3 pathway in astrocytes modulates the early time course of the neuronal dysfunction following lenti-Htt82Q-injection. Similarly, it is possible that the induced lesion is too severe to be reduced by surrounding astrocytes.

c) A role for the UPS in reactive astrocytes during ND?

i) The ubiquitin/proteasome system in HD

A role of the UPS in HD comes from studies that observed a co-localization between Ubiquitin and proteasome subunits with mHtt aggregates in brain of patients and mouse models of HD (**Davies et al., 1997; DiFiglia et al., 1997**). These results suggest that mHtt can be ubiquitinated and thus targeted for proteasomal degradation (**Thompson et al., 2009; Juenemann et al., 2013**). Early *in vitro* studies pointed towards an impairment of the UPS in HD cellular models. By contrast, studies in

mouse models of HD reported no global impairment of the UPS activity (**Bowman et al., 2005; Bett et al., 2006; Tydlacka et al., 2008; Maynard et al., 2009**). Moreover, inhibition of UPS in a knock-in mouse model of HD resulted in increased accumulation of the toxic N-terminal fragments of mHtt but not full-length mHtt, suggesting an efficient degradation of N-terminal mHtt fragments by the UPS (**Li et al., 2010**). In any case, this degradation system has mainly been studied in neurons, in which mHtt aggregates are mainly found (**Davies et al., 1997; DiFiglia et al., 1997**). Indeed, only one study evaluated UPS activity in astrocytes in mouse models of HD. Using UPS reporter *in vivo* and *in vitro*, Tydlacka et al. showed that this system is more active in glial cells than neurons to clear mHtt. Although, they did not observe any difference in the UPS activity between WT and Hdh150 knock-in HD mice, proteasome inhibition increased the number of mHtt aggregates in cultured glial cells (**Tydlacka et al., 2008**).

Upon inflammatory conditions, cytokine production such as IFNγ results in the formation of a proteasome variant termed immunoproteasome (**Ferrington and Gregerson, 2012**). Immunoproteasome-specific subunits (β1i, β2i and β5i) were observed in neurons in HD patients and mouse models of HD (**Diaz-Hernandez et al., 2003**). However, it is not known whether reactive astrocytes display immunoproteasomes in HD, but have been observed in other ND. Indeed, they were evidenced in reactive astrocytes as well as neurons and activated microglia in AD, PD, ALS or MS. For example, Orre et al. showed by double immunofluorescence staining that reactive astrocytes and activated microglia located around amyloid depositions upregulated immunoproteasome catalytic subunits in brains from patients with AD and in the APP/PS1dE9 mouse model of AD (**Orre et al., 2013**). Thus, there is evidence for a modulation of the UPS in reactive astrocytes in ND models, although in HD, this phenomenon remains largely unresolved.

ii) The UPS and astrocyte reactivity in HD

We studied the effect of manipulating astrocyte reactivity on Htt aggregates in the lentiviral-based model of HD. We found that SOCS3 influenced the formation of Htt aggregates, although we obtained inconsistent results in two experiments. The last experiment appears more reliable because it allows left-right comparisons and control for inter-individual variability. In addition, in the initial experiment, we detected Htt aggregates with ubiquitin, as Htt aggregates are ubiquinated. Yet, ubiquitin is an indirect marker and we would need to perform EM48 immunodetection to directly quantify Htt aggregates. In fact, reactive astrocytes seem to have a subtle effect on the formation of Htt aggregates, which is a dynamic and complex process. By looking at Htt inclusions we are only looking at the end-product of the pathway, and probably not at the pathogenic agent, as soluble or oligomeric forms of mHtt are thought to be more toxic (**Zuccato et al., 2010**). Additional experiments would be needed to study the formation of different mHtt species more dynamically and to replicate these findings in transgenic mouse models of HD.

Interestingly, our transcriptomic analysis revealed that activation of the JAK2/STAT3 pathway in wild-type astrocytes resulted in the downregulation of genes of the UPS and a concomitant upregulation in

lysosomal genes. These two pathways are involved in mHtt clearance, but with variable efficiency, specificity towards different mHtt forms and subcellular localization, as only the UPS is active in the nucleus (**Ortega and Lucas, 2014**). The UPS seems to be more efficient to degrade soluble mHtt than lysosomes (**Li et al., 2010**), but inclusions of mHtt can only be cleared by autophagy (**Ortega and Lucas, 2014**).

The few studies that have investigated UPS and immunoproteasomes in reactive astrocytes in ND found that their activity was increased. On the opposite, our results suggest that when the JAK2/STAT3 pathway is activated in astrocytes, it decreases the expression of several genes encoding E2-conjugating enzymes and E3-ubiquitin ligase proteins, pointing towards an altered ubiquitination process (**Figure 56**). We did not observe an increase in the expression of immunoproteasome subunits in JAK2ca astrocytes. This result suggests that induction of immunoproteasome formation in astrocytes observed in ND models is due to inflammatory conditions (neuronal dysfunction, microglial activation, pathological stimulus etc…) that do not originate from reactive astrocytes.

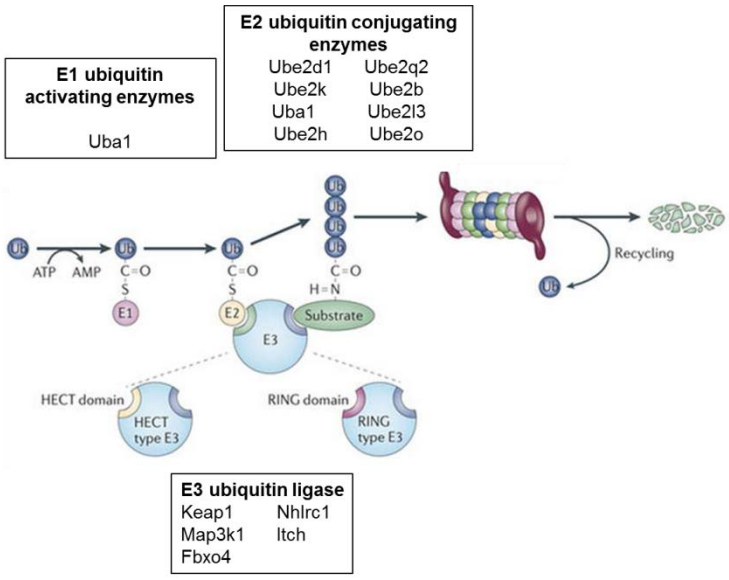

Figure 56. Impairment of the UPS in JAK2ca reactive astrocytes.
Activation of the JAK2/STAT3 pathway in striatal astrocytes decreases in the expression of genes UPS encoding enzymes, as observed in our transcriptomic analysis (§ III.D.1). Particularly, genes encoding E1 ubiquitin activating enzymes, E2 ubiquitin conjugating enzymes and E3 ubiquitin ligase enzymes are strongly downregulated by JAK2ca.

These results show that astrocyte reactivity through the JAK2/STAT3 pathway modulate protein degradation pathways in reactive astrocytes. To further validate these microarray results, it would be of interest to study the function of UPS in JAK2ca astrocytes for example by monitoring the activity of fluorescently tagged proteasomes, detecting proteasome subunits and lysosomal enzymes or measuring of their catalytic activity.

Where are Htt aggregates located?

In the lentivirus-based model of HD, Htt82Q is primarily expressed and forms aggregates in neurons. In patients with HD and mouse models, aggregates are mainly found in neurons even if mHtt is expressed in all brain cells. Several studies also reported mHtt inclusions in glial cells, although less frequently and smaller than neuronal aggregates (**Shin et al., 2005; Faideau et al., 2010; Tong et al., 2014**). Therefore, further experiments would be needed to determine the location of mHtt aggregates in the lentiviral-based model of HD and to evaluate if mHtt aggregates location is changed with modulation of the JAK2/STAT3.

In fact, in the field of ND, there is growing evidence that misfolded or aggregates of disease-causing proteins can spread from cell to cell and that this propagation is a key feature of ND pathogenesis (**Garden and La Spada, 2012; Guo and Lee, 2014**). However, until recently, this question was rather less investigated in HD compared with other ND (**Guo and Lee, 2014**). Indeed, a recent study convincingly suggests that mHtt can propagate from cell to cell through cortico-striatal connexions. Pecho-Vrieseling et al. showed with several *in vitro*, *ex vivo* on organotypic slices and *in vivo* in mice that mHtt aggregates could form in naïve WT neurons (**Pecho-Vrieseling et al., 2014**). Particularly, they injected lentiviral vectors in WT mice, to express the exon 1 of Htt with 72 polyQ repeats along with GFP in cortical neurons to visualize the infected cells and their projections onto striatal MSN. By this approach, authors were able to show the propagation of mHtt aggregates in MSN highly innervated by cortical axons. *In vitro*, they showed that inhibition of vesicular exocytosis decreased this phenomenon (**Pecho-Vrieseling et al., 2014**). However, for HD as for other ND, this trans-cellular propagation of misfolded proteins or aggregates has only been observed between neurons and not between neurons and glial cells.

How reactive astrocytes can modulate mHtt aggregation?

We found that inhibition of astrocyte reactivity by blockade of the JAK2/STAT3 pathway increased the number of mHtt aggregates after lenti-Htt82Q injection in the mouse striatum. First, we controlled by qRT-PCR that the expression of virally encoded human Htt was not different between SOCS3 and GFP control groups, indicating that the effect on aggregates was not due to a direct effect on the viral promoter. There are two main hypotheses that can be drawn from these results (**Figure 57**). First, the “neuronal” pathway is based on the observation that the majority of mHtt is expressed in neurons due to the viral vector used, therefore, mHtt processing (production, cleavage and aggregation) occurs predominantly in striatal neurons. It is possible that reactive astrocytes release molecules such as cytokines, chemokines, growth factors, signaling molecules or metabolic substrates that could modulate mHtt processing in neurons, at different levels (cleavage, ubiquination and aggregation), influencing the formation of mHtt aggregates into neurons. Indeed, the JAK2/STAT3 pathway, responsible for the establishment of astrocyte reactivity in this model, regulates the expression of hundreds of genes in reactive astrocytes that can affect their ability to release such molecules (**Figure 58**). The second hypothesis would be the “astrocyte pathway”, whereby astrocytes may be able to

take up mHtt (soluble, cleaved fragment or aggregates) by trans-cellular transport and degrade it. The shift in protein degradation pathways favoring autophagy could affect the way mHtt is processed in reactive astrocytes and favor the clearance of inclusions by astrocytes.

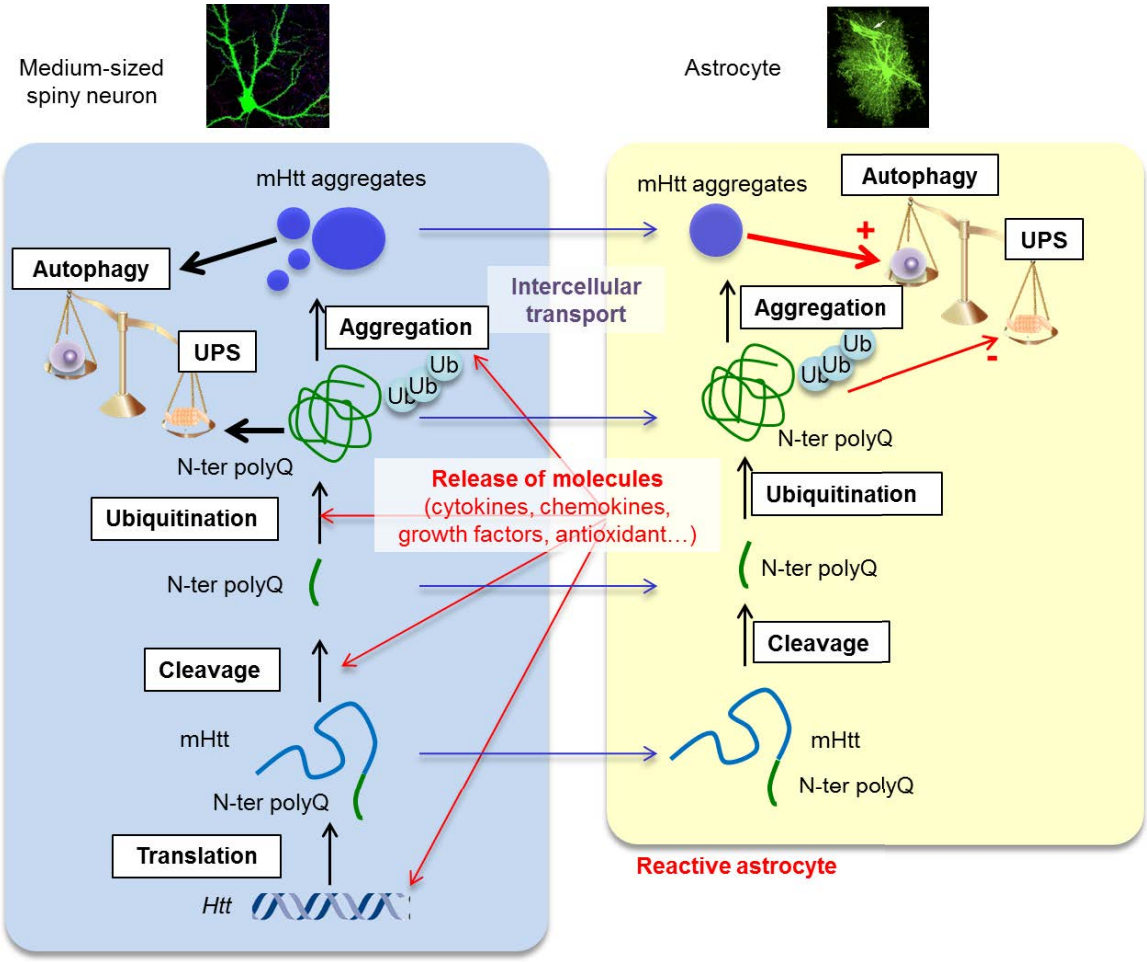

Figure 57. Astrocyte reactivity and mHtt processing and aggregation in HD.
MHtt is cleaved and N-terminal mHtt fragments are polyubiquinated. They can be targeted to the proteasome and degraded or they aggregate and form mHtt inclusions. In the lentiviral-based model of HD, astrocytes express low levels of transgene and mHtt aggregates are mainly found in neurons (as in patients and several mouse models). Nevertheless, it is possible that reactive astrocytes uptake mHtt by transcellular transport or phagocytosis. Reactive astrocytes could uptake either full-length mHtt, cleaved N-terminal fragments or mHtt aggregates and process to their degradation. Our transcriptomic data suggest that, when astrocytes are reactive (red arrows), there is a shift from the UPS system to autophagy. This could influence how astrocytes clear mHtt. Alternatively, reactive astrocytes can release a number of molecules such as cytokines, chemokines or growth factors that could influence the ability of striatal neurons to process mHtt at several levels (cleavage, UPS degradation or aggregation).

Altogether, further experiments will be needed to evaluate the functionality of UPS and lysosmal pathways in reactive astrocytes in the lentiviral-based model of HD and upon modulation of the JAK2/STAT3 pathway.

2) Targeting the JAK2/STAT3 pathway in astrocytes does not influence disease phenotype in N171-82Q mouse model of HD

We aimed at targeting the JAK2/STAT3 pathway in a widely used transgenic mouse model of HD, the N171-82Q model. N171-82Q and WT mice from our colony were injected in the striatum with AAV vectors encoding JAK2ca or SOCS3 to induce or prevent endogenous astrocyte reactivity, respectively. We could not evidence the effects of SOCS3 overexpression on the reactive phenotype of astrocytes in this model. However, a recent and elegant study has well demonstrated that astrocytes displayed abnormal K^+ buffering capacities, in the absence of an activated phenotype in symptomatic R6/2 HD mice (**Tong et al., 2014**). Therefore, it seems that in several mouse models of HD, astrocytes can display abnormal functions without recapitulating a reactive phenotype. As the JAK2/STAT3 pathway regulates key cellular processes in astrocytes, it would have been conceivable that its blockade might have an impact on the neighboring striatal neurons. Furthermore, we showed that JAK2ca overexpression in astrocytes induced their reactivity in N171-82Q HD mice. Therefore, we were able to successfully manipulate astrocyte reactivity in this model with AAV vectors.

a) Experimental issue: differences between animal cohorts

In a first cohort of N171-82Q mice from the Jackson's laboratory, we were able to evidence behavioral and histological alterations in N171-82Q that were reminiscent of symptoms in patients with HD, as previously described (**Schilling et al., 1999**). N171-82Q mice displayed shortened lifespan, weight loss and progressive appearance of behavioral symptoms. At the cellular level, N171-82Q showed significant brain atrophy and ventricle enlargement, decreased levels of striatal markers (DARPP32 and D2R) and the presence of mHtt aggregates throughout the brain.

By contrast, we observed a milder phenotype of N171-82Q from our colony that was used for AAV injections. Indeed, WT mice displayed abnormal motor behavior at the rotarod test, possibly due to a lack of motivation. Post-mortem analysis revealed no striatal atrophy in the N171-82Q in the control group. Furthermore, detection of mHtt aggregates showed qualitatively less inclusions in the striatum than the first cohort of HD mice. It is possible that a genetic drift occurred in our colony, which may explain the difference in both behavioral and histological characteristics observed between the two cohorts. Particularly, the decreased number of aggregates in the striatum might reflect lower expression of mHtt in this cohort of mice and therefore, explain their milder phenotype. We can hypothesize that the cellular alterations due the expression of mHtt were not as strong in the second cohort. Therefore, it is hard to conclude on the potential effects of SOCS3 as these mice displayed almost no alterations.

b) Selective induction of astrocyte reactivity does not influence neuronal dysfunction in N171-82Q mice

As previously mentioned, the N171-82Q HD mice display very mild astrocyte reactivity in the striatum, visible only with an enhanced detection of the gold standard GFAP marker. This was actually an advantage as we could selectively induce astrocyte reactivity through JAK2ca overexpression, in the absence of endogenous reactive astrocytes. JAK2ca induced robust astrocyte reactivity, in most of the dorso-lateral striatum in all JAK2ca-injected mice. We did not observe any effect of inducing astrocyte reactivity in striatal astrocytes on neuronal dysfunction with immunostaining. However, we detected a decrease in mRNA levels of striatal markers *d2r* and *darpp32* in HD mice, yet due to the small number of animals, it did not reach significance. It is possible, especially for immunodetection that the technique used lack sensitivity and that more functional approach, such as electrophysiology might have unraveled subtle toxic effects of JAK2ca-activated astrocytes on neurons.

Overall, our results suggest that reactive astrocytes do not primarily influence neuronal dysfunction in mouse model of HD *in vivo*. If they do play a role, it is likely to have a limited contribution to HD pathogenesis.

D. Deciphering the functional features of reactive astrocytes and their consequences on neurons

1) Activation of the JAK2/STAT3 pathway alters expression of genes involved in multiple key cellular functions in reactive astrocytes

The JAK2/STAT3 pathway is a central player in astrocyte reactivity in pathological conditions. However the functional consequences of its activation on astrocyte functions are not totally understood. Thus, we aimed at characterizing the effects of the JAK2/STAT3 pathway activation in astrocytes by injecting WT mice with AAV-JAK2ca. By contrast to a pathological state, in which a number of factors can influence astrocyte phenotype (neuronal death, microglial activation, aggregated proteins, BBB disruption, immune cells infiltration…), AAV-JAK2ca is only expressed in astrocytes and modifies a specific intracellular pathway within astrocytes.

a) Transcriptomic analysis of FACS-isolated infected astrocytes

Because the JAK2/STAT3 pathway regulates the gene transcription, we analyzed the transcriptome of astrocytes overexpressing JAK2ca or the control GFP. For this experiment, mice were injected in the striatum, as we were primarily interested in studying astrocyte reactivity in the context of HD. For that, we developed a method to sort infected astrocytes by FACS, based on their expression of AAV-

mediated GFP. First, we compared expression of genes between the GFP^+ cells (POS) mainly composed of astrocytes and the GFP^- cells (NEG) containing non-infected astrocytes, other brain cells and debris. We validated that this method yielded to a pure population of infected astrocytes as fold enrichment for astrocyte transcripts were higher than those of other cell types including neurons, microglia and myelinating oligodendrocytes. It is to note however, that for the latter, fold enrichment were lower compared with neurons and microglia. Indeed, we did not use a myelin removal kit as performed in other transcriptomic studies on brain tissue (**Lovatt et al., 2007; Orre et al., 2014a; Orre et al., 2014b**). Therefore, this kit should be used in future experiments with this method to ensure a minimal contamination with myelinating oligodendrocyte transcripts in the POS population.

b) Activation of the JAK2/STAT3 pathway induced the expression of genes involved in antigen presentation and lysosomal protein degradation

We used this approach to analyze FACS-isolated infected astrocytes either resting (GFP) or reactive (JAK2ca). We validated that JAK2ca, as previously observed by immunofluorescence and qRT-PCR, induced the expression of reactive astrocyte markers including *gfap* and *serpina3n*. Surprisingly, *vimentin* mRNA levels were not detected in sorted astrocytes neither in the JAK2ca nor the GFP group, whereas *vimentin* increased at the mRNA levels was observed consistently in our previous experiments. This result highlight the fact that, as previously mentioned (see § III.K.4), we performed microarray experiment with lesser cDNA input than recommended by the manufacturer. Therefore, it is not surprising that a lot of genes were undetectable in this experiment. Again, we used microarray analysis as a screen to pinpoint relevant and robust changes in gene expression with JAK2ca and to validate these changes by qRT-PCR and functional studies with other methods (immunofluorescence, western blot, ELISA etc…).

Our results showed that, upon activation, the JAK2/STAT3 pathway triggers profound changes in the expression of hundreds of genes in astrocytes (**Figure 58**). Intriguingly, by performing DAVID pathway analysis, we found that the majority of the cellular functions modified by JAK2ca in reactive astrocytes are associated with dysfunctions observed in ND such as protein degradation pathways (UPS and lysosome) and oxidative metabolism. In addition, genes associated with inflammatory processes such as lysosomal degradation and antigen processing and presentation are robustly induced in JAK2ca astrocytes.

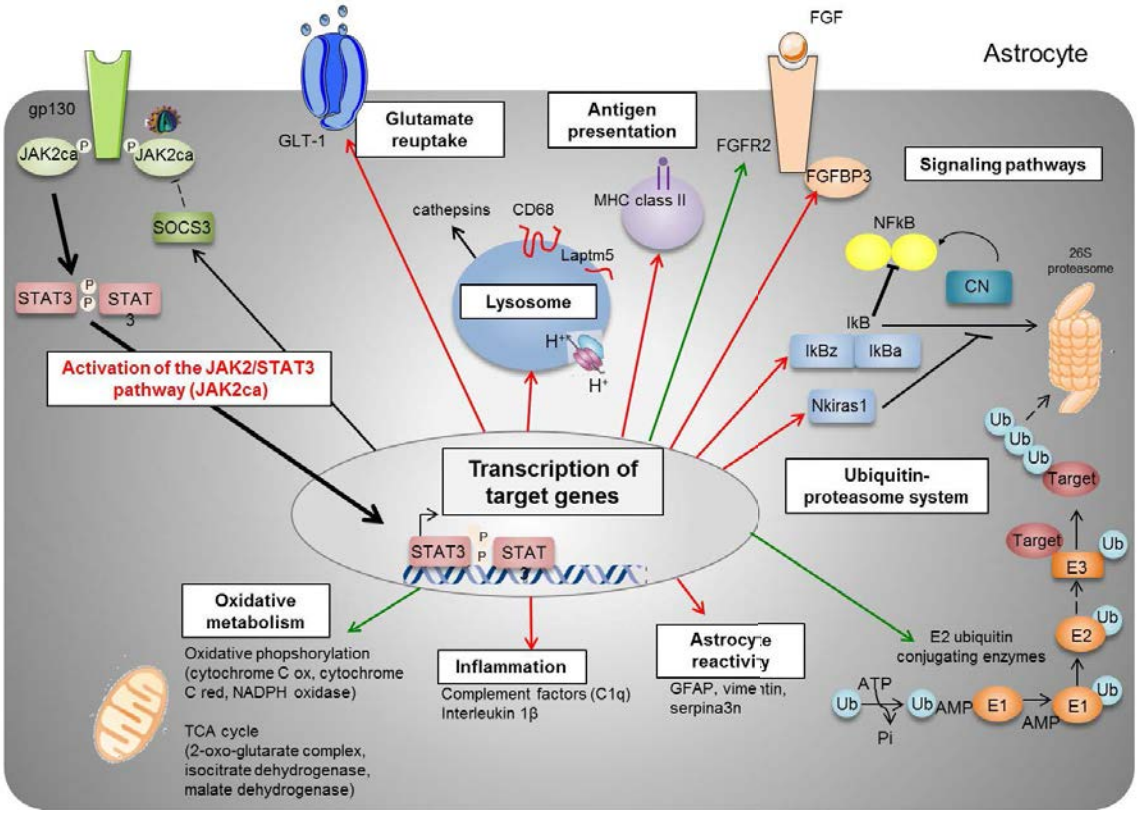

Figure 58. Consequences of the JAK2/STAT3 pathway activation in reactive astrocytes.
A viral construct encoding a constitutively active form of JAK2 (JAK2ca) phosphorylates STAT3, which is translocated to the nucleus and activates the transcription of target genes. Activation of the JAK2/STAT3 pathway in astrocytes upregulate (red arrows) and downregulate (green arrows) numerous genes involved in key cellular functions. Activation of the JAK2/STAT3 pathway results in the activation of astrocytes, with the induction of the expression of reactive astrocyte markers (GFAP, vimentin, serpina3n) as well as genes involved in inflammation (complement factors, interleukins). Importantly, activation of the JAK2/STAT3 pathway in astrocytes reduces several genes encoding enzymes of the oxidative phosphorylation (cytochrome C oxidase, cytochrome C reductase and TCA cycle in the mitochondria.

Recent data from the literature have studied the transcriptome of reactive astrocytes, in various pathological situations and with several approaches to isolate these cells (**Zamanian et al., 2012; Orre et al., 2013; Orre et al., 2014a; Orre et al., 2014b**). Interestingly, several intracellular pathways are consistently increased in reactive astrocytes including in our experiments with JAK2ca. For example, several genes of the antigen presentation pathway are upregulated in reactive astrocytes after LPS injection (**Zamanian et al., 2012**), in aged mice (**Orre et al., 2014b**), around amyloid plaques in a mouse model of AD (**Orre et al., 2014a**) and in JAK2ca astrocytes from our results. It is interesting to note that, in our model, astrocyte reactivity is induced by stimulation of an intracellular signaling pathway, in the absence of exogenous stimulus (toxin, neuronal death, microglial activation). In addition, several genes associated with inflammatory processes are also consistently upregulated such as *C1q, Il-1b and Klf6*. Very interestingly, transcriptomic study of astrocyte gene expression from B.Barre's lab showed that they express genes involved in evolutionary conserved phagocytic

pathways such as the Ced-1/Draper/Megf10 (**Cahoy et al., 2008**). Furthermore, they recently showed that activation of this pathway in astrocytes was necessary for the refinement of synaptic connexions both during development and in the adult brain (**Chung et al., 2013**). Intriguingly, *Megf10* is significantly downregulated in JAK2ca astrocytes along with an increase gene expression of its ligand *Mfge8*. This result suggests that, activation of the JAK2/STAT3 pathway in striatal astrocytes of an adult mouse does not induce the expression of genes involved in this phagocytic machinery.

By contrast, activation of the JAK2/STAT3 pathway in astrocytes strongly increases the expression of genes of the lysosomal degradation pathway, which was not found in other studies (**Figure 57**). (**Zamanian et al., 2012; Orre et al., 2014a; Orre et al., 2014b**). For instance, *lysozyme*, encoding a glycoside hydrolase was robustly upregulated more than 3-fold in JAK2ca astrocytes. This enzyme is involved in the antibacterial response. In addition, several cathepsins (S, Z, B and C) were upregulated approximately 2-fold in JAK2ca astrocytes. Cathepsin S is a lysosomal cysteine proteinase that may participate in the degradation of antigenic proteins to peptides for presentation on MHC class II molecules. Cathepsin Z has recently been reported as involved specifically in the degradation of mHtt but not mutant SOD1 in various mouse cell lines (**Bhutani et al., 2012**). Indeed, authors showed that Cathepsin Z is crucial for lysosomal degradation of mHtt in neurons by inhibiting lysosome function with lysosomal enzyme-specific inhibitors and cathepsin Z knockdown (**Bhutani et al., 2012**). Upon LPS injection, cathepsin C is upregulated and released from microglial cells (**Fan et al., 2012**). Interestingly, downregulation of cathepsin D and beclin-1, a tumor suppressor and a target gene of the JAK2/STAT3 pathway, in primary neurons and astrocytes, is associated with excitotoxic cell death after QA treatment (**Braidy et al., 2014**). Overall, there is evidence of a strong link between the induction of lysosomal pathway by the JAK2/STAT3 pathway and autophagy degradation system in ND.

In this context, to validate these results obtained at the mRNA level, it would be interesting to study the function of lysosomes in reactive astrocytes. For example, we could detect lysosome protein subunits by immunofluorescence or western blotting. More importantly, we could monitor lysosome activity *in vivo* in reactive astrocytes by co-injecting viral vectors encoding the lyso-tracker and JAK2ca. It would be particularly interesting to demonstrate the functional modulation of lysosomal degradation in reactive astrocytes in the context of ND. Indeed, in culture, astrocytes are able to clear amyloid peptide β and Mfeg8 is involved in amyloid clearance (**Boddaert et al., 2007**).

c) Unraveling the regional heterogeneity of reactive astrocytes

Last, it would be particularly interesting to repeat this experiment by injecting JAK2ca in other brain regions (cortex, hippocampus) to compare the transcriptomic changes in reactive astrocytes from one region to another. This experiment would allow studying the regional heterogeneity of reactive astrocytes. Indeed, astrocyte population is now recognized as heterogeneous as neurons (see § II.A.3). Several studies have reported that astrocytes are morphologically and functionally distinct according to the brain region (**Emsley and Macklis, 2006; Doyle et al., 2008; Oberheim et al.,**

2012). However, heterogeneity of reactive astrocytes, in a pathological condition, represents one step even further (**Anderson et al., 2014**). While the morphological heterogeneity of reactive astrocytes between brain regions is easy to evidence, their functional heterogeneity remains largely unknown. In this context, JAK2ca is a powerful tool, allowing the comparison of the same stimulus specifically in astrocytes, in various brain regions, in the absence of exogenous, pathological stimulus. Thus, studying changes in gene expression of regionally distinct astrocytes might highlight specific patterns or regulation of astrocyte functions depending of the brain area. In this study, we showed that the JAK2/STAT3 pathway is a universal inducer of astrocyte reactivity, highly conserved between ND models and brain regions. However, depending on the cellular environment of specific brain areas such as the striatum, the cortex or hippocampus, reactive astrocytes, even though activated by the same intracellular pathway, might have different effects on surrounding cells, including neurons. This concept is particularly relevant in the field of ND that are characterized by the selective loss of neurons in specific brain regions. Therefore, understanding reactive astrocyte regional heterogeneity might bring some insights on neuronal vulnerability in ND.

2) The JAK2/STAT3 pathway regulates astrocyte control of synaptic transmission in the mouse hippocampus

Astrocytes are protagonists of the synaptic transmission in the brain. Their distal processes ensheath synapses conferring to astrocytes a key anatomical location between the pre and the post-synaptic elements (**Araque et al., 1999**). Astrocytes modulate synaptic transmission through the of release gliotransmitters such as glutamate, D-serine, ATP or GABA (**Araque et al., 2014**). The impact of astrocyte reactivity on their ability to modulate synaptic transmission in the hippocampus has mostly been studied with experimentally activated astrocytes or in mouse models of AD, as synaptic dysfunction is a hallmark of AD pathogenesis.

We took advantage on viral vectors that are versatile tools to inject an AAV encoding either JAK2ca or GFP in the CA1 region of the hippocampus in WT mice and we performed electrophysiological recordings on brain slices of these mice. We showed that selective activation of the JAK2/STAT3 pathway in hippocampal astrocytes impairs glutamatergic synaptic transmission at Schaffer collateral (SC)-CA1 pyramidal cell synapses. Furthermore, LTP was also decreased in JAK2ca-injected mice compared with GFP and non-injected control mice. Interestingly, LTP is a form of synaptic plasticity and this phenomenon is thought to underlie experience-based behavior and learning (**Malenka and Bear, 2004**). JAK2ca mice display a decrease in synaptic plasticity of approximately 25%. Interestingly, similar synaptic deficits are observed in AD mouse models and were associated with abnormal learning behavior (**Saganich et al., 2006**). Therefore, it would be interesting to evaluate the memory and learning in JAK2ca and GFP mice, to determine if the decreased synaptic plasticity is associated with altered learning behavior.

Several mechanisms at the synaptic level could explain the influence of reactive astrocytes on synaptic transmission. Two recent studies have investigated the influence of reactive astrocytes on

synaptic transmission in the hippocampus of the APP/PS1dE9 mouse model of AD. They found that reactive astrocytes display alteration of GABA release, which results in a tonic inhibition in the dentate gyrus (**Jo et al., 2014; Wu et al., 2014**). Interestingly, we showed that the JAK2/STAT3 pathway mediates astrocyte reactivity in this mouse model of AD. Therefore, it would be interesting to study GABAergic transmission in the dentate dyrus in brain slices of JAK2ca-injected mice, to determine if we reproduce the synaptic defects observed in those mice. Indeed, there are numerous GABAergic interneurons that synapse onto CA1 pyramidal cells (**Klausberger, 2009**). We could also study by immunostaining or western blotting the expression of GABA transporters (GAT) and channels (bestrophin) that were upregulated in reactive astrocytes of AD mice (**Jo et al., 2014; Wu et al., 2014**). In another study highlighting the link between altered inhibitory transmission and astrocyte reactivity, Ortinski et al. showed that when astrocytes were activated by high titers of AAV-GFP in the hippocampus, it decreases inhibitory but not excitatory transmission in CA1 pyramidal cells (**Ortinski et al., 2010**).

Other gliotransmitters could be involved in this decreased synaptic transmission and plasticity. D-serine is the endogenous co-agonist on the glycine site of synaptic NDMARs (**Oliet and Mothet, 2006**, **2009; Papouin et al., 2012**). Astrocytes control synaptic NMDAR activity through D-serine release in the supraoptic nucleus (**Panatier et al., 2006**). More interestingly, astrocytes can detect synaptic activity triggered by single synapse stimulation at the SC-CA1 synapse in the hippocampus (**Panatier et al., 2011**). Therefore, it would be interesting to determine if D-serine release and occupancy at the glycine site of synaptic NMDARs is decreased in JAK2ca mice.

Last, we observed that *glt-1* mRNA levels are strongly increased in JAK2ca astrocytes, in the striatum. We could hypothesize that if the same effect occurs in hippocampal astrocytes and that this increase in mRNA levels is associated with a parallel increase in protein levels, GLT-1 could uptake more glutamate at the synaptic cleft, therefore resulting in a decrease synaptic transmission at excitatory synapses. It would be interesting to evaluate the protein levels of GLT-1 in samples from the hippocampus of JAK2ca mice. We could also perform functional assay of glutamate uptake to evaluate transporter activity in JAK2 and GFP mice (**Faideau et al., 2010**). Moreover, GLT-1-specific currents can be measured through the recording astrocytes during patch clamp experiments.

In conclusion, further experiments will be needed to understand the molecular mechanisms underlying this decrease in synaptic efficacy and plasticity. In any case, these results are intriguing and may provide direct evidence that the selective induction of astrocyte reactivity by targeting a relevant intracellular pathway is able to influence synaptic transmission, in the absence of a pathological stimulus.

VI. CONCLUSIONS - PERSPECTIVES

In this study, we provide evidence that the JAK2/STAT3 pathway, mediates astrocyte reactivity in various models of ND. We developed new viral tools allowing the selective manipulation of reactive astrocytes, *in vivo*, in the adult rodent brain. Importantly, while astrocytes are considered as a morphologically and functionally heterogeneous population of cells, our results suggest, on the opposite, that the molecular cascade mediating their reactivity upon pathological conditions, both acute and chronic, are highly conserved.

The universality of the JAK2/STAT3 pathway activation in reactive astrocytes is rather unexpected as the molecular triggers of astrocyte reactivity are likely to depend on the pathological stimulus, especially in ND. Therefore, our results suggest that the JAK2/STAT3 pathway is favored to mediate astrocyte reactivity, by subsequent inhibition of parallel signaling cascades, also associated with astrocyte reactivity, such as the NF-κB or FGFR pathways.

The contribution of reactive astrocytes to disease progression is controversial. Especially, in the context of HD, several studies have reported dysfunction of specific astrocyte functions including glutamate reuptake, K^+ buffering or release of anti-inflammatory cytokines. However, few of these studies have evaluated whether these dysfunctions were associated with the reactive phenotype of astrocytes. In this study, we aimed at globally modulating astrocyte reactivity in HD, rather than targeting specific cellular functions. We studied two complementary models of HD, the lentiviral-based model and the transgenic mouse model N171-82Q. Surprisingly, we found that, inducing or preventing astrocyte reactivity in both models does not primarily influence disease outcomes. Nevertheless, preventing astrocyte reactivity altered the number of mHtt aggregates in the lentiviral-based model of HD, suggesting that reactive astrocytes might influence mHtt aggregation in neurons. Further studies will be needed to determine if this effect is also observed in transgenic mouse models of HD and to decipher the molecular mechanisms involved.

In addition, it would also be interesting to use these versatile tools to evaluate the influence of reactive astrocytes to neuronal dysfunction and disease phenotype in other ND, such as AD or PD, especially as we showed that activation of this pathway is universal and conserved in these ND models. Experiments are ongoing in mouse models of AD.

Last, we studied the consequences of inducing astrocyte reactivity on astrocytes and neuron-astrocyte communication in two brain regions in the mouse brain. We carried out a transcriptomic analysis to study gene expression in activated striatal astrocytes. This is the first study to date that evaluated the consequences of JAK2/STAT3 pathway activation on astrocyte transcriptome, from isolated astrocytes of adult mice.

The JAK2/STAT3 pathway regulates cellular processes through transcriptional changes. Indeed, we found hundreds of genes significantly up- or down-regulated by JAK2ca. Strikingly, we found that activation of the JAK2/STAT3 pathway in astrocytes decreases the expression of genes involved in

oxidative metabolism or protein degradation pathways, highly relevant for the study of ND. Indeed, most of these cellular alterations are shared between different ND such as HD, AD, PD or ALS.
In addition, we studied the functional impact of inducing astrocyte reactivity on synaptic transmission in the hippocampus. Surprisingly, we showed it impairs synaptic efficacy and plasticity. Further experiments will be needed to decipher the molecular mechanisms involved in this effect. Although, it is particularly interesting that the selective activation of astrocytes, in the absence of a pathological stimulus, could influence synaptic transmission. Furthermore, these alterations are reminiscent of those observed in the hippocampus of AD mouse models. Because, we showed that the JAK2/STAT3 pathway mediates astrocyte reactivity in two mouse models of AD, it would be interesting to determine if the cellular alterations responsible for the decreased synaptic transmission are conserved between JAK2ca astrocytes and reactive astrocytes in AD models.
Viral vectors are versatile tools. Therefore, the tools developed during this project allow the comparison at the molecular, cellular and functional levels of reactive astrocytes, in different brain regions as well as in different species (rat, mice and even primates).

Altogether, our results suggest that the JAK2/STAT3 pathway is a key player of astrocyte reactivity, in virtually all pathological brain conditions. However, its modulation in reactive astrocytes of mouse models of HD did not predominantly influence disease outcomes. Therefore, comparing the effects of its modulation in reactive astrocytes in other ND models would validate the functional relevance of targeting the JAK2/STAT3 pathway to study astrocyte reactivity.

VII. GENERAL CONCLUSION

Neurons and astrocytes interact through a complex and essential interplay in the brain. It is now well accepted that, particularly in ND, dysfunction of astrocytes and thus, of neuron-astrocyte interactions, may contribute to disease phenotype. Evidence towards both beneficial and detrimental roles of reactive astrocytes has been equally demonstrated, although it may largely depend on the combination of several factors such as types of injury or disease, brain region, molecular triggers, intracellular signaling pathways and potential alterations of intercellular communication (neurons, microglia, oligodendrocytes, endothelial cells etc…). Thus, it appears important to develop new strategies to understand and characterize reactive astrocytes from a functional point of view. This would allow the development of novel therapeutic strategies in order to enhance endogenous support capacities of astrocytes while diminishing potentially harmful reactions. In this context, we decided to study one of the most well known intracellular signaling cascade associated with astrocyte reactivity: the JAK2/STAT3 pathway. We show that targeting this pathway in both in WT and mouse models of ND would provide insights on reactive astrocyte functions and their contribution to chronic pathological conditions.

ANNEXE

VII. ANNEXES

A. Abbreviations

AD	Alzheimer's disease
ALDH1L1	Aldehyde dehydrogenase 1 family, member l1
ALS	Amyotrophic lateral sclerosis
AMPAR	α-amino-3-hydroxy-5-methyl-4-isoxazolepropionic acid receptor
App	Amyloid beta precusor protein
Aqp4	Aquaporin 4
AVs	Autophagic vesicles
Aβ	Amyloid beta peptide
BBB	Blood-brain barrier
BDNF	Brain-derived neurotrophic factor
BLBP	Brain lipid binding protein
BMP	Bone morphogenic proteins
BSA	Bovin serum albumin
cAMP	Cyclic adenosine monophosphate
CBF	Cerebral blood flow
CBP	Creb-binding protein
CIS	Cytokine-inducible SRC homology 2 domain-containing protein
CLC	Cardiotrophin-like cytokine
CN	Calcineurin
CNS	Central nervous system
CNTF	Ciliary neurotrophic factor
CREB	Cyclic amp-response binding element
CT-1	Cardiotrophin-1
Cx	Connexins
D2R	Dopamine 2 receptor
DARPP32	Dopamine- and cAMP-regulated phosphoprotein 32 kDa
EAAT1/2	Excitatory amino acid transporter 1/2
EFG	Epidermal growth factor
ERK	Extracellular signal-regulated kinase
ERK	Extracellular signal-regulated kinase
FGF	Fibroblast growth factor
FGFR	Fibroblast growth factor receptor
GLAST	Glutamate aspartate transporter
GLT-1	Glutamate transporter -1
GPCR	G-protein coupled receptor
GPe	External globus pallidus
HAT	Histone acetyltransferases
HD	Huntington's disease
HDAC	Histone deacetylases (hdac)
HEK293T	Human embryonic kidney 293 cells
Hes5	Hairy and enhancer of split 5
HIP1	Huntingtin-interacting protein 1 (hap1)
Htt	Huntingtin
IGF-1	Insulin growth factor 1
Il-1β	Interleukin-1β
Il-6	Interleukin-6
IP_3	Inositol-3-phosphate
iRNA	interference RNA
JAK	Janus kinase
JNK	C-jun n-terminal kinase
Kir4.1	Inward rectifier-type potassium channel
KO	Knockout
LPS	Lipopolysaccharide

MAPK	Mitogen-activated protein kinase
MAPKK	Mitogen activated protein kinase kinase
MAPKKK	Mitogen activated protein kinase kinase kinase
MCT	Monocarboxylate transporters
miRNA	Micro-RNA
MOK-G	G protein of the mokola lyssaviruses
mTOR	Mammalian target of rapamycin
Nfat	Nuclear factor of activated T-cells
NF-κB	Nuclear factor of kappa light polypeptide gene enhancer in b-cells
NMDAR	N-méthyl-d-aspartate receptor
Nrf2	Nuclear factor erythroid 2- related factor 2
NSC	Neural stem cell
OsM	Oncostatin M
PD	Parkinson's disease
PGC-1α	Proliferator-activated receptor gamma coactivator 1-α ()
PGK	Phosphoglycerate kinase
PS1	Presenilin
RBX2	RING- box-2
Rev	Regulator of expression of virion proteins
RGC	Retinal ganglion cell
ROS	Reactive oxygen species
RTK	Receptor tyrosine kinases
S100β	S100 calcium binding protein B
SCI	Spinal cord injury
SEZ	Subependymal zone
SH2	SRC homology 2
shRNA	Small hairpin RNA
siRNA	Small interfering RNA
SNpc	Substancia nigra pars compacta
SNpr	Substancia nigra pars reticulata
Socs	Suppressor of cytokine signaling
SOD	Superoxide dismutase
Sox2	Sex determining region Y box 2
TBI	Traumatic brain injury
TCA	Tricyclic acid
TFEB	Transcription factor E-B
TGFβ1	Transforming growth factor beta 1
TrkB	Tropomyosin receptor kinase b
TSPs	Thrombospondins
VG	Viral genome
VSV-G	G protein of the vesicular stomatitis virus
WMI	White matter injury

B. Publications and communications

Publications

Ben Haim L., Ceyzeriat, K., Carrillo-De Sauvage, M.A., Aubry, F., Auregan, G., Guillermier, M., Ruiz, M. Petit, F., Houitte, D., Faivre, E., Vandesquille, M., Aron-Badin, R., Dhenain, M., Déglon, N., Hantraye, P., Brouillet, E., Bonvento, G., Escartin, C. **The JAK/STAT3 pathway is a universal inducer of astrocyte reactivity in of Alzheimer's and Huntington's diseases.** (under review at the Journal of Neuroscience)

Damiano M.,Diguet E., Malgorn C., Galvan L., Petit F., **Benhaim L.**, Guillermier M., Houitte D., Dufour N., Hantraye P., Canals J.M., Alberch J., Delzescaux T., Déglon N., Beal F.M., Brouillet E. **Mitochondrial complex II defects in genetic models of Huntington's disease expressing N-terminal fragments of mutant huntingtin.** Hum. Mol. Genet., (2013); 22(19):3869-82

Lavisse S., Guillermier M., Hérard A.S., Petit F., Delahaye M., Van Camp N., **Ben Haim L.**, Lebon V., Remy P., Dollé F., Delzescaux T., Bonvento G., Hantraye P., Escartin C. **Reactive astrocytes overexpress TSPO and are detected by TSPO positron emission tomography imaging**. J Neurosci. (2012); 32(32):10809-18.

Calvo C.F., Fontaine R.H., Soueid J., Tammela T., Makinen T., Alfaro-Cervello C., Bonnaud F., Miguez A., **Benhaim L.**, Xu Y., Barallobre M.J., Moutkine I., Lyytikkä J.,Tatlisumak T., Pytowski B., Zalc B., Richardson W., Kessaris N., Garcia-Verdugo J.M., Alitalo K., Eichmann A., Thomas J.L.. **Vascular endothelial growth factor receptor 3 directly regulates murine neurogenesis.** Genes Dev. (2011); 25(8):831-44.

Oral communications

The JAK/STAT3 pathway is a universal inducer of astrocyte reactivity in Alzheimer and Huntington's diseases, October 01-03 2014, Astrocytes in brain function and dysfunction, Paris, France.

STAT3 pathway mediates astrocyte activation in neurodegenerative disease models, April, 28-29 2014, Astrocytes in Health and Disease, London, UK.

Selective modulation of astrocyte activation *in vivo* through lentiviral gene transfer: Contribution of reactive astrocytes to neuronal dysfunction in Huntington's disease, May, 15 2013, Brain, Cognition and Behaviour doctoral school colloquium.

Posters

Activation of the STAT3 pathway in reactive astrocytes: a common feature of several neurodegenerative disease models. L. Ben Haim, MA. Carrillo de Sauvage, F. Aubry, G. Auregan, E. Faivre, L. Francelle, M. Dhenain, E. Brouillet, G. Bonvento, C. Escartin., March, 20-22, 2013, Brain Repair Spring School, Cambridge, United-Kingdom.

Astrocyte reactivity is associated with decreased of N-Acetyl-Aspartate levels in absence of neurodegeneneration in the rat brain. Carrillo-de Sauvage M.A., **Ben Haim L**., Guillermier M., Valette J., Escartin C., XXVIth International Symposium on Cerebral Blood Flow, Metabolism and Function, May, 20-23, 2013, Shangai, China.

Imaging signatures of reactive astrocytes *in vivo*: detection by magnetic resonance spectroscopy and positon emission tomography of TSPO ligands. Carrillo-de Sauvage M.A. & Lavisse S, Guillermier M. , Hérard A.-S., Petit F., Delahaye M., Van Camp N., **Ben Haim L**., Lebon V.,

Dollé F., Delzescaux T., Bonvento G., Hantraye P., Valette J., Escartin C., Gordon Research Conference "*Glial* Biology: Functional Interactions among *Glia* & Neurons", March,3-8, 2013, Ventura Beach Marriott, Ventura, Californie, Etats-Unis.

Imaging signatures of reactive astrocytes *in vivo*: detection by magnetic resonance spectroscopy and positron emission tomography of TSPO ligands. Carrillo-de Sauvage M.A. & Lavisse S, Guillermier M. , Hérard A.-S., Petit F., Delahaye M., Van Camp N., **Ben Haim L.**, Lebon V., Dollé F., Delzescaux T., Bonvento G., Hantraye P., Valette J., Escartin C., 8th FENS Forum of European Neurosciences, July 2012, Barcelona, Spain.

Metabolic signatures of reactive astrocytes in the rat brain as detected by magnetic resonance spectroscopy. Carrillo-de Sauvage M.A., **Ben Haim L.**, Valette J. Escartin C. 10th ICBEM Intenational Conference on Brain Energy Metabolism, April 2012, California, USA

Astrocyte reactivity is associated with changes in the concentration of multiple striatal metabolites in situ. Carrillo-de Sauvage M.A. Bramoulle Y., **Ben Haim L**., Aubry F., Guillermier M., Auregan G., Valette J., Escartin C.. XI European Meeting on Glial Cells in Health and Disease, July, 3-6, 2013, Berlin, Germany.

Activation of the STAT3 pathway in reactive astrocytes: a common feature of several neurodegenerative disease models. L. Ben Haim, K.Ceyzeriat, MA. Carrillo de Sauvage, F. Aubry, G. Auregan, E. Faivre, L. Francelle, M. Dhenain, E. Brouillet, G. Bonvento, C. Escartin., November, 5-9 2013, Society for Neuroscience, San Diego, USA.

Activation of the STAT3 pathway in reactive astrocytes: a common feature of several neurodegenerative disease models. L. Ben Haim, K.Ceyzeriat, MA. Carrillo de Sauvage, F. Aubry, G. Auregan, E. Faivre, L. Francelle, M. Dhenain, E. Brouillet, G. Bonvento, C. Escartin., April, 7-9 2014, ED3C colloquium, Roscoff, France.

Activation of the STAT3 pathway in reactive astrocytes: a common feature of several neurodegenerative disease models. L. Ben Haim, K.Ceyzeriat, MA. Carrillo de Sauvage, F. Aubry, G. Auregan, E. Faivre, L. Francelle, M. Dhenain, E. Brouillet, G. Bonvento, C. Escartin., April, 28-29 2014, Astrocytes in Health and Disease, London, UK.

C. Article

The JAK/STAT3 pathway is a universal inducer of astrocyte reactivity in of Alzheimer's and Huntington's diseases.

Ben Haim L., Ceyzeriat, K., Carrillo-De Sauvage, M.A., Aubry, F., Auregan, G., Guillermier, M., Ruiz, M. Petit, F., Houitte, D., Faivre, E., Vandesquille, M., Aron-Badin, R., Dhenain, M., Déglon, N., Hantraye, P., Brouillet, E., Bonvento, G., Escartin, C. (Under review at the Journal of Neuroscience)

The Journal of Neuroscience

http://jneurosci.msubmit.net

JN-RM-3516-14

The JAK/STAT3 pathway is a universal inducer of astrocyte reactivity in Alzheimer's and Huntington's disease

Carole Escartin, CEA CNRS URA2210
Lucile Ben Haim, CEA CNRS URA2210
Kelly Ceyzériat, CEA CNRS URA2210
María Ángeles Carrillo-de Sauvage, CNRS UMR 7224, INSERM U 952, Universty of Murcia
Fabien Aubry, CEA CNRS URA2210
Gwennaëlle Auregan, CEA, Institute of Molecular Imaging (I2BM) and Molecular Imaging Research Center (MIRCen), Orsay, France
Martine Guillermier,
Marta Ruiz, CEA CNRS URA2210
Fanny Petit, CEA
Diane Houitte, CEA
Emilie Faivre, University of Ulster
Matthias Vandesquille, CEA CNRS URA2210
Romina Aron-Badin, CEA CNRS URA2210
Marc Dhenain, CEA/CNRS
Nicole Déglon, CEA CNRS URA2210
Philippe Hantraye, MIRCen
Emmanuel Brouillet, CEA
Gilles Bonvento, MIRCen

Commercial Interest: No

This is a confidential document and must not be discussed with others, forwarded in any form, or posted on websites without the express written consent of The Journal for Neuroscience.

The JAK/STAT3 pathway is a universal inducer of astrocyte reactivity in Alzheimer's and Huntington's disease

L. Ben Haim, K. Ceyzeriat, M.A. Carrillo-de Sauvage, F. Aubry, G. Auregan, M. Guillermier, M. Ruiz, F. Petit, D. Houitte, E. Faivre, M. Vandesquille, R. Aron-Badin, M. Dhenain, N. Déglon, P. Hantraye, E. Brouillet, G. Bonvento, C. Escartin

CEA, DSV, I²BM, MIRCen and CNRS URA2210, 92260 Fontenay-aux-roses, France

Abbreviated title: STAT3, a universal trigger of astrocyte reactivity

Corresponding author:

Carole Escartin

18, route du Panorama

92260 Fontenay-aux-roses

carole.escartin@cea.fr

Number of pages: 31

Number of figures: 9

Number of words in Abstract: 250

Introduction: 448

Discussion: 1314

Conflict of interest

The authors declare no competing financial interests.

Acknowledgements

We thank Dr C. Bjørbæk and Dr. S.E. Shoelson for providing us with the pcDNA3-SOCS3 plasmid. We thank N. Dufour, C. Joséphine and Dr. A. Bémelmans for viral vector production. We are grateful to P. Gipchtein and Dr. C. Jan for their help with immunostainings and Dr. MC. Gaillard for technical advice on qRT-PCR analysis. We thank T. Kortulewski and L. Irbah of the CEA/IRCM Microscopy platform for providing training and technical advice for confocal analysis.

This work was supported by the grants ANR 2010-JCJC-1402-1 and ANR 2011-BSV4-021-03 (to CE), ANR 2011-MALZ-003-02 (to GB) and Association France Alzheimer (to GB and MD), CEA and CNRS. LBH was a recipient of a PhD fellowship from the CEA (IRTELIS program).

The current affiliation for Nicole Déglon is the "Laboratory of Cellular and Molecular Neurotherapies", Department of Clinical Neurosciences, Lausanne University Hospital Lausanne, Switzerland.

Abstract

Astrocyte reactivity is a hallmark of neurodegenerative diseases (ND). Reactive astrocytes are observed in vulnerable brain regions in both patients and animal models of ND, but their effects on disease outcome remain highly debated. Elucidation of the signaling cascades inducing reactivity in astrocytes during ND would help characterize the function of these cells and identify novel molecular targets to modulate disease progression. The JAK/STAT3 pathway is associated with reactive astrocytes in models of acute injury, but it is unknown whether this pathway is directly responsible for astrocyte reactivity in progressive pathological conditions such as ND.

In this study, we examined whether the JAK/STAT3 pathway promotes astrocyte reactivity in several animal models of ND. The JAK/STAT3 pathway was activated in reactive astrocytes in two transgenic mouse models of Alzheimer's disease and in a mouse and a non-human primate lentiviral vector-based model of Huntington's disease. To determine whether this cascade was instrumental for astrocyte reactivity, we used a lentiviral vector that specifically targets astrocytes *in vivo* to overexpress the endogenous inhibitor of the JAK/STAT3 pathway (Suppressor of Cytokine Signaling 3, SOCS3). SOCS3 overexpression significantly inhibited this pathway in astrocytes, efficiently prevented astrocyte reactivity in models of both diseases and restored a resting phenotype to astrocytes.

Our data demonstrate that the JAK/STAT3 pathway is a common mediator of astrocyte reactivity that is highly conserved between disease states, species and brain regions. This universal signaling cascade represents a powerful target to study the functional features of reactive astrocytes and examine their role in ND.

Introduction

In response to multiple pathological conditions, astrocytes undergo molecular, morphological and functional changes referred to as astrocyte reactivity (Sofroniew and Vinters, 2010). They become hypertrophic, up-regulate intermediate filament proteins including GFAP and vimentin, and display functional alterations that are still not fully understood. Astrocyte reactivity occurs both in acute and progressive pathological conditions and is a hallmark of multiple neurodegenerative diseases (ND) (Sofroniew and Vinters, 2010). Astrocyte reactivity develops in vulnerable regions at the early stages of ND and progresses along with neurological symptoms and cell death. Reactive astrocytes are observed in close proximity to amyloid depositions in both patients with Alzheimer's disease (AD) and mouse models of AD (Probst et al., 1982; Itagaki et al., 1989). They are also found in the striatum and cortex of patients with Huntington's disease (HD) and some mouse models of HD (Vonsattel et al., 1985; Yu et al., 2003; Faideau et al., 2010).

The involvement of reactive astrocytes in disease progression is highly controversial. Although, they are generally considered as detrimental for neuronal function, several studies suggest that reactive astrocytes may have beneficial effects and promote neuronal survival (Escartin and Bonvento, 2008; Hamby and Sofroniew, 2010). In any case, elucidation of the precise molecular cascades that lead to astrocyte reactivity may help identify potential therapeutic targets to modulate disease progression.

Astrocytes can sense many extracellular signals such as cytokines, growth factors, nucleotides, endothelins or ephrins, that activate various intracellular signaling pathways such as the Mitogen-activated Protein Kinase (MAPK), the Nuclear Factor Kappa B (NF-κB) and the Janus Kinase/Signal Transducer and Activator of Transcription (JAK/STAT) pathways (Kang and Hebert, 2011). Among them, the JAK/STAT3 pathway appears as a central player in the induction of astrocyte reactivity. It is activated by a variety of cytokines and growth factors that signal through the gp130 receptor (Aaronson and Horvath, 2002). Activation of the JAK/STAT3 pathway has been observed in reactive astrocytes in several conditions of acute injury (Justicia et al., 2000; Okada et al., 2006; Herrmann et al., 2008; O'Callaghan et al., 2014), and in patients and mouse models of amyotrophic lateral sclerosis (ALS) (Shibata et al., 2009; 2010). However, it remains to be demonstrated whether the JAK/STAT3 pathway is directly responsible for astrocyte reactivity during progressive pathological conditions such as ND.

In this study, we show that the JAK/STAT3 pathway is activated in reactive astrocytes in several mouse and non-human primate models of AD and HD. Overexpression of Suppressor of Cytokine Signaling 3 (SOCS3), the endogenous inhibitor of the JAK/STAT3 pathway in astrocytes *in vivo,* inhibited this pathway and prevented astrocyte reactivity. These results identify the JAK/STAT3 pathway as a universal and instrumental signaling cascade that triggers astrocyte reactivity in multiple progressive pathological conditions.

Materials and methods

Transgenic mouse models. Amyloid precursor protein (APP) /Presenilin 1 (PS1) mice (B6.Cg-Tg (APPswe, PSEN1dE9) 85Dbo) (http://jaxmice.jax.org/strain/005864.html) harbor the chimeric mouse/human APP gene with Swedish mutations K594N and M595L (APPswe) and the human PS1 variant lacking exon 9 on a C57BL/6J (http://jaxmice.jax.org/strain/000664.html) background (Jankowsky et al., 2004). APP/PS1dE9 breeding pairs were obtained from the Jackson Laboratory (Bar Harbor, ME). Triple transgenic AD (3xTg-AD) mice express the mutated human APPswe, PS1M146V and tauP301L transgenes on a mixed 129Sv (http://jaxmice.jax.org/strain/002448.html) and C57BL/6J background (Oddo et al., 2003). Breeding pairs of 3xTg-AD mice were obtained from the Mutant Mouse Regional Resource Centers. We used 8 month-old APP/PS1dE9 heterozygous females, 12 month-old 3xTg-AD homozygous females and their respective age-matched wild type (WT) control mice. Genotyping by PCR was performed at 4-6 weeks of age for APP/PS1dE9 mice. All experimental procedures were approved by a local ethics committee and submitted to the French Ministry of Education and Research (approval number #10-057). They were performed in strict accordance with the recommendations of the European Union (86/609/EEC) for the care and use of laboratory animals.

Lentiviral vectors and injections in mice. We used self-inactivated lentiviral vectors containing the central polypurine tract sequence, the mouse phosphoglycerate kinase I promoter and the woodchuck post-regulatory element sequence. We used two types of vectors to mediate transgene expression in either neurons or astrocytes. To target neurons, lentiviral vectors were pseudotyped with the G protein of the vesicular stomatitis virus (Naldini et al., 1996). To target astrocytes, lentiviral vectors were pseudotyped with the G protein of the mokola lyssaviruses and contained four copies of the target sequence of the neuronal miRNA124 to repress transgene expression in neurons (Colin et al., 2009). Lentiviral vectors are referred to as “lenti-name of the transgene” in the subsequent parts of the manuscript. Neuron-targeted vectors encoded the first 171 N-terminal amino acids of human huntingtin (Htt) cDNA with either 18 (lenti-Htt18Q) or 82 (lenti-Htt82Q) polyglutamine repeats (de Almeida et al., 2002). Astrocyte-targeted vectors encoded either the enhanced green fluorescent protein cDNA (lenti-GFP) or the murine SOCS3 cDNA (lenti-SOCS3) (Bjorbaek et al., 1998).

The construction, purification, and titration of these lentiviruses have been described previously (Hottinger et al., 2000). Lentiviral vectors were diluted in 0.1 M PBS with 1% BSA at a final concentration of 100 ng p24/µl. Mice were anesthetized with a mixture of ketamine (150 mg/kg) and xylazine (10 mg/kg). Lidocaine (5 mg/kg) was injected subcutaneously under the scalp 5 min before the beginning of surgery. C57BL/6J and 3xTg-AD mice received bilateral stereotaxic injections of diluted lentiviral vectors in the striatum or the subiculum respectively, administered by a 10 µl Hamilton syringe via a 28 gauge blunt needle. The stereotaxic coordinates used for the striatum were: antero-posterior (AP), + 1 mm; lateral (L), +/- 2 mm from bregma; ventral (V), -2.5 mm from the dura; and for the subiculum: AP - 2.92 mm; L +/- 1.5 mm; V - 1.5 mm with ear bars set at 4 mm and a tooth bar set at 0 mm. Mice received a total volume of 2.5 or 3.5 µl per injection site at a rate of 0.25 µl/min. At the end of the injection, the needle was left in place for 5 min before being slowly removed. The skin was sutured and mice were allowed to recover.

For the lentiviral vector-based HD model (de Almeida et al., 2002), 8 week-old male C57BL/6J mice were injected with lenti-Htt18Q (100 ng p24) and lenti-GFP (150 ng p24) in the left striatum and with lenti-Htt82Q (100 ng p24) and lenti-GFP (150 ng p24) in the right striatum.

To inhibit the JAK/STAT3 pathway in the HD model, 8 week-old male C57BL/6 mice were bilaterally injected in the striatum with lenti-Htt82Q (150 ng p24) and co-injected with the control lenti-GFP (200ng p24) in the left striatum and with lenti-SOCS3 (150 ng p24) and lenti-GFP (50 ng p24) in the right striatum. To inhibit the JAK/STAT3 pathway in the AD model, 7-8 month-old 3xTg-AD female mice were injected in the subiculum either with lenti-GFP (250 ng p24) or with lenti-SOCS3 (200 ng p24) and lenti-GFP (50 ng p24). Co-injections with lenti-GFP were performed to visualize the infected area and the morphology of infected cells because SOCS3 cannot be detected by immunohistochemistry due to the lack of specific antibodies. Post mortem analysis was performed 6 weeks post-injection for HD mice and 4.5 months post injection for 3xTg-AD mice.

Primate model of HD

Three adult male cynomolgus monkeys (*Macaca fascicularis,* 4.2 ± 0.08 kg) were used in this study according to European (EU Directive 86/609/EEC) and French regulations (French Act Rural Code R 214-87 to 131). The animal facility was approved by veterinarian inspectors (authorization n°A 92-032-

02) and complies with Standards for Humane Care and Use of Laboratory Animals of the Office of Laboratory Animal Welfare (OLAW – n°#A5826-01).

Magnetic Resonance Imaging (MRI) was performed on each macaque to calculate stereotactic coordinates for lentiviral injection. MRI was performed on a 7 Tesla scanner (Varian, CA, USA) with the following parameters: TR/ TE/ TI: 15 ms / 5500 ms / 10 ms, flip angle: 90°, 0.45×0.45×1 mm with coronal acquisition on a 256 × 256 × 40 matrix. For lentiviral injections, animals were anesthetized with a mixture of ketamine (10 mg/kg) and xylazine (1 mg/kg) and were kept under intravenous infusion of propofol (1% Rapinovet, 0.05 to 0.25 $mg.kg^{-1}.min^{-1}$) throughout the procedure with continuous monitoring of cardiac and respiratory frequencies, blood pressure and temperature. Animals were placed in a custom-made stereotaxic frame and a KDS injection micropump connected to a Hamilton syringe and a 26 gauge needle were used to perform 5 bilateral injections of 5 µl of lenti-Htt82Q at a rate of 1 µl/min. The injection sites comprised two deposits in the pre-commissural caudate (anterior commissure (AC) +5, AC +3) and three deposits in the commissural and post-commissural putamen (AC, AC -2, AC -5). Post-mortem analysis was performed 16 to 18 months later.

Immunohistochemistry. For histological processing, animals were killed with an overdose of sodium pentobarbital. Animals were either transcardially perfused with 4% paraformaldehyde (PFA) or their brains post-fixed for 24h in 4% PFA. Brains were cryoprotected by incubation in a 30% sucrose solution. Coronal brain sections (mice: 30 µm; monkey: 40 µm) were cut on a freezing microtome, collected serially and stored at - 20°C until further analysis. Antigen retrieval protocols were used for STAT3 and 4G8 staining according to the manufacturer's instructions. For STAT3 immunofluorescence, slices were permeabilized with 100% methanol at - 20°C for 20 min. For 4G8 staining, slices were pretreated in 70% formic acid for 5 min. Sections were then blocked with 4.5% normal goat serum (Sigma, Saint-Louis, MO) and incubated with primary antibodies directed against the following proteins: 4G8 (1:500, mouse, Signet Covance, Princeton, NJ), EM48 (1:200, mouse, Chemicon, Billerica, MA), GFAP-Cy3 (1:1000, mouse, Invitrogen, Carlsbad, CA), S100β (1:500, mouse, Invitrogen), STAT3 (STAT3α, 1:200, rabbit, Cell Signaling Technology, Danvers, MA), vimentin (1:1000, chicken, Abcam, Cambridge, England). Anti-STAT3 antibody was diluted in Signal Boost antibody diluent (Cell Signaling Technology). Brain sections were incubated for 36 h with STAT3 antibody and overnight at 4°C for all other antibodies. After rinsing, brain slices were incubated

for 1-2 h at room temperature with fluorescent secondary Alexa fluor®-conjugated antibodies (Invitrogen). Slices were stained with DAPI (1:2000, Sigma), mounted with FluorSave reagent (Calbiochem, La Jolla, CA) and analyzed by either epifluorescence (DM6000 Leica, Nussloch, Germany) or confocal microscopy (LSM 510; Zeiss, Thornwood, NY and TCS SPE or SP8, Leica).

qRT-PCR. Mice were killed with an overdose of sodium pentobarbital. Mouse brains were rapidly collected and sliced into 1 mm-thick coronal sections with a brain matrix. The GFP-positive (GFP^+) area on each slice was dissected with 1 mm-diameter punches (Ted Pella, CA) under a fluorescence macroscope (Leica MacroFluo, Leica). Punches were stored in RNA later (Sigma) until further processing. Total RNA was isolated from striatal punches with Trizol (Invitrogen) and cDNA was synthesized from 0.2 µg of RNA with the VILO kit (Invitrogen) and diluted at 0.15 ng/µl. The Platinum SYBR Green qPCR SuperMix UDG (Invitrogen) was used to perform qRT-PCR. Three housekeeping genes were tested and the peptidylprolyl isomerase A (*cyclophilin A*) gene was selected as the best normalizing gene, because it showed the minimal, non-significant, variation between groups. The abundance of each transcript of interest was then normalized to the abundance of *cyclophilin A* with the ΔCt method. The efficiency of qRT-PCR was between 85 and 110% for each set of primers. Distilled water and RT-negative reactions were used as negative controls. The sequences of oligonucleotides used for qRT-PCR are as follows: *ccl2* (forward: ACCAGCACCAGCCAACTCT; reverse AGGCCCAGAAGCATGACA), *cyclophilin A* (forward ATGGCAAATGCTGGACCAAA; reverse GCCTTCTTTCACCTTCCCAAA) *gfap* (forward ACGACTATCGCCGCCAACT; reverse GCCGCTCTAGGGACTCGTTC), *socs3* (forward CGAGAAGATTCCGCTGGTACTGA; reverse TGATCCAGGAACTCCCGAATG), *vimentin* (forward TCGAGGTGGAGCGGGACAAC; reverse TGCAGGGTGCTTTCGGCTTC), *iba1* (forward CCAGCCTAAGACAACCAGCGTC; reverse GCTGTATTTGGGATCATCGAGGAA).

Western blotting. Mice were killed with an overdose of sodium pentobarbital and their brains were rapidly collected and sliced into 1 mm-thick coronal sections with a brain matrix. The striatum or the dorsal hippocampus were dissected out. Samples were then homogenized with a glass homogenizer in 50 mM Tris-HCl, pH 7.4, 100 mM NaCl, 1% SDS, with protease (Roche, Indianapolis, IN) and phosphatase (Sigma) inhibitor cocktails. Protein concentration was determined by the BCA method.

Protein samples were diluted in NuPAGE LDS sample buffer with NuPAGE® Sample Reducing agent (Life technologies, Carlsbad, CA) boiled for 5 min, loaded on a 4-12% Bis-Tris gel, submitted to SDS-PAGE and transferred to a nitrocellulose membrane, with an iBlot transfer device (Life technologies). Membranes were blotted overnight at 4°C with antibodies against GAPDH (1:4000, mouse, Abcam) or IκBα (1: 500, mouse, Cell Signaling Technology) diluted in Tris Buffer saline with 0.1% Tween-20 and 5% BSA. After rinsing, secondary antibodies coupled to horseradish peroxidase were incubated with the membrane for 1 h (for IκBα: 1:500; Cell Signaling Technology and for GAPDH: 1:5000, Vector Laboratories, Burlingame, CA). Antibody binding was detected by a Fusion FX7 camera system (Fisher scientific, Whaltam, MA) after incubation with the enhanced chemiluminescence Clarity substrate (BioRad, Hercules, CA). Band intensity for IκBα were measured with Image J and normalized to GAPDH. Positive controls for NF-κB pathway activation were included. They were prepared from HeLA cells treated with TNFα (Cell Signaling Technology).

Quantification of immunostaining. Immunostaining was quantified from stacked confocal images (18 steps, Z-step: 1 µm, maximum intensity stack) acquired with the 40x objective on three slices per mouse and three fields on each slice. The $GFAP^+$ area was measured on each 40x Z-stack image with the threshold function of Image J Software (http://imagej.nih.gov/ij/, 1997-2012, Bethesda, MA). The $GFAP^+$ area was divided by the area of the image and expressed as a percentage. The average number of $GFAP^+$ cells expressing STAT3 in the nucleus ($nSTAT3^+/GFAP^+$ cells) was quantified on these images. In lenti-GFP injected mice, we also quantified the average number of GFP^+ infected astrocytes co-expressing STAT3 ($GFP^+/STAT3^+$ cells) or GFAP ($GFP^+/GFAP^+$ cells). Finally, astrocyte soma was manually segmented and the corresponding mean gray value for STAT3 staining was measured with Image J. We then determined the number of cells with a mean gray value for STAT3 over a fixed threshold for each experiment. These cells were considered as cells expressing high levels of STAT3. Unfortunately, the presence of autofluorescent puncta in the subiculum, made it impossible to quantify reliably the intensity of STAT3 staining in WT and 3xTg-AD mice. Microscope settings and Image J thresholds were identical for all images and mice, within each experiment.

Statistical analysis. Results are expressed as mean ± SEM. Statistical analysis was performed with Statview software. We used Student's t-test to compare two experimental groups and a Student's

paired t-test for left-right comparisons. The fraction of cells expressing high levels of STAT3 was normalized by the arcsine transformation, before applying a Student t-test. The results of qRT-PCR were analyzed using one-way ANOVA test and Scheffé *post-hoc* test. The significance level was set at $p < 0.05$.

Results

Astrocyte reactivity is observed in vulnerable brain regions in AD and HD mouse models

Reactive astrocytes overexpressing GFAP were found around $4G8^+$ amyloid depositions in both the APP/PS1dE9 and the 3xTg-AD transgenic mouse models of AD, consistent with previous findings (Oddo et al., 2003; Ruan et al., 2009). In particular, astrocytes overexpressed GFAP and displayed hypertrophic processes in the stratum lacunosum moleculare and the dentate gyrus of 8 month-old APP/PS1d9 mice (Fig. 1A, see also Fig. 2A, B). We quantified this phenomenon by counting the number of pixels that were positive for GFAP staining on confocal images of the hippocampus. The $GFAP^+$ area was four time larger in APP/PS1d9 mice than in WT mice ($p = 0.0010$, df = 5, n = 3-4 mice/group, Student's t-test; Fig. 1B). Astrocytes in APP/PS1dE9 mice also strongly expressed vimentin (Fig. 2B). The APP/PS1dE9 mouse is a quickly-evolving model of AD, with substantial deposits of amyloid at 6 months of age (Jankowsky et al., 2004). We thus analyzed astrocyte reactivity in 3xTg-AD mice, a more progressive model of AD. We observed astrocyte reactivity around amyloid depositions primarily in the subiculum in female 3xTg-AD mice at 12 months of age (Fig. 1C, 3). In this region, the $GFAP^+$ area was 13 fold larger in 3xTg-AD mice than in age-matched controls ($p < 0.0001$, df = 6, n = 3-5 mice/group, Student's t-test; Fig. 1D). Furthermore, astrocytes displayed a reactive morphology with enlarged soma and processes and over-expressed vimentin, which was nearly undetectable in WT mice (Fig. 3B).

We also characterized astrocyte reactivity in mouse models of HD. We studied two HD transgenic mouse models, N171-82Q mice (Schilling et al., 1999) and Hdh140 knock-in HD mice (Menalled et al., 2003). Although these models recapitulate the typical features of HD, we found that they displayed undetectable or very late astrocyte reactivity in the striatum and cortex, similar to what has been described in other mouse models (Tong et al., 2014). We thus focused on a lentiviral-based model of HD that has been extensively used (Ruiz and Deglon, 2012). This model reproduces both neuronal death and strong astrocyte reactivity that are observed in HD patients (Faideau et al., 2010). C57BL/6 mice were injected in the left striatum with a lentiviral vector encoding normal Htt with 18 glutamines (lenti-Htt18Q) and in the right striatum with a lentiviral vector encoding mutated Htt with 82 glutamines (lenti-Htt82Q). Mice were studied 6 weeks later. As described previously (Faideau et al., 2010; Galvan et al., 2012), overexpression of Htt82Q in neurons led to the formation of intraneuronal $EM48^+$ aggregates (Fig. 1E). In the lenti-Htt82Q injected striatum, astrocytes strongly up-regulated both

GFAP and vimentin, relative to the contralateral striatum injected with lenti-Htt18Q (Fig. 1E and 4A). The $GFAP^+$ area within the injected area was six times larger in the Htt82Q-side than in the Htt18Q-side ($p = 0.0098$, df = 5, n = 6 mice, Student's paired t-test; Fig. 1F).

The JAK/STAT3 pathway is activated in reactive astrocytes in AD and HD mouse models

We next evaluated whether astrocyte reactivity observed in these models was associated with activation of the JAK/STAT3 pathway.

The phosphorylated form of STAT3 (pSTAT3) was undetectable by immunofluorescence or western blotting in these progressive models of ND. Following activation, pSTAT3 translocates to the nucleus where it stimulates the transcription of a set of target genes including the *Stat3* gene itself (Campbell et al., 2014). We thus considered STAT3 nuclear localization and increased immunoreactivity as indexes of JAK/STAT3 pathway activation, as reported in previous publications (Escartin et al., 2006; Tyzack et al., 2014). This also enabled us to identify cell types displaying an active JAK/STAT3 pathway.

Interestingly, STAT3 staining was predominantly observed in astrocytes in all models. In the 8 month-old APP/PS1dE9 mice, there was an accumulation of STAT3 in the nucleus of $GFAP^+$ and $vimentin^+$ reactive astrocytes, whereas in age-matched WT mice, STAT3 was expressed at basal level throughout astrocyte cytoplasm (Fig. 2A, B). The number of $GFAP^+$ astrocytes expressing STAT3 in the nucleus ($nSTAT3^+/GFAP^+$ cells) was higher in APP/PS1dE9 mice than in age-matched WT mice ($p = 0.0235$, df = 5, n = 3-4 mice/group, Student's t-test; Fig. 2C). We also measured STAT3 immunoreactivity in astrocyte cell bodies. The percentage of cells with high STAT3 expression was more than 3 fold higher in APP/PS1dE9 mice than in WT mice, reflecting STAT3 activation in this mouse model of AD ($p = 0.0226$, df = 5, n = 3-4 mice/group, Student's t-test; Fig. 2D).

In the subiculum of 12 month-old female 3xTg-AD mice, there was also a strong increase in STAT3 immunoreactivity in the nucleus of reactive astrocytes overexpressing GFAP and vimentin, (Fig. 3A, B). The number of astrocytes co-expressing GFAP and STAT3 in the nucleus was more than 10 fold higher in 3xTg-AD mice than in age-matched WT mice ($p < 0.0001$, df = 6, n = 3-5 mice/group, Student's t-test; Fig. 3C).

We then investigated whether the JAK/STAT3 pathway was also activated in the mouse model of HD. STAT3 staining was strongly up-regulated in reactive astrocytes found in the lenti-Htt82Q-injected

striatum (Fig. 4A). Indeed, there were four time more nSTAT3^{+}/GFAP^{+} astrocytes in the Htt82Q striatum than in the Htt18Q striatum (p = 0,0004, df = 5, n = 6 mice, Student's paired t-test; Fig. 4B). Cells expressing high levels of STAT3 were also more abundant in the Htt82Q striatum than in the Htt18Q striatum (p = 0.0060, df = 5, n = 6 mice, Student's paired t-test; Fig. 4C).

We sought to evaluate whether the JAK/STAT3 pathway was also activated in reactive astrocytes in other species. We took advantage of the fact that lentiviral vectors can be used in several animal species, including non-human primates. Injection of lenti-Htt82Q in the macaque putamen leads to the formation of Htt aggregates, neuronal death and motor symptoms (Palfi et al., 2007). We found that the injection of lenti-Htt82Q into the macaque putamen induced the formation of EM48^{+} aggregates of Htt and led to strong astrocyte reactivity (Fig. 5). There was a prominent accumulation of STAT3 in the nucleus of GFAP^{+}-reactive astrocytes. In contrast, at a distance from the injection area, resting astrocytes of the same animal expressed nearly undetectable levels of both GFAP and STAT3 (Fig. 5).

These results suggest that the JAK/STAT3 pathway is a common signaling cascade for astrocyte reactivity in several models of ND, which involve different pathological mechanisms, brain regions and animal species.

The NF-κB pathway is not activated in 3xTg-AD mice and in the lentiviral-based model of HD

Other pathways such as the NF-κB have been associated with astrocyte reactivity (Kang and Hebert, 2011). Therefore, we used western blotting to measure the abundance of IκBα, the inhibitor of the NF-κKB pathway, which is degraded upon pathway activation (Hayden and Ghosh, 2008).

We performed this experiment with 3xTg-AD mice and lenti-Htt82Q injected mice, because astrocyte reactivity was the strongest in these models. In 3xTg-AD mice, the abundance of IκBα normalized to GAPDH was similar to that in WT mice (p = 0.4037, df = 8, n = 4-6 mice/group, Student's t-test; Fig. 6A), while the positive control of cells treated with the cytokine TNFα displayed the expected decrease in IκBα levels (Fig. 6A, B). Similarly, the abundance of IκBα normalized to GAPDH was not different between the Htt18Q-striatum and the Htt82Q-striatum (p = 0.8062, df = 5, n = 6 mice, Student's paired t-test; Fig. 6B).

The JAK/STAT3 pathway is responsible for astrocyte reactivity in AD and HD models

We sought to investigate directly whether the JAK/STAT3 pathway was responsible for astrocyte reactivity; therefore we inhibited this pathway by overexpressing its endogenous inhibitor SOCS3 through selective lentiviral gene transfer in astrocytes.

We used Mokola-pseudotyped lentiviral vectors that efficiently and selectively target astrocytes (Colin et al., 2009 and see Fig. 7C, 8D). We did not detect transgene expression in other brain cell types such as $NeuN^+$-neurons, $IBA1^+$-microglia, $NG2^+$-oligodendrocyte progenitors or MBP^+-myelinating oligodendrocytes (data not shown). In addition, we checked that infection of astrocytes with a control lentiviral vector (lenti-GFP) did not lead to their activation in the striatum of WT mice or in the subiculum of 3xTg-AD mice. In both models, GFAP expression was similar between lenti-GFP controls and non-injected mice (data not shown).

We detected SOCS3 overexpression by qRT-PCR following lenti-SOCS3 injection (Fig. 9A), but we were not able to show SOCS3 expression by immunohistochemistry due to the lack of specific antibodies. Therefore, for each experiment, we co-injected lenti-GFP with lenti-SOCS3 to visualize infected cells and their morphology. Indeed, we controlled that injection of two lentiviral vectors leads to a large majority of infected astrocytes co-expressing the two transgenes (88.7 ± 2 %). Control mice were injected with lenti-GFP alone, at the same total virus load.

We injected lenti-SOCS3 + lenti-GFP or lenti-GFP alone into the subiculum of 7 to 8 month-old 3xTg-AD mice and analyzed the mice 4.5 months later. We first tested whether SOCS3 overexpression in astrocytes was able to inhibit the JAK/STAT3 pathway *in situ*. SOCS3 strongly decreased STAT3 expression in astrocytes from 3xTg-AD mice (Fig. 7A). The number of GFP^+-astrocytes showing STAT3 immunoreactivity in the nucleus was significantly lower in mice co-infected with lenti-SOCS3 than in those infected with lenti-GFP alone ($p = 0.0375$, df = 6, n = 3-5 mice/group, Student's t-test; Fig. 7B). Furthermore, GFAP expression was 73% lower in the SOCS3 group than in the GFP controls, although this difference was not statistically significant ($p = 0.0827$, df = 6, n = 3-5 mice/group, Student's t-test; Fig. 7C, D). There were significantly fewer GFP^+-astrocytes co-expressing GFAP in the SOCS3 group than in the control (- 94%, $p = 0.0149$, df = 6, n = 3-5 mice/group, Student's t-test; Fig. 7E). GFP expression in infected astrocytes allowed us to visualize their morphology in both groups. Astrocytes in the subiculum of 3xTg-AD mice displayed a morphology characteristic of reactive astrocytes with enlarged soma and large $GFAP^+$ primary

processes (Fig. 7A, C). By contrast, SOCS3-infected astrocytes displayed complex ramifications composed of thin cytoplasmic processes radially organized around the soma, typical of resting astrocytes of the mouse brain (Wilhelmsson et al., 2006, Fig. 7A, C). We also performed immunostaining for S100β, a ubiquitous marker of astrocytes, to verify that SOCS3 did not globally impair protein expression in astrocytes. The abundance of S100β was similar between 3xTg-AD mice injected with lenti-SOCS3 or lenti-GFP (Fig. 7F).

We performed the same experiment with the lentiviral-based model of HD. C57BL/6 mice were injected with lenti-Htt82Q and lenti-GFP in the left striatum and with lenti-Htt82Q, lenti-SOCS3 and lenti-GFP in the right hemisphere, at the same total virus load. Again, SOCS3 efficiently prevented the activation of the JAK/STAT3 pathway in astrocytes (Fig. 8A). The number of infected cells co-expressing STAT3 was 87% lower in the striatum injected with lenti-SOCS3 than in the control striatum ($p = 0.0072$, df = 3, n = 4 mice, Student's paired t-test; Fig. 8B). In addition, the percentage of cells highly fluorescent for STAT3 was strongly reduced by SOCS3 ($p = 0.0118$, df = 3, n = 4 mice, Student's paired t-test; Fig. 8C). SOCS3-expressing astrocytes displayed a bushy morphology with thin cytoplasmic processes and numerous ramifications whereas reactive astrocytes in the control striatum showed enlarged and tortuous primary processes (Fig. 8D). Inhibition of the JAK/STAT3 pathway by SOCS3 prevented the increase of GFAP expression in the lenti-Htt82Q-injected area (Fig. 8D). The $GFAP^+$ area was 86% smaller in the striatum injected with lenti-SOCS3 than in the control striatum ($p = 0.0035$, df = 3, n = 4 mice, Student's paired t-test; Fig. 8E). In addition, the number of $GFP^+/GFAP^+$ cells was significantly decreased by SOCS3 ($p = 0.0036$, df = 3, n=4 mice, Student's paired t-test, Fig. 8F). On the contrary, the abundance of the ubiquitous astrocyte marker S100β was not altered by SOCS3 (Fig. 8G).

Activation of the JAK/STAT3 pathway results in the transcriptional activation of many genes including *gfap* and *vimentin*. Therefore, we studied the mRNA abundance of reactive astrocyte markers to characterize further the effect of SOCS3. We only used the lentiviral-based HD model, because the infected area in the subiculum of 3xTg-AD mice was too small to be dissected out for qRT-PCR analysis. The abundance of *gfap* and *vimentin* mRNA was more than 2 fold higher in the Htt82Q striatum than in the Htt18Q striatum, consistent with immunofluorescence results (Fig. 9B, C). Expression of SOCS3 in astrocytes normalized the expression of these two genes to levels comparable to controls (p = 0.0463 and 0.0138 versus Htt82Q for *gfap* and *vimentin* respectively, df =

2, n = 3-5 mice/group, ANOVA and Scheffé's test; Fig. 9B, C). We also studied the mRNA abundance of some markers of neuroinflammation. The expression of the microglial marker *iba1* and the chemokine *Ccl2* were increased 2.3 and 4.1-fold respectively by Htt82Q and reduced to Htt18Q control levels by SOCS3 (Fig. 9D, E). These results suggest that inhibition of the JAK/STAT3 pathway in reactive astrocytes restores a resting-like status to astrocytes and reduces the neuroinflammatory response.

Overall, our results identify the JAK/STAT3 pathway as a pivotal and universal signaling cascade for astrocyte reactivity in various models of ND.

Discussion

Activation of the JAK/STAT3 pathway is a universal feature of astrocyte reactivity

The JAK/STAT3 pathway is known to trigger astrocyte reactivity, which has been widely studied in models of acute injury (Sofroniew, 2009; Kang and Hebert, 2011). We aimed to decipher the role of the JAK/STAT3 pathway in astrocyte reactivity during progressive pathological conditions such as ND. The active phosphorylated form of STAT3 (pSTAT3) could not be detected by immunohistochemistry; therefore, we used increased STAT3 expression and nuclear localization as alternative indicators of pathway activation, as described previously by us and others (Escartin et al., 2006; Tyzack et al., 2014). We showed that the JAK/STAT3 pathway is activated in reactive astrocytes in mouse models of both AD and HD and in a primate model of HD. Wan *et al.* also reported the activation of this pathway in the hippocampus of AD patients, although pSTAT3 immunoreactivity was mainly found in neurons and in a few $GFAP^+$ astrocytes (Wan et al., 2010).

Importantly, the etiology of the two ND studied here is very different and involves particular vulnerable brain regions. Thus, activation of the JAK/STAT3 pathway appears to be a universal feature of astrocyte reactivity, which is conserved across animal models and multiple brain disorders, both acute and progressive. Both resting and reactive astrocytes are now considered as highly heterogeneous cells in terms of their morphological or functional features (Matyash and Kettenmann, 2010; Anderson et al., 2014). However, our results suggest that the molecular cascades triggering reactivity are in fact highly conserved between disease states, species and brain regions.

In addition to the three mouse models described in detail in this study, we examined astrocyte reactivity in two transgenic mouse models of HD: N171-82Q mice and Hdh140 mice. Both models displayed behavioral abnormalities and striatal atrophy. However, we did not observe substantial astrocyte reactivity in end-stage N171-82Q mice or before 17 months of age in Hdh140 mice. Interestingly, the JAK/STAT3 pathway was also found activated in the few reactive astrocytes of an old Hdh140 mouse. This limited astrocyte reactivity in HD transgenic mice is consistent with the literature (Tong et al., 2014), but differs greatly from what is observed in HD patients (Faideau et al., 2010). This discrepancy may be related to the absence of massive neuronal death in HD mouse models. Thus, we focused on the lentiviral-based model of HD that reproduces neuronal death in the striatum, along with strong astrocyte reactivity.

Astrocyte reactivity in ND models is mediated by STAT3

Immunohistological and biochemical techniques have shown that the JAK/STAT3 pathway is activated in reactive astrocytes in several models of acute injury (Justicia et al., 2000; Xia et al., 2002) and in ND (Shibata et al., 2010). Experiments involving pharmacological inhibitors of the JAK/STAT3 pathway later suggested that this pathway was needed for astrocyte reactivity, including in the MPTP model of PD (Sriram et al., 2004). However, the JAK/STAT3 pathway is active in all brain cells; therefore, it is possible that such inhibitors affect other cell types besides astrocytes. More recently, genetic approaches have been developed to knock-out the expression of STAT3 specifically in astrocytes with the Cre-LoxP system. STAT3 conditional knock-out strongly reduces astrocyte reactivity following acute injuries (Okada et al., 2006; Herrmann et al., 2008; Wanner et al., 2013; Tyzack et al., 2014). However, the use of a non-inducible Cre recombinase expressed under a *nestin* or *gfap* promoter, may trigger side effects, because these promoters are active during embryonic development (Alvarez-Buylla et al., 2001). By contrast, our strategy based on SOCS3 overexpression by lentiviral gene transfer results in an efficient inhibition of the JAK/STAT3 pathway specifically in astrocytes, in the adult brain. This selective approach allowed us to demonstrate that the JAK/STAT3 pathway is responsible for astrocyte reactivity in two models of ND.

In agreement with these findings, we observed no evidence for an activation of the NF-κB pathway in these models. This pathway is associated with astrocyte reactivity in acute disorders such as spinal cord and peripheral nerve injury (Kang and Hebert, 2011). In AD and HD, the NF-κB pathway is altered in neurons (Granic et al., 2009; Khoshnan and Patterson, 2011); but is activated in the peripheral immune cells of HD patients (Trager et al., 2014), and in astrocytes in mouse models of both diseases (Hsiao et al., 2013; Medeiros and LaFerla, 2013). However, the specific requirement of this pathway for the establishment of reactivity in astrocytes has not been tested in these ND. Frakes *et al.,* reported that the NF-κB pathway is activated mainly in microglial cells in the SOD^{G93A} mouse model of ALS (Frakes et al., 2014). Indeed, inhibition of the NF-κB pathway in astrocytes reduced their reactivity very moderately and only transiently (Crosio et al., 2011). In both studies, inhibition of the NF-κB pathway in astrocytes did not influence disease phenotype, further suggesting that this pathway does not play a major role in reactive astrocytes during ND.

There are multiple levels of crosstalk between the NF-κB and the JAK/STAT3 pathways (Fan et al., 2013); therefore, it is possible that the NF-κB pathway secondarily activates the JAK/STAT3 pathway

or that STAT3 inhibits the NF-κB pathway (Yu et al., 2002). Although other signaling pathways may be active in astrocytes or in other cell types during the disease, our experiments based on the specific inhibition by SOCS3, show that the JAK/STAT3 pathway is ultimately responsible for triggering astrocyte reactivity in these ND.

Viral vectors are versatile tools; therefore, our approach based on a lentiviral vector encoding an inhibitor of the JAK/STAT3 pathway could be easily extended to any animal model of brain disease, including those affecting different brain regions. However, one limitation is that lentiviral vectors transduce a small volume of brain cells, especially in the subiculum, preventing qRT-PCR or biochemical analysis by western blotting.

What are the effects of STAT3-mediated astrocyte reactivity?

The JAK/STAT3 pathway is a central intracellular cascade involved in the regulation of cell proliferation and survival both in the developing and adult brain (Campbell, 2005; Nicolas et al., 2013). In addition, it plays a key role in astrogliogenesis (He et al., 2005), and it participates in the regulation of synaptic plasticity and receptor signaling in neurons (Nicolas et al., 2013). What are the consequences of the activation of this highly conserved signaling pathway within astrocytes in the adult brain? Activation of the JAK/STAT3 pathway induces the expression of proteins of the cytoskeleton such as GFAP and vimentin, but it may also trigger profound changes in transcription, as shown in astrocyte cultures after exposure to pro-inflammatory signals (Hamby et al., 2012). In addition, activation of the JAK/STAT3 pathway in astrocytes by the cytokine CNTF enhances glutamate buffering and promotes metabolic plasticity in the rat brain (Escartin et al., 2006; 2007), suggesting that STAT3-induced astrocyte reactivity triggers an adaptive and beneficial response. This is in accordance with experiments showing that loss of STAT3 in astrocytes is associated with poor outcome following acute brain injury (Okada et al., 2006; Herrmann et al., 2008). Reactive astrocytes may also release several signaling molecules (e.g. cytokines, chemokines, gliotransmitters and reactive oxygen species) that affect neighboring cells such as neurons and microglial cells (Burda and Sofroniew, 2014). Indeed, we found an increased expression of neuroinflammation markers in the lenti-based model of HD, which was restored to basal levels by SOCS3. This observation suggests that reactive astrocytes are responsible for microglial activation in this model and illustrates the complex dialogue occurring between glial cells in ND.

Our study extends previous findings obtained in acute models of brain injury (trauma, spinal cord injury, ischemia, infection), and suggests that the JAK/STAT3 pathway is a universal signaling cascade, involved in almost all pathological situations in brain, both acute and progressive. Therefore, manipulation of the JAK/STAT3 pathway seems to be a very promising strategy to study the functional features of reactive astrocyte as well as the contribution of these cells to disease progression, particularly in the context of ND.

Figure legends

Figure 1. Mouse models of AD and HD display astrocyte reactivity in vulnerable regions of the brain.

A-C, Images of brain sections from mouse models of AD showing double staining for amyloid plaques (4G8, green) and astrocytes (GFAP, red). **A,** GFAP is strongly expressed in hippocampal astrocytes of 8-month-old APP/PS1dE9 mice around amyloid depositions (arrowheads) in the stratum lacunosum moleculare and the dentate gyrus. **B,** Quantification of the $GFAP^+$ area in the hippocampus of APP/PS1dE9 and WT mice. **C,** In the subiculum, 3xTg-AD mice display amyloid depositions that are surrounded by $GFAP^+$ reactive astrocytes (arrowheads). **D,** Quantification of the $GFAP^+$ area in the subiculum of 12-month-old 3xTg-AD mice and age-matched WT mice. **E,** Mice injected with lenti-Htt82Q in the striatum display $EM48^+$ aggregates of mutated Htt (green). Expression of the mutated Htt in striatal neurons leads to astrocyte reactivity (arrowheads) as shown by increased GFAP and vimentin staining (red). **F,** Quantification of the $GFAP^+$ area in the lenti-Htt82Q-injected striatum relative to the control striatum injected with lenti-Htt18Q.

N = 3-6/ group. ** $p < 0.01$; *** $p < 0.001$. Scale bars: 100 µm and 20 µm.

Figure 2. The JAK/STAT3 pathway is activated in reactive astrocytes in APP/PS1dE9 mice.

A-B, Images of brain sections from 8-month-old APP/PS1dE9 mice showing double staining for STAT3 (green) and reactive astrocyte markers (**A**: GFAP, **B**: vimentin). **A-B,** APP/PS1dE9 mice display reactive astrocytes that over-express GFAP, vimentin and STAT3, around amyloid plaques (arrowhead) in the hippocampus. STAT3 accumulates in the nucleus of reactive astrocytes (see enlargement). **C,** The number of $GFAP^+$ astrocytes co-expressing STAT3 in the nucleus ($nSTAT3^+/GFAP^+$ cells) is significantly higher in APP/PS1dE9 mice than in WT mice. **D,** The percentage of cells showing strong staining for STAT3 is higher in APP/PS1dE9 mice than in WT mice. N = 3-4/ group. * $p < 0.05$. Scale bars: 20 µm and 5 µm.

Figure 3. The JAK/STAT3 pathway is activated in reactive astrocytes in 3xTg-AD mice.

A-B, Images of brain sections from the subiculum of 12-month-old 3xTg-AD mice. STAT3 (green) accumulates in the nucleus of reactive astrocytes labeled with GFAP (**A**, red) or vimentin (**B**, red),

especially around amyloid plaques (arrowheads). **C,** The number of nSTAT3$^+$/GFAP$^+$ cells is significantly higher in 3xTg-AD mice than in age-matched WT controls. N = 3-5/ group. *** $p < 0.001$. Scale bars: 20 µm and 5 µm.

Figure 4. The JAK/STAT3 pathway is activated in reactive astrocytes in the mouse model of HD.

A, Images of brain sections showing double staining for GFAP (red) and STAT3 (green) on mouse brain sections, 6 weeks after the infection of striatal neurons with lenti-Htt18Q or lenti-Htt82Q. Astrocytes in the Htt82Q striatum are hypertrophic and express higher levels of STAT3 in their nucleus relative to resting astrocytes in the Htt18Q striatum. **B-C,** The number of nSTAT3$^+$/GFAP$^+$ cells (**B**) and the percentage of cells displaying strong staining for STAT3 (**C**) are significantly higher in the Htt82Q striatum than in the Htt18Q striatum. N = 6. * $p < 0.05$. Scale bars: 20 µm and 5 µm.

Figure 5. The JAK/STAT3 pathway is activated in reactive astrocytes in the primate model of HD.

A, Images of brain sections from macaques injected with lenti-Htt82Q in the putamen showing triple staining for STAT3 (green), GFAP (red) and EM48 (magenta). Seventeen months after infection with lenti-Htt82Q, EM48$^+$ aggregates of Htt are observed in the putamen, as well as prominent astrocyte reactivity. The immunoreactivity for STAT3 is much stronger in GFAP$^+$ reactive astrocytes than in resting astrocytes found outside the injected area in the same animal. Images are representative of all three macaques. Scale bars: 40 µm and 10 µm.

Figure 6. The NF-κB pathway is not activated in 3xTg-AD mice and the lentiviral-based model of HD

Western blot for IκBα and GAPDH in (**A**) 3xTg-Ad mice (3xTg) or their age-matched WT controls (WT) or (**B**) mice injected in the left striatum with lenti-Htt18Q (18Q) and in the right striatum with lenti-Htt82Q (82Q). IκBα expression is similar between 3xTg-AD mice and WT mice and between the left and right striatum of mice injected with lenti-Htt. The abundance of IκBα is lower in HeLA cells treated with TNFα (positive control, +) than in untreated cells (negative control, -). N = 4-6 mice/group.

Figure 7. The JAK/STAT3 pathway is responsible for astrocyte reactivity in 3xTg-AD mice.

A, Images of double staining for GFP (green) and STAT3 (red) in 7-8 month-old 3xTg-AD mice injected in the subiculum with lenti-GFP or lenti-SOCS3 + lenti-GFP (same total virus load). STAT3 expression becomes undetectable in astrocytes infected with lenti-SOCS3. **B,** The number of GFP^+ astrocytes co-expressing STAT3 in the nucleus (GFP^+/$nSTAT3^+$ cells) is significantly lower in the SOCS3 group than in the GFP control group. **C,** Images of GFP (green) and GFAP (red) staining in brain sections from 3xTg-AD mice injected with lenti-GFP or lenti-SOCS3 + lenti-GFP in the hippocampus. Lenti-SOCS3 injection strongly reduces GFAP expression in the injected area (delimited by white dots), in 3xTg-AD mice. Note that infected astrocytes in the SOCS3 group have a bushy morphology typical of resting astrocytes, whereas cells in the GFP group are hypertrophic with enlarged primary processes. **D,** Quantification of the $GFAP^+$ area in 3xTg-AD mice injected with lenti-SOCS3 + lenti-GFP or lenti-GFP alone. **E,** The number of GFP^+ astrocytes co-expressing GFAP is significantly lower in the SOCS3 group than in the GFP control group. **F,** Immunofluorescent labeling for the astrocyte marker S100β shows that its expression is not altered by SOCS3. N = 3-5/ group. * $p < 0.05$. Scale bars: 500 µm, 20 µm. Infected astrocytes in both groups are identified by their expression of GFP.

Figure 8. The JAK/STAT3 pathway is responsible for astrocyte reactivity in the lentiviral-based mouse model of HD.

A, Immunofluorescent staining of GFP (green) and STAT3 (red) in mice injected in the right striatum with lenti-Htt82Q + lenti-GFP and the left striatum with lenti-Htt82Q + lenti-SOCS3 + lenti-GFP. STAT3 expression becomes undetectable in astrocytes infected with lenti-SOCS3. **B-C,** The number of GFP^+/$nSTAT3^+$ astrocytes (**B**) and the percentage of cells showing strong staining for STAT3 (**C**) is significantly lower in the right striatum injected with lenti-SOCS3 than in the control striatum. **D,** SOCS3 expression strongly reduces GFAP expression (red) in the injected area (GFP^+, green). Infected astrocytes in the SOCS3 group display thin processes and complex ramifications, unlike hypertrophic reactive astrocytes in the control group. **E,** Quantification confirms that the $GFAP^+$ area is significantly smaller in the striatum injected with lenti-SOCS3 than in the control striatum. **F,** The number of GFP^+ astrocytes co-expressing GFAP is significantly higher in the striatum expressing

SOCS3 than in the control striatum. **G,** Immunofluorescent staining for the astrocyte marker S100β (red). N = 4. * $p < 0.05$; ** $p < 0.01$. Scale bars: 500 µm and 20 µm.

Figure 9. SOCS3 normalizes the expression of markers of astrocyte reactivity and neuroinflammation.

qRT-PCR analysis on mice injected in the striatum with lenti-Htt18Q + lenti-GFP; lenti-Htt82Q + lenti-GFP; or lenti-Htt82Q + lenti-SOCS3 + lenti-GFP (same total virus load). **A,** *Socs3* mRNA is overexpressed after lenti-SOCS3 injection. The expression of *gfap* (**B**)**,** *vimentin* (**C**), *iba1* (**D**) and *ccl2* (**E**) is induced by lenti-Htt82Q and is restored to levels observed in the Htt18Q control by the expression of SOCS3. N = 3-5/group. * $p < 0.05$, ** $p < 0.01$; *** $p < 0.001$.

References

Aaronson DS, Horvath CM (2002) A road map for those who don't know JAK-STAT. Science 296:1653-1655.

Alvarez-Buylla A, Garcia-Verdugo JM, Tramontin AD (2001) A unified hypothesis on the lineage of neural stem cells. Nature reviews Neuroscience 2:287-293.

Anderson MA, Ao Y, Sofroniew MV (2014) Heterogeneity of reactive astrocytes. Neurosci Lett 565:23-29.

Bjorbaek C, Elmquist JK, Frantz JD, Shoelson SE, Flier JS (1998) Identification of SOCS-3 as a potential mediator of central leptin resistance. Molecular cell 1:619-625.

Burda JE, Sofroniew MV (2014) Reactive gliosis and the multicellular response to CNS damage and disease. Neuron 81:229-248.

Campbell IL (2005) Cytokine-mediated inflammation, tumorigenesis, and disease-associated JAK/STAT/SOCS signaling circuits in the CNS. Brain research Brain research reviews 48:166-177.

Campbell IL, Erta M, Lim SL, Frausto R, May U, Rose-John S, Scheller J, Hidalgo J (2014) Trans-signaling is a dominant mechanism for the pathogenic actions of interleukin-6 in the brain. The Journal of neuroscience : the official journal of the Society for Neuroscience 34:2503-2513.

Colin A, Faideau M, Dufour N, Auregan G, Hassig R, Andrieu T, Brouillet E, Hantraye P, Bonvento G, Deglon N (2009) Engineered lentiviral vector targeting astrocytes in vivo. Glia 57:667-679.

Crosio C, Valle C, Casciati A, Iaccarino C, Carri MT (2011) Astroglial inhibition of NF-kappaB does not ameliorate disease onset and progression in a mouse model for amyotrophic lateral sclerosis (ALS). PloS one 6:e17187.

de Almeida LP, Ross CA, Zala D, Aebischer P, Deglon N (2002) Lentiviral-mediated delivery of mutant huntingtin in the striatum of rats induces a selective neuropathology modulated by polyglutamine repeat size, huntingtin expression levels, and protein length. J Neurosci 22:3473-3483.

Escartin C, Bonvento G (2008) Targeted activation of astrocytes: a potential neuroprotective strategy. Mol Neurobiol 38:231-241.

Escartin C, Brouillet E, Gubellini P, Trioulier Y, Jacquard C, Smadja C, Knott GW, Kerkerian-Le Goff L, Deglon N, Hantraye P, Bonvento G (2006) Ciliary neurotrophic factor activates astrocytes,

redistributes their glutamate transporters GLAST and GLT-1 to raft microdomains, and improves glutamate handling in vivo. J Neurosci 26:5978-5989.

Escartin C, Pierre K, Colin A, Brouillet E, Delzescaux T, Guillermier M, Dhenain M, Déglon N, Hantraye P, Pellerin L, Bonvento G (2007) CNTF-activated astrocytes display metabolic plasticity and increased resistance to metabolic insults. In: Society for Neuroscience. San Diego, CA, USA.

Faideau M, Kim J, Cormier K, Gilmore R, Welch M, Auregan G, Dufour N, Guillermier M, Brouillet E, Hantraye P, Deglon N, Ferrante RJ, Bonvento G (2010) In vivo expression of polyglutamine-expanded huntingtin by mouse striatal astrocytes impairs glutamate transport: a correlation with Huntington's disease subjects. Human molecular genetics 19:3053-3067.

Fan Y, Mao R, Yang J (2013) NF-kappaB and STAT3 signaling pathways collaboratively link inflammation to cancer. Protein & cell 4:176-185.

Frakes AE, Ferraiuolo L, Haidet-Phillips AM, Schmelzer L, Braun L, Miranda CJ, Ladner KJ, Bevan AK, Foust KD, Godbout JP, Popovich PG, Guttridge DC, Kaspar BK (2014) Microglia induce motor neuron death via the classical NF-kappaB pathway in amyotrophic lateral sclerosis. Neuron 81:1009-1023.

Galvan L, Lepejova N, Gaillard MC, Malgorn C, Guillermier M, Houitte D, Bonvento G, Petit F, Dufour N, Hery P, Gerard M, Elalouf JM, Deglon N, Brouillet E, de Chaldee M (2012) Capucin does not modify the toxicity of a mutant Huntingtin fragment in vivo. Neurobiology of aging 33:1845 e1845-1846.

Granic I, Dolga AM, Nijholt IM, van Dijk G, Eisel UL (2009) Inflammation and NF-kappaB in Alzheimer's disease and diabetes. Journal of Alzheimer's disease : JAD 16:809-821.

Hamby ME, Sofroniew MV (2010) Reactive astrocytes as therapeutic targets for CNS disorders. Neurotherapeutics 7:494-506.

Hamby ME, Coppola G, Ao Y, Geschwind DH, Khakh BS, Sofroniew MV (2012) Inflammatory mediators alter the astrocyte transcriptome and calcium signaling elicited by multiple g-protein-coupled receptors. J Neurosci 32:14489-14510.

Hayden MS, Ghosh S (2008) Shared principles in NF-kappaB signaling. Cell 132:344-362.

He F, Ge W, Martinowich K, Becker-Catania S, Coskun V, Zhu W, Wu H, Castro D, Guillemot F, Fan G, de Vellis J, Sun YE (2005) A positive autoregulatory loop of Jak-STAT signaling controls the onset of astrogliogenesis. Nat Neurosci 8:616-625.

Herrmann JE, Imura T, Song B, Qi J, Ao Y, Nguyen TK, Korsak RA, Takeda K, Akira S, Sofroniew MV (2008) STAT3 is a critical regulator of astrogliosis and scar formation after spinal cord injury. J Neurosci 28:7231-7243.

Hottinger AF, Azzouz M, Deglon N, Aebischer P, Zurn AD (2000) Complete and long-term rescue of lesioned adult motoneurons by lentiviral-mediated expression of glial cell line-derived neurotrophic factor in the facial nucleus. J Neurosci 20:5587-5593.

Hsiao HY, Chen YC, Chen HM, Tu PH, Chern Y (2013) A critical role of astrocyte-mediated nuclear factor-kappaB-dependent inflammation in Huntington's disease. Human molecular genetics 22:1826-1842.

Itagaki S, McGeer PL, Akiyama H, Zhu S, Selkoe D (1989) Relationship of microglia and astrocytes to amyloid deposits of Alzheimer disease. J Neuroimmunol 24:173-182.

Jankowsky JL, Fadale DJ, Anderson J, Xu GM, Gonzales V, Jenkins NA, Copeland NG, Lee MK, Younkin LH, Wagner SL, Younkin SG, Borchelt DR (2004) Mutant presenilins specifically elevate the levels of the 42 residue beta-amyloid peptide in vivo: evidence for augmentation of a 42-specific gamma secretase. Hum Mol Genet 13:159-170.

Justicia C, Gabriel C, Planas AM (2000) Activation of the JAK/STAT pathway following transient focal cerebral ischemia: signaling through Jak1 and Stat3 in astrocytes. Glia 30:253-270.

Kang W, Hebert JM (2011) Signaling pathways in reactive astrocytes, a genetic perspective. Mol Neurobiol 43:147-154.

Khoshnan A, Patterson PH (2011) The role of IkappaB kinase complex in the neurobiology of Huntington's disease. Neurobiology of disease 43:305-311.

Matyash V, Kettenmann H (2010) Heterogeneity in astrocyte morphology and physiology. Brain Res Rev 63:2-10.

Medeiros R, LaFerla FM (2013) Astrocytes: conductors of the Alzheimer disease neuroinflammatory symphony. Exp Neurol 239:133-138.

690 Menalled LB, Sison JD, Dragatsis I, Zeitlin S, Chesselet MF (2003) Time course of early motor and
691 neuropathological anomalies in a knock-in mouse model of Huntington's disease with 140
692 CAG repeats. J Comp Neurol 465:11-26.
693 Naldini L, Blomer U, Gallay P, Ory D, Mulligan R, Gage FH, Verma IM, Trono D (1996) In vivo gene
694 delivery and stable transduction of nondividing cells by a lentiviral vector. Science 272:263-
695 267.
696 Nicolas CS, Amici M, Bortolotto ZA, Doherty A, Csaba Z, Fafouri A, Dournaud P, Gressens P,
697 Collingridge GL, Peineau S (2013) The role of JAK-STAT signaling within the CNS. Jak-Stat
698 2:e22925.
699 O'Callaghan JP, Kelly KA, VanGilder RL, Sofroniew MV, Miller DB (2014) Early Activation of STAT3
700 Regulates Reactive Astrogliosis Induced by Diverse Forms of Neurotoxicity. PloS one
701 9:e102003.
702 Oddo S, Caccamo A, Shepherd JD, Murphy MP, Golde TE, Kayed R, Metherate R, Mattson MP,
703 Akbari Y, LaFerla FM (2003) Triple-transgenic model of Alzheimer's disease with plaques and
704 tangles: intracellular Abeta and synaptic dysfunction. Neuron 39:409-421.
705 Okada S, Nakamura M, Katoh H, Miyao T, Shimazaki T, Ishii K, Yamane J, Yoshimura A, Iwamoto Y,
706 Toyama Y, Okano H (2006) Conditional ablation of Stat3 or Socs3 discloses a dual role for
707 reactive astrocytes after spinal cord injury. Nat Med 12:829-834.
708 Palfi S, Brouillet E, Jarraya B, Bloch J, Jan C, Shin M, Conde F, Li XJ, Aebischer P, Hantraye P,
709 Deglon N (2007) Expression of mutated huntingtin fragment in the putamen is sufficient to
710 produce abnormal movement in non-human primates. Molecular therapy : the journal of the
711 American Society of Gene Therapy 15:1444-1451.
712 Probst A, Ulrich J, Heitz PU (1982) Senile dementia of Alzheimer type: astroglial reaction to
713 extracellular neurofibrillary tangles in the hippocampus. An immunocytochemical and electron-
714 microscopic study. Acta Neuropathol 57:75-79.
715 Ruan L, Kang Z, Pei G, Le Y (2009) Amyloid deposition and inflammation in APPswe/PS1dE9 mouse
716 model of Alzheimer's disease. Current Alzheimer research 6:531-540.
717 Ruiz M, Deglon N (2012) Viral-mediated overexpression of mutant huntingtin to model HD in various
718 species. Neurobiology of disease 48:202-211.

719 Schilling G, Becher MW, Sharp AH, Jinnah HA, Duan K, Kotzuk JA, Slunt HH, Ratovitski T, Cooper
720 JK, Jenkins NA, Copeland NG, Price DL, Ross CA, Borchelt DR (1999) Intranuclear inclusions
721 and neuritic aggregates in transgenic mice expressing a mutant N-terminal fragment of
722 huntingtin. Hum Mol Genet 8:397-407.
723 Shibata N, Yamamoto T, Hiroi A, Omi Y, Kato Y, Kobayashi M (2010) Activation of STAT3 and
724 inhibitory effects of pioglitazone on STAT3 activity in a mouse model of SOD1-mutated
725 amyotrophic lateral sclerosis. Neuropathology : official journal of the Japanese Society of
726 Neuropathology 30:353-360.
727 Shibata N, Kakita A, Takahashi H, Ihara Y, Nobukuni K, Fujimura H, Sakoda S, Sasaki S, Iwata M,
728 Morikawa S, Hirano A, Kobayashi M (2009) Activation of signal transducer and activator of
729 transcription-3 in the spinal cord of sporadic amyotrophic lateral sclerosis patients. Neuro-
730 degenerative diseases 6:118-126.
731 Sofroniew MV (2009) Molecular dissection of reactive astrogliosis and glial scar formation. Trends
732 Neurosci 32:638-647.
733 Sofroniew MV, Vinters HV (2010) Astrocytes: biology and pathology. Acta Neuropathol 119:7-35.
734 Sriram K, Benkovic SA, Hebert MA, Miller DB, O'Callaghan JP (2004) Induction of gp130-related
735 cytokines and activation of JAK2/STAT3 pathway in astrocytes precedes up-regulation of glial
736 fibrillary acidic protein in the 1-methyl-4-phenyl-1,2,3,6-tetrahydropyridine model of
737 neurodegeneration: key signaling pathway for astrogliosis in vivo? J Biol Chem 279:19936-
738 19947.
739 Tong X, Ao Y, Faas GC, Nwaobi SE, Xu J, Haustein MD, Anderson MA, Mody I, Olsen ML, Sofroniew
740 MV, Khakh BS (2014) Astrocyte Kir4.1 ion channel deficits contribute to neuronal dysfunction
741 in Huntington's disease model mice. Nat Neurosci 17:694-703.
742 Trager U, Andre R, Lahiri N, Magnusson-Lind A, Weiss A, Grueninger S, McKinnon C, Sirinathsinghji
743 E, Kahlon S, Pfister EL, Moser R, Hummerich H, Antoniou M, Bates GP, Luthi-Carter R,
744 Lowdell MW, Bjorkqvist M, Ostroff GR, Aronin N, Tabrizi SJ (2014) HTT-lowering reverses
745 Huntington's disease immune dysfunction caused by NFkappaB pathway dysregulation. Brain
746 : a journal of neurology 137:819-833.
747 Tyzack GE, Sitnikov S, Barson D, Adams-Carr KL, Lau NK, Kwok JC, Zhao C, Franklin RJ, Karadottir
748 RT, Fawcett JW, Lakatos A (2014) Astrocyte response to motor neuron injury promotes

structural synaptic plasticity via STAT3-regulated TSP-1 expression. Nature communications 5:4294.

Vonsattel JP, Myers RH, Stevens TJ, Ferrante RJ, Bird ED, Richardson EP, Jr. (1985) Neuropathological classification of Huntington's disease. J Neuropathol Exp Neurol 44:559-577.

Wan J, Fu AK, Ip FC, Ng HK, Hugon J, Page G, Wang JH, Lai KO, Wu Z, Ip NY (2010) Tyk2/STAT3 signaling mediates beta-amyloid-induced neuronal cell death: implications in Alzheimer's disease. The Journal of neuroscience : the official journal of the Society for Neuroscience 30:6873-6881.

Wanner IB, Anderson MA, Song B, Levine J, Fernandez A, Gray-Thompson Z, Ao Y, Sofroniew MV (2013) Glial scar borders are formed by newly proliferated, elongated astrocytes that interact to corral inflammatory and fibrotic cells via STAT3-dependent mechanisms after spinal cord injury. The Journal of neuroscience : the official journal of the Society for Neuroscience 33:12870-12886.

Wilhelmsson U, Bushong EA, Price DL, Smarr BL, Phung V, Terada M, Ellisman MH, Pekny M (2006) Redefining the concept of reactive astrocytes as cells that remain within their unique domains upon reaction to injury. Proc Natl Acad Sci U S A 103:17513-17518.

Xia XG, Hofmann HD, Deller T, Kirsch M (2002) Induction of STAT3 signaling in activated astrocytes and sprouting septal neurons following entorhinal cortex lesion in adult rats. Mol Cell Neurosci 21:379-392.

Yu Z, Zhang W, Kone BC (2002) Signal transducers and activators of transcription 3 (STAT3) inhibits transcription of the inducible nitric oxide synthase gene by interacting with nuclear factor kappaB. Biochem J 367:97-105.

Yu ZX, Li SH, Evans J, Pillarisetti A, Li H, Li XJ (2003) Mutant huntingtin causes context-dependent neurodegeneration in mice with Huntington's disease. J Neurosci 23:2193-2202.

Figure 1

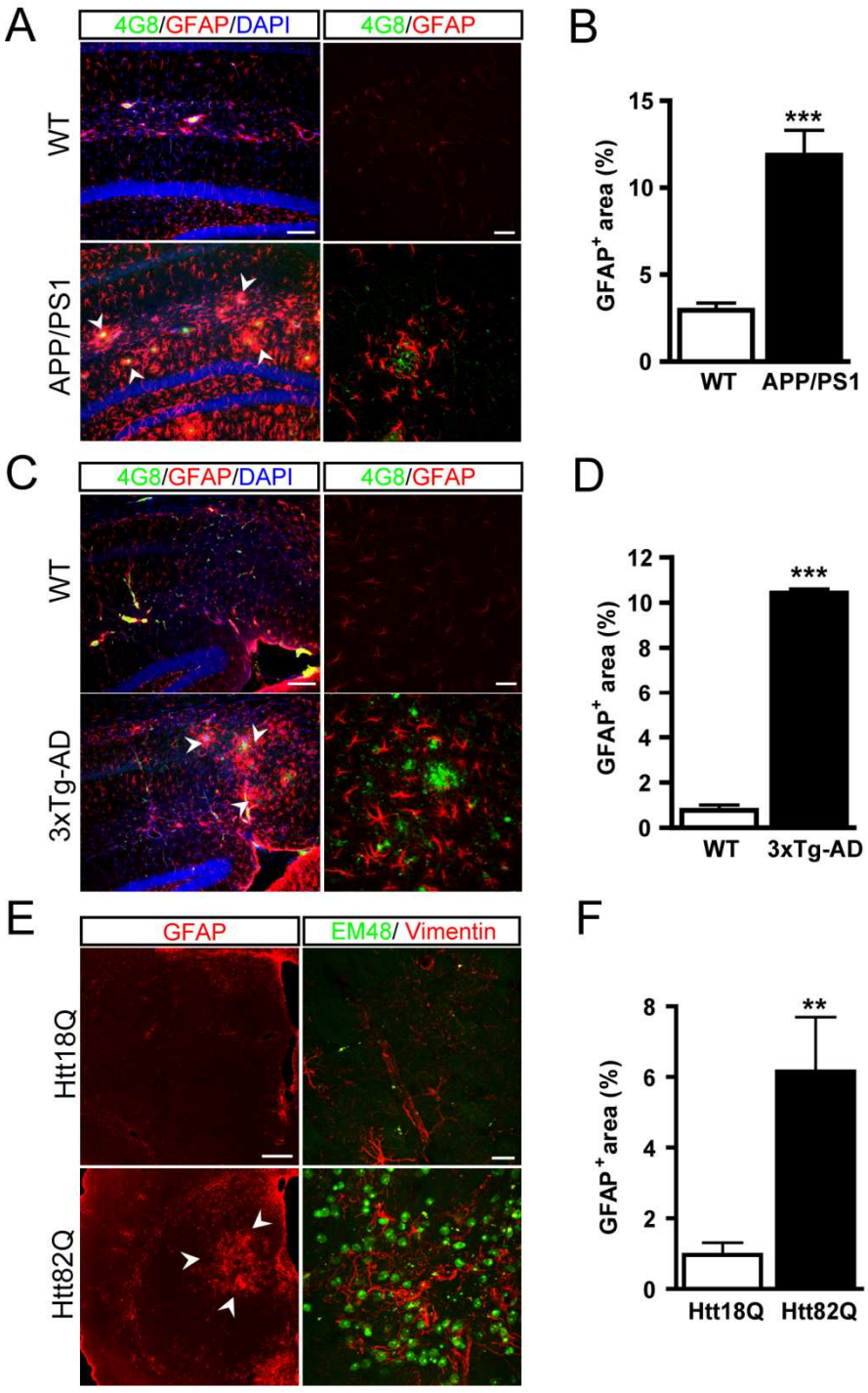
A
4G8/GFAP/DAPI
4G8/GFAP
WT
APP/PS1
B
GFAP+ area (%)
15
10
5
0
***
WT
APP/PS1
C
4G8/GFAP/DAPI
4G8/GFAP
WT
3xTg-AD
D
GFAP+ area (%)
12
10
8
6
4
2
0
***
WT
3xTg-AD
E
GFAP
EM48/ Vimentin
Htt18Q
Htt82Q
F
GFAP+ area (%)
8
6
4
2
0
**
Htt18Q
Htt82Q

Figure 2

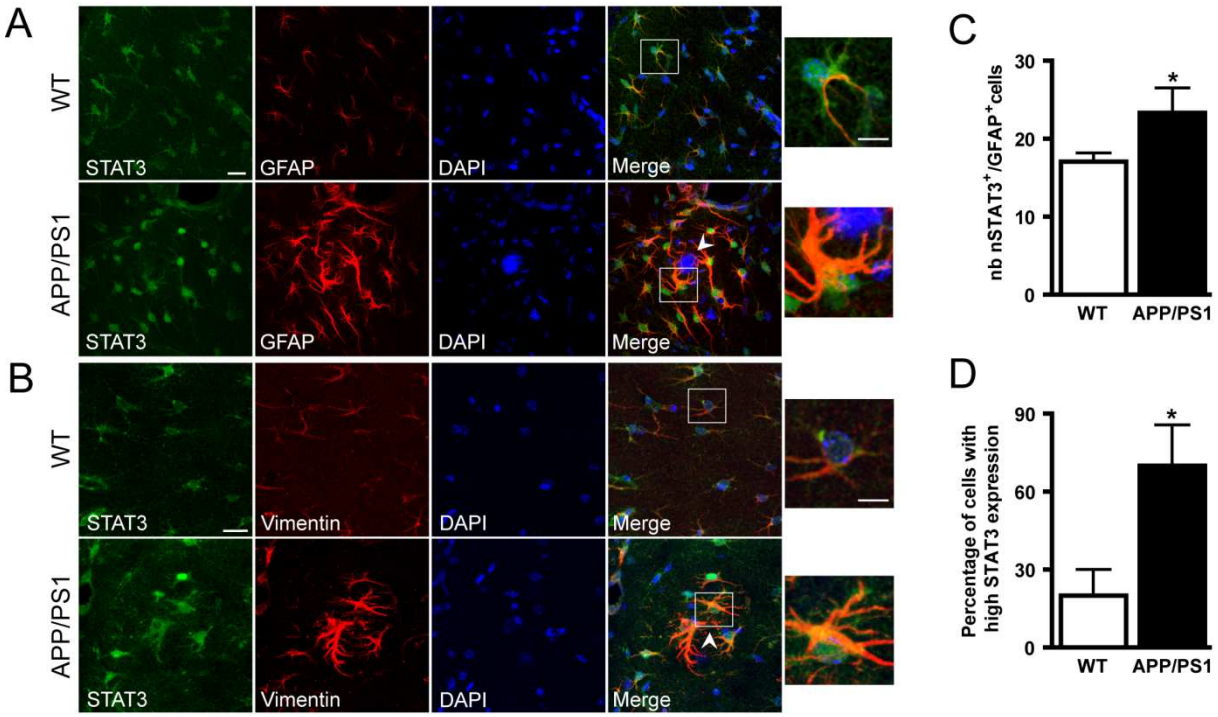
A
WT
APP/PS1
STAT3
GFAP
DAPI
Merge
B
Vimentin
C
nb nSTAT3+/GFAP+cells
30
20
10
0
WT
APP/PS1
*
D
Percentage of cells with high STAT3 expression
90
60
30
0

Figure 3

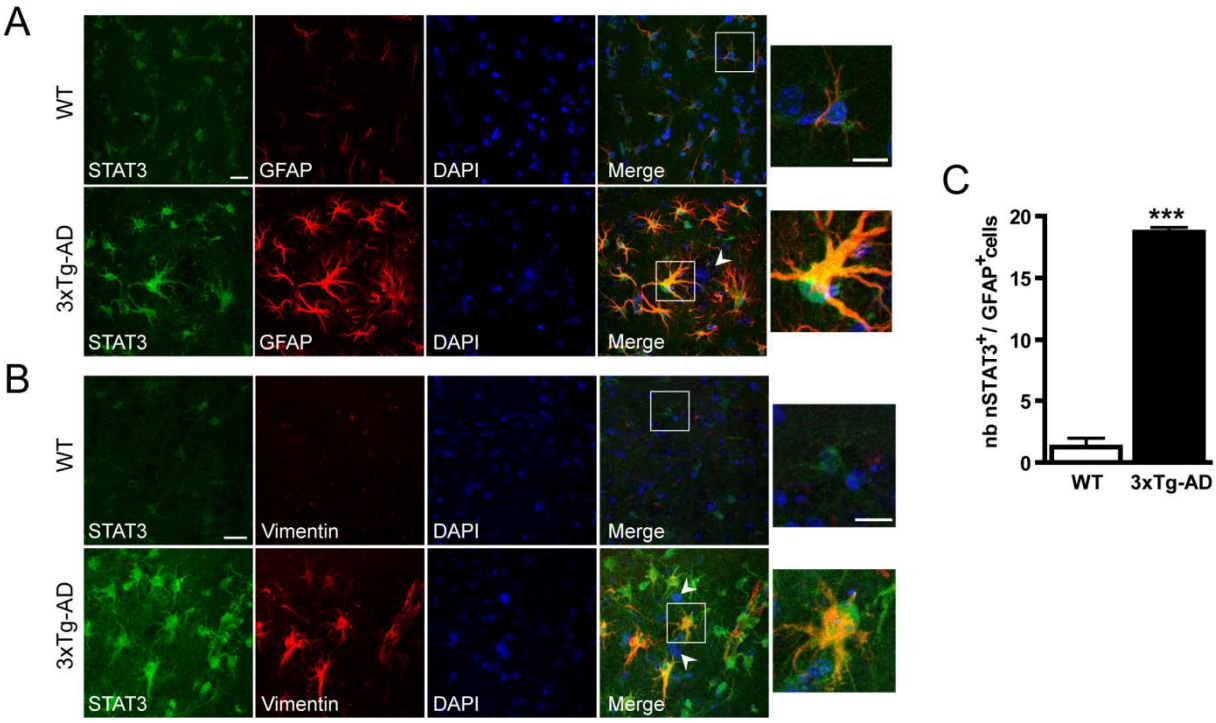
A
WT
3xTg-AD
STAT3
GFAP
DAPI
Merge
B
Vimentin
C
nb nSTAT3+/ GFAP+cells
20
15
10
5
0
***
WT
3xTg-AD

Figure 4

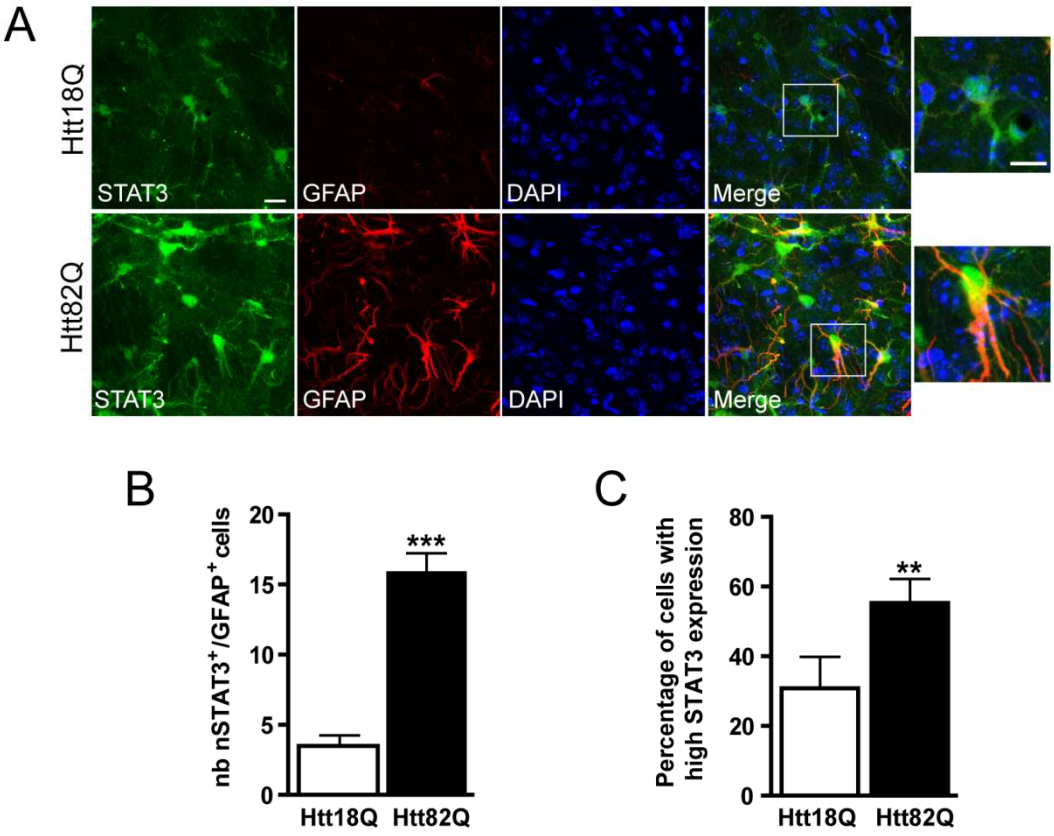
A
Htt18Q
Htt82Q
STAT3
GFAP
DAPI
Merge
B
nb nSTAT3+/GFAP+ cells
20
15
10
5
0
***
Htt18Q
Htt82Q
C
Percentage of cells with high STAT3 expression
80
60
40
20
0
**
Htt18Q
Htt82Q

Figure 5

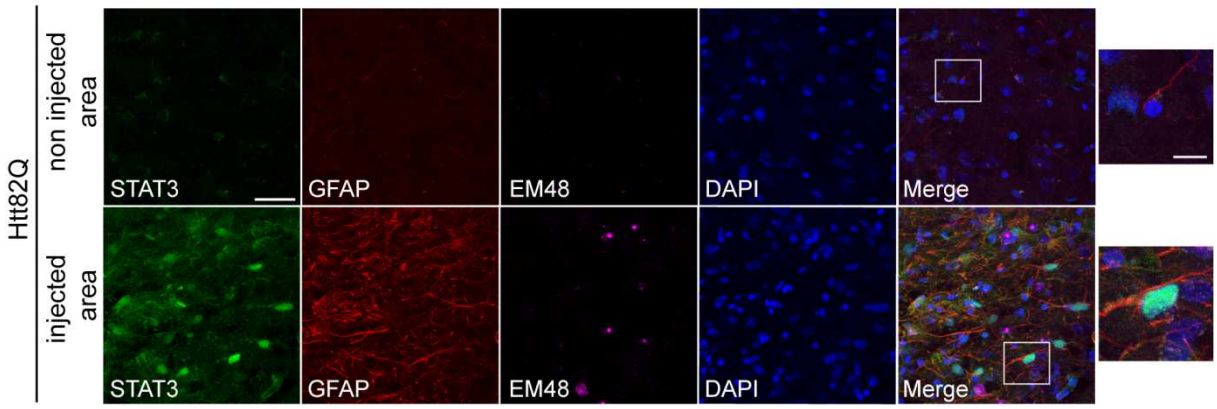
Htt82Q
non injected area
injected area
STAT3
GFAP
EM48
DAPI
Merge
STAT3
GFAP
EM48
DAPI
Merge

Figure 6

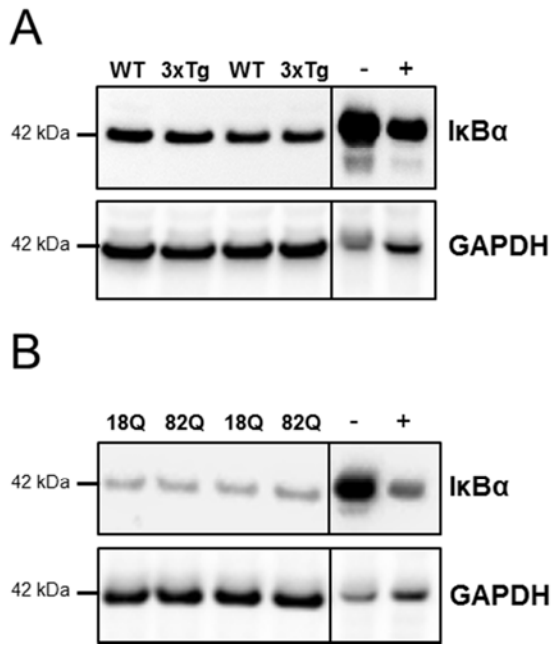
A
WT
3xTg
WT
3xTg
-
+
42 kDa
IκBα
42 kDa
GAPDH
B
18Q
82Q
18Q
82Q
-
+
42 kDa
IκBα
42 kDa
GAPDH

Figure 7

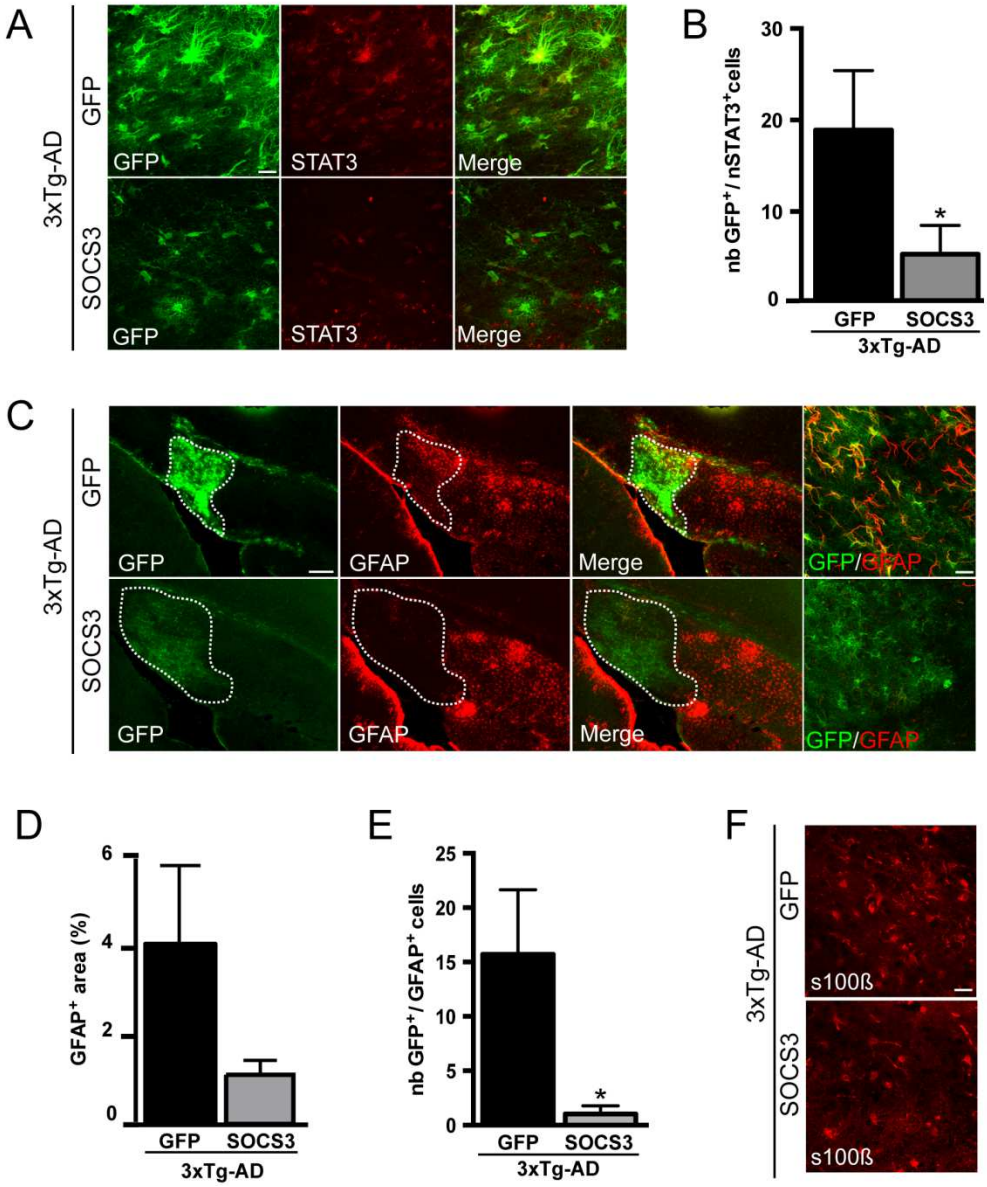
A
3xTg-AD
GFP
SOCS3
GFP
STAT3
Merge
GFP
STAT3
Merge
B
nb GFP+ / nSTAT3+cells
30
20
10
0
*
GFP
SOCS3
3xTg-AD
C
3xTg-AD
GFP
SOCS3
GFP
GFAP
Merge
GFP/GFAP
GFP
GFAP
Merge
GFP/GFAP
D
GFAP+ area (%)
6
4
2
0
GFP
SOCS3
3xTg-AD
E
nb GFP+ / GFAP+ cells
25
20
15
10
5
0
*
GFP
SOCS3
3xTg-AD
F
3xTg-AD
GFP
SOCS3
s100ß
s100ß

Figure 8

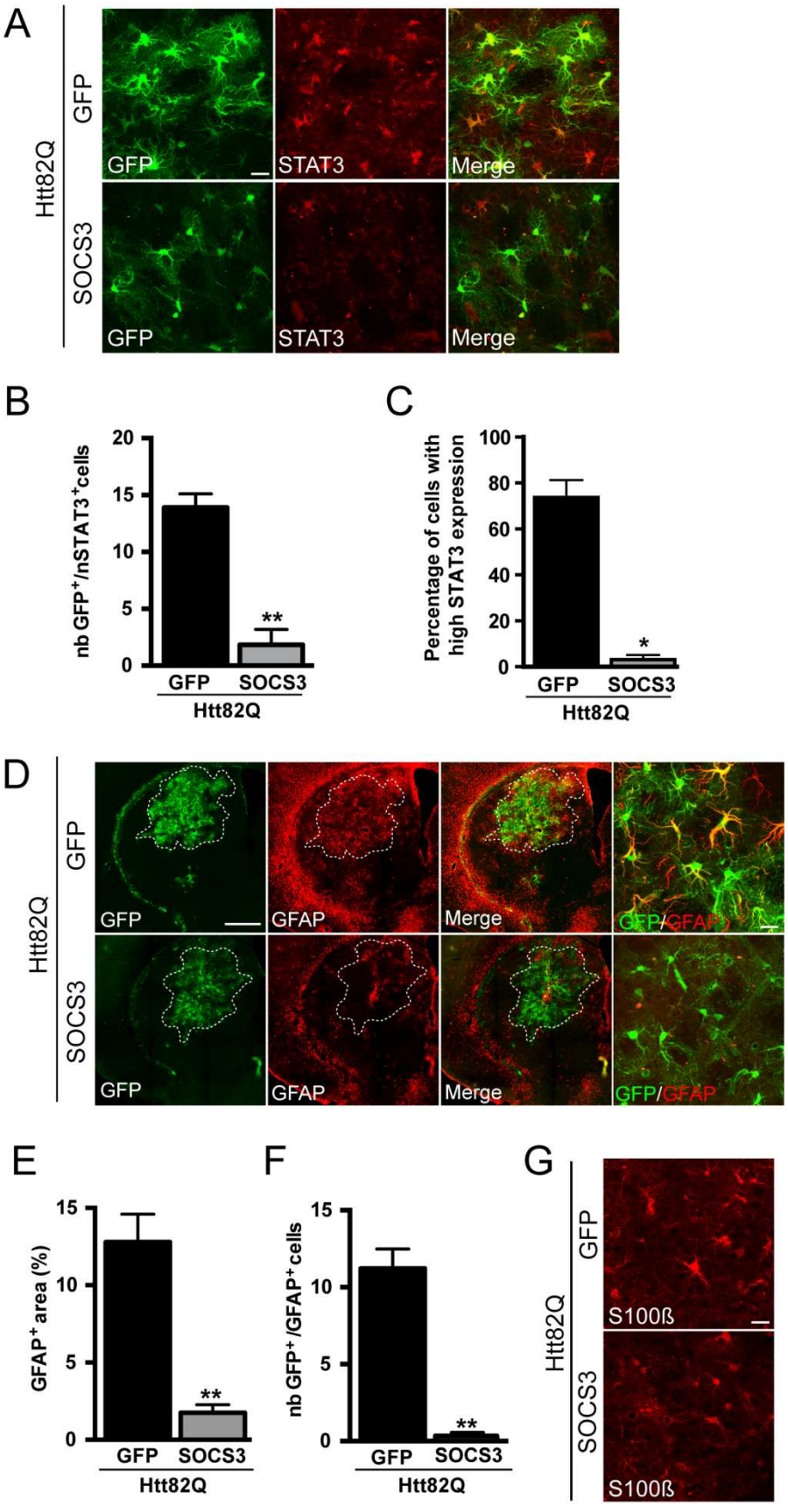
A
Htt82Q
GFP
SOCS3
GFP
STAT3
Merge
GFP
STAT3
Merge
B
nb GFP+/nSTAT3+cells
20
15
10
5
0
**
GFP
SOCS3
Htt82Q
C
Percentage of cells with high STAT3 expression
100
80
60
40
20
0
*
GFP
SOCS3
Htt82Q
D
Htt82Q
GFP
SOCS3
GFP
GFAP
Merge
GFP/GFAP
GFP
GFAP
Merge
GFP/GFAP
E
GFAP+ area (%)
15
10
5
0
**
GFP
SOCS3
Htt82Q
F
nb GFP+ /GFAP+ cells
15
10
5
0
**
GFP
SOCS3
Htt82Q
G
Htt82Q
GFP
SOCS3
S100ß
S100ß

Figure 9

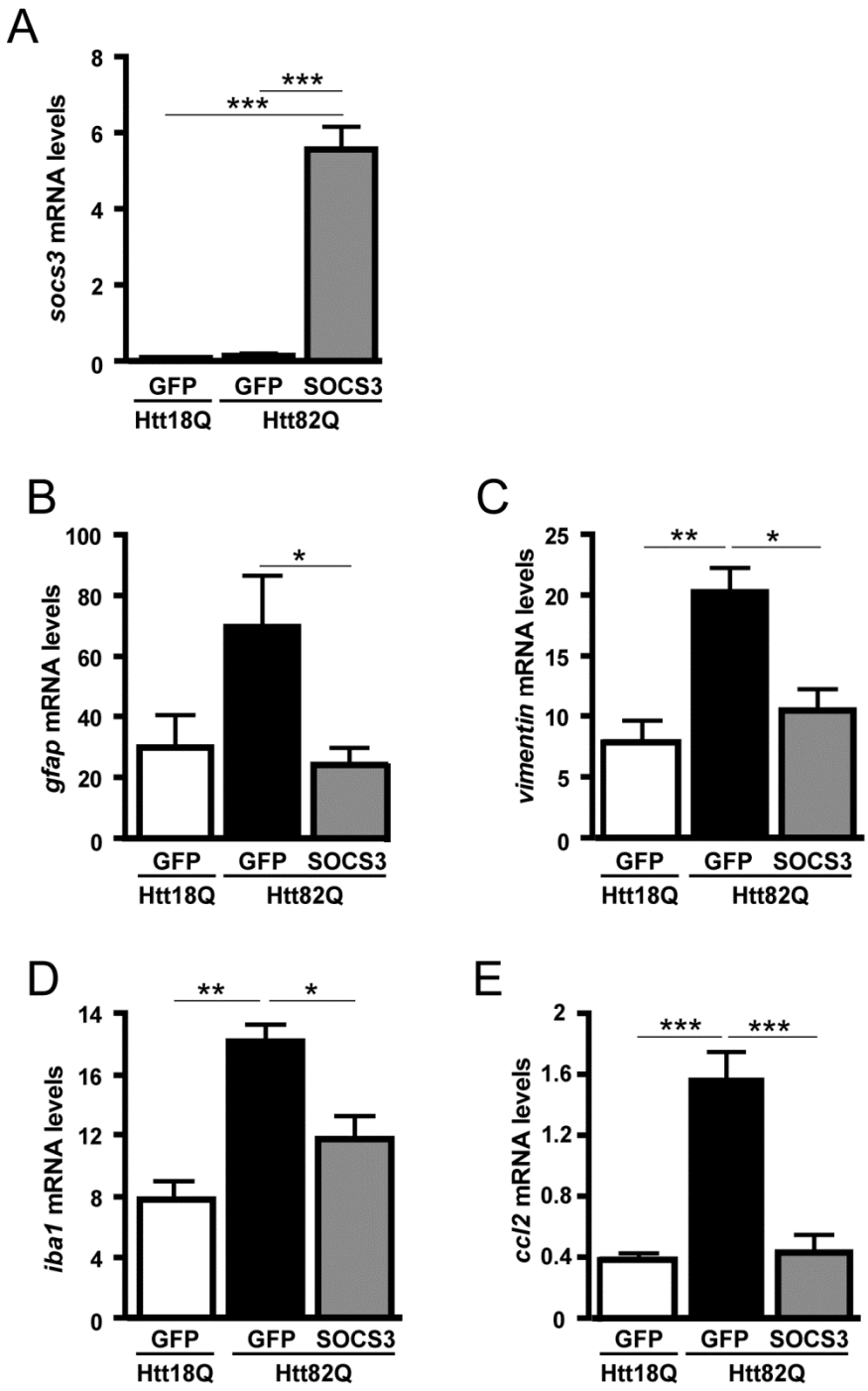
A
socs3 mRNA levels
8
6
4
2
0
***
***
GFP
GFP
SOCS3
Htt18Q
Htt82Q
B
gfap mRNA levels
100
80
60
40
20
0
*
GFP
GFP
SOCS3
Htt18Q
Htt82Q
C
vimentin mRNA levels
25
20
15
10
5
0
**
*
GFP
GFP
SOCS3
Htt18Q
Htt82Q
D
iba1 mRNA levels
14
16
12
8
4
0
**
*
GFP
GFP
SOCS3
Htt18Q
Htt82Q
E
ccl2 mRNA levels
2
1.6
1.2
0.8
0.4
0
***
***
GFP
GFP
SOCS3
Htt18Q
Htt82Q

D. References

Abbott NJ, Ronnback L, Hansson E (2006) Astrocyte-endothelial interactions at the blood-brain barrier. Nature reviews Neuroscience 7:41-53.

Acuna AI, Esparza M, Kramm C, Beltran FA, Parra AV, Cepeda C, Toro CA, Vidal RL, Hetz C, Concha, II, Brauchi S, Levine MS, Castro MA (2013) A failure in energy metabolism and antioxidant uptake precede symptoms of Huntington's disease in mice. Nature communications 4:2917.

Albrecht PJ, Dahl JP, Stoltzfus OK, Levenson R, Levison SW (2002) Ciliary neurotrophic factor activates spinal cord astrocytes, stimulating their production and release of fibroblast growth factor-2, to increase motor neuron survival. Experimental neurology 173:46-62.

Alexander WS, Starr R, Fenner JE, Scott CL, Handman E, Sprigg NS, Corbin JE, Cornish AL, Darwiche R, Owczarek CM, Kay TW, Nicola NA, Hertzog PJ, Metcalf D, Hilton DJ (1999) SOCS1 is a critical inhibitor of interferon gamma signaling and prevents the potentially fatal neonatal actions of this cytokine. Cell 98:597-608.

Allaman I, Belanger M, Magistretti PJ (2011) Astrocyte-neuron metabolic relationships: for better and for worse. Trends in neurosciences 34:76-87.

Allaman I, Gavillet M, Belanger M, Laroche T, Viertl D, Lashuel HA, Magistretti PJ (2010) Amyloid-beta aggregates cause alterations of astrocytic metabolic phenotype: impact on neuronal viability. The Journal of neuroscience : the official journal of the Society for Neuroscience 30:3326-3338.

Allen NJ (2013) Role of glia in developmental synapse formation. Current opinion in neurobiology 23:1027-1033.

Allen NJ, Bennett ML, Foo LC, Wang GX, Chakraborty C, Smith SJ, Barres BA (2012) Astrocyte glypicans 4 and 6 promote formation of excitatory synapses via GluA1 AMPA receptors. Nature 486:410-414.

Alvarez JI, Katayama T, Prat A (2013) Glial influence on the blood brain barrier. Glia 61:1939-1958.

Amantea D, Tassorelli C, Russo R, Petrelli F, Morrone LA, Bagetta G, Corasaniti MT (2011) Neuroprotection by leptin in a rat model of permanent cerebral ischemia: effects on STAT3 phosphorylation in discrete cells of the brain. Cell death & disease 2:e238.

Anderson MA, Ao Y, Sofroniew MV (2014) Heterogeneity of reactive astrocytes. Neurosci Lett 565:23-29.

Araque A, Parpura V, Sanzgiri RP, Haydon PG (1999) Tripartite synapses: glia, the unacknowledged partner. Trends in neurosciences 22:208-215.

Araque A, Carmignoto G, Haydon PG, Oliet SH, Robitaille R, Volterra A (2014) Gliotransmitters travel in time and space. Neuron 81:728-739.

Arrasate M, Finkbeiner S (2012) Protein aggregates in Huntington's disease. Experimental neurology 238:1-11.

Arrasate M, Mitra S, Schweitzer ES, Segal MR, Finkbeiner S (2004) Inclusion body formation reduces levels of mutant huntingtin and the risk of neuronal death. Nature 431:805-810.

Arregui L, Benitez JA, Razgado LF, Vergara P, Segovia J (2011) Adenoviral astrocyte-specific expression of BDNF in the striata of mice transgenic for Huntington's disease delays the onset of the motor phenotype. Cellular and molecular neurobiology 31:1229-1243.

Attwell D, Buchan AM, Charpak S, Lauritzen M, Macvicar BA, Newman EA (2010) Glial and neuronal control of brain blood flow. Nature 468:232-243.

Avola R, Di Tullio MA, Fisichella A, Tayebati SK, Tomassoni D (2004) Glial fibrillary acidic protein and vimentin expression is regulated by glucocorticoids and neurotrophic factors in primary rat astroglial cultures. Clinical and experimental hypertension 26:323-333.

Awasaki T, Lee T (2011) Orphan nuclear receptors control neuronal remodeling during fly metamorphosis. Nature neuroscience 14:6-7.

Babon JJ, Nicola NA (2012) The biology and mechanism of action of suppressor of cytokine signaling 3. Growth factors 30:207-219.

Babon JJ, Sabo JK, Zhang JG, Nicola NA, Norton RS (2009) The SOCS box encodes a hierarchy of affinities for Cullin5: implications for ubiquitin ligase formation and cytokine signalling suppression. Journal of molecular biology 387:162-174.

Bardehle S, Kruger M, Buggenthin F, Schwausch J, Ninkovic J, Clevers H, Snippert HJ, Theis FJ, Meyer-Luehmann M, Bechmann I, Dimou L, Gotz M (2013) Live imaging of astrocyte responses to acute injury reveals selective juxtavascular proliferation. Nature neuroscience 16:580-586.

Barnabe-Heider F, Goritz C, Sabelstrom H, Takebayashi H, Pfrieger FW, Meletis K, Frisen J (2010) Origin of new glial cells in intact and injured adult spinal cord. Cell stem cell 7:470-482.

Barres BA (2008) The mystery and magic of glia: a perspective on their roles in health and disease. Neuron 60:430-440.

Bauer S, Kerr BJ, Patterson PH (2007) The neuropoietic cytokine family in development, plasticity, disease and injury. Nature reviews Neuroscience 8:221-232.

Beal MF, Henshaw DR, Jenkins BG, Rosen BR, Schulz JB (1994) Coenzyme Q10 and nicotinamide block striatal lesions produced by the mitochondrial toxin malonate. Annals of neurology 36:882-888.

Beenhakker MP, Huguenard JR (2010) Astrocytes as gatekeepers of GABAB receptor function. The Journal of neuroscience : the official journal of the Society for Neuroscience 30:15262-15276.

Behrens PF, Franz P, Woodman B, Lindenberg KS, Landwehrmeyer GB (2002) Impaired glutamate transport and glutamate-glutamine cycling: downstream effects of the Huntington mutation. Brain : a journal of neurology 125:1908-1922.

Belanger M, Magistretti PJ (2009) The role of astroglia in neuroprotection. Dialogues in clinical neuroscience 11:281-295.

Belanger M, Allaman I, Magistretti PJ (2011a) Brain energy metabolism: focus on astrocyte-neuron metabolic cooperation. Cell metabolism 14:724-738.

Belanger M, Allaman I, Magistretti PJ (2011b) Differential effects of pro- and anti-inflammatory cytokines alone or in combinations on the metabolic profile of astrocytes. Journal of neurochemistry 116:564-576.

Beppu K, Sasaki T, Tanaka KF, Yamanaka A, Fukazawa Y, Shigemoto R, Matsui K (2014) Optogenetic countering of glial acidosis suppresses glial glutamate release and ischemic brain damage. Neuron 81:314-320.

Berg A, Zelano J, Pekna M, Wilhelmsson U, Pekny M, Cullheim S (2013) Axonal regeneration after sciatic nerve lesion is delayed but complete in GFAP- and vimentin-deficient mice. PloS one 8:e79395.

Bergles DE, Jahr CE (1998) Glial contribution to glutamate uptake at Schaffer collateral-commissural synapses in the hippocampus. The Journal of neuroscience : the official journal of the Society for Neuroscience 18:7709-7716.

Bernardinelli Y, Randall J, Janett E, Nikonenko I, Konig S, Jones EV, Flores CE, Murai KK, Bochet CG, Holtmaat A, Muller D (2014) Activity-dependent structural plasticity of perisynaptic astrocytic domains promotes excitatory synapse stability. Current biology : CB 24:1679-1688.

Bertram L, Lill CM, Tanzi RE (2010) The genetics of Alzheimer disease: back to the future. Neuron 68:270-281.

Bethea JR, Castro M, Keane RW, Lee TT, Dietrich WD, Yezierski RP (1998) Traumatic spinal cord injury induces nuclear factor-kappaB activation. The Journal of neuroscience : the official journal of the Society for Neuroscience 18:3251-3260.

Bett JS, Goellner GM, Woodman B, Pratt G, Rechsteiner M, Bates GP (2006) Proteasome impairment does not contribute to pathogenesis in R6/2 Huntington's disease mice: exclusion of proteasome activator REGgamma as a therapeutic target. Human molecular genetics 15:33-44.

Bhutani N, Piccirillo R, Hourez R, Venkatraman P, Goldberg AL (2012) Cathepsins L and Z are critical in degrading polyglutamine-containing proteins within lysosomes. The Journal of biological chemistry 287:17471-17482.

Birch AM, Katsouri L, Sastre M (2014) Modulation of inflammation in transgenic models of Alzheimer's disease. Journal of neuroinflammation 11:25.

Bjorkqvist M et al. (2008) A novel pathogenic pathway of immune activation detectable before clinical onset in Huntington's disease. The Journal of experimental medicine 205:1869-1877.

Boddaert J, Kinugawa K, Lambert JC, Boukhtouche F, Zoll J, Merval R, Blanc-Brude O, Mann D, Berr C, Vilar J, Garabedian B, Journiac N, Charue D, Silvestre JS, Duyckaerts C, Amouyel P, Mariani J, Tedgui A, Mallat Z (2007) Evidence of a role for lactadherin in Alzheimer's disease. The American journal of pathology 170:921-929.

Boillee S, Vande Velde C, Cleveland DW (2006) ALS: a disease of motor neurons and their nonneuronal neighbors. Neuron 52:39-59.
Bouchard J, Truong J, Bouchard K, Dunkelberger D, Desrayaud S, Moussaoui S, Tabrizi SJ, Stella N, Muchowski PJ (2012) Cannabinoid receptor 2 signaling in peripheral immune cells modulates disease onset and severity in mouse models of Huntington's disease. The Journal of neuroscience : the official journal of the Society for Neuroscience 32:18259-18268.
Bowman AB, Yoo SY, Dantuma NP, Zoghbi HY (2005) Neuronal dysfunction in a polyglutamine disease model occurs in the absence of ubiquitin-proteasome system impairment and inversely correlates with the degree of nuclear inclusion formation. Human molecular genetics 14:679-691.
Boyle K, Robb L (2008) The role of SOCS3 in modulating leukaemia inhibitory factor signalling during murine placental development. Journal of reproductive immunology 77:1-6.
Bracchi-Ricard V, Lambertsen KL, Ricard J, Nathanson L, Karmally S, Johnstone J, Ellman DG, Frydel B, McTigue DM, Bethea JR (2013) Inhibition of astroglial NF-kappaB enhances oligodendrogenesis following spinal cord injury. Journal of neuroinflammation 10:92.
Bradford J, Shin JY, Roberts M, Wang CE, Li XJ, Li S (2009) Expression of mutant huntingtin in mouse brain astrocytes causes age-dependent neurological symptoms. Proceedings of the National Academy of Sciences of the United States of America 106:22480-22485.
Bradford J, Shin JY, Roberts M, Wang CE, Sheng G, Li S, Li XJ (2010) Mutant huntingtin in glial cells exacerbates neurological symptoms of Huntington disease mice. The Journal of biological chemistry 285:10653-10661.
Braidy N, Brew BJ, Inestrosa NC, Chung R, Sachdev P, Guillemin GJ (2014) Changes in Cathepsin D and Beclin-1 mRNA and protein expression by the excitotoxin quinolinic acid in human astrocytes and neurons. Metabolic brain disease 29:873-883.
Brambilla R, Cottini L, Fumagalli M, Ceruti S, Abbracchio MP (2003) Blockade of A2A adenosine receptors prevents basic fibroblast growth factor-induced reactive astrogliosis in rat striatal primary astrocytes. Glia 43:190-194.
Brambilla R, Hurtado A, Persaud T, Esham K, Pearse DD, Oudega M, Bethea JR (2009) Transgenic inhibition of astroglial NF-kappa B leads to increased axonal sparing and sprouting following spinal cord injury. Journal of neurochemistry 110:765-778.
Brambilla R, Bracchi-Ricard V, Hu WH, Frydel B, Bramwell A, Karmally S, Green EJ, Bethea JR (2005) Inhibition of astroglial nuclear factor kappaB reduces inflammation and improves functional recovery after spinal cord injury. The Journal of experimental medicine 202:145-156.
Brenner M, Johnson AB, Boespflug-Tanguy O, Rodriguez D, Goldman JE, Messing A (2001) Mutations in GFAP, encoding glial fibrillary acidic protein, are associated with Alexander disease. Nature genetics 27:117-120.
Bromberg JF, Wrzeszczynska MH, Devgan G, Zhao Y, Pestell RG, Albanese C, Darnell JE, Jr. (1999) Stat3 as an oncogene. Cell 98:295-303.
Brooks AJ, Dai W, O'Mara ML, Abankwa D, Chhabra Y, Pelekanos RA, Gardon O, Tunny KA, Blucher KM, Morton CJ, Parker MW, Sierecki E, Gambin Y, Gomez GA, Alexandrov K, Wilson IA, Doxastakis M, Mark AE, Waters MJ (2014) Mechanism of activation of protein kinase JAK2 by the growth hormone receptor. Science 344:1249783.
Brosius Lutz A, Barres BA (2014) Contrasting the glial response to axon injury in the central and peripheral nervous systems. Developmental cell 28:7-17.
Brouillet E, Hantraye P, Ferrante RJ, Dolan R, Leroy-Willig A, Kowall NW, Beal MF (1995) Chronic mitochondrial energy impairment produces selective striatal degeneration and abnormal choreiform movements in primates. Proceedings of the National Academy of Sciences of the United States of America 92:7105-7109.
Brown AM, Ransom BR (2007) Astrocyte glycogen and brain energy metabolism. Glia 55:1263-1271.
Bruce AW, Donaldson IJ, Wood IC, Yerbury SA, Sadowski MI, Chapman M, Gottgens B, Buckley NJ (2004) Genome-wide analysis of repressor element 1 silencing transcription factor/neuron-restrictive silencing factor (REST/NRSF) target genes. Proceedings of the National Academy of Sciences of the United States of America 101:10458-10463.
Buffo A, Rite I, Tripathi P, Lepier A, Colak D, Horn AP, Mori T, Gotz M (2008) Origin and progeny of reactive gliosis: A source of multipotent cells in the injured brain. Proceedings of the National Academy of Sciences of the United States of America 105:3581-3586.

Burda JE, Sofroniew MV (2014) Reactive gliosis and the multicellular response to CNS damage and disease. Neuron 81:229-248.

Bush TG, Puvanachandra N, Horner CH, Polito A, Ostenfeld T, Svendsen CN, Mucke L, Johnson MH, Sofroniew MV (1999) Leukocyte infiltration, neuronal degeneration, and neurite outgrowth after ablation of scar-forming, reactive astrocytes in adult transgenic mice. Neuron 23:297-308.

Bushong EA, Martone ME, Jones YZ, Ellisman MH (2002) Protoplasmic astrocytes in CA1 stratum radiatum occupy separate anatomical domains. The Journal of neuroscience : the official journal of the Society for Neuroscience 22:183-192.

Cabezas R, Avila M, Gonzalez J, El-Bacha RS, Baez E, Garcia-Segura LM, Jurado Coronel JC, Capani F, Cardona-Gomez GP, Barreto GE (2014) Astrocytic modulation of blood brain barrier: perspectives on Parkinson's disease. Frontiers in cellular neuroscience 8:211.

Cahoy JD, Emery B, Kaushal A, Foo LC, Zamanian JL, Christopherson KS, Xing Y, Lubischer JL, Krieg PA, Krupenko SA, Thompson WJ, Barres BA (2008) A transcriptome database for astrocytes, neurons, and oligodendrocytes: a new resource for understanding brain development and function. The Journal of neuroscience : the official journal of the Society for Neuroscience 28:264-278.

Calkins MJ, Vargas MR, Johnson DA, Johnson JA (2010) Astrocyte-specific overexpression of Nrf2 protects striatal neurons from mitochondrial complex II inhibition. Toxicological sciences : an official journal of the Society of Toxicology 115:557-568.

Campbell IL, Erta M, Lim SL, Frausto R, May U, Rose-John S, Scheller J, Hidalgo J (2014) Trans-signaling is a dominant mechanism for the pathogenic actions of interleukin-6 in the brain. The Journal of neuroscience : the official journal of the Society for Neuroscience 34:2503-2513.

Cao F, Hata R, Zhu P, Nakashiro K, Sakanaka M (2010) Conditional deletion of Stat3 promotes neurogenesis and inhibits astrogliogenesis in neural stem cells. Biochemical and biophysical research communications 394:843-847.

Carbonell WS, Mandell JW (2003) Transient neuronal but persistent astroglial activation of ERK/MAP kinase after focal brain injury in mice. Journal of neurotrauma 20:327-336.

Carmona MA, Murai KK, Wang L, Roberts AJ, Pasquale EB (2009) Glial ephrin-A3 regulates hippocampal dendritic spine morphology and glutamate transport. Proceedings of the National Academy of Sciences of the United States of America 106:12524-12529.

Carrero I, Gonzalo MR, Martin B, Sanz-Anquela JM, Arevalo-Serrano J, Gonzalo-Ruiz A (2012) Oligomers of beta-amyloid protein (Abeta1-42) induce the activation of cyclooxygenase-2 in astrocytes via an interaction with interleukin-1beta, tumour necrosis factor-alpha, and a nuclear factor kappa-B mechanism in the rat brain. Experimental neurology 236:215-227.

Carter SF, Scholl M, Almkvist O, Wall A, Engler H, Langstrom B, Nordberg A (2012) Evidence for astrocytosis in prodromal Alzheimer disease provided by 11C-deuterium-L-deprenyl: a multitracer PET paradigm combining 11C-Pittsburgh compound B and 18F-FDG. Journal of nuclear medicine : official publication, Society of Nuclear Medicine 53:37-46.

Castro MA, Beltran FA, Brauchi S, Concha, II (2009) A metabolic switch in brain: glucose and lactate metabolism modulation by ascorbic acid. Journal of neurochemistry 110:423-440.

Cattaneo E, Zuccato C, Tartari M (2005) Normal huntingtin function: an alternative approach to Huntington's disease. Nature reviews Neuroscience 6:919-930.

Cearley CN, Wolfe JH (2006) Transduction characteristics of adeno-associated virus vectors expressing cap serotypes 7, 8, 9, and Rh10 in the mouse brain. Molecular therapy : the journal of the American Society of Gene Therapy 13:528-537.

Cepeda C, Cummings DM, Andre VM, Holley SM, Levine MS (2010) Genetic mouse models of Huntington's disease: focus on electrophysiological mechanisms. ASN neuro 2:e00033.

Chadi G, Gomide VC (2004) FGF-2 and S100beta immunoreactivities increase in reactive astrocytes, but not in microglia, in ascending dopamine pathways following a striatal 6-OHDA-induced partial lesion of the nigrostriatal system. Cell biology international 28:849-861.

Chatton JY, Marquet P, Magistretti PJ (2000) A quantitative analysis of L-glutamate-regulated Na+ dynamics in mouse cortical astrocytes: implications for cellular bioenergetics. The European journal of neuroscience 12:3843-3853.

Chaturvedi RK, Beal MF (2013) Mitochondria targeted therapeutic approaches in Parkinson's and Huntington's diseases. Molecular and cellular neurosciences 55:101-114.

Chen PC, Vargas MR, Pani AK, Smeyne RJ, Johnson DA, Kan YW, Johnson JA (2009) Nrf2-mediated neuroprotection in the MPTP mouse model of Parkinson's disease: Critical role for the astrocyte. Proceedings of the National Academy of Sciences of the United States of America 106:2933-2938.
Chiba T, Yamada M, Aiso S (2009) Targeting the JAK2/STAT3 axis in Alzheimer's disease. Expert opinion on therapeutic targets 13:1155-1167.
Cho KS, Park SH, Joo SH, Kim SH, Shin CY (2010) The effects of IL-32 on the inflammatory activation of cultured rat primary astrocytes. Biochemical and biophysical research communications 402:48-53.
Chou SY, Weng JY, Lai HL, Liao F, Sun SH, Tu PH, Dickson DW, Chern Y (2008) Expanded-polyglutamine huntingtin protein suppresses the secretion and production of a chemokine (CCL5/RANTES) by astrocytes. The Journal of neuroscience : the official journal of the Society for Neuroscience 28:3277-3290.
Chung WS, Clarke LE, Wang GX, Stafford BK, Sher A, Chakraborty C, Joung J, Foo LC, Thompson A, Chen C, Smith SJ, Barres BA (2013) Astrocytes mediate synapse elimination through MEGF10 and MERTK pathways. Nature 504:394-400.
Cicchetti F, Soulet D, Freeman TB (2011) Neuronal degeneration in striatal transplants and Huntington's disease: potential mechanisms and clinical implications. Brain : a journal of neurology 134:641-652.
Cimica V, Chen HC, Iyer JK, Reich NC (2011) Dynamics of the STAT3 transcription factor: nuclear import dependent on Ran and importin-beta1. PloS one 6:e20188.
Clarke LE, Barres BA (2013) Emerging roles of astrocytes in neural circuit development. Nature reviews Neuroscience 14:311-321.
Clarke SR, Shetty AK, Bradley JL, Turner DA (1994) Reactive astrocytes express the embryonic intermediate neurofilament nestin. Neuroreport 5:1885-1888.
Clasadonte J, Haydon PG (2012) Astrocytes and Epilepsy. In: Jasper's Basic Mechanisms of the Epilepsies, 4th Edition (Noebels JL, Avoli M, Rogawski MA, Olsen RW, Delgado-Escueta AV, eds). Bethesda (MD).
Cole-Edwards KK, Musto AE, Bazan NG (2006) c-Jun N-terminal kinase activation responses induced by hippocampal kindling are mediated by reactive astrocytes. The Journal of neuroscience : the official journal of the Society for Neuroscience 26:8295-8304.
Colin A, Faideau M, Dufour N, Auregan G, Hassig R, Andrieu T, Brouillet E, Hantraye P, Bonvento G, Deglon N (2009) Engineered lentiviral vector targeting astrocytes in vivo. Glia 57:667-679.
Cooper JK, Schilling G, Peters MF, Herring WJ, Sharp AH, Kaminsky Z, Masone J, Khan FA, Delanoy M, Borchelt DR, Dawson VL, Dawson TM, Ross CA (1998) Truncated N-terminal fragments of huntingtin with expanded glutamine repeats form nuclear and cytoplasmic aggregates in cell culture. Human molecular genetics 7:783-790.
Cortes CJ, La Spada AR (2014) The many faces of autophagy dysfunction in Huntington's disease: from mechanism to therapy. Drug discovery today 19:963-971.
Crosio C, Valle C, Casciati A, Iaccarino C, Carri MT (2011) Astroglial inhibition of NF-kappaB does not ameliorate disease onset and progression in a mouse model for amyotrophic lateral sclerosis (ALS). PloS one 6:e17187.
Crotti A, Benner C, Kerman BE, Gosselin D, Lagier-Tourenne C, Zuccato C, Cattaneo E, Gage FH, Cleveland DW, Glass CK (2014) Mutant Huntingtin promotes autonomous microglia activation via myeloid lineage-determining factors. Nature neuroscience 17:513-521.
Dallerac G, Chever O, Rouach N (2013) How do astrocytes shape synaptic transmission? Insights from electrophysiology. Frontiers in cellular neuroscience 7:159.
Danbolt NC (2001) Glutamate uptake. Progress in neurobiology 65:1-105.
Davies SW, Turmaine M, Cozens BA, DiFiglia M, Sharp AH, Ross CA, Scherzinger E, Wanker EE, Mangiarini L, Bates GP (1997) Formation of neuronal intranuclear inclusions underlies the neurological dysfunction in mice transgenic for the HD mutation. Cell 90:537-548.
Deglon N, Tseng JL, Bensadoun JC, Zurn AD, Arsenijevic Y, Pereira de Almeida L, Zufferey R, Trono D, Aebischer P (2000) Self-inactivating lentiviral vectors with enhanced transgene expression as potential gene transfer system in Parkinson's disease. Human gene therapy 11:179-190.
Delzor A, Escartin C, Deglon N (2013) Lentiviral vectors: a powerful tool to target astrocytes in vivo. Current drug targets 14:1336-1346.

Desmaris N, Bosch A, Salaun C, Petit C, Prevost MC, Tordo N, Perrin P, Schwartz O, de Rocquigny H, Heard JM (2001) Production and neurotropism of lentivirus vectors pseudotyped with lyssavirus envelope glycoproteins. Molecular therapy : the journal of the American Society of Gene Therapy 4:149-156.
Di Castro MA, Chuquet J, Liaudet N, Bhaukaurally K, Santello M, Bouvier D, Tiret P, Volterra A (2011) Local Ca2+ detection and modulation of synaptic release by astrocytes. Nature neuroscience 14:1276-1284.
Di Giorgio FP, Carrasco MA, Siao MC, Maniatis T, Eggan K (2007) Non-cell autonomous effect of glia on motor neurons in an embryonic stem cell-based ALS model. Nature neuroscience 10:608-614.
Diamond JS, Jahr CE (1997) Transporters buffer synaptically released glutamate on a submillisecond time scale. The Journal of neuroscience : the official journal of the Society for Neuroscience 17:4672-4687.
Diaz-Hernandez M, Hernandez F, Martin-Aparicio E, Gomez-Ramos P, Moran MA, Castano JG, Ferrer I, Avila J, Lucas JJ (2003) Neuronal induction of the immunoproteasome in Huntington's disease. The Journal of neuroscience : the official journal of the Society for Neuroscience 23:11653-11661.
DiFiglia M, Sapp E, Chase KO, Davies SW, Bates GP, Vonsattel JP, Aronin N (1997) Aggregation of huntingtin in neuronal intranuclear inclusions and dystrophic neurites in brain. Science 277:1990-1993.
Dimou L, Gotz M (2014) Glial cells as progenitors and stem cells: new roles in the healthy and diseased brain. Physiological reviews 94:709-737.
Dineley KT, Hogan D, Zhang WR, Taglialatela G (2007) Acute inhibition of calcineurin restores associative learning and memory in Tg2576 APP transgenic mice. Neurobiology of learning and memory 88:217-224.
Dong XX, Wang Y, Qin ZH (2009) Molecular mechanisms of excitotoxicity and their relevance to pathogenesis of neurodegenerative diseases. Acta pharmacologica Sinica 30:379-387.
Doyle JP, Dougherty JD, Heiman M, Schmidt EF, Stevens TR, Ma G, Bupp S, Shrestha P, Shah RD, Doughty ML, Gong S, Greengard P, Heintz N (2008) Application of a translational profiling approach for the comparative analysis of CNS cell types. Cell 135:749-762.
Dragatsis I, Levine MS, Zeitlin S (2000) Inactivation of Hdh in the brain and testis results in progressive neurodegeneration and sterility in mice. Nature genetics 26:300-306.
Dragunow M, Hughes P (1993) Differential expression of immediate-early proteins in non-nerve cells after focal brain injury. International journal of developmental neuroscience : the official journal of the International Society for Developmental Neuroscience 11:249-255.
Drouet V, Ruiz M, Zala D, Feyeux M, Auregan G, Cambon K, Troquier L, Carpentier J, Aubert S, Merienne N, Bourgois-Rocha F, Hassig R, Rey M, Dufour N, Saudou F, Perrier AL, Hantraye P, Deglon N (2014) Allele-specific silencing of mutant huntingtin in rodent brain and human stem cells. PloS one 9:e99341.
Dvoriantchikova G, Barakat D, Brambilla R, Agudelo C, Hernandez E, Bethea JR, Shestopalov VI, Ivanov D (2009) Inactivation of astroglial NF-kappa B promotes survival of retinal neurons following ischemic injury. The European journal of neuroscience 30:175-185.
Eclancher F, Kehrli P, Labourdette G, Sensenbrenner M (1996) Basic fibroblast growth factor (bFGF) injection activates the glial reaction in the injured adult rat brain. Brain research 737:201-214.
Eclancher F, Perraud F, Faltin J, Labourdette G, Sensenbrenner M (1990) Reactive astrogliosis after basic fibroblast growth factor (bFGF) injection in injured neonatal rat brain. Glia 3:502-509.
Eddleston M, Mucke L (1993) Molecular profile of reactive astrocytes--implications for their role in neurologic disease. Neuroscience 54:15-36.
Eid T, Behar K, Dhaher R, Bumanglag AV, Lee TS (2012) Roles of glutamine synthetase inhibition in epilepsy. Neurochemical research 37:2339-2350.
Elsaeidi F, Bemben MA, Zhao XF, Goldman D (2014) Jak/Stat signaling stimulates zebrafish optic nerve regeneration and overcomes the inhibitory actions of Socs3 and Sfpq. The Journal of neuroscience : the official journal of the Society for Neuroscience 34:2632-2644.
Emsley JG, Macklis JD (2006) Astroglial heterogeneity closely reflects the neuronal-defined anatomy of the adult murine CNS. Neuron glia biology 2:175-186.
Endo TA, Masuhara M, Yokouchi M, Suzuki R, Sakamoto H, Mitsui K, Matsumoto A, Tanimura S, Ohtsubo M, Misawa H, Miyazaki T, Leonor N, Taniguchi T, Fujita T, Kanakura Y, Komiya S,

Yoshimura A (1997) A new protein containing an SH2 domain that inhibits JAK kinases. Nature 387:921-924.
Ernst M, Jenkins BJ (2004) Acquiring signalling specificity from the cytokine receptor gp130. Trends in genetics : TIG 20:23-32.
Ernst MB, Wunderlich CM, Hess S, Paehler M, Mesaros A, Koralov SB, Kleinridders A, Husch A, Munzberg H, Hampel B, Alber J, Kloppenburg P, Bruning JC, Wunderlich FT (2009) Enhanced Stat3 activation in POMC neurons provokes negative feedback inhibition of leptin and insulin signaling in obesity. The Journal of neuroscience : the official journal of the Society for Neuroscience 29:11582-11593.
Escartin C, Bonvento G (2008) Targeted activation of astrocytes: a potential neuroprotective strategy. Molecular neurobiology 38:231-241.
Escartin C, Rouach N (2013) Astroglial networking contributes to neurometabolic coupling. Frontiers in neuroenergetics 5:4.
Escartin C, Brouillet E, Gubellini P, Trioulier Y, Jacquard C, Smadja C, Knott GW, Kerkerian-Le Goff L, Deglon N, Hantraye P, Bonvento G (2006) Ciliary neurotrophic factor activates astrocytes, redistributes their glutamate transporters GLAST and GLT-1 to raft microdomains, and improves glutamate handling in vivo. The Journal of neuroscience : the official journal of the Society for Neuroscience 26:5978-5989.
Escartin C, Pierre K, Colin A, Brouillet E, Delzescaux T, Guillermier M, Dhenain M, Deglon N, Hantraye P, Pellerin L, Bonvento G (2007) Activation of astrocytes by CNTF induces metabolic plasticity and increases resistance to metabolic insults. The Journal of neuroscience : the official journal of the Society for Neuroscience 27:7094-7104.
Faideau M, Kim J, Cormier K, Gilmore R, Welch M, Auregan G, Dufour N, Guillermier M, Brouillet E, Hantraye P, Deglon N, Ferrante RJ, Bonvento G (2010) In vivo expression of polyglutamine-expanded huntingtin by mouse striatal astrocytes impairs glutamate transport: a correlation with Huntington's disease subjects. Human molecular genetics 19:3053-3067.
Fan K, Wu X, Fan B, Li N, Lin Y, Yao Y, Ma J (2012) Up-regulation of microglial cathepsin C expression and activity in lipopolysaccharide-induced neuroinflammation. Journal of neuroinflammation 9:96.
Fan Y, Mao R, Yang J (2013) NF-kappaB and STAT3 signaling pathways collaboratively link inflammation to cancer. Protein & cell 4:176-185.
Faulkner JR, Herrmann JE, Woo MJ, Tansey KE, Doan NB, Sofroniew MV (2004) Reactive astrocytes protect tissue and preserve function after spinal cord injury. The Journal of neuroscience : the official journal of the Society for Neuroscience 24:2143-2155.
Feigin A, Leenders KL, Moeller JR, Missimer J, Kuenig G, Spetsieris P, Antonini A, Eidelberg D (2001) Metabolic network abnormalities in early Huntington's disease: an [(18)F]FDG PET study. Journal of nuclear medicine : official publication, Society of Nuclear Medicine 42:1591-1595.
Fernandez AM, Fernandez S, Carrero P, Garcia-Garcia M, Torres-Aleman I (2007) Calcineurin in reactive astrocytes plays a key role in the interplay between proinflammatory and anti-inflammatory signals. The Journal of neuroscience : the official journal of the Society for Neuroscience 27:8745-8756.
Fernandez AM, Jimenez S, Mecha M, Davila D, Guaza C, Vitorica J, Torres-Aleman I (2012) Regulation of the phosphatase calcineurin by insulin-like growth factor I unveils a key role of astrocytes in Alzheimer's pathology. Molecular psychiatry 17:705-718.
Ferrante RJ, Andreassen OA, Dedeoglu A, Ferrante KL, Jenkins BG, Hersch SM, Beal MF (2002) Therapeutic effects of coenzyme Q10 and remacemide in transgenic mouse models of Huntington's disease. The Journal of neuroscience : the official journal of the Society for Neuroscience 22:1592-1599.
Ferrante RJ, Andreassen OA, Jenkins BG, Dedeoglu A, Kuemmerle S, Kubilus JK, Kaddurah-Daouk R, Hersch SM, Beal MF (2000) Neuroprotective effects of creatine in a transgenic mouse model of Huntington's disease. The Journal of neuroscience : the official journal of the Society for Neuroscience 20:4389-4397.
Ferrington DA, Gregerson DS (2012) Immunoproteasomes: structure, function, and antigen presentation. Progress in molecular biology and translational science 109:75-112.
Fischer AJ, Omar G, Eubanks J, McGuire CR, Dierks BD, Reh TA (2004) Different aspects of gliosis in retinal Muller glia can be induced by CNTF, insulin, and FGF2 in the absence of damage. Molecular vision 10:973-986.

Flotte TR, Carter BJ (1995) Adeno-associated virus vectors for gene therapy. Gene therapy 2:357-362.
Flugge G, Araya-Callis C, Garea-Rodriguez E, Stadelmann-Nessler C, Fuchs E (2014) NDRG2 as a marker protein for brain astrocytes. Cell and tissue research 357:31-41.
Foo LC, Allen NJ, Bushong EA, Ventura PB, Chung WS, Zhou L, Cahoy JD, Daneman R, Zong H, Ellisman MH, Barres BA (2011) Development of a method for the purification and culture of rodent astrocytes. Neuron 71:799-811.
Forno LS, DeLanney LE, Irwin I, Di Monte D, Langston JW (1992) Astrocytes and Parkinson's disease. Progress in brain research 94:429-436.
Frakes AE, Ferraiuolo L, Haidet-Phillips AM, Schmelzer L, Braun L, Miranda CJ, Ladner KJ, Bevan AK, Foust KD, Godbout JP, Popovich PG, Guttridge DC, Kaspar BK (2014) Microglia induce motor neuron death via the classical NF-kappaB pathway in amyotrophic lateral sclerosis. Neuron 81:1009-1023.
Freeman MR, Rowitch DH (2013) Evolving concepts of gliogenesis: a look way back and ahead to the next 25 years. Neuron 80:613-623.
Freeman SM, Whartenby KA, Freeman JL, Abboud CN, Marrogi AJ (1996) In situ use of suicide genes for cancer therapy. Seminars in oncology 23:31-45.
Fukuda AM, Badaut J (2012) Aquaporin 4: a player in cerebral edema and neuroinflammation. Journal of neuroinflammation 9:279.
Furman JL, Norris CM (2014) Calcineurin and glial signaling: neuroinflammation and beyond. Journal of neuroinflammation 11:158.
Furman JL, Sama DM, Gant JC, Beckett TL, Murphy MP, Bachstetter AD, Van Eldik LJ, Norris CM (2012) Targeting astrocytes ameliorates neurologic changes in a mouse model of Alzheimer's disease. The Journal of neuroscience : the official journal of the Society for Neuroscience 32:16129-16140.
Gadea A, Lopez-Colome AM (2001) Glial transporters for glutamate, glycine, and GABA: II. GABA transporters. Journal of neuroscience research 63:461-468.
Gallo V, Patrizio M, Levi G (1991) GABA release triggered by the activation of neuron-like non-NMDA receptors in cultured type 2 astrocytes is carrier-mediated. Glia 4:245-255.
Galvan L, Lepejova N, Gaillard MC, Malgorn C, Guillermier M, Houitte D, Bonvento G, Petit F, Dufour N, Hery P, Gerard M, Elalouf JM, Deglon N, Brouillet E, de Chaldee M (2012) Capucin does not modify the toxicity of a mutant Huntingtin fragment in vivo. Neurobiology of aging 33:1845 e1845-1846.
Gan L, Vargas MR, Johnson DA, Johnson JA (2012) Astrocyte-specific overexpression of Nrf2 delays motor pathology and synuclein aggregation throughout the CNS in the alpha-synuclein mutant (A53T) mouse model. The Journal of neuroscience : the official journal of the Society for Neuroscience 32:17775-17787.
Garcia-Marin V, Garcia-Lopez P, Freire M (2007) Cajal's contributions to glia research. Trends in neurosciences 30:479-487.
Garden GA, La Spada AR (2012) Intercellular (mis)communication in neurodegenerative disease. Neuron 73:886-901.
Gauthier LR, Charrin BC, Borrell-Pages M, Dompierre JP, Rangone H, Cordelieres FP, De Mey J, MacDonald ME, Lessmann V, Humbert S, Saudou F (2004) Huntingtin controls neurotrophic support and survival of neurons by enhancing BDNF vesicular transport along microtubules. Cell 118:127-138.
Gavillet M, Allaman I, Magistretti PJ (2008) Modulation of astrocytic metabolic phenotype by proinflammatory cytokines. Glia 56:975-989.
Ge WP, Miyawaki A, Gage FH, Jan YN, Jan LY (2012) Local generation of glia is a major astrocyte source in postnatal cortex. Nature 484:376-380.
Genoud C, Quairiaux C, Steiner P, Hirling H, Welker E, Knott GW (2006) Plasticity of astrocytic coverage and glutamate transporter expression in adult mouse cortex. PLoS biology 4:e343.
Gervais FG, Singaraja R, Xanthoudakis S, Gutekunst CA, Leavitt BR, Metzler M, Hackam AS, Tam J, Vaillancourt JP, Houtzager V, Rasper DM, Roy S, Hayden MR, Nicholson DW (2002) Recruitment and activation of caspase-8 by the Huntingtin-interacting protein Hip-1 and a novel partner Hippi. Nature cell biology 4:95-105.
Giacobini E, Gold G (2013) Alzheimer disease therapy--moving from amyloid-beta to tau. Nature reviews Neurology 9:677-686.

Giaume C, Koulakoff A, Roux L, Holcman D, Rouach N (2010) Astroglial networks: a step further in neuroglial and gliovascular interactions. Nature reviews Neuroscience 11:87-99.
Giralt A, Friedman HC, Caneda-Ferron B, Urban N, Moreno E, Rubio N, Blanco J, Peterson A, Canals JM, Alberch J (2010) BDNF regulation under GFAP promoter provides engineered astrocytes as a new approach for long-term protection in Huntington's disease. Gene therapy 17:1294-1308.
Gong YH, Parsadanian AS, Andreeva A, Snider WD, Elliott JL (2000) Restricted expression of G86R Cu/Zn superoxide dismutase in astrocytes results in astrocytosis but does not cause motoneuron degeneration. The Journal of neuroscience : the official journal of the Society for Neuroscience 20:660-665.
Goritz C, Mauch DH, Pfrieger FW (2005) Multiple mechanisms mediate cholesterol-induced synaptogenesis in a CNS neuron. Molecular and cellular neurosciences 29:190-201.
Goritz C, Thiebaut R, Tessier LH, Nieweg K, Moehle C, Buard I, Dupont JL, Schurgers LJ, Schmitz G, Pfrieger FW (2007) Glia-induced neuronal differentiation by transcriptional regulation. Glia 55:1108-1122.
Gourine AV, Kasymov V, Marina N, Tang F, Figueiredo MF, Lane S, Teschemacher AG, Spyer KM, Deisseroth K, Kasparov S (2010) Astrocytes control breathing through pH-dependent release of ATP. Science 329:571-575.
Grafton ST, Mazziotta JC, Pahl JJ, St George-Hyslop P, Haines JL, Gusella J, Hoffman JM, Baxter LR, Phelps ME (1992) Serial changes of cerebral glucose metabolism and caudate size in persons at risk for Huntington's disease. Archives of neurology 49:1161-1167.
Granic I, Dolga AM, Nijholt IM, van Dijk G, Eisel UL (2009) Inflammation and NF-kappaB in Alzheimer's disease and diabetes. Journal of Alzheimer's disease : JAD 16:809-821.
Grison A, Mantovani F, Comel A, Agostoni E, Gustincich S, Persichetti F, Del Sal G (2011) Ser46 phosphorylation and prolyl-isomerase Pin1-mediated isomerization of p53 are key events in p53-dependent apoptosis induced by mutant huntingtin. Proceedings of the National Academy of Sciences of the United States of America 108:17979-17984.
Grivennikov SI, Karin M (2010) Dangerous liaisons: STAT3 and NF-kappaB collaboration and crosstalk in cancer. Cytokine & growth factor reviews 21:11-19.
Grondin R, Kaytor MD, Ai Y, Nelson PT, Thakker DR, Heisel J, Weatherspoon MR, Blum JL, Burright EN, Zhang Z, Kaemmerer WF (2012) Six-month partial suppression of Huntingtin is well tolerated in the adult rhesus striatum. Brain : a journal of neurology 135:1197-1209.
Group THsDCR (1993) A novel gene containing a trinucleotide repeat that is expanded and unstable on Huntington's disease chromosomes. . Cell 72:971-983.
Gu X, Andre VM, Cepeda C, Li SH, Li XJ, Levine MS, Yang XW (2007) Pathological cell-cell interactions are necessary for striatal pathogenesis in a conditional mouse model of Huntington's disease. Molecular neurodegeneration 2:8.
Gu X, Li C, Wei W, Lo V, Gong S, Li SH, Iwasato T, Itohara S, Li XJ, Mody I, Heintz N, Yang XW (2005) Pathological cell-cell interactions elicited by a neuropathogenic form of mutant Huntingtin contribute to cortical pathogenesis in HD mice. Neuron 46:433-444.
Gu XL, Long CX, Sun L, Xie C, Lin X, Cai H (2010) Astrocytic expression of Parkinson's disease-related A53T alpha-synuclein causes neurodegeneration in mice. Molecular brain 3:12.
Guo JL, Lee VM (2014) Cell-to-cell transmission of pathogenic proteins in neurodegenerative diseases. Nature medicine 20:130-138.
Haan S, Wuller S, Kaczor J, Rolvering C, Nocker T, Behrmann I, Haan C (2009) SOCS-mediated downregulation of mutant Jak2 (V617F, T875N and K539L) counteracts cytokine-independent signaling. Oncogene 28:3069-3080.
Haidet-Phillips AM, Hester ME, Miranda CJ, Meyer K, Braun L, Frakes A, Song S, Likhite S, Murtha MJ, Foust KD, Rao M, Eagle A, Kammesheidt A, Christensen A, Mendell JR, Burghes AH, Kaspar BK (2011) Astrocytes from familial and sporadic ALS patients are toxic to motor neurons. Nature biotechnology 29:824-828.
Halassa MM, Fellin T, Takano H, Dong JH, Haydon PG (2007) Synaptic islands defined by the territory of a single astrocyte. The Journal of neuroscience : the official journal of the Society for Neuroscience 27:6473-6477.
Halassa MM, Florian C, Fellin T, Munoz JR, Lee SY, Abel T, Haydon PG, Frank MG (2009) Astrocytic modulation of sleep homeostasis and cognitive consequences of sleep loss. Neuron 61:213-219.

Hamby ME, Sofroniew MV (2010) Reactive astrocytes as therapeutic targets for CNS disorders. Neurotherapeutics : the journal of the American Society for Experimental NeuroTherapeutics 7:494-506.
Hamby ME, Coppola G, Ao Y, Geschwind DH, Khakh BS, Sofroniew MV (2012) Inflammatory mediators alter the astrocyte transcriptome and calcium signaling elicited by multiple G-protein-coupled receptors. The Journal of neuroscience : the official journal of the Society for Neuroscience 32:14489-14510.
Hamilton NB, Attwell D (2010) Do astrocytes really exocytose neurotransmitters? Nature reviews Neuroscience 11:227-238.
Han X, Chen M, Wang F, Windrem M, Wang S, Shanz S, Xu Q, Oberheim NA, Bekar L, Betstadt S, Silva AJ, Takano T, Goldman SA, Nedergaard M (2013) Forebrain engraftment by human glial progenitor cells enhances synaptic plasticity and learning in adult mice. Cell stem cell 12:342-353.
Hanneken A, Ying W, Ling N, Baird A (1994) Identification of soluble forms of the fibroblast growth factor receptor in blood. Proceedings of the National Academy of Sciences of the United States of America 91:9170-9174.
Hayden MS, Ghosh S (2008) Shared principles in NF-kappaB signaling. Cell 132:344-362.
He F, Ge W, Martinowich K, Becker-Catania S, Coskun V, Zhu W, Wu H, Castro D, Guillemot F, Fan G, de Vellis J, Sun YE (2005) A positive autoregulatory loop of Jak-STAT signaling controls the onset of astrogliogenesis. Nature neuroscience 8:616-625.
Hebert MA, O'Callaghan JP (2000) Protein phosphorylation cascades associated with methamphetamine-induced glial activation. Annals of the New York Academy of Sciences 914:238-262.
Henneberger C, Papouin T, Oliet SH, Rusakov DA (2010) Long-term potentiation depends on release of D-serine from astrocytes. Nature 463:232-236.
Herculano-Houzel S (2014) The glia/neuron ratio: How it varies uniformly across brain structures and species and what that means for brain physiology and evolution. Glia 62:1377-1391.
Herrmann JE, Imura T, Song B, Qi J, Ao Y, Nguyen TK, Korsak RA, Takeda K, Akira S, Sofroniew MV (2008) STAT3 is a critical regulator of astrogliosis and scar formation after spinal cord injury. The Journal of neuroscience : the official journal of the Society for Neuroscience 28:7231-7243.
Hipp MS, Park SH, Hartl FU (2014) Proteostasis impairment in protein-misfolding and -aggregation diseases. Trends in cell biology 24:506-514.
Hirsch EC, Hunot S (2009) Neuroinflammation in Parkinson's disease: a target for neuroprotection? The Lancet Neurology 8:382-397.
Hirsch EC, Jenner P, Przedborski S (2013) Pathogenesis of Parkinson's disease. Movement disorders : official journal of the Movement Disorder Society 28:24-30.
Hoffmann A, Baltimore D (2006) Circuitry of nuclear factor kappaB signaling. Immunological reviews 210:171-186.
Hogan PG, Chen L, Nardone J, Rao A (2003) Transcriptional regulation by calcium, calcineurin, and NFAT. Genes & development 17:2205-2232.
Holmberg CI, Staniszewski KE, Mensah KN, Matouschek A, Morimoto RI (2004) Inefficient degradation of truncated polyglutamine proteins by the proteasome. The EMBO journal 23:4307-4318.
Hottinger AF, Azzouz M, Deglon N, Aebischer P, Zurn AD (2000) Complete and long-term rescue of lesioned adult motoneurons by lentiviral-mediated expression of glial cell line-derived neurotrophic factor in the facial nucleus. The Journal of neuroscience : the official journal of the Society for Neuroscience 20:5587-5593.
Houades V, Koulakoff A, Ezan P, Seif I, Giaume C (2008) Gap junction-mediated astrocytic networks in the mouse barrel cortex. The Journal of neuroscience : the official journal of the Society for Neuroscience 28:5207-5217.
Hsiao HY, Chern Y (2010) Targeting glial cells to elucidate the pathogenesis of Huntington's disease. Molecular neurobiology 41:248-255.
Hsiao HY, Chen YC, Chen HM, Tu PH, Chern Y (2013) A critical role of astrocyte-mediated nuclear factor-kappaB-dependent inflammation in Huntington's disease. Human molecular genetics 22:1826-1842.

Hsieh HL, Wang HH, Wu WB, Chu PJ, Yang CM (2010) Transforming growth factor-beta1 induces matrix metalloproteinase-9 and cell migration in astrocytes: roles of ROS-dependent ERK- and JNK-NF-kappaB pathways. Journal of neuroinflammation 7:88.

Huang Y, Mucke L (2012) Alzheimer mechanisms and therapeutic strategies. Cell 148:1204-1222.

Huang YH, Bergles DE (2004) Glutamate transporters bring competition to the synapse. Current opinion in neurobiology 14:346-352.

Hunter JM, Lesort M, Johnson GV (2007) Ubiquitin-proteasome system alterations in a striatal cell model of Huntington's disease. Journal of neuroscience research 85:1774-1788.

Hutchins AP, Diez D, Takahashi Y, Ahmad S, Jauch R, Tremblay ML, Miranda-Saavedra D (2013) Distinct transcriptional regulatory modules underlie STAT3's cell type-independent and cell type-specific functions. Nucleic acids research 41:2155-2170.

Hwang CJ, Yun HM, Jung YY, Lee DH, Yoon NY, Seo HO, Han JY, Oh KW, Choi DY, Han SB, Yoon DY, Hong JT (2014) Reducing Effect of IL-32alpha in the Development of Stroke Through Blocking of NF-kappaB, but Enhancement of STAT3 Pathways. Molecular neurobiology.

Ilieva H, Polymenidou M, Cleveland DW (2009) Non-cell autonomous toxicity in neurodegenerative disorders: ALS and beyond. The Journal of cell biology 187:761-772.

Itoh K, Chiba T, Takahashi S, Ishii T, Igarashi K, Katoh Y, Oyake T, Hayashi N, Satoh K, Hatayama I, Yamamoto M, Nabeshima Y (1997) An Nrf2/small Maf heterodimer mediates the induction of phase II detoxifying enzyme genes through antioxidant response elements. Biochemical and biophysical research communications 236:313-322.

Janelsins MC, Mastrangelo MA, Park KM, Sudol KL, Narrow WC, Oddo S, LaFerla FM, Callahan LM, Federoff HJ, Bowers WJ (2008) Chronic neuron-specific tumor necrosis factor-alpha expression enhances the local inflammatory environment ultimately leading to neuronal death in 3xTg-AD mice. The American journal of pathology 173:1768-1782.

Jankovic J (2008) Parkinson's disease: clinical features and diagnosis. Journal of neurology, neurosurgery, and psychiatry 79:368-376.

Jankowsky JL, Fadale DJ, Anderson J, Xu GM, Gonzales V, Jenkins NA, Copeland NG, Lee MK, Younkin LH, Wagner SL, Younkin SG, Borchelt DR (2004) Mutant presenilins specifically elevate the levels of the 42 residue beta-amyloid peptide in vivo: evidence for augmentation of a 42-specific gamma secretase. Human molecular genetics 13:159-170.

Jayakumar AR, Tong XY, Ruiz-Cordero R, Bregy A, Bethea JR, Bramlett HM, Norenberg MD (2014) Activation of NF-kappaB Mediates Astrocyte Swelling and Brain Edema in Traumatic Brain Injury. Journal of neurotrauma.

Jeffrey KL, Camps M, Rommel C, Mackay CR (2007) Targeting dual-specificity phosphatases: manipulating MAP kinase signalling and immune responses. Nature reviews Drug discovery 6:391-403.

Jenkins BG, Koroshetz WJ, Beal MF, Rosen BR (1993) Evidence for impairment of energy metabolism in vivo in Huntington's disease using localized 1H NMR spectroscopy. Neurology 43:2689-2695.

Jia H, Pallos J, Jacques V, Lau A, Tang B, Cooper A, Syed A, Purcell J, Chen Y, Sharma S, Sangrey GR, Darnell SB, Plasterer H, Sadri-Vakili G, Gottesfeld JM, Thompson LM, Rusche JR, Marsh JL, Thomas EA (2012) Histone deacetylase (HDAC) inhibitors targeting HDAC3 and HDAC1 ameliorate polyglutamine-elicited phenotypes in model systems of Huntington's disease. Neurobiology of disease 46:351-361.

Jo S et al. (2014) GABA from reactive astrocytes impairs memory in mouse models of Alzheimer's disease. Nature medicine 20:886-896.

Johnson JA, el Barbary A, Kornguth SE, Brugge JF, Siegel FL (1993) Glutathione S-transferase isoenzymes in rat brain neurons and glia. The Journal of neuroscience : the official journal of the Society for Neuroscience 13:2013-2023.

Juenemann K, Schipper-Krom S, Wiemhoefer A, Kloss A, Sanz Sanz A, Reits EA (2013) Expanded polyglutamine-containing N-terminal huntingtin fragments are entirely degraded by mammalian proteasomes. The Journal of biological chemistry 288:27068-27084.

Jung ES, An K, Hong HS, Kim JH, Mook-Jung I (2012) Astrocyte-originated ATP protects Abeta(1-42)-induced impairment of synaptic plasticity. The Journal of neuroscience : the official journal of the Society for Neuroscience 32:3081-3087.

Justicia C, Gabriel C, Planas AM (2000) Activation of the JAK/STAT pathway following transient focal cerebral ischemia: signaling through Jak1 and Stat3 in astrocytes. Glia 30:253-270.

Kaltschmidt B, Widera D, Kaltschmidt C (2005) Signaling via NF-kappaB in the nervous system. Biochimica et biophysica acta 1745:287-299.
Kamakura S, Oishi K, Yoshimatsu T, Nakafuku M, Masuyama N, Gotoh Y (2004) Hes binding to STAT3 mediates crosstalk between Notch and JAK-STAT signalling. Nature cell biology 6:547-554.
Kang W, Hebert JM (2011) Signaling pathways in reactive astrocytes, a genetic perspective. Molecular neurobiology 43:147-154.
Kang W, Balordi F, Su N, Chen L, Fishell G, Hebert JM (2014) Astrocyte activation is suppressed in both normal and injured brain by FGF signaling. Proceedings of the National Academy of Sciences of the United States of America 111:E2987-2995.
Kanski R, van Strien ME, van Tijn P, Hol EM (2014) A star is born: new insights into the mechanism of astrogenesis. Cellular and molecular life sciences : CMLS 71:433-447.
Katzman R (1986) Alzheimer's disease. The New England journal of medicine 314:964-973.
Kershaw NJ, Murphy JM, Lucet IS, Nicola NA, Babon JJ (2013a) Regulation of Janus kinases by SOCS proteins. Biochemical Society transactions 41:1042-1047.
Kershaw NJ, Murphy JM, Liau NP, Varghese LN, Laktyushin A, Whitlock EL, Lucet IS, Nicola NA, Babon JJ (2013b) SOCS3 binds specific receptor-JAK complexes to control cytokine signaling by direct kinase inhibition. Nature structural & molecular biology 20:469-476.
Khoshnan A, Patterson PH (2011) The role of IkappaB kinase complex in the neurobiology of Huntington's disease. Neurobiology of disease 43:305-311.
Kiechle T, Dedeoglu A, Kubilus J, Kowall NW, Beal MF, Friedlander RM, Hersch SM, Ferrante RJ (2002) Cytochrome C and caspase-9 expression in Huntington's disease. Neuromolecular medicine 1:183-195.
Kile BT, Schulman BA, Alexander WS, Nicola NA, Martin HM, Hilton DJ (2002) The SOCS box: a tale of destruction and degradation. Trends in biochemical sciences 27:235-241.
Kinouchi R, Takeda M, Yang L, Wilhelmsson U, Lundkvist A, Pekny M, Chen DF (2003) Robust neural integration from retinal transplants in mice deficient in GFAP and vimentin. Nature neuroscience 6:863-868.
Kiu H, Nicholson SE (2012) Biology and significance of the JAK/STAT signalling pathways. Growth factors 30:88-106.
Klausberger T (2009) GABAergic interneurons targeting dendrites of pyramidal cells in the CA1 area of the hippocampus. The European journal of neuroscience 30:947-957.
Koistinaho M, Kettunen MI, Goldsteins G, Keinanen R, Salminen A, Ort M, Bures J, Liu D, Kauppinen RA, Higgins LS, Koistinaho J (2002) Beta-amyloid precursor protein transgenic mice that harbor diffuse A beta deposits but do not form plaques show increased ischemic vulnerability: role of inflammation. Proceedings of the National Academy of Sciences of the United States of America 99:1610-1615.
Koistinaho M, Lin S, Wu X, Esterman M, Koger D, Hanson J, Higgs R, Liu F, Malkani S, Bales KR, Paul SM (2004) Apolipoprotein E promotes astrocyte colocalization and degradation of deposited amyloid-beta peptides. Nature medicine 10:719-726.
Kordasiewicz HB, Stanek LM, Wancewicz EV, Mazur C, McAlonis MM, Pytel KA, Artates JW, Weiss A, Cheng SH, Shihabuddin LS, Hung G, Bennett CF, Cleveland DW (2012) Sustained therapeutic reversal of Huntington's disease by transient repression of huntingtin synthesis. Neuron 74:1031-1044.
Kraft AW, Hu X, Yoon H, Yan P, Xiao Q, Wang Y, Gil SC, Brown J, Wilhelmsson U, Restivo JL, Cirrito JR, Holtzman DM, Kim J, Pekny M, Lee JM (2013) Attenuating astrocyte activation accelerates plaque pathogenesis in APP/PS1 mice. FASEB journal : official publication of the Federation of American Societies for Experimental Biology 27:187-198.
Kriegstein A, Alvarez-Buylla A (2009) The glial nature of embryonic and adult neural stem cells. Annual review of neuroscience 32:149-184.
Krutzik PO, Crane JM, Clutter MR, Nolan GP (2008) High-content single-cell drug screening with phosphospecific flow cytometry. Nature chemical biology 4:132-142.
Kuchibhotla KV, Lattarulo CR, Hyman BT, Bacskai BJ (2009) Synchronous hyperactivity and intercellular calcium waves in astrocytes in Alzheimer mice. Science 323:1211-1215.
Kucukdereli H, Allen NJ, Lee AT, Feng A, Ozlu MI, Conatser LM, Chakraborty C, Workman G, Weaver M, Sage EH, Barres BA, Eroglu C (2011) Control of excitatory CNS synaptogenesis by

astrocyte-secreted proteins Hevin and SPARC. Proceedings of the National Academy of Sciences of the United States of America 108:E440-449.
Kullmann DM, Asztely F (1998) Extrasynaptic glutamate spillover in the hippocampus: evidence and implications. Trends in neurosciences 21:8-14.
Lagier-Tourenne C et al. (2013) Targeted degradation of sense and antisense C9orf72 RNA foci as therapy for ALS and frontotemporal degeneration. Proceedings of the National Academy of Sciences of the United States of America 110:E4530-4539.
Landles C, Bates GP (2004) Huntingtin and the molecular pathogenesis of Huntington's disease. Fourth in molecular medicine review series. EMBO reports 5:958-963.
Lee Y, Messing A, Su M, Brenner M (2008) GFAP promoter elements required for region-specific and astrocyte-specific expression. Glia 56:481-493.
Leibinger M, Muller A, Andreadaki A, Hauk TG, Kirsch M, Fischer D (2009) Neuroprotective and axon growth-promoting effects following inflammatory stimulation on mature retinal ganglion cells in mice depend on ciliary neurotrophic factor and leukemia inhibitory factor. The Journal of neuroscience : the official journal of the Society for Neuroscience 29:14334-14341.
Leonard WJ (2001) Cytokines and immunodeficiency diseases. Nature reviews Immunology 1:200-208.
Lepore AC, Dejea C, Carmen J, Rauck B, Kerr DA, Sofroniew MV, Maragakis NJ (2008) Selective ablation of proliferating astrocytes does not affect disease outcome in either acute or chronic models of motor neuron degeneration. Experimental neurology 211:423-432.
Levy DE, Darnell JE, Jr. (2002) Stats: transcriptional control and biological impact. Nature reviews Molecular cell biology 3:651-662.
Li L et al. (2008) Protective role of reactive astrocytes in brain ischemia. Journal of cerebral blood flow and metabolism : official journal of the International Society of Cerebral Blood Flow and Metabolism 28:468-481.
Li X, Wang CE, Huang S, Xu X, Li XJ, Li H, Li S (2010) Inhibiting the ubiquitin-proteasome system leads to preferential accumulation of toxic N-terminal mutant huntingtin fragments. Human molecular genetics 19:2445-2455.
Lievens JC, Rival T, Iche M, Chneiweiss H, Birman S (2005) Expanded polyglutamine peptides disrupt EGF receptor signaling and glutamate transporter expression in Drosophila. Human molecular genetics 14:713-724.
Lievens JC, Woodman B, Mahal A, Spasic-Boscovic O, Samuel D, Kerkerian-Le Goff L, Bates GP (2001) Impaired glutamate uptake in the R6 Huntington's disease transgenic mice. Neurobiology of disease 8:807-821.
Lin RC, Matesic DF, Marvin M, McKay RD, Brustle O (1995) Re-expression of the intermediate filament nestin in reactive astrocytes. Neurobiology of disease 2:79-85.
Ling SC, Polymenidou M, Cleveland DW (2013) Converging mechanisms in ALS and FTD: disrupted RNA and protein homeostasis. Neuron 79:416-438.
Liu Z, Li Y, Cui Y, Roberts C, Lu M, Wilhelmsson U, Pekny M, Chopp M (2014) Beneficial effects of gfap/vimentin reactive astrocytes for axonal remodeling and motor behavioral recovery in mice after stroke. Glia.
Lobsiger CS, Cleveland DW (2007) Glial cells as intrinsic components of non-cell-autonomous neurodegenerative disease. Nature neuroscience 10:1355-1360.
Lovatt D, Sonnewald U, Waagepetersen HS, Schousboe A, He W, Lin JH, Han X, Takano T, Wang S, Sim FJ, Goldman SA, Nedergaard M (2007) The transcriptome and metabolic gene signature of protoplasmic astrocytes in the adult murine cortex. The Journal of neuroscience : the official journal of the Society for Neuroscience 27:12255-12266.
Lowenstein PR, Castro MG (2002) Progress and challenges in viral vector-mediated gene transfer to the brain. Current opinion in molecular therapeutics 4:359-371.
Lu B, Al-Ramahi I, Valencia A, Wang Q, Berenshteyn F, Yang H, Gallego-Flores T, Ichcho S, Lacoste A, Hild M, Difiglia M, Botas J, Palacino J (2013) Identification of NUB1 as a suppressor of mutant Huntington toxicity via enhanced protein clearance. Nature neuroscience 16:562-570.
Magistretti PJ (2006) Neuron-glia metabolic coupling and plasticity. The Journal of experimental biology 209:2304-2311.
Magistretti PJ, Pellerin L, Rothman DL, Shulman RG (1999) Energy on demand. Science 283:496-497.
Malenka RC, Bear MF (2004) LTP and LTD: an embarrassment of riches. Neuron 44:5-21.

Mandell JW, VandenBerg SR (1999) ERK/MAP kinase is chronically activated in human reactive astrocytes. Neuroreport 10:3567-3572.
Mandell JW, Gocan NC, Vandenberg SR (2001) Mechanical trauma induces rapid astroglial activation of ERK/MAP kinase: Evidence for a paracrine signal. Glia 34:283-295.
Maragakis NJ, Rothstein JD (2006) Mechanisms of Disease: astrocytes in neurodegenerative disease. Nature clinical practice Neurology 2:679-689.
Marchetto MC, Muotri AR, Mu Y, Smith AM, Cezar GG, Gage FH (2008) Non-cell-autonomous effect of human SOD1 G37R astrocytes on motor neurons derived from human embryonic stem cells. Cell stem cell 3:649-657.
Marco S, Giralt A, Petrovic MM, Pouladi MA, Martinez-Turrillas R, Martinez-Hernandez J, Kaltenbach LS, Torres-Peraza J, Graham RK, Watanabe M, Lujan R, Nakanishi N, Lipton SA, Lo DC, Hayden MR, Alberch J, Wesseling JF, Perez-Otano I (2013) Suppressing aberrant GluN3A expression rescues synaptic and behavioral impairments in Huntington's disease models. Nature medicine 19:1030-1038.
Martinez-Vicente M, Talloczy Z, Wong E, Tang G, Koga H, Kaushik S, de Vries R, Arias E, Harris S, Sulzer D, Cuervo AM (2010) Cargo recognition failure is responsible for inefficient autophagy in Huntington's disease. Nature neuroscience 13:567-576.
Mattson MP, Camandola S (2001) NF-kappaB in neuronal plasticity and neurodegenerative disorders. The Journal of clinical investigation 107:247-254.
Matyash V, Kettenmann H (2010) Heterogeneity in astrocyte morphology and physiology. Brain research reviews 63:2-10.
Mauch DH, Nagler K, Schumacher S, Goritz C, Muller EC, Otto A, Pfrieger FW (2001) CNS synaptogenesis promoted by glia-derived cholesterol. Science 294:1354-1357.
Maynard CJ, Bottcher C, Ortega Z, Smith R, Florea BI, Diaz-Hernandez M, Brundin P, Overkleeft HS, Li JY, Lucas JJ, Dantuma NP (2009) Accumulation of ubiquitin conjugates in a polyglutamine disease model occurs without global ubiquitin/proteasome system impairment. Proceedings of the National Academy of Sciences of the United States of America 106:13986-13991.
McBride JL, Pitzer MR, Boudreau RL, Dufour B, Hobbs T, Ojeda SR, Davidson BL (2011) Preclinical safety of RNAi-mediated HTT suppression in the rhesus macaque as a potential therapy for Huntington's disease. Molecular therapy : the journal of the American Society of Gene Therapy 19:2152-2162.
McCown TJ (2011) Adeno-Associated Virus (AAV) Vectors in the CNS. Current gene therapy 11:181-188.
McDowell AL, Dixon LJ, Houchins JD, Bilotta J (2004) Visual processing of the zebrafish optic tectum before and after optic nerve damage. Visual neuroscience 21:97-106.
Medeiros R, LaFerla FM (2013) Astrocytes: conductors of the Alzheimer disease neuroinflammatory symphony. Experimental neurology 239:133-138.
Medeiros R, Figueiredo CP, Pandolfo P, Duarte FS, Prediger RD, Passos GF, Calixto JB (2010) The role of TNF-alpha signaling pathway on COX-2 upregulation and cognitive decline induced by beta-amyloid peptide. Behavioural brain research 209:165-173.
Medeiros R, Prediger RD, Passos GF, Pandolfo P, Duarte FS, Franco JL, Dafre AL, Di Giunta G, Figueiredo CP, Takahashi RN, Campos MM, Calixto JB (2007) Connecting TNF-alpha signaling pathways to iNOS expression in a mouse model of Alzheimer's disease: relevance for the behavioral and synaptic deficits induced by amyloid beta protein. The Journal of neuroscience : the official journal of the Society for Neuroscience 27:5394-5404.
Meisingset TW, Risa O, Brenner M, Messing A, Sonnewald U (2010) Alteration of glial-neuronal metabolic interactions in a mouse model of Alexander disease. Glia 58:1228-1234.
Menalled LB, Sison JD, Dragatsis I, Zeitlin S, Chesselet MF (2003) Time course of early motor and neuropathological anomalies in a knock-in mouse model of Huntington's disease with 140 CAG repeats. The Journal of comparative neurology 465:11-26.
Menet V, Prieto M, Privat A, Gimenez y Ribotta M (2003) Axonal plasticity and functional recovery after spinal cord injury in mice deficient in both glial fibrillary acidic protein and vimentin genes. Proceedings of the National Academy of Sciences of the United States of America 100:8999-9004.
Mennerick S, Zorumski CF (1994) Glial contributions to excitatory neurotransmission in cultured hippocampal cells. Nature 368:59-62.

Messing A, Head MW, Galles K, Galbreath EJ, Goldman JE, Brenner M (1998) Fatal encephalopathy with astrocyte inclusions in GFAP transgenic mice. The American journal of pathology 152:391-398.
Miklossy G, Hilliard TS, Turkson J (2013) Therapeutic modulators of STAT signalling for human diseases. Nature reviews Drug discovery 12:611-629.
Milnerwood AJ, Gladding CM, Pouladi MA, Kaufman AM, Hines RM, Boyd JD, Ko RW, Vasuta OC, Graham RK, Hayden MR, Murphy TH, Raymond LA (2010) Early increase in extrasynaptic NMDA receptor signaling and expression contributes to phenotype onset in Huntington's disease mice. Neuron 65:178-190.
Mitani A, Tanaka K (2003) Functional changes of glial glutamate transporter GLT-1 during ischemia: an in vivo study in the hippocampal CA1 of normal mice and mutant mice lacking GLT-1. The Journal of neuroscience : the official journal of the Society for Neuroscience 23:7176-7182.
Molofsky AV, Krencik R, Ullian EM, Tsai HH, Deneen B, Richardson WD, Barres BA, Rowitch DH (2012) Astrocytes and disease: a neurodevelopmental perspective. Genes & development 26:891-907.
Molofsky AV, Kelley KW, Tsai HH, Redmond SA, Chang SM, Madireddy L, Chan JR, Baranzini SE, Ullian EM, Rowitch DH (2014) Astrocyte-encoded positional cues maintain sensorimotor circuit integrity. Nature 509:189-194.
Moumne L, Betuing S, Caboche J (2013) Multiple Aspects of Gene Dysregulation in Huntington's Disease. Frontiers in neurology 4:127.
Muller HW, Junghans U, Kappler J (1995) Astroglial neurotrophic and neurite-promoting factors. Pharmacology & therapeutics 65:1-18.
Mutch WA, Hansen AJ (1984) Extracellular pH changes during spreading depression and cerebral ischemia: mechanisms of brain pH regulation. Journal of cerebral blood flow and metabolism : official journal of the International Society of Cerebral Blood Flow and Metabolism 4:17-27.
Myer DJ, Gurkoff GG, Lee SM, Hovda DA, Sofroniew MV (2006) Essential protective roles of reactive astrocytes in traumatic brain injury. Brain : a journal of neurology 129:2761-2772.
Na YJ, Jin JK, Kim JI, Choi EK, Carp RI, Kim YS (2007) JAK-STAT signaling pathway mediates astrogliosis in brains of scrapie-infected mice. Journal of neurochemistry 103:637-649.
Nagai M, Re DB, Nagata T, Chalazonitis A, Jessell TM, Wichterle H, Przedborski S (2007) Astrocytes expressing ALS-linked mutated SOD1 release factors selectively toxic to motor neurons. Nature neuroscience 10:615-622.
Nagele RG, D'Andrea MR, Lee H, Venkataraman V, Wang HY (2003) Astrocytes accumulate A beta 42 and give rise to astrocytic amyloid plaques in Alzheimer disease brains. Brain research 971:197-209.
Naka T, Narazaki M, Hirata M, Matsumoto T, Minamoto S, Aono A, Nishimoto N, Kajita T, Taga T, Yoshizaki K, Akira S, Kishimoto T (1997) Structure and function of a new STAT-induced STAT inhibitor. Nature 387:924-929.
Nakazawa T, Takeda M, Lewis GP, Cho KS, Jiao J, Wilhelmsson U, Fisher SK, Pekny M, Chen DF, Miller JW (2007) Attenuated glial reactions and photoreceptor degeneration after retinal detachment in mice deficient in glial fibrillary acidic protein and vimentin. Investigative ophthalmology & visual science 48:2760-2768.
Namekata K, Harada C, Kohyama K, Matsumoto Y, Harada T (2008) Interleukin-1 stimulates glutamate uptake in glial cells by accelerating membrane trafficking of Na+/K+-ATPase via actin depolymerization. Molecular and cellular biology 28:3273-3280.
Ng CW, Yildirim F, Yap YS, Dalin S, Matthews BJ, Velez PJ, Labadorf A, Housman DE, Fraenkel E (2013) Extensive changes in DNA methylation are associated with expression of mutant huntingtin. Proceedings of the National Academy of Sciences of the United States of America 110:2354-2359.
Nicolas CS, Amici M, Bortolotto ZA, Doherty A, Csaba Z, Fafouri A, Dournaud P, Gressens P, Collingridge GL, Peineau S (2013) The role of JAK-STAT signaling within the CNS. Jak-Stat 2:e22925.
Nicolas CS et al. (2012) The Jak/STAT pathway is involved in synaptic plasticity. Neuron 73:374-390.
Nimmerjahn A, Mukamel EA, Schnitzer MJ (2009) Motor behavior activates Bergmann glial networks. Neuron 62:400-412.
Nobuta H, Ghiani CA, Paez PM, Spreuer V, Dong H, Korsak RA, Manukyan A, Li J, Vinters HV, Huang EJ, Rowitch DH, Sofroniew MV, Campagnoni AT, de Vellis J, Waschek JA (2012)

STAT3-mediated astrogliosis protects myelin development in neonatal brain injury. Annals of neurology 72:750-765.
O'Callaghan JP, Sriram K (2004) Focused microwave irradiation of the brain preserves in vivo protein phosphorylation: comparison with other methods of sacrifice and analysis of multiple phosphoproteins. Journal of neuroscience methods 135:159-168.
O'Callaghan JP, Kelly KA, VanGilder RL, Sofroniew MV, Miller DB (2014) Early activation of STAT3 regulates reactive astrogliosis induced by diverse forms of neurotoxicity. PloS one 9:e102003.
O'Shea JJ, Holland SM, Staudt LM (2013a) JAKs and STATs in immunity, immunodeficiency, and cancer. The New England journal of medicine 368:161-170.
O'Shea JJ, Kontzias A, Yamaoka K, Tanaka Y, Laurence A (2013b) Janus kinase inhibitors in autoimmune diseases. Annals of the rheumatic diseases 72 Suppl 2:ii111-115.
Oberheim NA, Goldman SA, Nedergaard M (2012) Heterogeneity of astrocytic form and function. Methods in molecular biology 814:23-45.
Oberheim NA, Tian GF, Han X, Peng W, Takano T, Ransom B, Nedergaard M (2008) Loss of astrocytic domain organization in the epileptic brain. The Journal of neuroscience : the official journal of the Society for Neuroscience 28:3264-3276.
Oberheim NA, Takano T, Han X, He W, Lin JH, Wang F, Xu Q, Wyatt JD, Pilcher W, Ojemann JG, Ransom BR, Goldman SA, Nedergaard M (2009) Uniquely hominid features of adult human astrocytes. The Journal of neuroscience : the official journal of the Society for Neuroscience 29:3276-3287.
Oddo S, Caccamo A, Kitazawa M, Tseng BP, LaFerla FM (2003a) Amyloid deposition precedes tangle formation in a triple transgenic model of Alzheimer's disease. Neurobiology of aging 24:1063-1070.
Oddo S, Caccamo A, Shepherd JD, Murphy MP, Golde TE, Kayed R, Metherate R, Mattson MP, Akbari Y, LaFerla FM (2003b) Triple-transgenic model of Alzheimer's disease with plaques and tangles: intracellular Abeta and synaptic dysfunction. Neuron 39:409-421.
Oeckinghaus A, Hayden MS, Ghosh S (2011) Crosstalk in NF-kappaB signaling pathways. Nature immunology 12:695-708.
Oikonomou G, Shaham S (2011) The glia of Caenorhabditis elegans. Glia 59:1253-1263.
Okada S, Nakamura M, Katoh H, Miyao T, Shimazaki T, Ishii K, Yamane J, Yoshimura A, Iwamoto Y, Toyama Y, Okano H (2006) Conditional ablation of Stat3 or Socs3 discloses a dual role for reactive astrocytes after spinal cord injury. Nature medicine 12:829-834.
Okamoto S, Pouladi MA, Talantova M, Yao D, Xia P, Ehrnhoefer DE, Zaidi R, Clemente A, Kaul M, Graham RK, Zhang D, Vincent Chen HS, Tong G, Hayden MR, Lipton SA (2009) Balance between synaptic versus extrasynaptic NMDA receptor activity influences inclusions and neurotoxicity of mutant huntingtin. Nature medicine 15:1407-1413.
Okaty BW, Sugino K, Nelson SB (2011) Cell type-specific transcriptomics in the brain. The Journal of neuroscience : the official journal of the Society for Neuroscience 31:6939-6943.
Oliet SH, Mothet JP (2006) Molecular determinants of D-serine-mediated gliotransmission: from release to function. Glia 54:726-737.
Oliet SH, Mothet JP (2009) Regulation of N-methyl-D-aspartate receptors by astrocytic D-serine. Neuroscience 158:275-283.
Oliet SH, Piet R, Poulain DA (2001) Control of glutamate clearance and synaptic efficacy by glial coverage of neurons. Science 292:923-926.
Oliva AA, Jr., Kang Y, Sanchez-Molano J, Furones C, Atkins CM (2012) STAT3 signaling after traumatic brain injury. Journal of neurochemistry 120:710-720.
Orre M, Kamphuis W, Osborn LM, Jansen AH, Kooijman L, Bossers K, Hol EM (2014a) Isolation of glia from Alzheimer's mice reveals inflammation and dysfunction. Neurobiology of aging.
Orre M, Kamphuis W, Osborn LM, Melief J, Kooijman L, Huitinga I, Klooster J, Bossers K, Hol EM (2014b) Acute isolation and transcriptome characterization of cortical astrocytes and microglia from young and aged mice. Neurobiology of aging 35:1-14.
Orre M, Kamphuis W, Dooves S, Kooijman L, Chan ET, Kirk CJ, Dimayuga Smith V, Koot S, Mamber C, Jansen AH, Ovaa H, Hol EM (2013) Reactive glia show increased immunoproteasome activity in Alzheimer's disease. Brain : a journal of neurology 136:1415-1431.
Ortega Z, Lucas JJ (2014) Ubiquitin-proteasome system involvement in Huntington's disease. Frontiers in molecular neuroscience 7:77.

Ortega Z, Diaz-Hernandez M, Lucas JJ (2007) Is the ubiquitin-proteasome system impaired in Huntington's disease? Cellular and molecular life sciences : CMLS 64:2245-2257.
Ortinski PI, Dong J, Mungenast A, Yue C, Takano H, Watson DJ, Haydon PG, Coulter DA (2010) Selective induction of astrocytic gliosis generates deficits in neuronal inhibition. Nature neuroscience 13:584-591.
Owen JB, Di Domenico F, Sultana R, Perluigi M, Cini C, Pierce WM, Butterfield DA (2009) Proteomics-determined differences in the concanavalin-A-fractionated proteome of hippocampus and inferior parietal lobule in subjects with Alzheimer's disease and mild cognitive impairment: implications for progression of AD. Journal of proteome research 8:471-482.
Palazuelos J, Aguado T, Pazos MR, Julien B, Carrasco C, Resel E, Sagredo O, Benito C, Romero J, Azcoitia I, Fernandez-Ruiz J, Guzman M, Galve-Roperh I (2009) Microglial CB2 cannabinoid receptors are neuroprotective in Huntington's disease excitotoxicity. Brain : a journal of neurology 132:3152-3164.
Palfi S, Brouillet E, Jarraya B, Bloch J, Jan C, Shin M, Conde F, Li XJ, Aebischer P, Hantraye P, Deglon N (2007) Expression of mutated huntingtin fragment in the putamen is sufficient to produce abnormal movement in non-human primates. Molecular therapy : the journal of the American Society of Gene Therapy 15:1444-1451.
Panatier A, Vallee J, Haber M, Murai KK, Lacaille JC, Robitaille R (2011) Astrocytes are endogenous regulators of basal transmission at central synapses. Cell 146:785-798.
Panatier A, Theodosis DT, Mothet JP, Touquet B, Pollegioni L, Poulain DA, Oliet SH (2006) Glia-derived D-serine controls NMDA receptor activity and synaptic memory. Cell 125:775-784.
Pannasch U, Rouach N (2013) Emerging role for astroglial networks in information processing: from synapse to behavior. Trends in neurosciences 36:405-417.
Pannasch U, Freche D, Dallerac G, Ghezali G, Escartin C, Ezan P, Cohen-Salmon M, Benchenane K, Abudara V, Dufour A, Lubke JH, Deglon N, Knott G, Holcman D, Rouach N (2014) Connexin 30 sets synaptic strength by controlling astroglial synapse invasion. Nature neuroscience 17:549-558.
Papadeas ST, Kraig SE, O'Banion C, Lepore AC, Maragakis NJ (2011) Astrocytes carrying the superoxide dismutase 1 (SOD1G93A) mutation induce wild-type motor neuron degeneration in vivo. Proceedings of the National Academy of Sciences of the United States of America 108:17803-17808.
Papouin T, Ladepeche L, Ruel J, Sacchi S, Labasque M, Hanini M, Groc L, Pollegioni L, Mothet JP, Oliet SH (2012) Synaptic and extrasynaptic NMDA receptors are gated by different endogenous coagonists. Cell 150:633-646.
Park KK, Hu Y, Muhling J, Pollett MA, Dallimore EJ, Turnley AM, Cui Q, Harvey AR (2009) Cytokine-induced SOCS expression is inhibited by cAMP analogue: impact on regeneration in injured retina. Molecular and cellular neurosciences 41:313-324.
Parsons MP, Raymond LA (2014) Extrasynaptic NMDA receptor involvement in central nervous system disorders. Neuron 82:279-293.
Paukert M, Agarwal A, Cha J, Doze VA, Kang JU, Bergles DE (2014) Norepinephrine controls astroglial responsiveness to local circuit activity. Neuron 82:1263-1270.
Pecho-Vrieseling E, Rieker C, Fuchs S, Bleckmann D, Esposito MS, Botta P, Goldstein C, Bernhard M, Galimberti I, Muller M, Luthi A, Arber S, Bouwmeester T, van der Putten H, Di Giorgio FP (2014) Transneuronal propagation of mutant huntingtin contributes to non-cell autonomous pathology in neurons. Nature neuroscience 17:1064-1072.
Pekny M, Nilsson M (2005) Astrocyte activation and reactive gliosis. Glia 50:427-434.
Pekny M, Johansson CB, Eliasson C, Stakeberg J, Wallen A, Perlmann T, Lendahl U, Betsholtz C, Berthold CH, Frisen J (1999) Abnormal reaction to central nervous system injury in mice lacking glial fibrillary acidic protein and vimentin. The Journal of cell biology 145:503-514.
Pellerin L, Magistretti PJ (1994) Glutamate uptake into astrocytes stimulates aerobic glycolysis: a mechanism coupling neuronal activity to glucose utilization. Proceedings of the National Academy of Sciences of the United States of America 91:10625-10629.
Pelvig DP, Pakkenberg H, Stark AK, Pakkenberg B (2008) Neocortical glial cell numbers in human brains. Neurobiology of aging 29:1754-1762.
Perkins ND (2007) Integrating cell-signalling pathways with NF-kappaB and IKK function. Nature reviews Molecular cell biology 8:49-62.

Petit JM, Tobler I, Allaman I, Borbely AA, Magistretti PJ (2002) Sleep deprivation modulates brain mRNAs encoding genes of glycogen metabolism. The European journal of neuroscience 16:1163-1167.
Pfrieger FW (2009) Roles of glial cells in synapse development. Cellular and molecular life sciences : CMLS 66:2037-2047.
Pfrieger FW, Barres BA (1997) Synaptic efficacy enhanced by glial cells in vitro. Science 277:1684-1687.
Pfrieger FW, Slezak M (2012) Genetic approaches to study glial cells in the rodent brain. Glia 60:681-701.
Pihlaja R, Koistinaho J, Malm T, Sikkila H, Vainio S, Koistinaho M (2008) Transplanted astrocytes internalize deposited beta-amyloid peptides in a transgenic mouse model of Alzheimer's disease. Glia 56:154-163.
Pinteaux E, Trotter P, Simi A (2009) Cell-specific and concentration-dependent actions of interleukin-1 in acute brain inflammation. Cytokine 45:1-7.
Pirttimaki T, Parri HR, Crunelli V (2013) Astrocytic GABA transporter GAT-1 dysfunction in experimental absence seizures. The Journal of physiology 591:823-833.
Porter JT, McCarthy KD (1997) Astrocytic neurotransmitter receptors in situ and in vivo. Progress in neurobiology 51:439-455.
Pringsheim T, Wiltshire K, Day L, Dykeman J, Steeves T, Jette N (2012) The incidence and prevalence of Huntington's disease: a systematic review and meta-analysis. Movement disorders : official journal of the Movement Disorder Society 27:1083-1091.
Ram PA, Waxman DJ (1999) SOCS/CIS protein inhibition of growth hormone-stimulated STAT5 signaling by multiple mechanisms. The Journal of biological chemistry 274:35553-35561.
Ramaswamy S, Kordower JH (2012) Gene therapy for Huntington's disease. Neurobiology of disease 48:243-254.
Ravikumar B, Rubinsztein DC (2006) Role of autophagy in the clearance of mutant huntingtin: a step towards therapy? Molecular aspects of medicine 27:520-527.
Regan MR, Huang YH, Kim YS, Dykes-Hoberg MI, Jin L, Watkins AM, Bergles DE, Rothstein JD (2007) Variations in promoter activity reveal a differential expression and physiology of glutamate transporters by glia in the developing and mature CNS. The Journal of neuroscience : the official journal of the Society for Neuroscience 27:6607-6619.
Reiman EM (2014) Alzheimer's disease and other dementias: advances in 2013. The Lancet Neurology 13:3-5.
Riedel G, Platt B, Micheau J (2003) Glutamate receptor function in learning and memory. Behavioural brain research 140:1-47.
Rigamonti D, Sipione S, Goffredo D, Zuccato C, Fossale E, Cattaneo E (2001) Huntingtin's neuroprotective activity occurs via inhibition of procaspase-9 processing. The Journal of biological chemistry 276:14545-14548.
Robb L, Boyle K, Rakar S, Hartley L, Lochland J, Roberts AW, Alexander WS, Metcalf D (2005) Genetic reduction of embryonic leukemia-inhibitory factor production rescues placentation in SOCS3-null embryos but does not prevent inflammatory disease. Proceedings of the National Academy of Sciences of the United States of America 102:16333-16338.
Robertson SA, Koleva RI, Argetsinger LS, Carter-Su C, Marto JA, Feener EP, Myers MG, Jr. (2009) Regulation of Jak2 function by phosphorylation of Tyr317 and Tyr637 during cytokine signaling. Molecular and cellular biology 29:3367-3378.
Roos M, Schachner M, Bernhardt RR (1999) Zebrafish semaphorin Z1b inhibits growing motor axons in vivo. Mechanisms of development 87:103-117.
Rosas HD, Doros G, Gevorkian S, Malarick K, Reuter M, Coutu JP, Triggs TD, Wilkens PJ, Matson W, Salat DH, Hersch SM (2014) PRECREST: a phase II prevention and biomarker trial of creatine in at-risk Huntington disease. Neurology 82:850-857.
Rose CR, Karus C (2013) Two sides of the same coin: sodium homeostasis and signaling in astrocytes under physiological and pathophysiological conditions. Glia 61:1191-1205.
Ross CA, Tabrizi SJ (2011) Huntington's disease: from molecular pathogenesis to clinical treatment. The Lancet Neurology 10:83-98.
Ross CA, Aylward EH, Wild EJ, Langbehn DR, Long JD, Warner JH, Scahill RI, Leavitt BR, Stout JC, Paulsen JS, Reilmann R, Unschuld PG, Wexler A, Margolis RL, Tabrizi SJ (2014) Huntington

disease: natural history, biomarkers and prospects for therapeutics. Nature reviews Neurology 10:204-216.
Rothstein JD, Martin L, Levey AI, Dykes-Hoberg M, Jin L, Wu D, Nash N, Kuncl RW (1994) Localization of neuronal and glial glutamate transporters. Neuron 13:713-725.
Rothstein JD, Patel S, Regan MR, Haenggeli C, Huang YH, Bergles DE, Jin L, Dykes Hoberg M, Vidensky S, Chung DS, Toan SV, Bruijn LI, Su ZZ, Gupta P, Fisher PB (2005) Beta-lactam antibiotics offer neuroprotection by increasing glutamate transporter expression. Nature 433:73-77.
Rouach N, Koulakoff A, Abudara V, Willecke K, Giaume C (2008) Astroglial metabolic networks sustain hippocampal synaptic transmission. Science 322:1551-1555.
Roze E, Saudou F, Caboche J (2008) Pathophysiology of Huntington's disease: from huntingtin functions to potential treatments. Current opinion in neurology 21:497-503.
Ruan L, Kang Z, Pei G, Le Y (2009) Amyloid deposition and inflammation in APPswe/PS1dE9 mouse model of Alzheimer's disease. Current Alzheimer research 6:531-540.
Ruiz M, Deglon N (2012) Viral-mediated overexpression of mutant huntingtin to model HD in various species. Neurobiology of disease 48:202-211.
Sabelstrom H, Stenudd M, Reu P, Dias DO, Elfineh M, Zdunek S, Damberg P, Goritz C, Frisen J (2013) Resident neural stem cells restrict tissue damage and neuronal loss after spinal cord injury in mice. Science 342:637-640.
Saft C, Zange J, Andrich J, Muller K, Lindenberg K, Landwehrmeyer B, Vorgerd M, Kraus PH, Przuntek H, Schols L (2005) Mitochondrial impairment in patients and asymptomatic mutation carriers of Huntington's disease. Movement disorders : official journal of the Movement Disorder Society 20:674-679.
Saganich MJ, Schroeder BE, Galvan V, Bredesen DE, Koo EH, Heinemann SF (2006) Deficits in synaptic transmission and learning in amyloid precursor protein (APP) transgenic mice require C-terminal cleavage of APP. The Journal of neuroscience : the official journal of the Society for Neuroscience 26:13428-13436.
Sama MA, Mathis DM, Furman JL, Abdul HM, Artiushin IA, Kraner SD, Norris CM (2008) Interleukin-1beta-dependent signaling between astrocytes and neurons depends critically on astrocytic calcineurin/NFAT activity. The Journal of biological chemistry 283:21953-21964.
Sarafian TA, Montes C, Imura T, Qi J, Coppola G, Geschwind DH, Sofroniew MV (2010) Disruption of astrocyte STAT3 signaling decreases mitochondrial function and increases oxidative stress in vitro. PloS one 5:e9532.
Saudou F, Finkbeiner S, Devys D, Greenberg ME (1998) Huntingtin acts in the nucleus to induce apoptosis but death does not correlate with the formation of intranuclear inclusions. Cell 95:55-66.
Saura J (2007) Microglial cells in astroglial cultures: a cautionary note. Journal of neuroinflammation 4:26.
Sawaishi Y (2009) Review of Alexander disease: beyond the classical concept of leukodystrophy. Brain & development 31:493-498.
Schapira AH, Olanow CW, Greenamyre JT, Bezard E (2014) Slowing of neurodegeneration in Parkinson's disease and Huntington's disease: future therapeutic perspectives. Lancet 384:545-555.
Scherzinger E, Lurz R, Turmaine M, Mangiarini L, Hollenbach B, Hasenbank R, Bates GP, Davies SW, Lehrach H, Wanker EE (1997) Huntingtin-encoded polyglutamine expansions form amyloid-like protein aggregates in vitro and in vivo. Cell 90:549-558.
Schilling G, Becher MW, Sharp AH, Jinnah HA, Duan K, Kotzuk JA, Slunt HH, Ratovitski T, Cooper JK, Jenkins NA, Copeland NG, Price DL, Ross CA, Borchelt DR (1999) Intranuclear inclusions and neuritic aggregates in transgenic mice expressing a mutant N-terminal fragment of huntingtin. Human molecular genetics 8:397-407.
Schipper-Krom S, Juenemann K, Reits EA (2012) The Ubiquitin-Proteasome System in Huntington's Disease: Are Proteasomes Impaired, Initiators of Disease, or Coming to the Rescue? Biochemistry research international 2012:837015.
Schipper-Krom S, Juenemann K, Jansen AH, Wiemhoefer A, van den Nieuwendijk R, Smith DL, Hink MA, Bates GP, Overkleeft H, Ovaa H, Reits E (2014) Dynamic recruitment of active proteasomes into polyglutamine initiated inclusion bodies. FEBS letters 588:151-159.

Schneider A, Martin-Villalba A, Weih F, Vogel J, Wirth T, Schwaninger M (1999) NF-kappaB is activated and promotes cell death in focal cerebral ischemia. Nature medicine 5:554-559.
Schummers J, Yu H, Sur M (2008) Tuned responses of astrocytes and their influence on hemodynamic signals in the visual cortex. Science 320:1638-1643.
Schurr A, Payne RS, Miller JJ, Rigor BM (1997) Glia are the main source of lactate utilized by neurons for recovery of function posthypoxia. Brain research 774:221-224.
Schwarcz R, Bruno JP, Muchowski PJ, Wu HQ (2012) Kynurenines in the mammalian brain: when physiology meets pathology. Nature reviews Neuroscience 13:465-477.
Schwarz DS, Ding H, Kennington L, Moore JT, Schelter J, Burchard J, Linsley PS, Aronin N, Xu Z, Zamore PD (2006) Designing siRNA that distinguish between genes that differ by a single nucleotide. PLoS genetics 2:e140.
Seo H, Sonntag KC, Isacson O (2004) Generalized brain and skin proteasome inhibition in Huntington's disease. Annals of neurology 56:319-328.
Sepers MD, Raymond LA (2014) Mechanisms of synaptic dysfunction and excitotoxicity in Huntington's disease. Drug discovery today 19:990-996.
Shibata N, Yamamoto T, Hiroi A, Omi Y, Kato Y, Kobayashi M (2010) Activation of STAT3 and inhibitory effects of pioglitazone on STAT3 activity in a mouse model of SOD1-mutated amyotrophic lateral sclerosis. Neuropathology : official journal of the Japanese Society of Neuropathology 30:353-360.
Shibata N, Kakita A, Takahashi H, Ihara Y, Nobukuni K, Fujimura H, Sakoda S, Sasaki S, Iwata M, Morikawa S, Hirano A, Kobayashi M (2009) Activation of signal transducer and activator of transcription-3 in the spinal cord of sporadic amyotrophic lateral sclerosis patients. Neuro-degenerative diseases 6:118-126.
Shibuki K, Gomi H, Chen L, Bao S, Kim JJ, Wakatsuki H, Fujisaki T, Fujimoto K, Katoh A, Ikeda T, Chen C, Thompson RF, Itohara S (1996) Deficient cerebellar long-term depression, impaired eyeblink conditioning, and normal motor coordination in GFAP mutant mice. Neuron 16:587-599.
Shin JY, Fang ZH, Yu ZX, Wang CE, Li SH, Li XJ (2005) Expression of mutant huntingtin in glial cells contributes to neuronal excitotoxicity. The Journal of cell biology 171:1001-1012.
Shoulson I, Fahn S (1979) Huntington disease: clinical care and evaluation. Neurology 29:1-3.
Shuai K, Liu B (2003) Regulation of JAK-STAT signalling in the immune system. Nature reviews Immunology 3:900-911.
Sigrist SJ, Plested AJ (2009) How to button a bouton with alpha2deltas. Nature neuroscience 12:1357-1358.
Silvestroni A, Faull RL, Strand AD, Moller T (2009) Distinct neuroinflammatory profile in post-mortem human Huntington's disease. Neuroreport 20:1098-1103.
Sirko S et al. (2013) Reactive glia in the injured brain acquire stem cell properties in response to sonic hedgehog. [corrected]. Cell stem cell 12:426-439.
Slow EJ, Graham RK, Osmand AP, Devon RS, Lu G, Deng Y, Pearson J, Vaid K, Bissada N, Wetzel R, Leavitt BR, Hayden MR (2005) Absence of behavioral abnormalities and neurodegeneration in vivo despite widespread neuronal huntingtin inclusions. Proceedings of the National Academy of Sciences of the United States of America 102:11402-11407.
Smith KM, Matson S, Matson WR, Cormier K, Del Signore SJ, Hagerty SW, Stack EC, Ryu H, Ferrante RJ (2006) Dose ranging and efficacy study of high-dose coenzyme Q10 formulations in Huntington's disease mice. Biochimica et biophysica acta 1762:616-626.
Smith PD, Sun F, Park KK, Cai B, Wang C, Kuwako K, Martinez-Carrasco I, Connolly L, He Z (2009) SOCS3 deletion promotes optic nerve regeneration in vivo. Neuron 64:617-623.
Sofroniew MV (2009) Molecular dissection of reactive astrogliosis and glial scar formation. Trends in neurosciences 32:638-647.
Sofroniew MV, Vinters HV (2010) Astrocytes: biology and pathology. Acta neuropathologica 119:7-35.
Somjen GG (1988) Nervenkitt: notes on the history of the concept of neuroglia. Glia 1:2-9.
Sosunov AA, Guilfoyle E, Wu X, McKhann GM, 2nd, Goldman JE (2013) Phenotypic conversions of "protoplasmic" to "reactive" astrocytes in Alexander disease. The Journal of neuroscience : the official journal of the Society for Neuroscience 33:7439-7450.
Sosunov AA, Wu X, Tsankova NM, Guilfoyle E, McKhann GM, 2nd, Goldman JE (2014) Phenotypic heterogeneity and plasticity of isocortical and hippocampal astrocytes in the human brain. The Journal of neuroscience : the official journal of the Society for Neuroscience 34:2285-2298.

Spalding KL, Bergmann O, Alkass K, Bernard S, Salehpour M, Huttner HB, Bostrom E, Westerlund I, Vial C, Buchholz BA, Possnert G, Mash DC, Druid H, Frisen J (2013) Dynamics of hippocampal neurogenesis in adult humans. Cell 153:1219-1227.

Sriram K, Benkovic SA, Hebert MA, Miller DB, O'Callaghan JP (2004) Induction of gp130-related cytokines and activation of JAK2/STAT3 pathway in astrocytes precedes up-regulation of glial fibrillary acidic protein in the 1-methyl-4-phenyl-1,2,3,6-tetrahydropyridine model of neurodegeneration: key signaling pathway for astrogliosis in vivo? The Journal of biological chemistry 279:19936-19947.

Starr R, Metcalf D, Elefanty AG, Brysha M, Willson TA, Nicola NA, Hilton DJ, Alexander WS (1998) Liver degeneration and lymphoid deficiencies in mice lacking suppressor of cytokine signaling-1. Proceedings of the National Academy of Sciences of the United States of America 95:14395-14399.

Starr R, Willson TA, Viney EM, Murray LJ, Rayner JR, Jenkins BJ, Gonda TJ, Alexander WS, Metcalf D, Nicola NA, Hilton DJ (1997) A family of cytokine-inducible inhibitors of signalling. Nature 387:917-921.

Stevens B, Allen NJ, Vazquez LE, Howell GR, Christopherson KS, Nouri N, Micheva KD, Mehalow AK, Huberman AD, Stafford B, Sher A, Litke AM, Lambris JD, Smith SJ, John SW, Barres BA (2007) The classical complement cascade mediates CNS synapse elimination. Cell 131:1164-1178.

Su ZZ, Leszczyniecka M, Kang DC, Sarkar D, Chao W, Volsky DJ, Fisher PB (2003) Insights into glutamate transport regulation in human astrocytes: cloning of the promoter for excitatory amino acid transporter 2 (EAAT2). Proceedings of the National Academy of Sciences of the United States of America 100:1955-1960.

Sun F, Park KK, Belin S, Wang D, Lu T, Chen G, Zhang K, Yeung C, Feng G, Yankner BA, He Z (2011) Sustained axon regeneration induced by co-deletion of PTEN and SOCS3. Nature 480:372-375.

Sun JY, Anand-Jawa V, Chatterjee S, Wong KK (2003) Immune responses to adeno-associated virus and its recombinant vectors. Gene therapy 10:964-976.

Surmeier DJ, Ding J, Day M, Wang Z, Shen W (2007) D1 and D2 dopamine-receptor modulation of striatal glutamatergic signaling in striatal medium spiny neurons. Trends in neurosciences 30:228-235.

Suzuki A, Stern SA, Bozdagi O, Huntley GW, Walker RH, Magistretti PJ, Alberini CM (2011) Astrocyte-neuron lactate transport is required for long-term memory formation. Cell 144:810-823.

Takahashi Y, Carpino N, Cross JC, Torres M, Parganas E, Ihle JN (2003) SOCS3: an essential regulator of LIF receptor signaling in trophoblast giant cell differentiation. The EMBO journal 22:372-384.

Takano T, Han X, Deane R, Zlokovic B, Nedergaard M (2007) Two-photon imaging of astrocytic Ca2+ signaling and the microvasculature in experimental mice models of Alzheimer's disease. Annals of the New York Academy of Sciences 1097:40-50.

Takata N, Hirase H (2008) Cortical layer 1 and layer 2/3 astrocytes exhibit distinct calcium dynamics in vivo. PloS one 3:e2525.

Tanaka K, Watase K, Manabe T, Yamada K, Watanabe M, Takahashi K, Iwama H, Nishikawa T, Ichihara N, Kikuchi T, Okuyama S, Kawashima N, Hori S, Takimoto M, Wada K (1997) Epilepsy and exacerbation of brain injury in mice lacking the glutamate transporter GLT-1. Science 276:1699-1702.

Thompson LM et al. (2009) IKK phosphorylates Huntingtin and targets it for degradation by the proteasome and lysosome. The Journal of cell biology 187:1083-1099.

Tian R, Wu X, Hagemann TL, Sosunov AA, Messing A, McKhann GM, Goldman JE (2010) Alexander disease mutant glial fibrillary acidic protein compromises glutamate transport in astrocytes. Journal of neuropathology and experimental neurology 69:335-345.

Tien AC, Tsai HH, Molofsky AV, McMahon M, Foo LC, Kaul A, Dougherty JD, Heintz N, Gutmann DH, Barres BA, Rowitch DH (2012) Regulated temporal-spatial astrocyte precursor cell proliferation involves BRAF signalling in mammalian spinal cord. Development 139:2477-2487.

Tilleux S, Hermans E (2007) Neuroinflammation and regulation of glial glutamate uptake in neurological disorders. Journal of neuroscience research 85:2059-2070.

Tong X, Ao Y, Faas GC, Nwaobi SE, Xu J, Haustein MD, Anderson MA, Mody I, Olsen ML, Sofroniew MV, Khakh BS (2014) Astrocyte Kir4.1 ion channel deficits contribute to neuronal dysfunction in Huntington's disease model mice. Nature neuroscience 17:694-703.

Tsai HH, Li H, Fuentealba LC, Molofsky AV, Taveira-Marques R, Zhuang H, Tenney A, Murnen AT, Fancy SP, Merkle F, Kessaris N, Alvarez-Buylla A, Richardson WD, Rowitch DH (2012) Regional astrocyte allocation regulates CNS synaptogenesis and repair. Science 337:358-362.

Tsuda M, Kohro Y, Yano T, Tsujikawa T, Kitano J, Tozaki-Saitoh H, Koyanagi S, Ohdo S, Ji RR, Salter MW, Inoue K (2011) JAK-STAT3 pathway regulates spinal astrocyte proliferation and neuropathic pain maintenance in rats. Brain : a journal of neurology 134:1127-1139.

Tsukada S, Iino M, Takayasu Y, Shimamoto K, Ozawa S (2005) Effects of a novel glutamate transporter blocker, (2S, 3S)-3-[3-[4-(trifluoromethyl)benzoylamino]benzyloxy]aspartate (TFB-TBOA), on activities of hippocampal neurons. Neuropharmacology 48:479-491.

Tydlacka S, Wang CE, Wang X, Li S, Li XJ (2008) Differential activities of the ubiquitin-proteasome system in neurons versus glia may account for the preferential accumulation of misfolded proteins in neurons. The Journal of neuroscience : the official journal of the Society for Neuroscience 28:13285-13295.

Tyzack GE, Sitnikov S, Barson D, Adams-Carr KL, Lau NK, Kwok JC, Zhao C, Franklin RJ, Karadottir RT, Fawcett JW, Lakatos A (2014) Astrocyte response to motor neuron injury promotes structural synaptic plasticity via STAT3-regulated TSP-1 expression. Nature communications 5:4294.

Ullian EM, Sapperstein SK, Christopherson KS, Barres BA (2001) Control of synapse number by glia. Science 291:657-661.

Uwechue NM, Marx MC, Chevy Q, Billups B (2012) Activation of glutamate transport evokes rapid glutamine release from perisynaptic astrocytes. The Journal of physiology 590:2317-2331.

Vainchenker W, Constantinescu SN (2013) JAK/STAT signaling in hematological malignancies. Oncogene 32:2601-2613.

Vargas MR, Johnson DA, Sirkis DW, Messing A, Johnson JA (2008) Nrf2 activation in astrocytes protects against neurodegeneration in mouse models of familial amyotrophic lateral sclerosis. The Journal of neuroscience : the official journal of the Society for Neuroscience 28:13574-13581.

Venugopal R, Jaiswal AK (1998) Nrf2 and Nrf1 in association with Jun proteins regulate antioxidant response element-mediated expression and coordinated induction of genes encoding detoxifying enzymes. Oncogene 17:3145-3156.

Villanueva EC, Myers MG, Jr. (2008) Leptin receptor signaling and the regulation of mammalian physiology. International journal of obesity 32 Suppl 7:S8-12.

Vonsattel JP, Myers RH, Stevens TJ, Ferrante RJ, Bird ED, Richardson EP, Jr. (1985) Neuropathological classification of Huntington's disease. Journal of neuropathology and experimental neurology 44:559-577.

Voskuhl RR, Peterson RS, Song B, Ao Y, Morales LB, Tiwari-Woodruff S, Sofroniew MV (2009) Reactive astrocytes form scar-like perivascular barriers to leukocytes during adaptive immune inflammation of the CNS. The Journal of neuroscience : the official journal of the Society for Neuroscience 29:11511-11522.

Walker FO (2007) Huntington's disease. Lancet 369:218-228.

Walrafen P, Verdier F, Kadri Z, Chretien S, Lacombe C, Mayeux P (2005) Both proteasomes and lysosomes degrade the activated erythropoietin receptor. Blood 105:600-608.

Wan J, Fu AK, Ip FC, Ng HK, Hugon J, Page G, Wang JH, Lai KO, Wu Z, Ip NY (2010) Tyk2/STAT3 signaling mediates beta-amyloid-induced neuronal cell death: implications in Alzheimer's disease. The Journal of neuroscience : the official journal of the Society for Neuroscience 30:6873-6881.

Wang CE, Tydlacka S, Orr AL, Yang SH, Graham RK, Hayden MR, Li S, Chan AW, Li XJ (2008) Accumulation of N-terminal mutant huntingtin in mouse and monkey models implicated as a pathogenic mechanism in Huntington's disease. Human molecular genetics 17:2738-2751.

Wang L, Lin F, Wang J, Wu J, Han R, Zhu L, Difiglia M, Qin Z (2012) Expression of mutant N-terminal huntingtin fragment (htt552-100Q) in astrocytes suppresses the secretion of BDNF. Brain research 1449:69-82.

Wanner IB, Anderson MA, Song B, Levine J, Fernandez A, Gray-Thompson Z, Ao Y, Sofroniew MV (2013) Glial scar borders are formed by newly proliferated, elongated astrocytes that interact to corral inflammatory and fibrotic cells via STAT3-dependent mechanisms after spinal cord injury. The Journal of neuroscience : the official journal of the Society for Neuroscience 33:12870-12886.

White JK, Auerbach W, Duyao MP, Vonsattel JP, Gusella JF, Joyner AL, MacDonald ME (1997) Huntingtin is required for neurogenesis and is not impaired by the Huntington's disease CAG expansion. Nature genetics 17:404-410.

Wilhelmsson U, Bushong EA, Price DL, Smarr BL, Phung V, Terada M, Ellisman MH, Pekny M (2006) Redefining the concept of reactive astrocytes as cells that remain within their unique domains upon reaction to injury. Proceedings of the National Academy of Sciences of the United States of America 103:17513-17518.

Wilhelmsson U, Li L, Pekna M, Berthold CH, Blom S, Eliasson C, Renner O, Bushong E, Ellisman M, Morgan TE, Pekny M (2004) Absence of glial fibrillary acidic protein and vimentin prevents hypertrophy of astrocytic processes and improves post-traumatic regeneration. The Journal of neuroscience : the official journal of the Society for Neuroscience 24:5016-5021.

Wojtowicz AM, Dvorzhak A, Semtner M, Grantyn R (2013) Reduced tonic inhibition in striatal output neurons from Huntington mice due to loss of astrocytic GABA release through GAT-3. Frontiers in neural circuits 7:188.

Wu Z, Asokan A, Samulski RJ (2006) Adeno-associated virus serotypes: vector toolkit for human gene therapy. Molecular therapy : the journal of the American Society of Gene Therapy 14:316-327.

Wu Z, Guo Z, Gearing M, Chen G (2014) Tonic inhibition in dentate gyrus impairs long-term potentiation and memory in an Alzhiemer's disease model. Nature communications 5:4159.

Wyss-Coray T, Loike JD, Brionne TC, Lu E, Anankov R, Yan F, Silverstein SC, Husemann J (2003) Adult mouse astrocytes degrade amyloid-beta in vitro and in situ. Nature medicine 9:453-457.

Xia XG, Hofmann HD, Deller T, Kirsch M (2002) Induction of STAT3 signaling in activated astrocytes and sprouting septal neurons following entorhinal cortex lesion in adult rats. Molecular and cellular neurosciences 21:379-392.

Xiao Q, Yan P, Ma X, Liu H, Perez R, Zhu A, Gonzales E, Burchett JM, Schuler DR, Cirrito JR, Diwan A, Lee JM (2014) Enhancing astrocytic lysosome biogenesis facilitates Abeta clearance and attenuates amyloid plaque pathogenesis. The Journal of neuroscience : the official journal of the Society for Neuroscience 34:9607-9620.

Xu Z, Xue T, Zhang Z, Wang X, Xu P, Zhang J, Lei X, Li Y, Xie Y, Wang L, Fang M, Chen Y (2011) Role of signal transducer and activator of transcription-3 in up-regulation of GFAP after epilepsy. Neurochemical research 36:2208-2215.

Yamanaka K, Chun SJ, Boillee S, Fujimori-Tonou N, Yamashita H, Gutmann DH, Takahashi R, Misawa H, Cleveland DW (2008) Astrocytes as determinants of disease progression in inherited amyotrophic lateral sclerosis. Nature neuroscience 11:251-253.

Yang J, Liao X, Agarwal MK, Barnes L, Auron PE, Stark GR (2007) Unphosphorylated STAT3 accumulates in response to IL-6 and activates transcription by binding to NFkappaB. Genes & development 21:1396-1408.

Yang Y, Vidensky S, Jin L, Jie C, Lorenzini I, Frankl M, Rothstein JD (2011) Molecular comparison of GLT1+ and ALDH1L1+ astrocytes in vivo in astroglial reporter mice. Glia 59:200-207.

Yiu G, He Z (2006) Glial inhibition of CNS axon regeneration. Nature reviews Neuroscience 7:617-627.

Yoshida Y, Kumar A, Koyama Y, Peng H, Arman A, Boch JA, Auron PE (2004) Interleukin 1 activates STAT3/nuclear factor-kappaB cross-talk via a unique TRAF6- and p65-dependent mechanism. The Journal of biological chemistry 279:1768-1776.

Yoshii Y, Otomo A, Pan L, Ohtsuka M, Hadano S (2011) Loss of glial fibrillary acidic protein marginally accelerates disease progression in a SOD1(H46R) transgenic mouse model of ALS. Neuroscience research 70:321-329.

Yoshimura A, Naka T, Kubo M (2007) SOCS proteins, cytokine signalling and immune regulation. Nature reviews Immunology 7:454-465.

Yoshimura A, Mori H, Ohishi M, Aki D, Hanada T (2003) Negative regulation of cytokine signaling influences inflammation. Current opinion in immunology 15:704-708.

Yoshimura A, Ohkubo T, Kiguchi T, Jenkins NA, Gilbert DJ, Copeland NG, Hara T, Miyajima A (1995) A novel cytokine-inducible gene CIS encodes an SH2-containing protein that binds to

tyrosine-phosphorylated interleukin 3 and erythropoietin receptors. The EMBO journal 14:2816-2826.
Yu Z, Zhang W, Kone BC (2002) Signal transducers and activators of transcription 3 (STAT3) inhibits transcription of the inducible nitric oxide synthase gene by interacting with nuclear factor kappaB. The Biochemical journal 367:97-105.
Yu ZX, Li SH, Evans J, Pillarisetti A, Li H, Li XJ (2003) Mutant huntingtin causes context-dependent neurodegeneration in mice with Huntington's disease. The Journal of neuroscience : the official journal of the Society for Neuroscience 23:2193-2202.
Zamanian JL, Xu L, Foo LC, Nouri N, Zhou L, Giffard RG, Barres BA (2012) Genomic analysis of reactive astrogliosis. The Journal of neuroscience : the official journal of the Society for Neuroscience 32:6391-6410.
Zennou V, Serguera C, Sarkis C, Colin P, Perret E, Mallet J, Charneau P (2001) The HIV-1 DNA flap stimulates HIV vector-mediated cell transduction in the brain. Nature biotechnology 19:446-450.
Zhang JG, Metcalf D, Rakar S, Asimakis M, Greenhalgh CJ, Willson TA, Starr R, Nicholson SE, Carter W, Alexander WS, Hilton DJ, Nicola NA (2001) The SOCS box of suppressor of cytokine signaling-1 is important for inhibition of cytokine action in vivo. Proceedings of the National Academy of Sciences of the United States of America 98:13261-13265.
Zhang S, Li W, Wang W, Zhang SS, Huang P, Zhang C (2013) Expression and activation of STAT3 in the astrocytes of optic nerve in a rat model of transient intraocular hypertension. PloS one 8:e55683.
Zhang Y, Li M, Drozda M, Chen M, Ren S, Mejia Sanchez RO, Leavitt BR, Cattaneo E, Ferrante RJ, Hayden MR, Friedlander RM (2003) Depletion of wild-type huntingtin in mouse models of neurologic diseases. Journal of neurochemistry 87:101-106.
Zou H, Yan D, Mohi G (2011) Differential biological activity of disease-associated JAK2 mutants. FEBS letters 585:1007-1013.
Zuccato C, Valenza M, Cattaneo E (2010) Molecular mechanisms and potential therapeutical targets in Huntington's disease. Physiological reviews 90:905-981.
Zuccato C, Tartari M, Crotti A, Goffredo D, Valenza M, Conti L, Cataudella T, Leavitt BR, Hayden MR, Timmusk T, Rigamonti D, Cattaneo E (2003) Huntingtin interacts with REST/NRSF to modulate the transcription of NRSE-controlled neuronal genes. Nature genetics 35:76-83.
Zufferey R, Donello JE, Trono D, Hope TJ (1999) Woodchuck hepatitis virus posttranscriptional regulatory element enhances expression of transgenes delivered by retroviral vectors. Journal of virology 73:2886-2892.
Zufferey R, Dull T, Mandel RJ, Bukovsky A, Quiroz D, Naldini L, Trono D (1998) Self-inactivating lentivirus vector for safe and efficient in vivo gene delivery. Journal of virology 72:9873-9880.